



TU/e



Supported by



The 3rd International Conference on Sustainable Building Materials

第三届可持续建筑材料国际会议

ABSTRACT BOOK

摘要集



24-27 September, 2023 | Wuhan · China

2023年9月24-27日 | 中国·武汉

CONTENTS

TOPIC A: Advances in cementitious binders..... 1

Effect of different particle sizes of coarse aggregates on chloride diffusion by AC impedance spectroscopy	1
Characterization of N-(C)-A-S-H gels: insight from molecular dynamics and experimental study	2
Sodium tripolyphosphate as CaCO ₃ phase controlling additive in carbonated wollastonite composites: Microstructural evolution and carbonation mechanism	4
Effect of ceramsite sand on mechanical properties and impermeability of Limestone Calcined Clay Cement (LC3) mortar	5
Pozzolanic activity of mechanochemically and thermally activated coal-series kaolin in cement-based materials.....	6
Effect of recycled fine aggregate as internal curing medium on mechanical properties and autogenous shrinkage of UHPC.....	7
Effect of calcium leaching on the chloride-binding properties of Portland cement.....	8
Development of coarse aggregate-engineered cementitious composites (CA-ECC) with the characteristics of low carbon and shrinkage.....	10
Experimental study on novel low carbon ultra-high performance concrete: mechanical properties and microstructure characterization.....	11
Machine Learning Predictions of Rheological Parameters in 3D Printed Cement Composites: Influential Components and Printability Enhancement.....	12
Spin, orbital, charge ordering, and elastic properties of ferrite cement C ₄ AF.....	13
Key Technologies for Multiple Protection of Concrete Durability Under Severe Environment	14
Study on the Properties of Cementitious Materials by Carbonated Recycled Cement Powder Based on ACC Induction.....	15
Using CaO-SiO ₂ -Al ₂ O ₃ ternary phase diagram, this study uses analytical reagentssuch as CaCO ₃ , Al ₂ O ₃ , SiO ₂ and Fe ₂ O ₃ to prepare ordinary Portland cement by firing	16
Applications of the half-calcined Na ₃ PO ₄ -doped dolomite in magnesium oxychloride cement .	17
Evaluation of protected paste volume by Dirichlet tessellation tile areas assigned to air voids as a random point process.....	18
Sustainable BOF slag binder activated by EDTA-4Na	19
Flowability, mechanical properties and post-cracking behavior of ultra-high performance concrete (UHPC) reinforced by polyoxymethylene (POM) fiber and steel fiber	21
Straw Wool Geopolymer Board: Straw-Geopolymer Compatibility and Its Insulation Performance.....	23
Nanostructure evolution of the Fe(OH) ₃ phase in the hydration products of calcium sulfoaluminate cement at different temperature	24
The compressive fatigue performance of ultra-high performance cementitious composites with nanofillers	25
Effect of Volcanic Rock on the Properties of Cement Mortar under Sulfate Attack	26
Utilising Low Al/Si Materials Manufacturing Ternesite - Ye'elimité Cement and its Long-age	

ICSBM 2023

3rd International Conference of Sustainable Building Materials

25-27 September, Wuhan, China

Performance.....	28
Prediction of deformations of alkali-activated slag concrete under semi-adiabatic condition	30
Study on Polyaluminum Regulates Hydration Reaction and Durability of Slag-Portland Cement Material.....	33
A Mini Temperature Stress Testing Machine for Assessing Early-Age Cracking Potentials of Cementitious Materials.....	35
Effects of calcined phosphogypsum replacement on hydration and properties of calcium sulfoaluminate cement at different curing temperatures	38
Effects of glass bubbles on the radiative cooling performance of cementitious cooling composites and its carbonation behavior: the role of content, size, and pre-crush.....	40
Influences of carbonate sources on the performance of calcium carbonate-metakaolin- cement composites	42
The Mechanism of Microwave Curing for Ultra-high Performance Concrete	43
Assessing the feasibility of partially replacing Portland cement with calcined Dutch clay	45
Enhancing Mechanical Properties of Portland Cement with Blending CO ₂ -intermixed High Belite Calcium Sulfoaluminate Cement	47
The role of mineral wool waste in geopolymers: the cementing properties and environmental impact.....	49
Effect of metakaolin and superplasticizer on drying shrinkage of hardened Portland cement pastes	51
Effect of CO ₂ curing on carbonation products and subsequent hydration of cementitious materials.....	53
Mechanism and Properties of Solidification of Simulated Intermediate and Low Level Radioactive High Concentration Borate Solution by Portland Cement.....	55
Self-sensing properties of alkali-activated materials	57
Machine learning based strength prediction model for cement clinker	58
Effect of steel slag powder on the properties of magnesium phosphate cement.....	60
Mechanisms of Steel Corrosion and Chloride Binding in Cement-Based Materials.....	61
Compatibility evaluation on phosphogypsum-based cementitious binder and cold-bonded aggregates to conventional cements and concretes	63
Silica-aerogel composites for thermal insulation application: Characteristics and reinforcement evaluation.....	65
Analysis on Influencing Factors of Field Test Results of Resistance to Chloride Ion Penetration	66
The Influence of nano silica on the Carbonation Resistance of Supersulfated Cement.....	67
水化硅酸钙的粘弹性研究.....	68
Nanoscale Mechanisms of C-S-H Decalcification in Seawater	69
Pre-wet-carbonated 10% cement in the production of CO ₂ -mixed cement pastes	70
Experimental and numerical investigation on thermal properties of alkali-activated concrete at elevated temperatures.....	71
Enhancing the early performance of BOFS-blended cement pastes by internal carbonation with 13X zeolite.....	72
Effects of Pre-curing and Water-cement Ratios on the Carbonation Curing of Cement-based	

ICSBM 2023

3rd International Conference of Sustainable Building Materials

25-27 September, Wuhan, China

Materials	73
Experimental and numerical investigation on thermal properties of alkali-activated concrete at elevated temperatures.....	74
Study of the rheological properties and flocculation mechanism of PAM on underwater non-dispersible slag/fly ash-based alkali-activated cementitious materials	75
Influence of different chain transfer agents on properties of polycarboxylate superplasticizers	76
Effect of the activation agents on the properties of the obtained geopolymers from high-calcium fly ash.....	78
Feasibility of preparing carbonated fly ash as supplementary cementitious material.....	80
Effects of the electrical double layer on nanoscale chloride transport in alkali-activated slag materials.....	82
Mechanical property, microstructure and anti-acid rain erosion performance of red mud-slag-based geopolymer	83
Characterization and Hydrophobic Surface Study of Gypsum based Composite by Modified Reduced Graphene Oxide	85
Preparation and Properties of the Alite-modified Calcium Sulfoaluminate Clinker by Using High Magnesium Limestone	86
Mechanism of Ba ion solution in LCCSB and its influence on carbonation reaction.....	88
Thermal responsive clay-hydrogel composite for additive construction.....	89
Coupled thermodynamic modelling and experimental study of alkali-activated slag cement under combined attack of chloride and sulfate salts.....	90

TOPIC B: Waste recovery, treatments and valorizations..... 91

Lightweight, deformable, and water-resistant cement mortars with recycled plastics enabled by in-situ polymerization.....	91
Evaluation of chloride diffusion in recycled aggregate concrete including slag using PSO-BP and GA-BP neural network.....	93
Ambiently dried silica aerogel from waste glass, production and sustainability analysis.....	94
Real-time Sensor-based Characterization of Recycled Coarse Aggregates (RCA)	96
Evaluation of Graphene Oxide on Microstructure and Micromechanical Properties of Ultra-high Performance Concrete with Recycled Fine Aggregate.....	98
Preparation of low calcium cement clinker based on solid waste	99
Preparation of polypropylene-encapsulated toluene diisocyanate microcapsules for self-healing concrete cracks	100
Effect of lightweight aggregate (LWA) and superabsorbent polymers (SAP) on autogenous shrinkage, hydration and properties of UHPC.....	101
The immobilization of Pb, Zn and Cd by spontaneous combustion gangue geopolymer and the depolymerization and reconstruction mechanism	103
Compressive strength and hydration kinetics of phosphate slag-cement materials under varied curing temperature	105
Effect of MgO content on high-temperature phase transformation of coal gangue.....	107
Intelligent Grasping Planning of Decoration Waste Using Generative Grasping Convolutional Neural Network	109

ICSBM 2023

3rd International Conference of Sustainable Building Materials

25-27 September, Wuhan, China

Recycle of contaminated-gypsum in BOF slag system.....	111
Mechanical and self-sensing properties of ultra high performance fiber reinforced concrete (UHPC) with steel slags	112
Design, Preparation, and Performance of Sustainable Concrete Incorporating Solid Waste of Manganese Residue	114
Role and Immobilization of cerium(IV) in Portland cement: A chemical analog of plutonium(IV)	115
Effect of Geometric Morphology of Recycled Fine Aggregate on the Rheology and Strength of Cement Mortar.....	117
Mechanical and Thermal Performance of Electric Arc Furnace Slag-based Alkali Activated Mortar.....	118
Synergistic Valorization of Hazardous Nickel-Chrome Plating Sludge in Alkali-Activated Electric Arc Furnace Slag-Fly Ash Blended Bricks: A Waste to Wealth Approach.....	120
Influence of Temperature in Accelerated Dry Carbonation of Recycled Concrete Fines	122
Assessment of mechanical and durability properties of concrete containing waste ceramic tiles as coarse aggregates.....	123
Limitation of Innovation and Sustainability - Example of Industrial Floors in Germany.....	125
Developing Sustainable Building Materials through Utilization of Steel Industrial Solid Waste: A Case Study of Sintering Flue Gas Desulphurization Ash and Steel Slag Composite Cementitious Material.....	127
Effect of different heat treatment conditions on the activity of recycled powder.....	129
Future fossil-free steelmaking slags – prospect for sustainable use in building materials.....	130
Reactivity and Microstructure of De-chlorinated Ti-Extracted Residues.....	132
A novel method of co-disposal of steel slag and municipal solid waste incineration fly ash under alkali activation.....	133
A novel power ultrasonic-assisted mixing technology to prepare cement paste: dispersion, hydration dynamics and products evolution of Portland cement paste.....	135
Preparation and Performance Optimization of C ₂ S-C ₄ A ₃ \$/Q Phase Cement with High Volume of Mixed Solid Wastes.....	137
Synthesis of Novel Shrinkage-reducing Polycarboxylate Superplasticiser and its Performance on the workability and Shrinkage of Alkali-Activated Slag	139
Composition design of a low-carbon emission clinker using Phosphogypsum instead of limestone.....	140
Effective iron removal method for coal gangue applied in cement industry	141
Heavy metal solidification and reaction mechanism in alkali-activated MSWI fly ash specimens with natural zeolite	143
Solidification mechanisms of lead in high ferrite cement clinker.....	145
Study on the effect of sewage sludge ash on the properties of cement paste and its water film thickness	146
Understanding the microstructural evolution of 3D printing steel slag-cement with low-field NMR relaxation.....	147

TOPIC C: Alternative reinforcements for concrete structures..... 148

ICSBM 2023

3rd International Conference of Sustainable Building Materials

25-27 September, Wuhan, China

Effect of Accelerated Aging on the Bond Behavior of TRM Composites Through Single-lap Shear Tests.....	148
A comparative study of the composition and corrosion of concrete sewer pipes in the Netherlands.....	150
Effect of polymer fibres recycled from waste tyres on impact resistance of concrete after heat exposure.....	152
Enhancing the dynamic splitting tensile behaviour of ultra-high performance concrete using waste tyre steel fibres.....	153
Mixture design theory of ultra-high performance concrete (UHPC): From particle packing model to artificial intelligence techniques.....	155
Study on the deterioration of interfacial bond strength between LWAC and OC under the coupling effect of sulfate erosion and dry-wet cycles.....	157
Influence of SCMs on the resistance to chloride penetration of ultra-high performance fiber reinforced concrete	159
Two-dimensional concrete meso-aggregate modeling method based on voronoi method	160
Study on the design of alkali-activated concrete and its bonding properties with steel rebar ...	162
Enhancing Chloride Migration Resistance of Cement Mortar with Fly Ash Through the Addition of Nano-Metakaolin.....	163
Strength estimation of concrete model scale sections with FRP for floating wave energy converters	165
Formation of gradient interface in concrete repair and its durability under load and marine environment coupling effects	167
Alkalinity optimization and long-term life prediction for BFRP bars serving in simulated marine concrete environments	168
Effect of gneiss rock power on the performance of machine-made sand concrete	169
A widely applicable freeze–thaw damage model for concrete considering a nonuniform temperature field.....	170
The potential use of Juncus plant fibers as reinforcement in compressed stabilized earth blocks	173
Investigations on the effect of surface treatment of hemp fibers on the mechanical and micro-performance of fiber-cement composites under accelerated aging.....	175
Chloride induced mechanical degradation of ultra-high performance fiber-reinforced concrete: insights from corrosion evolution paths	177
Mesoscopic numerical investigation on the bond behaviour between GFRP bar and UHPC ..	178

TOPIC D: Functionalizing building materials..... 179

Long term development of mechanical properties of concretes with different water to cement ratio and internally cured concretes	179
Influence of expansive agent on the mechanical properties of steel-tube-confined high-performance concrete	181
Mechanism of inhibition of Temperature Rising Inhibitor on hydration of cement and supplementary cementitious materials	184
Understanding the role of carbon nanotubes in low-carbon concrete: from experiment to	

ICSBM 2023

3rd International Conference of Sustainable Building Materials

25-27 September, Wuhan, China

molecular dynamics	185
Salt scaling resistance of pre-cracked ultra-high performance concrete with the coupling of salt freeze-thaw and wet-dry cycles	186
Research on Heat Resistance and Shielding Performance of Serpentine Shielded Concrete	187
Formation of a layered structure porous glass-ceramics for neutron shielding	188
Fly ash as magneto-responsive additive for active rheology control of cementitious materials	189
Design and Application Performance of Phase Change Heat Storage Aggregates and Concrete	190
Development of nano-enhanced composite phase change material for Trombe wall applications	191
Surface Characterization of Carbonated Recycled Concrete Fines and Their Impact on Cement-Based, Lime-Based, and Alkali-Activated Materials.....	192
Understanding the Generation and Evolution of Hydrophobicity of Silane Modified Fly Ash/Slag Based Geopolymers	194
Biomimetic-Induced Hydroxyapatite for Autonomous Self-Healing in Cementitious Materials: Crack Repair and Rebar Corrosion Mitigation	195
Mechanical properties and underlying mechanisms of nickel coated carbon nanotubes reinforced ultra-high performance cementitious composite	197
Preparing energy conservation self-levelling mortar via fly ash cenospheres/paraffin using in floor radiant heating	199
Design of Core-Shell Aggregates and Research on the Mechanism of Heavy Metal Stabilization in Red Mud	201
Phosphorus removal improvement of porous concrete using highly adsorptive aggregates	202
The positive effects of power ultrasound assisted mixing on Portland cement pastes: dispersion, hydration dynamics and products evolution.....	204
Study on the Internal Generation Mechanism of Nano-SiO ₂ for Modification of Cement-based Materials	206
The Effect of CNTs on the diffusivity of Chloride Ions in C-A-S-H Gel.....	207
Electromagnetic absorption characteristics of alkali-activated slag-fly ash composite cementitious material.....	208
Novel C-M/A/F-S-H seeds: Synthesis, characterization and the effect on cement hydration ..	209
Temperature-responsive clays containing heat-sensitive gelatin for 3D printing	210
<i>TOPIC E: Green products & Bio-based materials.....</i>	211
Bio-concrete-organic-soil	211
The use of organic soil to create a bio-protection system for concrete for sustainable underground structures.	212
Research on Mechanical-Electro-Magnetic Properties and Microstructure of Carbon Fiber-Graphite Modified Foam Concrete	213
High performance bio-lightweight concrete using eco-aerogel coated miscanthus fibers.....	214
Effects of lime content on properties of autoclaved aerated concrete made of circulating fluidized bed ash	215
Use of rice husk ash for mitigating the autogenous shrinkage of UHPC	216

ICSBM 2023

3rd International Conference of Sustainable Building Materials

25-27 September, Wuhan, China

Retarding the setting time of alkali-activated slag paste by processing the alkali activator into pills and capsules	217
Calcined Clay Binders.....	219
Oxygen diffusion into unsaturated concrete and affecting chloride-induced corrosion of steel bars	220
Solidification and stabilization of heavy metals in municipal solid waste incineration fly ash using nano-alumina by alkali-activated treatment	221
New insights in the preparation of artificial aggregates: towards sustainable concrete.....	222
Development of Low-carbon Supersulfated Cement for Solidification and Stabilization of Hazardous Waste.....	224
Preparation and Characterization of Portland Cement Clinker Made by Non-traditional Raw Material.....	225
Bio-inspired functionally layered prepacked aggregate fibrous concrete slab under low velocity drop weight impact test	227
Synthesis of aragonite whisker from recycled concrete waste by carbonation method.....	228
Review of ultra-high performance concrete research	229
Thermal damage inhibitory effect of graphene oxide and silica fume synergy on the steam-cured manufactured sand concrete	230
Control of peroxophosphate gypsum slag dry hard cement by adding aluminum phase.....	231
Segregation Analysis of Hollow Microspheres as Lightweight Aggregate in Cementitious Composites	232
Sustainable Ultra-High Performance Concrete Using Low-Grade Waste Glass	233
Mechanical and Microstructural Properties of Sustainable Ultra-High Performance Concrete Using Low-Grade Waste Glass	234

POSTER CONTENTS

A comparative study of the composition and the corrosion products of concrete sewer pipes 235

Straw Wool Geopolymer Board Straw-Geopolymer Compatibility and Its Insulation Performance 236

Hydroceramics for durable passive cooling of the built environment 237

A novel power ultrasound assisted mixing technology to prepare cement paste: Effect on hydration process and compressive strength 238

Combined effect of NaAlO₂ and NaOH on the early age hydration of Portland cement with a high concentration of borate solution 239

Investigations on the effect of surface treatment of hemp fibers on the mechanical and micro-performance of fiber-cement composites 240

Micro-mechanism of SCMs on the chloride penetration of UHPFRC 241

Effects of calcined phosphogypsum replacement on hydration and properties of CSA cement at different curing temperatures 242

Segregation Analysis of Hollow Microspheres as Lightweight Aggregate in Cementitious Composites 243

Two-dimensional concrete meso-aggregate modeling method based on Voronoi method 244

Life Cycle Assessment of geopolymers for sustainable transition of cement industry 245

Formation of a layered structure porous glass-ceramics for neutron shielding 246

Effective iron removal from coal gangue applied in cement industry 247

Influence of Temperature in Accelerated Dry Carbonation of Recycled Concrete Fines 248

Ceramizable geopolymer-based fire-resistant coating 249

Effects of Pre-curing and Water-cement Ratios on the Carbonation Curing of Cement-based Materials 250

Experimental and numerical investigation on thermal properties of alkali-activated concrete at elevated temperatures 251

Mechanism of Temperature Rising Inhibitor on hydration of cement and supplementary cementitious materials 252

Alkalinity optimization and long-term life prediction for BFRP bars serving in marine concrete environment with different Ca(OH)₂ content 253

Influence of expansive agent on the mechanical properties of steel-tube-confined high-performance concrete (STCHPC) 254

Effects of calcined phosphogypsum replacement on hydration and properties of calcium sulfoaluminate cement at different curing temperatures 255

Characterization and Hydrophobic Surface Study of Gypsum based Composite by Modified Reduced Graphene Oxide 256

Sustainable BOF slag binder activated by EDTA-4Na 257

Towards performance carbonation improvement of supersulfated cement by nano-silica 258

Assessing the feasibility of partially replacing Portland cement with calcined Dutch clay 259

Thermal responsive clay-hydrogel composite for additive construction 260

ICSBM 2023

3rd International Conference of Sustainable Building Materials

25-27 September, Wuhan, China

Mechanism of Ba ion solution in LCCSB and its influence on carbonation reaction	261
Understanding the microstructural evolution of 3D printing steel slag-cement with low-field NMR relaxation	262

ICSBM 2023

3rd International Conference of Sustainable Building Materials
25-27 September, Wuhan, China

TOPIC A: Advances in cementitious binders

Effect of different particle sizes of coarse aggregates on chloride diffusion by AC impedance spectroscopy

BI Wenyan^{2,*}, CAI Dongxing¹, GUAN Xuemao^{1,*}

1. School of Materials Science and Engineering, Henan Polytechnic University, Jiaozuo 454000, China

2. School of Chemistry and Chemical Engineering, Henan Polytechnic University, Jiaozuo 454000, China)

Email of the corresponding author: biwenyan@hpu.edu.cn, guanxuemao@hpu.edu.cn

Keywords: Chloride diffusion, AC impedance spectroscopy, Coarse aggregates, concrete

Chloride ion corrosion causes concrete structures to be damaged and influences durability. This study established a new equivalent circuit model to investigate the relationship between different sizes of coarse aggregates and the chloride diffusion coefficient of concrete. The results indicate that the diffusion performance of chloride ions in concrete decreases with the increase of coarse aggregate size. The analysis shows that the correlation coefficient between the R_{ccp} of the connecting pore and the chloride diffusion coefficient is above 0.9. The functional relationship is $D_m = k\sqrt{R_{ccp}(r_x)} + \sqrt{R_{ccp}(t)}$ which can be used to predict the chloride diffusion coefficients of concrete mixed with different sizes of coarse aggregates at different hydration times by the AC impedance method.

ICSBM 2023

3rd International Conference of Sustainable Building Materials
25-27 September, Wuhan, China

Characterization of N-(C)-A-S-H gels: insight from molecular dynamics and experimental study

Yun Chen, ¹Faculty of Civil Engineering and Geosciences, Delft University of Technology, The Netherlands

Jorge S. Dolado, ²Centro de Física de Materiales CFM (CSIC-UPV/EHU), Spain. ³Donostia International Physics Center (DIPC), Spain

Bin Ma, ⁴Laboratory for Waste Management, Paul Scherrer Institut (PSI), Switzerland

Chen Liu, ¹Faculty of Civil Engineering and Geosciences, Delft University of Technology, The Netherlands

Zhenming Li, ⁵Department of Materials Science and Engineering, The University of Sheffield, Sheffield, United Kingdom

Suhong Yin, ⁶School of Materials Science and Engineering, South China University of Technology, China

Qijun Yu, ⁶School of Materials Science and Engineering, South China University of Technology, China

Guang Ye, ¹Faculty of Civil Engineering and Geosciences, Delft University of Technology, The Netherlands

Email of the corresponding author: Y.Chen-9@tudelft.nl

Keywords: N-(C)-A-S-H gel, atomic structure, chemical composition, molecular dynamics, sol-gel method

Sodium calcium aluminosilicate hydrate (N-(C)-A-S-H) gel is the main reaction product in medium Ca alkali-activated materials (AAMs). A better understanding of N-(C)-A-S-H gel can help establish the link between the composition, structure and engineering properties of AAMs, and thereby contributing to the tailored design of AAMs. However, few studies are devoted to the structural characterization of N-(C)-A-S-H gel compared to C-A-S-H gel and N-A-S-H gel, which are the main reaction product of high and low Ca AAMs, respectively. Thus, this study aims to investigate the chemical composition and atomic structure of N-(C)-A-S-H gels through molecular dynamics and experiments. The N-(C)-A-S-H gels with a Si/Al ratio of around 2 and Ca/Al ratios ranging from 0 to 0.5 were synthesized by using the sol-gel method, while the corresponding N-(C)-A-S-H gel models were constructed from the polymerization of Si(OH)₄ and Al(OH)₃ monomers with ReaxFF force field by using molecular dynamics (MD) simulation. The chemical compositions of the synthesized N-(C)-A-S-H gels were characterized by using X-ray fluorescence analysis (XRF) and thermogravimetric analysis (TGA), while their structural information was gained from X-ray diffraction (XRD) and Fourier transform infrared spectroscopy (FTIR). Also, a detailed structural analysis was performed on the constructed N-(C)-A-S-H gel models, including bonding information, X-ray diffraction, and Qⁿ distribution. The resulting Si/Al ratio in the synthesized N-(C)-A-S-H gels is lower than the initial Si/Al ratio used in the synthesis mixture, which is in good agreement with the finding of the constructed N-(C)-A-S-H gel model, where the final Si/Al ratio in the model is also lower than the Si/Al ratio in the initial configuration. For one reason, Si-O-Al is more favoured to be formed than Si-O-Si due to the lower formation energy. For another, Si has a higher tendency to remain in the alkaline solution than Al. These led to a lower Si/Al ratio in the N-(C)-A-S-H gels, either from

ICSBM 2023

3rd International Conference of Sustainable Building Materials
25-27 September, Wuhan, China

experiment or MD simulation, than the initial Si/Al. The Na/Al ratio in the synthesized N-(C-)A-S-H gels or the constructed model is also lower than the initial value. However, the Ca/Al ratio of the constructed N-(C-)A-S-H model was identical to the initial one, and the Ca/Al ratio of the synthesized N-(C-)A-S-H gels was only slightly lower than the initial value. Furthermore, it is found that the Na/Al ratio of the synthesized N-(C-)A-S-H gels lowered with the increasing Ca/Al ratio, also supported by the MD simulation results. These findings indicate that N-(C-)A-S-H gel shows a higher affinity for Ca than Na. All synthesized N-(C-)A-S-H gels showed X-ray amorphous, regardless of their Ca/Al ratios. However, a shift toward larger 2θ angles was observed with an increase in Ca/Al ratio, which is consistent with MD simulation results. Similar trending can be found in the paste level in the literature. According to Q^n distribution, all Si atoms presented in a tetrahedron environment with a four-coordinate configuration, while multi-coordinated Al atoms (Al^4 , Al^5 and Al^6) were found in the polyhedron arrangement. The existence of Al^5 and Al^6 in N-(C-)A-S-H gel model provides strong support to the current knowledge that Al^5 and Al^6 do not only come from raw material. The amounts of Si^3 and Si^4 in the constructed model decreased with an increase in the Ca/Al ratio, which is also confirmed by the FTIR results of the synthesized N-(C-)A-S-H gels. That means the increase in Ca/Al ratio can lead to a less cross-lined N-(C-)A-S-H gel structure. However, the N-(C-)A-S-H gel still maintained a three-dimensional network structure according to the MD simulation results. Overall, this study sheds light on the chemical composition and atomic structure of N-(C-)A-S-H gel and provides valuable insights into the link between the composition, structure, and properties of medium Ca AAMs.

ICSBM 2023

3rd International Conference of Sustainable Building Materials
25-27 September, Wuhan, China

Sodium tripolyphosphate as CaCO₃ phase controlling additive in carbonated wollastonite composites: Microstructural evolution and carbonation mechanism

Lulu Cheng^a, School of Civil Engineering, Wuhan University, Wuhan 430072, PR China

Yuxuan Chen^{a,b,*}, School of Civil Engineering, Wuhan University, Wuhan 430072, PR China;
Department of the Built Environment, Eindhoven University of Technology, P.O. Box 513, 5600 MB Eindhoven, The Netherlands

Tao Liu^b, Department of the Built Environment, Eindhoven University of Technology, P.O. Box 513, 5600 MB Eindhoven, The Netherlands

Qingliang Yu^{a,b,*} School of Civil Engineering, Wuhan University, Wuhan 430072, PR China;
Department of the Built Environment, Eindhoven University of Technology, P.O. Box 513, 5600 MB Eindhoven, The Netherlands

Email of the corresponding author: q.yu@bwk.tue.nl, Yuxuan.chen@whu.edu.cn

This study proposes sodium tripolyphosphate (STPP) as a phase controlling additive for the transition of amorphous calcium carbonate (ACC) and the evolution of CaCO₃ polymorph in carbonation-activated wollastonite composites. Moreover, mechanical performance and carbonation mechanism are investigated. Compared to the control binder, the introduction of STPP results in the formation of more ACC, vaterite, and aragonite during wollastonite carbonation. Besides, STPP prolongs the phase transition of ACC (including transient and stable ACC) into other CaCO₃ polymorphs. Transient ACC crystallizes within 3 days while stable ACC transforms to vaterite, aragonite, or calcite after 3 days. More importantly, the phase change of ACC improves binder efficiencies of all carbonated products, attributed to the cementitious effect. The 0.1 M STPP-containing binder exhibits the highest binder efficiency, reaching the compressive strength of 75.59 MPa. Our results contribute to unique pathways toward a more sustainable and carbon neutral cement industry.

ICSBM 2023

3rd International Conference of Sustainable Building Materials
25-27 September, Wuhan, China

Effect of ceramsite sand on mechanical properties and impermeability of Limestone Calcined Clay Cement (LC3) mortar

Shukai Cheng^{1,2*}, School of Civil Engineering and Architecture, Wuhan Institute of Technology, Wuhan, 430073, China; Hubei Provincial Engineering Research Center for Green Civil Engineering Materials and Structures, China

Xiao You¹, School of Civil Engineering and Architecture, Wuhan Institute of Technology, Wuhan, 430073, China

Ziyang Wu¹, School of Civil Engineering and Architecture, Wuhan Institute of Technology, Wuhan, 430073, China

Kang Chen¹, School of Civil Engineering and Architecture, Wuhan Institute of Technology, Wuhan, 430073, China

Email of the corresponding author: chengsk@wit.edu.cn

Keywords: ceramsite sand; limestone calcined clay cement; mechanical properties; impermeability; pore structure

Limestone Calcined Clay Cement (LC3) is a promising cementitious material. LC3 mortar was prepared by using light ceramsite sand, cement, metakaolin and limestone powder. This study proposes to improve the performance of LC3 mortar, especially its strength and impermeability, by using pre-wet ceramic sand. The effects of different content and prewetting state of ceramic sand on dry density, mechanical properties, hydration reaction, microstructure, ion erosion resistance and impermeability of LC3 mortar were studied. The results showed that the dry density and compressive strength of LC3 mortar decreased gradually with the increase of the mass ratio of ceramic sand to binder (M_s/M_b). The capillary water absorption rate of LC3 mortar increased, while its chloride penetration resistance increased. However, the compressive strength of LC3 mortar can be significantly improved by pre-wet ceramic sand. The results of isothermal calorimetric and thermogravimetric analysis show that the pre-wet clay can promote the reaction rate of LC3 system. After the addition of pre-wet ceramic sand, the permeability resistance and chloride ion erosion resistance of LC3 mortar are significantly improved, indicating that the pre-wet ceramic sand can promote the pozzolanic reaction of calcined clay, further refine its micro-pore structure and enhance its permeability resistance. In general, the introduction of ceramic sand into LC3 system for the study and preparation of lightweight mortar and lightweight concrete is of great significance for the progress of engineering structures and concrete materials.

Pozzolanic activity of mechanochemically and thermally activated coal-series kaolin in cement-based materials

Shukai Cheng^{1,2}, Hubei Provincial Engineering Research Center for Green Civil Engineering Materials and Structures, China; School of Civil Engineering and Architecture, Wuhan Institute of Technology, Wuhan, 430073, China

Ziqian Ye², School of Civil Engineering and Architecture, Wuhan Institute of Technology, Wuhan, 430073, China

Email of the corresponding author: chengsk@wit.edu.cn, 617108098@qq.com

Keywords: Coal-series kaolin; Thermal activation; Pozzolanic reactivity; Hydration; Supplementary cementitious materials.

The shortage of good quality supplementary cementitious materials (SCMs) for producing cement concrete eagerly demands an alternative pozzolan material. Thanks to the rich silica-alumina contents and large reserves in China, coal-series kaolin (CK) (a by-product of coal mining) is promising to be used as an effective SCMs in cement-based materials. This study investigated the effectiveness of using thermally activated CK coupled with mechanical grinding in ordinary Portland cement paste and mortar. The mineralogy, physicochemical structures, thermal decomposition, pozzolanic reactivity of this novel treated CK were evaluated and compared with two water-washed high-purity kaolinitic clays. The results showed that the large change of Al coordination environment in the thermally activated CK at a relatively low temperature (650 °C) rendered a high pozzolanic reactivity. The high content of kaolinite and reduced particle size by mechanical treatment were beneficial to enhancing the reactivity of thermally activated CK. With the use of thermoactivated CK, the early hydration of cement paste was significantly accelerated. The high degree of dihydroxylation, large specific surface area and high pozzolanic reaction of thermoactivated CK contributed to refining the pore structure and improving the compressive strength of blended mortar. The results of this study provided an implication of using treated CK as an alternative SCMs.

Effect of recycled fine aggregate as internal curing medium on mechanical properties and autogenous shrinkage of UHPC

Shukai Cheng^{1*}, School of Civil Engineering and Architecture, Wuhan Institute of Technology, Wuhan, 430073, China

Ziyang Wu², Hubei Provincial Engineering Research Center for Green Civil Engineering Materials and Structures, China

Email of the corresponding author: chengsk@wit.edu.cn

Keywords: Ultra-high performance concrete; Recycled fine aggregate; Mechanical properties; Autogenous shrinkage, Pore structure

The effects of pre-wetted treatment recycled fine aggregate with different particle sizes (0-0.6mm, 0.6-1.18mm and 1.18-2.36mm) and different substitution rates (10%, 20% and 30%) on the fluidity, autogenous shrinkage, mechanical properties and resistance to chloride ion penetration of ultra-high performance concrete (UHPC) were studied. The mechanism of the effect of recycled fine aggregate on the properties of UHPC was investigated by microhardness, TG-DTG, MIP and SEM. The results show that the particle size and content of recycled fine aggregate are the key factors that determine the workability, mechanical properties and shrinkage properties of UHPC. The addition of pre-wetted treatment recycled fine aggregate with different particle sizes increase the fluidity of UHPC and significantly reduce its early autogenous shrinkage, while it has a negative effect on the early compressive strength and resistance to chloride ion penetration of UHPC. However the microhardness and 28 days compressive strength of UHPC are enhanced. With the increase of recycled fine aggregate content, the fluidity and resistance to chloride ion penetration of UHPC decrease gradually. The UHPC incorporating pre-wetted recycled fine aggregate with 1.18-2.36mm particle size shows better performance. Compared with the control group, the 28 days compressive strength is increased by 7.01%, and the autogenous shrinking and resistance to chloride ion penetration are decreased by 82.5% and 30.6%, respectively. The pre-wetted recycled fine aggregate can release water in the UHPC matrix, reduce the internal self-drying process, and improve the degree of hydration reaction, which generate more hydration products and optimize the interface composition structure, and thus refine the internal pores of the matrix.

Effect of calcium leaching on the chloride-binding properties of Portland cement

Hongfeng Di, School of Materials Science and Engineering, Henan Polytechnic University, Jiaozuo, China

Xuemaο Guan, School of Materials Science and Engineering, Henan Polytechnic University, Jiaozuo, China

Songhui Liu, School of Materials Science and Engineering, Henan Polytechnic University, Jiaozuo, China

Email of the corresponding author: guanxuemaο@hpu.edu.cn

Keywords: Calcium leaching, hardened cement paste, pore structure, Chloride binding

Concrete is currently the world's largest civil engineering materials, long-term service in the ocean, salt lake environment of bridges, ports and terminals are very likely to be damaged by calcium leaching and chloride salt corrosion. The study of the adsorption law of free chloride ions adsorbed by concrete materials under chloride salt environment is mainly focused on cementitious materials without calcium leaching, while the experimental study related to the ability of cementitious materials to bind (physisorb and chemically bind) free chloride ions due to microstructural changes induced by calcium leaching in the marine complex aqueous environments is still less involved, in order to understand the effect of calcium leaching on the adsorption and binding properties of chloride ions in hardened cement pastes. In this paper, samples of particles with different degrees of calcium leaching were obtained by accelerating calcium leaching by soaking in 4 mol/L ammonium nitrate solution for different times, and then the particles were subjected to chlorine ion adsorption and desorption experiments. The phase composition and content of the samples were analyzed qualitatively and quantitatively by TG-DTG and X-ray diffractometer, the changes in micro-morphology and calcium-silicon ratio were tested by SEM-EDS, the changes in pore structure were characterized by nitrogen adsorption, and the chloride content was determined by silver nitrate titration. The results show that calcium leaching affects the CH content in the cement paste and the calcium-silicon ratio of C-S-H gel. Calcium leaching can change the composition of the material phases and the relative content of the material phases by dissolving calcium hydroxide and removing calcium from the C-S-H gel. The removal of calcium from the C-S-H gel significantly increased the porosity of the pore size in the range of 2~50 nm. When CH was present, the hardened cement paste was able to chemically bind chloride ions and existed in the formation of Friedel's salt; when CH was leached out, the Friedel's salt did not exist in the hardened cement paste, and CH was one of the necessary conditions for the generation of the Friedel's salt. Since calcium leaching can change the pore structure of C-S-H gel, and the total amount of adsorbed chloride ions in the sample after leaching is affected by the concentration of free chloride ions, in this paper, the capacity of adsorption of chloride ions on C-S-H gel was corrected, and two parameters, the specific surface area and the concentration of free chloride ions, were introduced. The analysis showed that the physical adsorption capacity of C-S-H gel for chloride ions after decalcification was only related to the calcium-silicon ratio and decreased with the decrease of the calcium-silicon ratio. The total amount of chloride ions adsorbed on the C-S-H gel was determined by the mass of the C-S-H gel, the calcium-silicon ratio, the specific surface area, and the concentration of free chloride ions. The total amount of physically adsorbed chloride ions did not change with the decalcification of C-S-H gel in the results of chloride adsorption experiments, because after the decalcification of C-S-H gel, the ability of physically adsorbing chloride ions was reduced, but the specific surface area of the C-S-H gel was significantly increased, and the increase in the adsorbed chloride ions caused by the increase in the specific surface made up for the decrease caused by the decrease in

ICSBM 2023

3rd International Conference of Sustainable Building Materials
25-27 September, Wuhan, China

the ability of physically adsorbing chloride ions.

Development of coarse aggregate-engineered cementitious composites (CA-ECC) with the characteristics of low carbon and shrinkage

Zhifu Dong, Civil engineering college¹ and Tongji University

Hailong Tan, Civil engineering college¹ and Tongji University

Jiangtao Yu, Civil engineering college¹ and Tongji University

Email of the corresponding author: yujiangtao@tongji.edu.cn

Coarse aggregate (CA) is an important component in ordinary cement concrete, However, CA is excluded from the mixture of engineered cementitious composites (ECC) since the negative impact on tensile behavior. This brings some issues to ECC, such as high shrinkage, high production costs, and insufficient greenness. In an attempt to improve above ECC's shortcomings and maintain good tensile behavior, this investigation attempted to introduce artificial fly ash cold-bonded aggregate as CA to produce special green and low-shrinkage engineered cementitious composites (CA-ECC). The aggregate particle size, volume fraction, and pre-wetting time were selected as the main parameter to study the effect of these parameters on the mechanical and shrinkage property. Simultaneously, the meso- and micro-experimental tests were conducted to understand the mechanism of the high tensile strain capacity of CA-ECC. The test results showed that all CA-ECC mixtures could still maintain the characteristic with multiple cracking and strain-hardening. Notably, the mixture of ECC with particle size 5~8mm aggregate, CA8-ECC, showed excellent tensile strain capacity with a value of 8.00%, almost two times that of conventional ECC (4.8%), CA0-ECC, indicating CA could also play 'flaw' to improve tensile strain capacity. Furthermore, through the meso- and micro-scale experiment, small particle aggregates were more evenly distributed in the matrix compared with larger aggregates and induced cracks bifurcation and deflection, which increased the area of the damage zone and benefited the realization of multiple cracking. The incorporation of CA slightly decreased the compressive strength and elastic modulus. However, the lowest compressive strength of all mixtures also surpassed the 50 MPa, which satisfied the demand for fundamental engineering.

As for the effect of CA on the shrinkage properties, as the lightweight aggregate, artificial fly ash aggregate could be introduced as internal curing (IC) agent to reduce autogenous shrinkage because of IC water released from fly ash aggregate. Compared with conventional ECC, CA0-0-0.28, the critical time of the mixture of ECC with aggregate, CA8-20-0.28 and CA15-20-0.28, i.e., the time the internal relative humidity (IRH) started to decline from 100%, were 16.8 and 7.4 hours longer than that of CA0-0-0.28. The IRH of CA-ECC during the unsaturation stage also developed slowly. The saturated stage and unsaturated stage would be further improved after the aggregate was pre-wetted and the IRH of ECC with pre-wetting aggregate could still maintain 90% at the age of 28 days, which meant the better impediment efficacy of pre-wetting aggregate on the self desiccation and decreased the autogenous shrinkage. In terms of the effect of aggregate on autogenous shrinkage, a similar trend with the influence of CA on the IRH could be found. The CA could evidently improve shrinkage performance. At the age of 8h and 28 days, the autogenous shrinkages of CA15-20-0.28 are 210 μe and 613 μe , which were 44% and 55% lower than conventional ECC. As the decrease in the particle size and the incorporation of pre-wetting aggregate, the autogenous shrinkage of ECC could be further improved. The mechanism of the influence of CA on shrinkage was discussed in the end according to the result of microstructure tests. Overall, the proper particle size of CA can maintain or improve the tensile behaviour as well as decrease the autogenous shrinkage and the risk of cracking at the early age. The present study extends the fundamental knowledge for developing ECC materials.

Experimental study on novel low carbon ultra-high performance concrete: mechanical properties and microstructure characterization

Benhao Gao; Lihua Xu*; Tao Tang; Kaidong Su; Yin Chi; Le Huang*

School of Civil Engineering, Wuhan University, 8 Dong Hu South Road, Wuhan 430072, China

Email of the corresponding author: xulihua@whu.edu.cn, huangle@whu.edu.cn

Keywords: Low-carbon ultra-high performance concrete (LC-UHPC); cement replacement ratio; mechanical performance; microstructural alteration

In this study, a tailored slag-based low-carbon ultra-high performance concrete (LC-UHPC) featured with low cement content (30%) was developed at room temperature, in which the dual roles of cement acted as the binder and the alkaline activator to the slag was explored. To evaluate the practical applicability of LC-UHPC, systematic investigations on the workability, mechanical properties, microstructure, hydration products, and environmental impact were conducted. The results showed that the substitution of cement with slag at a large proportion will induce notable modifications in the microstructures and phase compositions of LC-UHPC, leading to the alteration in the failure modes. Compared with OPC-UHPC, LC-UHPC with only 30% cement content possessed superior mechanical performance that exhibits comparable ultimate strength and peak strain, while a significant improvement in toughness by 58%. Moreover, in comparison with the fiber-free specimen, the ultimate strength and toughness of LC-UHPC containing 2.0% steel fiber content were further improved by 1.12 times and 31.17 times, respectively. At last, upon the analyses using SEM-EDS, XRD, TG, and thermodynamic modeling, it is revealed that 30% cement content in the binder is sufficient to activate the hydration activity of slag and generate a significant amount of densely packed hydration products at the microstructural level. The following conclusions were drawn: (1) Using cement as both binder and alkali activator allowed for a significant reduction in cement content in the UHPC system while effectively activating the hydration activity of slag. LC-UHPC achieved comparable workability and mechanical properties to OPC-UHPC while reducing cement content by 40%. This is attributed to the ability of LC-UHPC to generate sufficient hydration products and alkaline environment with only about 30% cement content, resulting in a dense microstructure. (2) The analysis results showed that with the decrease in cement content, the hydration products of LC-UHPC gradually transformed from C-S-H to C-A-S-H and the microstructure and the stress transfer paths can be changed, leading to an alteration of the failure mode under macroscopic mechanical responses. (3) The microstructure characterization and prediction of the phase alteration indicate that when the cement content exceeds 30%, the hydration products of cement can provide a sufficient alkaline environment to stimulate the hydration activity of slag. Additionally, the high content of slag replaces the unhydrated cement particles in the gel, significantly reducing the cement consumption of LC-UHPC without compromising its mechanical properties. (4) The carbon emissions in LC-UHPC were mainly contributed by cement (70%) and steel fibers (28%). The content of these two components was closely related to the strength and toughness of LC-UHPC. Based on the research findings, the tailored mixture of LC-UHPC consisting of 30% cement in mass, 1.0% steel fiber in volume, and 0.17 water-to-binder ratio achieves the optimal balance among the good working performance, superior mechanical properties, and extremely low carbon emission. This provides novel guidance for the design of a low-carbon UHPC cementitious materials system. This capability enables LC-UHPC to achieve a substantial reduction in cement content without compromising the mechanical performance, providing a new routine for the development of LC-UHPC.

Machine Learning Predictions of Rheological Parameters in 3D Printed Cement Composites: Influential Components and Printability Enhancement

Huaxing Gao^a, Yuxuan Chen^{a,**}, Qian Chen^a, Qingliang Yu^{a,*}

^a School of Civil Engineering, Wuhan University, Wuhan, 430072, PR China

Email of the corresponding author: Yuxuan.chen@whu.edu.cn, q.yu@bwk.tue.nl

Keywords: 3D printing concrete, Machine learning, Robustness, Rheology.

The rapid additive manufacturing of structures through layer-by-layer stacking using 3D printing is an advantageous advanced manufacturing technique in the context of Industry 4.0. However, there is still a lack of comprehensive research on the various factors that affect the printability of cement-based composites. In this study, experiments were designed considering seven factors: Portland cement (PC), sulphoaluminate cement (SAC), fly ash, silica fume (SF), superplasticizer (SP), water content, and the time after water addition. The aim was to investigate the effects of these factors on two key rheological parameters that influence printability, namely, plastic viscosity and yield stress, and to provide a printability prediction scheme based on this. In order to construct the machine learning model, a data set was obtained based on experimental means to study the influence of different influencing factors on the two rheological parameters yield stress and plastic viscosity. The experiment uses a rheometer Brookfield RSX-SST attached rheometer with a four-blade vane spindle. The shear stress and shear rate are output from the test results, and the corresponding rheological parameters yield stress and plastic viscosity are calculated by using the Bingham model. In this way, a data set containing 154 data points was established for model training. Six different regression prediction models, namely linear regression (LR), support vector machine regression (SVR), random forest regression (RF), multi-layer perceptron artificial neural network regression (MLP-ANN), ensemble regression were utilized to predict plastic viscosity and yield stress, considering 80% and 20% data for training and testing, respectively while the model's accuracy, MSE, RMSE, MAPE, and R2 were also calculated. The code has been generated in Python scripts. For the sorting problem of the importance of input features, Shapley additive explanations (SHAP) are also accompanied. The results demonstrated that the MLP-ANN and ensemble regression models exhibited best prediction accuracy, with R² reaching 0.985 and 0.979, respectively. Robustness comparisons revealed that water content and SP had the greatest influence on the two rheological parameters, the incorporation of SAC and SF have a positive effect on the rheological parameters, while the negative effect of fly ash on the rheological properties is relatively small, consistent with the experimental results unanimous. It can be observed that both yield stress and plastic viscosity increase with SAC dosage and time, owing to the acceleration of irreversible hydration reactions by SAC, bridging of AFt and gel products to form flocculation structures. Thus, more force is required to break down the formed flocculation structure under shear. The plastic viscosity of the mixture is closely related to the particle collision during the flow process, and the addition of SAC leads to an increase in plastic viscosity due to the higher surface interaction of SAC compared to SF and FA. The rheological parameter has a great influence on the printing window time, and the rheological parameter box is obtained based on multiple sets of printing tests, and is used to guide the printability of the slurry. The effectiveness of the model was confirmed by using the trained model to make predictions on data outside the dataset and verifying that the model can provide support for printability through additional printing tests.

ICSBM 2023

3rd International Conference of Sustainable Building Materials
25-27 September, Wuhan, China

Spin, orbital, charge ordering, and elastic properties of ferrite cement C_4AF

Tingting He, Junhao Shuai, Neng Li*

State Key Laboratory of Silicate Materials for Architectures, Wuhan University of Technology, Wuhan 430070, China

Email of the corresponding author: lineng@whut.edu.cn

Keywords: C_4AF , spin order, electronic structures, strong coulomb interaction effect, mechanical properties

Spin, orbital, and charge ordering of ferrite cement (C_4AF) is investigated, firstly, by the well-defined density functional theory approach as implemented in the VASP package. Both the generalized gradient approximation (GGA) as well as GGA plus the one-site Coulomb interaction (GGA+ U) methods are considered for the exchange–correlation energy functional. The obtained results show that C_4AF is found stable in anti-ferrimagnetic state. The DFT+ U methods was used to evaluate its effect on the electronic structure, and mechanical properties of C_4AF with two different phases of I_2mb (C_4AF -I) and $Pnma$ (C_4AF -P). The Fe-O bonds of the two phases are all weaker and display U due to the presence of Fe ions. The mechanical properties of C_4AF calculated using DFT+ U method significantly differ from those obtained without U considering, in which the former shows lower inferior mechanical properties than the latter.

Key Technologies for Multiple Protection of Concrete Durability Under Severe Environment

Jinxiang Hong^{1,2}, Song Mu^{1,2}, Jinshun Cai^{1,2}, Wei She^{1,2}, Dewen Sun^{1,2}

1 Sobute New Materials Co., Ltd, Nanjing 211103, PR China

2 State Key Laboratory of High Performance Civil Engineering Materials, Jiangsu Research Institute of Building Science Co., Ltd, Nanjing 210008, PR China

Based on the requirement of multi-level protection systems under severe environment, breakthroughs have been made in the key technologies such as biomimetic modified epoxy resin, amphiphilic solidification technology, biomimetic modified light adsorption materials and nanoparticles enhanced materials, integration of hydrophobic modification and steel corrosion inhibition, preparation of steel corrosion inhibitor with stable cation. Furthermore, the aging and debonding of coatings under severe cold and plateau radiation environment and poor pitting resistance of steel corrosion inhibitors exposed to severe environments of high temperature, high humidity and high salt have also been solved. Finally, the key materials for multi-protection and concrete durability guarantee technology were developed.

For protective coating materials, biomimetic, amphiphilic modification technology and properties adjustment of self-drainage and high permeability were applied to preparation of interface enhancement materials with strong adhesion and corrosion resistance on the dry/wet surface. It solved the problems of slow solidify, weak interface force and easy failure of coating materials on the wet and saturated surface and increased interface force on wet surface from 1.3 MPa to over 3.18 MPa, making a technical breakthrough of coating with low interface force on the wet/saturated surface. The research results have been applied in practical engineering, significantly developing the long-term external protection technology for concrete structures durability under severe environment of plateau and ocean.

For corrosion resistance of steel, a hydrophobic efficient steel corrosion inhibitor with a characteristic of responsive release was invented. The hydrophobic effect and corrosion resistance were combined by groups connection, effectively overcoming the poor dispersion of single hydrophobic group and corresponding weakening of concrete performance. It realized a corrosion area rate below 5% under severe environment of high temperature and salt, which was superior to similar technologies of domestic and foreign. The corrosion resistance of steel exposed to high chloride concentration environment was substantially improved, conquering a technical bottleneck of the declined pitting resistance of traditional organic corrosion inhibitors under high chloride concentration environment. The research results have been applied on a large scale, and the significant economic and social benefits have been achieved, developing a new direction of steel corrosion inhibition exposed to severe environment of marine and salinized soil.

For service life assessment, the calculation platform of concrete service life in the combination with effect of concrete surface protection and steel corrosion inhibition was well established. Moreover, the optimization design of multi-protection materials of concrete surface, matrix and steel surface exposed to severe environment was proposed, overcoming a technical bottleneck of the existing protective technologies without quantification design.

The research results provided a guidance for the engineering application, developing the life prediction methods of concrete structure durability under severe environment. It has been successfully applied in 10 projects, such as, Tianwan Nuclear Power Station, Tongminghai Bridge, Songhua River Bridge, Dalu Island Wharf, Taihu Tunnel, and Nanjing/Qidong-Yangzhou Expressway, providing technical support for multi-protection design, service life extension and application evaluation of reinforced concrete under severe environment.

Study on the Properties of Cementitious Materials by Carbonated Recycled Cement Powder Based on ACC Induction

This topic intends to study the mechanism of the formation of calcium carbonate after the carbonation of recycled cement powder, and then improve the reactivity and mechanical properties of carbonized waste concrete micro powder as a supplementary cementitious material by artificially controlling and inducing the in-situ formation of highly active amorphous calcium carbonate on the micro powder particles, so as to achieve the goal of efficient recycling of waste concrete powder in cement-based concrete and optimal utilization of CO₂. This study can provide a theoretical and experimental basis for the comprehensive and efficient utilization of CO₂ and the green reactivation treatment of recycled cement powder, as well as its multifunctional and rational utilization as the main material source in green low-carbon building materials.

The recycled cement powder was carbonized by CO₂ diffusion at low temperature. The formation process of induced carbonization and stable ACC was carried out by adding chemical polymer (Aspartic acid), inorganic ion (Mg²⁺) and solvent conditions (ethanol water), controlling environmental factors (temperature, humidity) and carbonization conditions (time, pressure, rate of CO₂ penetration). Through inductively coupled plasma emission spectrometry (ICP-OES), conductivity meter and pH meter, the process of ion dissolution at the solid-liquid interface was studied and analyzed, the change mode of supersaturation and pH value was established was established. The growth and evolution mechanism of ACC in the carbonization treatment of waste concrete was clarified, and the environmental boundary conditions for the formation of ACC were established.

Combined with the basic process principle of calcium carbonate crystal form induction transformation, adjust environmental factors (temperature, humidity, vacuum state) to induce ACC type recycled cement powder to transform from amorphous phase to crystalline phase, study the crystal form transformation process under the coupling condition of multiple factors of ACC in the recycled cement powder, and establish the basic relationship between the formation, output and induction factors of Amorphous carbon crystal phase (Vaterite, aragonite, Calcite), Reasonably regulate the stability and crystal transformation rate of ACC type recycled cement powder. XRD, SEM, TEM and FTIR were used to study the evolution of microscopic morphology and image changes during the phase transformation of amorphous calcium carbonate, reveal the Mode of action and mechanism of various regulatory factors on the transformation of amorphous calcium carbonate crystal in situ, and explore the development law of amorphous calcium carbonate crystal transformation rate under environmental control.

Subsequently, further research was conducted on the evolution law and internal mechanism of the cementitious ability of carbonized recycled cement powder under the control of different ACC crystal transformation. Subsequently, different activity evaluation methods (such as specific strength method, chemical dissolution method, XPS method, etc.) were used to evaluate the gelation activity of ACC type carbonized recycled cement powder with different mineralization rates and crystallization products, exploring the internal mechanism of the influence of ACC crystal phase transformation on the gelation activity of recycled cement powder. Based on the relationship between ACC cementitious ability and crystal phase transformation, a new activity evaluation system is established to reflect the impact of ACC crystal phase transformation on the cementitious performance of recycled cement powder, and to elucidate the optimization and improvement effect of ACC induction regulation on the cementitious performance of recycled cement powder.

Using CaO-SiO₂-Al₂O₃ ternary phase diagram, this study uses analytical reagentssuch as CaCO₃, Al₂O₃, SiO₂ and Fe₂O₃ to prepare ordinary Portland cement by firing

Using CaO-SiO₂-Al₂O₃ ternary phase diagram, this study uses analytical reagents such as CaCO₃, Al₂O₃, SiO₂ and Fe₂O₃ to prepare ordinary Portland cement by firing at 1400°C, and hydrates it in a mixing bucket for 7 days to prevent its hardening. After removal, it is dried and used as raw material of Full cycle cement with γ -C₂S as the main clinker phase.

According to the XRF of ordinary silicic cement obtained, cement is prepared by adding a small amount of tempering agent in the first cycle, and sintering is carried out in the subsequent cycle without adding the tempering material. The optimal sintering temperature of the full-cycle cement is 1260°C. The content of free calcium oxide in the produced clinker is all lower than 1wt%. The clinker phase of the full-cycle cement is γ -C₂S and no other phase appears in the five cycles, indicating that the clinker of the full-cycle cement has good stability. By grinding the clinker, controlling the target particle size, pressing molding, and then carbonizing hardening.

The full cycle clinker has good mechanical properties after carbonization. After 1 day of CO₂ carbonization, the bending strength of the test block is 65 MPa. After 7 days of carbonization, the flexural strength was increased to 85MPa. The weight percentage of CO₂ in the 7d carbonization sample can be as high as 10.28%. The morphology of calcium carbonate after carbonization is observed, and the resulting CaCO₃ is angular. In some locations, the plates are arranged in parallel, forming a brick-like structure. However, with the increase of the number of cycles, the strength gradually decreased and then tended to be stable, the morphology of calcium carbonate changed, and the amount of carbon sequestration gradually decreased, so a series of studies were carried out on this. The comprehensive test results show that the new clinker can save energy and reduce greenhouse gas emissions, and has a broad application prospect in the construction industry. Due to the low calcium content of cement, the CO₂ emissions generated by the decomposition of calcium carbonate are significantly reduced, and the required fuel is reduced, resulting in a significant reduction of CO₂ emissions in the flue gas. In addition to significantly reducing CO₂ emissions, a large amount of CO₂ is further absorbed into the cement mortar during the hardening process. All of these advantages effectively translate into the low-carbon properties of this cement.

The following conclusions can be drawn:

(1) Taking ordinary Portland cement as the main raw material and adding a small amount of tempering agent by chemometry method, the full-cycle cement with γ -C₂S as the main clinker phase is prepared. After the first cycle, the tempering agent does not need to be added again, the optimal firing temperature is 1260°C, and the clinker has self-powder, which can greatly reduce the grinding energy consumption.

(2) After the first cycle of clinker carbonization for 1 day, the flexural strength of the test block is 65 MPa; After 7 days of carbonization, the flexural strength was increased to 85MPa. With the increase of the number of cycles, the mechanical properties of clinker become worse and worse, and the fixed carbon content in the sample gradually decreases with the increase of the number of cycles, maintaining at 6-10%(carbonization 7d).

(3) The reason for the decline in strength is speculated to be that as the number of cycles increases, the contact area provided by clinker for the carbonization process decreases, the CaCO₃ generated decreases, and the strength decreases.

After repeated cycles, the mechanical properties of the all-component recyclable cement remain almost unchanged with the decrease of the number of cycles, saving natural resources, greatly reducing CO₂ emissions, and having significant economic benefits and social value.

Applications of the half-calcined Na₃PO₄-doped dolomite in magnesium oxychloride cement

Ju Huang¹, Yu Cui¹, Zanqun Liu¹, Dehua, Deng¹

1 School of Civil Engineering, Central South University, Changsha, Hunan, 410075, China

Email of the corresponding author: zanqun.liu@csu.edu.cn

Keywords: half-calcined dolomite; magnesium oxychloride cement; green cement; CO₂ emission.

The provision of residential and commercial buildings is responsible for over one-third of GHG emissions globally. To mitigate the colossal building-related emissions, magnesium oxychloride cement (MOC) has attracted intensive attention in recent decades. The high production cost and poor water resistance are two shortcomings that severely hamper the application of MOC. The latter now can be greatly improved by adding adequate phosphates to MOCs while the former continues to be a problem. Some studies have been carried out on the use of half-calcined dolomite (HCD) which is often calcined in a CO₂ atmosphere (973 K, 2 h) to replace the active MgO for the production of MOC. However, the prepared MOCs exhibit very poor mechanical properties, especially at very early ages. This paper investigated the use of the half-calcined Na₃PO₄-doped dolomite (HCND) as an alternative for MOC production. Obtained under much lower calcination temperatures for much short time, the HCND showed a much more mesoporous structure, higher BET surface area, smaller MgO particle size and the resultant higher activity, as compared to the conventional half-calcined dolomite (HCD). The heat evolution curves showed that MOC prepared using the HCD (HCD-MOC) had a very slow reaction rate and exhibited no strength after 1 day. The MOC prepared using the HCND (HCND-MOC), however, showed a very rapid reaction rate within the first 4-24 hours and gained a very high early strength after 1 day. The HCND-MOC also gained a much higher 28-day compressive strength (101.2 MPa) than that of HCD-MOC (40.3 MPa). The HCND-MOCs with different molar ratios of MgO/MgCl₂/H₂O were also prepared, and their strengths and bulk density were studied. The CO₂ emission and production cost of HCND-MOCs were estimated and compared with those of MOCs prepared using the commercial light-burned MgO (LBM-MOCs). The carbon emission from energy use (FDCO₂), raw materials (RMCO₂), and transportation (TDCO₂) are calculated (in a unit of kg CO₂/MPa/m³). The results showed that compared to the LBM-MOC having a molar ratio of MgO/MgCl₂/H₂O (E5113), the HCND-MOCs showed a reduction of 16.9-60.5% in FDCO₂, 41.0-72.0% in RMCO₂, 85.2-92.9% in TDCO₂ and, 41.9-72.0 % in total CO₂ emission, depending on their molar ratios of MgO/MgCl₂/H₂O. The production costs of HCND-MOCs are 14.6-63.8 % lower than the E5113. The reasons for the significant reduction in CO₂ emission and production cost include: (1) the much lower MgO content in HCNDs; (2) the higher strength of HCND-MOCs; (3) shorter transportation distance due to the universal accessibility of dolomite resources. The microstructures of HCND-MOCs were further revealed to explain the source of their outstanding performance. The main contribution of this study is providing a novel route to highly active half-calcined dolomite for the production of MOCs with extraordinary mechanical properties, water resistance capability, low carbon footprint, and low production cost.

ICSBM 2023

3rd International Conference of Sustainable Building Materials

25-27 September, Wuhan, China

Evaluation of protected paste volume by Dirichlet tessellation tile areas assigned to air voids as a random point process

Shin-ichi Igarashi, School of Geosciences and Civil Engineering, Kanazawa University

Kakuma-machi, Kanazawa 920-1192, Japan

Email of the corresponding author: igarashi@se.kanazawa-u.ac.jp

The effectiveness of air entrainment for frost protection is judged by the volume and spacing of air voids. Its significance is explained by the concept of protected paste volume, i.e., paste-void proximity. In this study, the protected paste volume was estimated by the area fraction of the Dirichlet tessellation tiles associated with the point pattern of air voids. Each tile area excluding aggregate particles was regarded as a region where an air void was responsible for protection from frost attack. The histogram of the tile areas was created from their frequencies and the characteristic distance was defined by the maximum tile area to cover most of the entire cement paste. The significance of the distance was verified by a Monte Carlo test for the simulation of random point patterns. The characteristic distance was found comparable with the spacing factor recommended for the general concrete in the moderate exposure condition. A virtual distance equivalent to the conventional spacing factor corresponds to an actual distance required for an air void to protect a most vulnerable local region to frost attack. The tessellation model is useful for intuitively realizing the extent of the protected paste volume to which an air void has to protect locally in cement paste for freeze-thaw durability. Furthermore, the effect of aggregate on the spacing distribution is also suggested by the tessellation model

Sustainable BOF slag binder activated by EDTA-4Na

Zhihan Jiang^{1*}, Xuan Ling¹, Katrin Schollbach^{1,2}, H.J.H. Brouwers¹

¹ Department of the Built Environment, Eindhoven University of Technology, Eindhoven 5600 MB, the Netherlands

² Tata Steel, R&D, Microstructure & Surface Characterization (MSC), P.O. Box 10.000, 1970 CA, IJmuiden, the Netherlands

Email of the corresponding author: z.jiang@tue.nl; pro_jzh@163.com;

Keywords: EDTA-4Na, BOF slag, sustainable cementitious materials, ligand-activated hydration, reaction kinetics

BOF slag is a by-product of the basic oxygen furnace steelmaking process and accounts for most steel slag outputs. Its principal mineral compositions are C₂S, brownmillerite (or even closer to srebrodolskite), wuestite, magnetite and f-CaO. The massive production and accumulation of BOF slag have caused the occupation of lands and potential pollution of water and soil. At the same time, abundant belite and brownmillerite within it offer great potential to be used as cementitious binders. However, the early hydration reactivity of belite is low. Furthermore, the hydration is also hindered by numerous impurities (mainly ferrous and ferric iron). Brownmillerite initially dissolves and hydrates quickly, while Fe-containing products' rapid formation impedes further hydration. To improve the hydraulic capacity of BOF slag, EDTA-4Na was used as the activator. EDTA-4Na is a hexadentate ligand widely utilized as a chelator for metal cations in many industries to remove insoluble deposits. Brownmillerite dissolution and the early hydration of belite were expected to accelerate due to the ligand-promoted dissolution of impurities (mainly ferrous and ferric iron) and thus forming stable Fe-EDTA complex ions rather than insoluble Fe-containing hydration products.

The effects of EDTA-4Na on BOF slag hydration were investigated by multiple techniques and methods. The hydration kinetic mechanism was revealed by the isothermal microcalorimeter (TAM Air, Thermometric). Mechanical strength and microstructural (pores) properties were tested by a strength testing bench and mercury porosimeter (AutoPore IV 9500, Micromeritics), respectively. Phase compositions and evolution were characterized by XRD patterns (D2, ENDEAVOR) and quantitative phase analysis (Rietveld refinement, TOPAS commercial). The information of chemical bonds was indicated by FTIR spectrums (PerkinElmer Frontier™ MIR/FIR Spectrometer). SEM/EDS (PhenomProX) was employed to observe and illustrate hydration products' morphology and chemical compositions. One batch leaching test was conducted, and the relevant elements concentrations were determined by the inductively coupled plasma atomic emission spectrometer (ICP-OES, SPECTROBLUE).

The normalized heat flow and cumulative heat release (by weight of binder) reveal the hydration kinetics of EDTA-4Na-activated BOF slag. Pure BOF slag paste only presented almost ignorable exothermic peaks. While with EDTA-4NA addition, distinct heat release peaks occurred, and increased concentration retarded the heat flow peaks. The induction stage for all EDTA-4NA-activated samples was short. The total exothermic heat of EDTA-4NA-activated BOF slag after 7 d hydration also increased significantly compared with pure BOF slag paste. Higher amount of EDTA-4NA addition only increased the whole heat release slightly. It is clear that the addition of EDTA-4NA accelerated the early hydration of BOF slag and promoted the degree of hydration. The 7-day compressive strengths of EDTA-4Na activated BOF slag paste were above 25 Mpa, which was a significant increase compared with below 3 Mpa of pure BOF slag paste. The XRD patterns and quantitative phase analysis (Rietveld refinement) demonstrate the phase evolution after different hydration periods. Main crystalline hydration products of BOF slag with EDTA-4NA activation were hydrogarnet (common general chemical formula

ICSBM 2023

3rd International Conference of Sustainable Building Materials
25-27 September, Wuhan, China

$\text{Ca}_3(\text{Al}_x\text{Fe}_{1-x})_2(\text{SiO}_4)_y(\text{OH})_{4(3-y)}$ and hydrotalcite (common general chemical formula $\text{Mg}_6(\text{Al}_{1-x}\text{Fe}_x)_2\text{CO}_3(\text{OH})_{16}\cdot 4\text{H}_2\text{O}$). Due to the substitution of cations or anions, it is hard to determine the definite chemical formulas for these two minerals. To quantify their amount accurately, in the Rietveld refinement, Katoite and hydroandradite were applied to represent hydrogarnet, and hydrotalcite and pyroaurite were used to represent hydrotalcite. The weight percentage of wuestite decreased apparently after just one day of hydration at high contents of EDTA-4NA addition. After that, it stayed almost still. In contrast, the weight percentage of magnetite remained almost steady throughout the period and was only slightly affected by the addition of EDTA-4NA. C_2S ($\alpha' + \beta$) dropped sharply at high concentration EDTA-4NA after just one day of hydration. The hydration products should (mainly) be C-S-H phase, considering the surge of amorphous content. Apparent declining of C_2S ($\alpha' + \beta$) appeared much later when the lower dosage of EDTA-4Na was used. The second reactive phase, srebrodolskite, decreased significantly after one day of hydration, especially at a high dosage of EDTA-4Na. While after that, it only further reacted slowly or just stabilized. Free lime almost disappeared within hydrated samples. Portlandite and Calcite rose slightly after longer days of hydration and at higher EDTA-4Na concentrations.

Overall, the addition of EDTA-4Na accelerated the early hydration of BOF slag (both belite and srebrodolskite phases) and promoted the degree of hydration. The compressive strength increased significantly. The main crystalline hydration products were hydrogarnet and hydrotalcite.

Flowability, mechanical properties and post-cracking behavior of ultra-high performance concrete (UHPC) reinforced by polyoxymethylene (POM) fiber and steel fiber

JIN Lang, CCCC Second Harbour Engineering Co., Ltd, Wuhan 430040, China

CHEN Feixiang, CCCC Second Harbour Engineering Co., Ltd, Wuhan 430040, China

XIAO Ji, CCCC Second Harbour Engineering Co., Ltd, Wuhan 430040, China

WEI Kai, CCCC Second Harbour Engineering Co., Ltd, Wuhan 430040, China

Email of the corresponding author: jinlang_me@163.com

Keywords: Ultra-high performance concrete (UHPC), Polyoxymethylene (POM) fiber, Mechanical properties, Post-cracking behavior, pull out behavior.

Ultra-high performance concrete (UHPC) by incorporating with a sufficient amount of fiber is a novel type of cementitious composite material with superior high compressive strength, excellent durability and super ductility compared to conventional concrete, especially after high temperature curing. The volume fraction, length, geometry, distribution and orientation of fibers are critical to the mechanical properties of UHPC. Types of fiber used in UHPC are mainly metal fibers, natural fibers and polymer fibers. POM fiber, whose specific density is 1420kg/m³, is a new type of synthetic fiber using recycled polyoxymethylene plastic as raw material. Application of POM fiber in the cement-based materials started from the first decade in 21st, lying on the concordant compatibility between POM fiber and cement paste. The objectives of this research is (1) to investigate the flowability, mechanical properties and post-cracking behavior of UHPC reinforced by POM fiber and steel fiber, (2) to explain the effects of POM fiber and steel fiber reinforced UHPC by investigating the bonding strength and pullout behavior between fibers and matrix, and (3) to explore the feasibility of replacing steel fiber by POM fiber.

An experimental approach is used to achieve these objectives. Round and flat POM fiber with different lengths were used. Steel fiber with different aspect ratios were used. The addition of POM fiber and steel fiber was 28.2kg/m³ and 157kg/m³ by 2% volume fraction in UHPC, individually. Cube specimens of 100mm×100mm×100mm were used for compressive strength testing at the loading rate of 1.2MPa/s. Specimens of 100mm×100mm×400mm prisms (span of 300mm) were used for four-point bending testing to obtain flexural strength and post-cracking behavior at the rate of 0.2mm/min. Dog bone specimens were used to evaluate the direct tensile strength at the rate of 0.2mm/min. The bonding strength of fiber and UHPC matrix were performed by single fiber pull-out experiments at the rate of 0.2mm/min. For the micro-scale, advanced materials characterization techniques, including mercury intrusion porosimetry (MIP), scanning electron microscopy (SEM) were employed to evaluate the porosity of UHPC and to characterize the microstructure.

In this study, the flowability, mechanical properties and post-cracking behavior of UHPC reinforced by different length (4mm~30mm) and shape (round, R=0.2mm, R=0.3mm; flat) of POM fibers and steel fibers (8mm, 13mm, 22mm) were investigated. Properties of UHPC reinforced by mixing POM fiber and steel fiber were also evaluated. Results showed that the flowability of UHPC-P decreased significantly along with the length of POM fiber while the flowability of UHPC-S increased. The compressive strength, flexural strength and tensile strength of UHPC-P was about 20%, 50% and 30% lower than that of UHPC-S, respectively, because of the weak bonding strength of POM fiber and the matrix. However, UHPC-P can

ICSBM 2023

3rd International Conference of Sustainable Building Materials

25-27 September, Wuhan, China

bear higher load and endure significant displacement after initial crack when the diameter is 0.2mm and the length is over 20mm because of the bridging effect of POM fibers. Microstructural results from MIP and SEM confirmed the change in mechanical properties. Based on the hybrid reinforcing effect of fibers, properties UHPC reinforced by mixing fibers can achieve high strength and capacity of reloading by a reasonable ratio.

The conclusions from this investigation are as follows:

- (1) The flowability of UHPC paste decreased rapidly along with the POM fiber length and it can be observed that UHPC paste cannot flow through a clogged fiber network because POM fibers tend to form lumps when the lengths is over 24mm. The flowability of UHPC paste reinforced by steel fiber decreased with the aspect ratio due to the increasing of quantity and total contacting surface of steel fiber.
- (2) The compressive strength of UHPC-P was about 120MPa, which was much lower than UHPC-S. Short POM fibers have little enhancement due to the disturbance effect of the dense packing state of the matrix which was negative to the strength.
- (3) The flexural strength of UHPC-P and UHPC-S was around 12-15MPa and over 25MPa, respectively, due to difference of the bond strength and fiber pull-out behavior of POM fiber and steel fiber. UHPC-P showed typical brittle failure and only one main crack came out. However UHPC-P was able to bear higher load and endure significant displacement and after initial crack when the diameter is 0.2mm and the length is over 20mm because of the bridging effect of POM fibers.
- (4) UHPC incorporating with POM fiber and steel fiber can achieve high compressive strength of over 150MPa, which is similar to UHPC-S, and capacity of reloading after initial crack when the volume ratio is 0.1:1.5 and 1:1.

Straw Wool Geopolymer Board: Straw-Geopolymer Compatibility and Its Insulation Performance

C.H. Koh¹, F. Gauvin¹, K. Schollbach¹, and H.J.H. Brouwers¹

¹Department of the Built Environment, Eindhoven University of Technology

Email of the corresponding author: k.c.h.koh.chuen.hon@tue.nl

Keywords: straw; fibres; geopolymer composites; insulation

Wood wool cement board (WWCB) is widely used in construction due to its advantages such as decay and insect resistance, lightweight nature, and acoustic and thermal insulation properties. However, the chemical incompatibility between wood and cement presents challenges in manufacturing. Geopolymer binders have shown compatibility with natural fibres, including waste straws. This study aims to replace high-energy ordinary Portland cement (OPC) with geopolymer and wood wool with agricultural by-product straws in the production of insulation boards. The resulting straw wool geopolymer board (SWGB) is lightweight, offers thermal insulation, and demonstrates good compatibility between geopolymer binders and straw fibres.

This study explores the use of wheat and barley straws as alternatives to wood wool in the production of geopolymer-based boards. Geopolymer precursors, specifically fly ash and ground granulated blast furnace slag, are utilized, along with sodium hydroxide and sodium silicate as alkali activators. To assess the compatibility between geopolymer and straws, different concentrations of alkali pre-treatment (0, 0.5, and 1.0M NaOH) are applied to both wheat and barley straws.

The developed samples undergo comprehensive testing to evaluate their mechanical strength according to EN 13168 standards (including bending and compressive strength), thermal properties such as thermal conductivities and heat capacity, hygric properties through sorption isotherm analysis, and acoustic performance specifically sound absorption. Additionally, the microstructure and porosity of the samples are examined to provide a thorough understanding of their physical characteristics. Furthermore, the chemical compositions and reactions of the samples are investigated to gain insights into their geopolymerisation process and overall chemical stability.

This study aims to showcase the compatibility between geopolymer and straw fibres in the production of high-performance insulation boards. By replacing OPC with geopolymer and substituting wood wool with straws, a more sustainable alternative is achieved in the construction industry. Both geopolymer and straws contribute to a significant reduction in the carbon footprint, making the proposed SWGB an environmentally friendly option

Nanostructure evolution of the Fe(OH)₃ phase in the hydration products of calcium sulfoaluminate cement at different temperature

Jiangchuan Li, School of Civil Engineering, Dalian University of Technology, Dalian, China

Jun Chang*, School of Civil Engineering, Dalian University of Technology, Dalian, China

Tian Zeng, School of Civil Engineering, Dalian University of Technology, Dalian, China

Email of the corresponding author: Jun Chang*, mlchang@163.com

Keywords: Calcium sulfoaluminate cement; Fe(OH)₃ phase; Temperature; Microstructure

Temperature is one of the most important factors affecting the hydration process and the crystallinity of the products of cement, and its effect on the gel phase cannot be ignored. The Fe(OH)₃ phase is an indispensable gel phase in calcium sulfoaluminate cement, which significantly contributes to the desirable properties of CSA cement (especially the Ferric-rich calcium sulfoaluminate (FR-CSA) cement). In order to thoroughly study the influence of temperature on the microstructure of Fe(OH)₃ gel phase, XRD, TGA, FTIR, SEM, TEM, N₂ adsorption-Brunauer Emmett Teller (BET) and Mössbauer spectroscopy were used to investigate the microstructure of Fe(OH)₃ phase synthesized by sol-gel method and Fe(OH)₃ phase in iron phase hydration products prepared by solid phase sintering at different temperatures. The results show that the chemically synthesized Fe(OH)₃ phase has a crystal structure, Goethite/Hematite is the only product of Fe(OH)₃ phase, and temperature has a significant effect on the crystallinity and microstructure of Fe(OH)₃. The increase of temperature leads to the gradual increase of the crystallinity of Fe(OH)₃ phase, changes the crystallization path of Fe (OH)₃ phase, and is conducive to the formation of Hematite crystal. At the same time, the microstructure changes from needle like structure of Goethite to sheet like structure of Hematite. In addition, no evidence of amorphous Fe(OH)₃ was found during the hydration process at different temperatures. XRD, TEM, and Mössbauer spectra indicate that Fe (OH)₃ has a clear crystal structure. Compared with the chemically synthesized Fe(OH)₃ phase, the hydrated Fe(OH)₃ phase exists as microcrystals, and its microstructure is mostly flaky, with significantly smaller particle sizes.

The compressive fatigue performance of ultra-high performance cementitious composites with nanofillers

Linwei Li¹, Xinyue Wang¹, Baoguo Han^{1,*}

¹ School of Civil Engineering, Dalian University of Technology, Dalian 116024, China

Email of the corresponding author: hithanbaoguo@163.com, hanbaoguo@dlut.edu.cn

Keywords: nanomaterial, fatigue performance, ultra-high performance cementitious composites

The ultra-high performance cementitious composites, known for their high stiffness, strength and strong durability, have been widely used in engineering structures, such as bridge deck, piers and wind turbine towers that are usually subjected to fatigue load. Nevertheless, despite the excellent properties, ultra-high performance cementitious composites are still porous and prone to cracking when the localized fatigue load is too larger or the fatigue load is of great high-frequency, which will reduce the service life and threaten the safety of the structures. This demonstrates the importance of improving fatigue performance of ultra-high performance cementitious composites.

Fatigue of cementitious composites is highly affected by internal imperfections. Cementitious composites under fatigue load shows a greater number of micro/nanoscale cracks and a higher proportion of bond cracks between the cementitious matrix and aggregate. Despite having a compact matrix, the ultra-high performance cementitious composites still cracks originating from inside weak regions, such as nanoscale pores, porous hydrated calcium silicate gels and calcium hydroxide crystals, etc. Thus, improvement of microstructure of ultra-high performance cementitious composites matrix has the potential to enhance fatigue performance. Previous studies have shown that the incorporation of steel fiber can improve the fatigue life and strength, and change the fatigue deformation of ultra-high performance cementitious composites. It should be noted that the ordinary steel fiber mainly focusses on limiting the development of macroscopic fatigue cracks, and ultrafine steel fiber targets the microscopic fatigue cracks. Nevertheless, the impact of steel fiber on the initiation of fatigue cracks nanoscopic of cementitious composites is relatively limited.

Therefore, the objective of this study is to develop anti-fatigue ultra-high performance cementitious composites by incorporating nanofillers, which can modify the microstructure of ultra-high performance cementitious composites. The investigations focus on the compressive fatigue performance of nanofillers modified ultra-high performance cementitious composites, including fatigue life, fatigue strength and fatigue deformation characteristics. Factors such as dimension, property, content, surface treatment of the nanomaterial are taken into consideration. The use of digital imaging processing method reveals the cracks and pores characteristic at the fatigue fracture surface. The results indicate that the fatigue life of ultra-high performance cementitious composites is significantly extended, and the fatigue strength and fatigue failure strain demonstrate an increase with the incorporation of nanofillers. Among the different types of nanofillers, one-dimensional nanofillers (carbon nanotubes), are proved to be more effective in improving the fatigue performance of the ultra-high performance cementitious composites. It is observed that surface treatment of carbon nanotubes, including hydroxylation, carboxylation, graphitization and nickel coating, does not enhance fatigue life and strength, but does contribute to an increase in the fatigue failure strain of carbon nanotube-modified ultra-high performance cementitious composites. Furthermore, the area of pores and cracks at the fatigue fracture surface is largely reduced with the incorporation of nanofillers, and the number of microscopic and nanoscopic cracks is increased. All in all, incorporating nanofillers has ability to improve the service life of structures fabricated by ultra-high performance cementitious composites.

Effect of Volcanic Rock on the Properties of Cement Mortar under Sulfate Attack

Yang Li, affiliation and addresses: College of Materials Science and Engineering, Nanjing Tech University, Nanjing, PR China

Yuang Liu, affiliation and addresses: College of Materials Science and Engineering, Nanjing Tech University, Nanjing, PR China

Zhuqing Yu^{1,2}, affiliation and addresses: ¹College of Materials Science and Engineering, Nanjing Tech University, Nanjing, PR China; ²State Key Laboratory of Materials-Oriented Chemical Engineering, Nanjing, P. R. China

Xiaodong Shen^{1,2}, affiliation and addresses: ¹College of Materials Science and Engineering, Nanjing Tech University, Nanjing, PR China; ²State Key Laboratory of Materials-Oriented Chemical Engineering, Nanjing, P. R. China

Email of the corresponding author: zyu@njtech.edu.cn

Keywords: Sulfate attack; Pore; Volcanic rock; Mechanical property; Length change.

Sulfate attack is one of the chemical mechanisms of concrete deterioration, which is highly related to the durability of concrete. It can cause expansion, crack and mechanical property degradation of concrete due to the formation of ettringite and gypsum. In order to improve the sulfate resistance of the cement-based materials, there are three main approaches, such as (1) by reducing the content of tricalcium aluminate (C_3A) in cement to decrease the formation of ettringite; (2) by decreasing the water to binder ratio to improve the compactness of the cement-based material and block the entry of external sulfate ions; (3) by adding a certain amount of supplementary cementitious material to reduce the amount of $Ca(OH)_2$ and produce more calcium silicate hydrate (C-S-H). However, the reduction of C_3A content does not prevent the degradation caused by gypsum type erosion. In the dense and narrow cement-based material structure, the formation and crystallization pressure of ettringite will be greater, resulting in greater expansion. The addition of supplementary cementitious material will introduce a large amount of aluminum phase and generate more ettringite.

In recent years, some researches state that the pore in the cement-based material plays a role in the resistance of sulfate attack. Our previous study also shows that the cement mortar made with coral sand (a kind of porous material) has better resistance to sulfate attack than that made with standard sand. The pore can provide additional space to accommodate the formation of ettringite and postpone the damage generated by ettringite. Volcanic rock is also a kind of porous material. It is igneous rock with high silica content. The chemical property of volcanic rock is stable. Therefore, the aim of this study is to investigate the properties of cement mortar made with volcanic rock under sulfate attack. During the experimental work, standard sand is partially replaced by volcanic rock, such as 0%, 20%, and 50%. The used water to cement ratio is designed as 0.6 since volcanic rock has a higher water absorption than standard sand. All mortar samples are cured under water for 28 days and then exposed to 5 wt% Na_2SO_4 solution. After a certain exposure time, the visual appearance, mechanical properties, length and mass change, phase composition and microstructure development of the cement mortar are investigated.

Current results show that the flexural strength of the mortar sample increases when 20% standard sand is replaced by volcanic rock. When 50% standard sand is replaced, the flexural strength of the mortar sample decreases slightly. The compressive strength of the mortar sample increases with the increase of volcanic rock from 20% to 50%. The surface of volcanic rock is rough and porous. Volcanic rock can be filled with a large amounts of C-S-H gel resulting in the improvement of the strength of mortar. During the exposure period to 120 days, the mass of

ICSBM 2023

3rd International Conference of Sustainable Building Materials

25-27 September, Wuhan, China

mortar increases continuously. It can be inferred that the formation of reaction products due to sulfate attack may continue to grow in the mortar.

Utilising Low Al/Si Materials Manufacturing Ternesite - Ye'elimite Cement and its Long-age Performance

Yangrui Li¹, Yanfei Yue^{1,*}, Yalun Yang¹, Wensheng Zhang², Yujie Fang¹, Jueshi Qian^{1,*}

1 College of Materials Science and Engineering, Chongqing University, Chongqing, 400044, China

2 State Key Laboratory of Green Building Materials, China Building Materials Academy, Beijing, 100024, China)

Email of the corresponding author: yanfei.yue@cqu.edu.cn, qianjueshi@163.com

Keywords: Ternesite-ye'elimite cement; Clinker; Low Al/Si material; Ternesite content; Long-age performance

Ternesite-ye'elimite cement (TYC) is the new cement that introduces ternesite ($C_5S_2\bar{S}$) into SAC system, and the main minerals in the cement clinker are ternesite and ye'elimite. Compared with belite sulfoaluminate cement, the formation temperature of ternesite is lower than that of belite, which can effectively reduce the sintering temperature of the cement and reduce the energy consumption of coal. The elements of ternesite are richer than belite, which can reduce the amount of limestone, and improve the utilization of solid waste raw materials. In addition, ternesite has higher hydration activity than belite in sulphoaluminate system, which is conducive to improving the performance of the cement. Therefore, TYC plays an important role in promoting the green, low carbon and high performance development of the cement and the utilization of solid waste resources, and has a broad application prospect in the field of building materials and solid waste. Although the preparation of TYC has been studied in the past, the proportion of ternesite in TYC was low. Ye'elimite still plays a dominant role in the hydration of TYC, and the high content of ye'elimite means that TYC still has a high demand for high-grade aluminum raw materials. This demand not only leads to the supply pressure of non-renewable natural resources, but also leads to the high production cost of TYC and huge resistance in the market application. Belite sulfoaluminate cement has grown rapidly because its clinker can utilize a wide range of industrial wastes as well as low-grade industrial raw materials. Theoretically, raw materials with low Al/Si ratio that can be calcined into belite sulfoaluminate cement clinker could also be used as raw materials for TYC. However, due to the low formation temperature of ternesite and the different raw materials used to prepare TYC may affect the firing of the cement clinker. Further studies are needed to expand the selection range of TYC raw materials, make more efficient use of low Al/Si ratio raw materials to design and burn TYC with adjustable ternesite content. Therefore, the effect of different calcination conditions on the firing of TYC clinker that prepared different amounts raw materials of low Al/Si ratio was investigated by designing four groups of TYC clinker with different ternesite contents. The influence of ternesite content on the long-age physical and mechanical properties was studied and hydration process of the cement was analysed via microscopic tests of hydration products. The results of the study show that TYC clinker with low Al/Si ratio raw materials was best prepared when mineralizers were added and the calcination temperature was 1150 °C. The content of ternesite in four groups of cement clinker were very close to the design content, among which the content of ternesite in T-67 cement clinker was 65.28 %, which meets the requirements of experimental design. The morphology of TYC clinker had different sizes, close packing degrees and overall porosity caused by different ternesite contents, which had certain effects on the cement hydration. With the increase of ternesite content in the cement, the initial-setting and final-setting time of the cement were prolonged, the compressive strength and the pH value decreased, due to its lower hydration velocity compared to ye'elimite. But the compressive strength and the pH value

ICSBM 2023

3rd International Conference of Sustainable Building Materials

25-27 September, Wuhan, China

showed a steady and sustainable growth of age, indicating that ternesite plays a key role on the long-term characteristics of TYC which could correct the strength fluctuation of ye'elinite especially at later age. In short, it is feasible to prepare TYC from raw materials with low Al/Si ratio.

Prediction of deformations of alkali-activated slag concrete under semi-adiabatic condition

Zhenming Li ¹, Department of Materials Science and Engineering, The University of Sheffield, Sheffield, United Kingdom

Chen Liu ², Department of Materials and Environment (Microlab), Faculty of Civil Engineering and Geoscience, Delft University of Technology, Delft, the Netherlands

Kangting Yin ³, College of Mechanics and Materials, Hohai University, Nanjing, China

Guang Ye ², Department of Materials and Environment (Microlab), Faculty of Civil Engineering and Geoscience, Delft University of Technology, Delft, the Netherlands

Email of the corresponding author: Zhenming.li@sheffield.ac.uk

Keywords: Thermal deformation; autogenous shrinkage; coefficient of thermal expansion; reaction heat; alkali-activated materials

Alkali-activated concrete has shown great potential to be used in civil engineering. Ground granulated blast furnace slag (hereinafter termed slag) is currently the most widely used precursor to make alkali-activated materials. Previous studies have revealed that alkali-activated slag concrete (AASC) shows large shrinkage under isothermal condition. In practice, however, concrete is usually serving under non-isothermal conditions due to the presence of reaction heat and changes in the environmental temperature. Hence not only autogenous and drying but also thermal deformations are involved. In literature, very little information is available regarding thermal deformation of AASC and its prediction.

In this paper, the deformation of AASC under semi-adiabatic condition is investigated and predicted as the sum of autogenous and thermal deformations (Eq. 1). The autogenous deformation of AASC is simulated, based on the experimental data obtained under isothermal condition with the consideration of equivalent age (Eq. 2). Arrhenius law was used to calculate the equivalent age based on temperature history (Eq. 3). The thermal deformation of AASC is simulated based on temperature history and coefficient of thermal expansion (CTE) measured with two Autogenous Deformation Testing Machines (ADTM) (Eq. 4).

The semi-adiabatic temperature history of the concrete was realized by the insulation of moulds of ADTM1. The moulds were made of 40 mm-thick foam plastics with a low coefficient of heat conductivity (0.03 J/(s·m·K)), around two-order lower than that of normal weight aggregate concrete. The temperature of concrete was measured by thermocouples located in the center of the concrete specimen. The CTE of the concrete was measured by ADTM2. In most of the time, the temperature of concrete in ADTM2 was kept the same as that in ADTM1. At certain ages, however, the temperature of concrete in ADTM2 was manually changed by 1 °C. The corresponding deformation during the small temperature change was recorded to obtain the CTE.

$$\varepsilon_{tot} = \varepsilon_{au} + \varepsilon_{th} \quad (1)$$

where ε_{au} and ε_{th} is the autogenous and thermal deformation, respectively.

$$\varepsilon_{au,semi}(t) = \varepsilon_{au,iso}(t_{eq}) \quad (2)$$

where $\varepsilon_{au,semi}$ and $\varepsilon_{au,iso}$ is the autogenous shrinkage under semi-adiabatic condition and

isothermal condition at 20 °C, respectively. t_{eq} is the equivalent age.

$$t_{eq}(T) = \int_0^t \exp\left(-\frac{E_a}{R} \cdot \left(\frac{1}{T(\tau)} - \frac{1}{T_{ref}}\right)\right) \cdot d\tau \quad (3)$$

where T is the temperature history under semi-adiabatic condition. E_a is the apparent activation energy. R is the universal gas constant, 8.314 J/(K·mol). T_{ref} is the reference temperature, 20 °C, i.e. 293 K.

$$\varepsilon_{th}(t) = \sum_{k=1}^n \alpha_{CTE}(k) \cdot \Delta T(k) \quad (4)$$

where ε_{th} is the thermal deformation. α_{CTE} is the CTE. ΔT is the temperature change of the concrete.

The CTE evolution of AASC is shown in Figure 1. The CTE first decreased along with the hardening of the concrete then gradually increased with time. This can be explained by the self-desiccation process which leads to a lower internal relative humidity of the concrete. Despite the fluctuation of the curve, the two-stage evolution of CTE is in line with the results of previous studies on Portland cement (PC) paste or concrete. It can also be seen that AASC shows higher CTE than PC systems, the CTE of which normally falls in the range of 5-13×10⁻⁶/°C. This information is worthy consideration for the establishment of model codes for AASC in future.

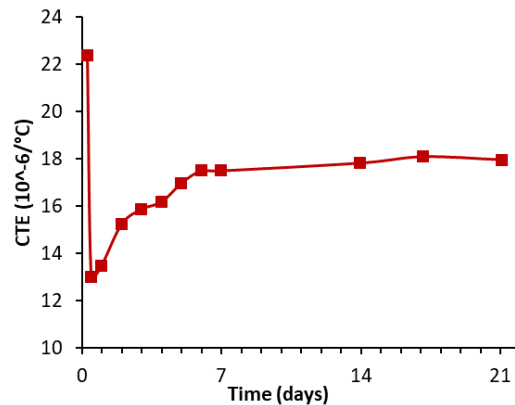


Figure 1. CTE of AASC.

The predicted deformations of AASC are shown in Figure 2 (left). The comparison between predicted and measured total deformations of AASC is shown in Figure 2 (right). It can be seen that the prediction agrees pretty well with the experimental result. In the first day, there is a small discrepancy between the two curves, as shown in the panel in Figure 2 (right). This might result from the small number of data points obtained for some inputs in the very early age. For example, as shown in Figure. 1, the CTE of concrete changed significantly in the first 2d, but only 4 points were measured in this period. Within each time interval, the CTE was assumed as a constant, which can lead to simulation error in the thermal deformation. Besides, in the prediction of autogenous shrinkage (Eq. 2), the apparent activation energy was taken as 57.6 KJ/mol from the literature. On one hand, this value can vary with mixture design, hence, the activation energy of the AASC studied here may be different. On the other hand, this value changes with the reaction degree. Therefore, the assumption of the activation energy as constant can lead to error in simulating autogenous shrinkage. Last but not the least, the coupled effects of autogenous and thermal deformation, e.g., the influence of temperature variations on capillary tension, were not considered in the simulation. Despite, the general agreement between the simulated and measured results indicates the validity of the simulation approach used in this study.

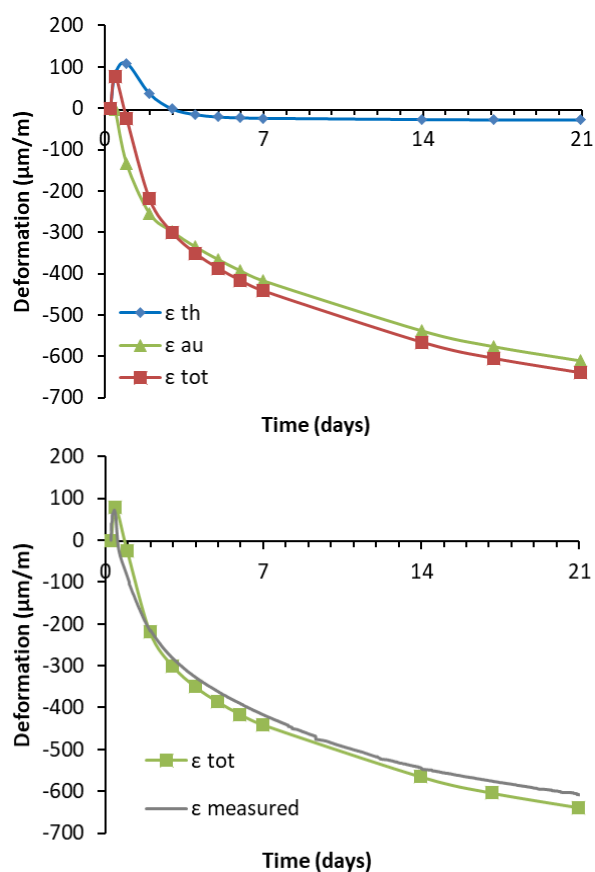


Figure 2. Simulated autogenous, thermal and total deformations of AASC under semi-adiabatic condition (left). Comparison between the simulated and measured total deformation of AASC (right).

In this study, the deformation of AASC is simulated as the sum of autogenous and thermal deformations. The thermal deformation of the concrete is calculated based on the semi-adiabatic temperature evolution and measured CTE of the concrete. The good agreement between the simulated and measured deformations indicate the feasibility of the approach used. The results on CTE and thermal deformation of AASC can be useful for structural design of this concrete.

Study on Polyaluminum Regulates Hydration Reaction and Durability of Slag-Portland Cement Material

Li Zonggang, School of Materials Science and Engineering, Wuhan University of Technology, Wuhan, China

Li Bo, State Key Laboratory of Silicate Materials for Architectures, Wuhan University of Technology, Wuhan, China

Chen Wei, State Key Laboratory of Silicate Materials for Architectures, Wuhan University of Technology, Wuhan, China

Email of the corresponding author: chen.wei@whut.edu.cn

Keywords: Polyaluminum; hydration reaction; microstructure; durability; micromechanical properties

Silico-aluminum vitreous body is the main component of many industrial wastes represented by slag. It has potential hydraulic properties and can undergo hydration and hardening reactions when the excitation conditions are reached. Current research has found that Keggin-Al13 can be hydrolyzed to form penta-coordinated aluminum ions. By changing the ion migration and penetration capacity of the IP C-A-S-H hydration product layer on the surface of the silica-alumina vitreous particles, the degree of hydration can be improved. Existing research results are mainly the effect of polyaluminum chloride (PAC) on the macroscopic properties of 60wt% slag blended slag portland cement and the alkali slag system. PAC contains more chloride ions and is not suitable for reinforced concrete. From the perspective of practical engineering applications, the durability of slag-silicate materials is very important. These aspects need to be studied.

Based on the theory that Keggin-Al13 can promote the hydration of silico-aluminous vitreous body, polyaluminum sulfate (PAS) and polyaluminum chloride are used as the control modification materials. The influence of two kinds of polyaluminum with different amounts of 40wt%, 60wt%, 80wt% slag doped slag Portland cement materials on working performance, mechanical properties, density and micro-mechanism of hydration were studied. Combined with the research content and the practical application of the project, the ability of two kinds of polyaluminum with different dosages to its chloride permeability and the carbonization resistance of 60% by weight slag cementitious materials was studied. Finally, the microscopic mechanical properties of the modified slurry were studied.

The specific research contents of the paper is as follows:

(1) The paper studies the effect of two kinds of polyaluminum with different content on the working performance and mechanical properties of slag-silicate cement paste with different content of slag. It was found that the two polyaluminums can increase the standard consistency water consumption of the cementitious materials under different slag content, and the increase effect is proportional to the polyaluminum content. The fluidity, initial and final setting time of the modified slurry and the polyaluminum content is inversely proportional. When the content of polyaluminum sulfate is too high, the fluidity of the slurry basically disappears. Both types of polyaluminum have improved the compressive strength of the test blocks with different amounts of slag content, and the modification effect of polyaluminum sulfate is better. After modified with aluminum in each slag content, the porosity change of the sample is inversely proportional to the strength change.

(2) The hydration micro-mechanism of the modified slurry was studied, and it was found that the two types of polyaluminum did not change the type of hydration products in the slurry, but the addition of polyaluminum could promote the hydration of slag particles and dissolve magnesium ions, Aluminum ions, calcium ions, etc. further promote the transformation of calcium hydroxide

ICSBM 2023

3rd International Conference of Sustainable Building Materials

25-27 September, Wuhan, China

phase, AFm phase, hydrotalcite phase to C-A-S-H gel and other materials in the entire gelling system, making the material more compact. After PAS is incorporated, the nano-hardness and elastic modulus of the material are improved, the calcium-silicon ratio of the material is increased, and the calcium-aluminum ratio of the material is reduced.

(3) The incorporation of polyaluminum sulfate can improve the combination of the hardened mortar density and the mortar binding ability, thereby enhancing the carbonization resistance and its chloride permeability of modified mortar with 60% by weight slag. Polyaluminum chloride has no promoting effect on the material's chloride permeability, and it has a negative effect when the amount is too high, but it can improve the material's resistance to carbonization to a certain extent.

A Mini Temperature Stress Testing Machine for Assessing Early-Age Cracking Potentials of Cementitious Materials

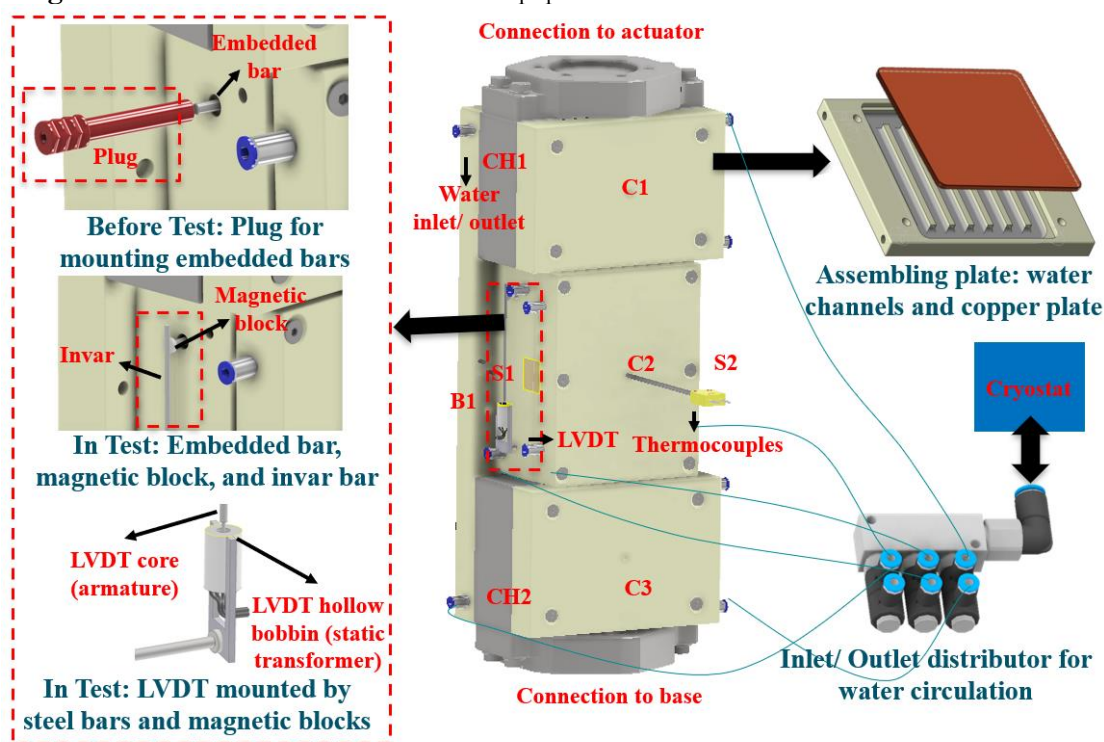
Minfei Liang^{1*}, Erik Schlangen¹, and Branko Šavija¹

¹MicroLab, Faculty of Civil Engineering and Geosciences, Delft University of Technology, Delft, 2628 CN, The Netherlands

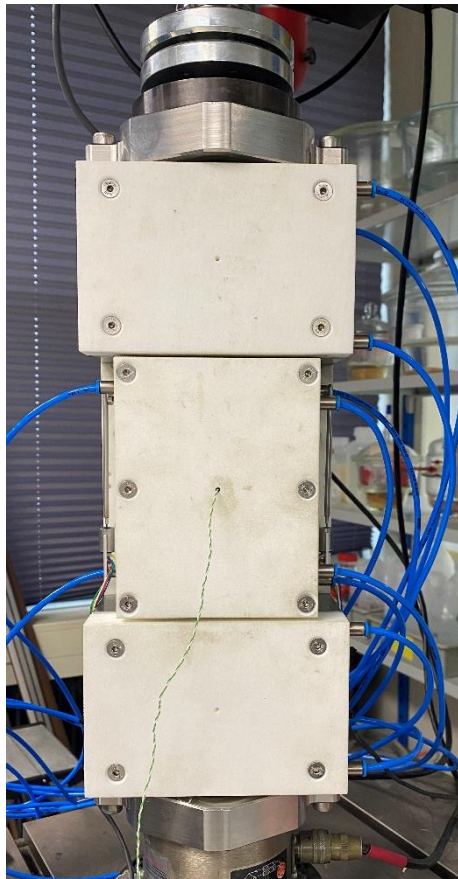
Email of the corresponding author: M.Liang-1@tudelft.nl

Keywords: Early-age cracking, Temperature Stress Testing Machine, Elastic modulus, Autogenous deformation, Creep/ Relaxation.

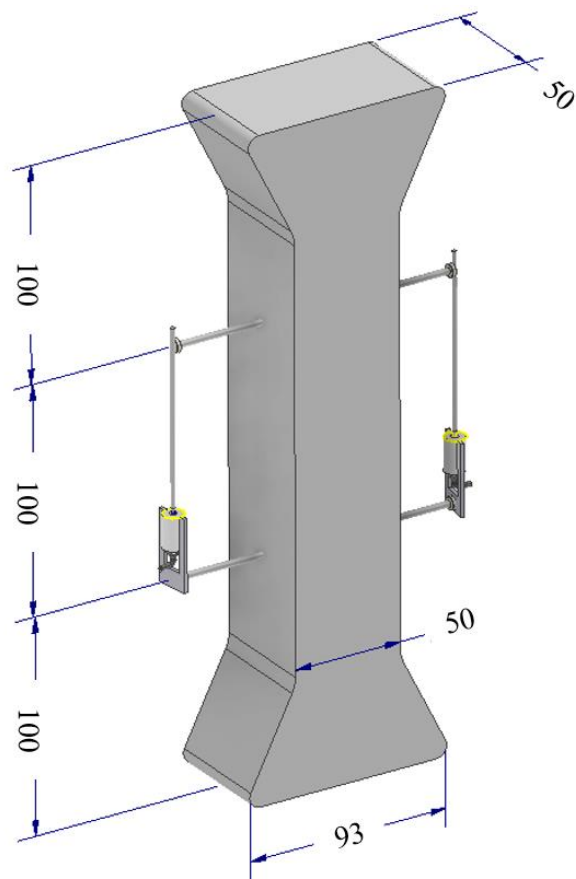
In the development of novel sustainable construction materials, early age cracking (EAC) is an important issue that needs to be properly addressed before its engineering application. Temperature Stress Testing Machine (TSTM) is a versatile tool for measuring various early-age properties and behaviors of cementitious materials, but investigating the EAC problem with traditional TSTM may encounter some problems of efficiency brought by the complexity of testing systems. In this paper, a Mini-TSTM is developed to efficiently test the behaviors and properties of sustainable cementitious materials related to EAC. The developed Mini-TSTM addressed several issues that occurred in classical TSTM tests: the effort needed to set up and execute the experiment, continuous control for full-restrained conditions, and the influence of friction. The design, implementation, and methods of the new setup and experiments are shown in Fig.1 and will be introduced in detail in the paper.



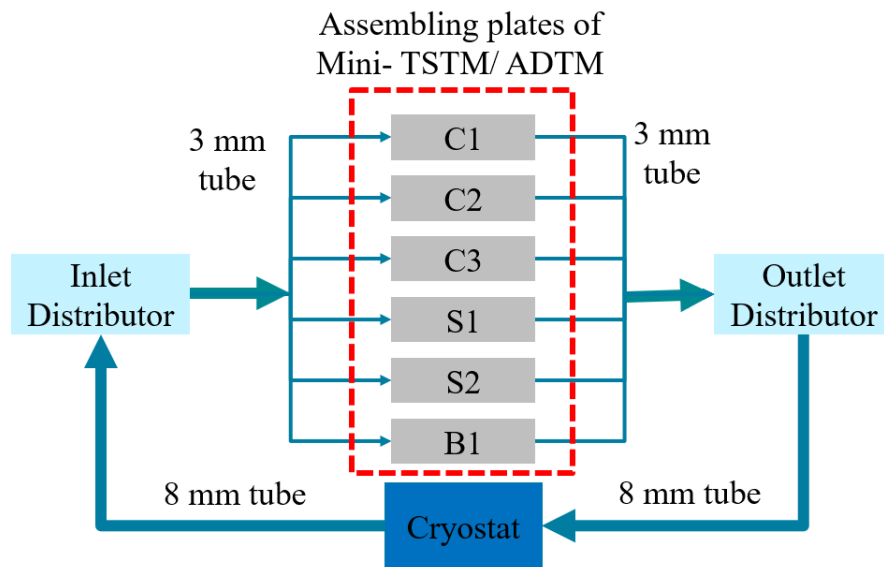
(a)



(b)



(c)



(d)

Fig. 1 The mini-TSTM: (a) overall design; (b) the efficient TSTM installed in the loading machine; (c) geometry of the dog-bone specimen (unit: mm); (d) parallel connection of water circulation system.

A systematic validation scheme, from the perspective of experiments and theories, was devised to examine the reasonability of the proposed setup. The developed setup obtained reasonable testing results on early age stress (EAS), autogenous deformation, elastic modulus, creep, and

coefficient of thermal expansion (CTE) of CEM III/B and CEM I paste using different testing methods. The repeatability of the developed testing method was verified using the same batch of CEM III/B cement. A viscoelastic model was developed and could accurately predict the EAS based on the input of autogenous deformation, elastic modulus, and creep, which allowed a theoretical validation of the developed setup and testing methods. The viscoelastic model explained the variation in early autogenous deformation due to different cement batches does not significantly influence the EAS results. The above testing and modeling results together validate the developed Mini-TSTM and Mini-ADTM setup. Specifically, this paper leads to the following findings:

- 1) The Mini Autogenous Deformation Testing Machine (Mini-ADTM) and Mini-TSTM, made mainly by 3D printing techniques, improved the testing efficiency and addressed several issues in big TSTM tests, including the difficulty in pre-test installation and post-test disassembling, continuous control for full-restraint condition, LVDT installation, and friction between the specimen and supporting table.
- 2) The Mini-ADTM and Mini-TSTM showed good consistency in the EAS test. The expanding/shrinking process detected by the Mini-ADTM matched well with the stress decreasing (compression)/ increasing (tension) detected by the Mini-TSTM. The influence of cement type and w/b ratios on EAC potentials were correctly reflected. The heating/ cooling efficiency of the proposed setup was examined in a CTE test, which obtained reasonable results compared with existing studies.
- 3) The Mini-ADTM and Mini-TSTM showed good repeatability. In EAS tests of CEM I, all mixes obtained similar EAS despite a significant difference found in the measurement of early chemical shrinkage and autogenous expansion. In EAS tests of CEM III/B, the results also showed good repeatability in the measurement of both autogenous deformation and EAS.
- 4) The Mini-ADTM and Mini-TSTM found that batch difference of CEM III/B mix with a low w/b ratio (0.30 in this study) can result in a completely different EAC potential. In some cases, the autogenous expansion that typically happens in high-volume slag cement concrete does not occur, while the onset of autogenous shrinkage is significantly earlier which can lead to higher EAC risk.
- 5) The measured autogenous deformation, elastic modulus, and creep can be used as the input of a viscoelastic model to predict the EAS with good accuracy, which validated that the proposed setup correctly simulated and measured the process of EAS evolution. By comparing the results of the viscoelastic model and elastic model, it is found that in some cases neglecting viscoelastic behavior will be conservative and result in a lower risk for EAC, but in other cases, the opposite will happen and the risk for EAC will increase. Simulating the EAS evolution of one batch of CEM III/B based on the elastic modulus and creep data measured on another batch of CEM III/B shows good accuracy. The same holds for CEM I mixes.
- 6) It was shown quantitatively (i.e., using the viscoelastic model) that the lower elastic modulus and relaxation are the reasons that the initial chemical shrinkage and autogenous expansion at an early age played a much less significant role in stress development than autogenous shrinkage afterward.
- 7) In real application stresses will increase further due to thermal stresses which should be added to the stress resulting from autogenous shrinkage. The Mini TSTM and Mini ADTM are ready for investigating this in the near future.

Effects of calcined phosphogypsum replacement on hydration and properties of calcium sulfoaluminate cement at different curing temperatures

Yishun Liao^{1,2,3,*}, Jinxin Yao¹, Kejin Wang⁴, Haoran Huang¹, Guoxi Jang¹, Shengwen Tang⁵, Yibing Zuo⁶

1: School of Urban Construction, Wuhan University of Science and Technology, Wuhan 430065, China

2: Hubei Provincial Engineering Research Center of Urban Regeneration, Wuhan 430065, China

3: Institute of High Performance Engineering Structure, Wuhan University of Science and Technology, Wuhan 430065, China

4: Department of Civil, Construction, and Environmental Engineering, Iowa State University, Ames, IA 50011, USA

5: State Key Laboratory of Water Resources and Hydropower Engineering Science, Wuhan University, Wuhan 430072, China

6: School of Civil and Hydraulic Engineering, Huazhong University of Science and Technology, Wuhan 430074, China

Email of the corresponding author: Liaoyishun@wust.edu.cn

Keywords: Calcium sulfoaluminate cement; Calcined phosphogypsum; Hydration products; Hydration kinetics; Thermodynamic modelling.

The effects of calcined phosphogypsum (CPG) dosage on the heat of hydration, electrical resistivity, hydration products, and bound water content of calcium sulfoaluminate (CSA) cement pastes were investigated at curing temperatures of 20° C, 35° C, and 50°C. Hydration kinetics was studied to elucidate the hydration mechanism, and thermodynamic modelling was performed to predict the phase assemblages. Calorimetry tests indicate that CSA cement hydrates faster at higher temperatures, with the amount of CPG playing a significant role in accelerating hydration. Electrical resistivity tests show that the early hydration of the cement pastes is accelerated, and the time interval between the induction period and the acceleration period is shortened at 50°C. Porosity becomes the dominant factor determining electrical resistivity during later stages of hydration. Elevated temperatures result in the heterogeneous distribution of hydration products, leading to a loose structure and decreased electrical resistivity. X-ray diffraction (XRD) analyses reveal that the addition of CPG promotes the hydration of ye'elimite in CSA cement pastes. Higher temperatures accelerate the hydration process and the consumption of ye'elimite and CPG. The presence of sufficient gypsum enhances the formation of AFt. Measurements of bound water content indicate that the addition of CPG accelerates the hydration process and influences the formation of different hydration products. Higher temperatures promote the formation of AFm, while the presence of CPG inhibits the decomposition of AFt. The compressive strength of CSA cement pastes is influenced by curing temperature and CPG content. At 6 h, the addition of CPG significantly increases the compressive strength at 35°C and 50°C compared to 20°C. At elevated temperatures, CPG is rapidly consumed, and hydration products are generated quickly, resulting in a loose structure and strength loss during later stages of hydration. However, an appropriate increase in CPG content under high temperatures can effectively counteract the adverse effects of AFt decomposition caused by insufficient CPG

ICSBM 2023

3rd International Conference of Sustainable Building Materials
25-27 September, Wuhan, China

content in the late stage of cement paste formation. Excessive AFt formation in sample during curing at 35°C for three days results in cracking due to expansion. This significantly compromises the compressive strength of the sample. However, at 50°C, a transformation of some AFt into AFm occurs, preventing excessive AFt formation and mitigating the risk of cracking, contributing to improved structural integrity in the sample. At 50°C, the growth rate and nucleation rate of CSA cement significantly increase compared to 20°C. The addition of CPG accelerates the nucleation rate of hydration products in CSA cement paste at 35°C and 50°C. This acceleration can be attributed to the elevated temperature, which increases the rate of ion release from CSA clinker and CPG, thereby modifying the hydration kinetics of the cement paste during high-temperature curing conditions. The thermodynamic modeling provides a reasonable assessment of the evolution of hydration products in the CSA clinker mixed with CPG system, with the ettringite content obtained from the model closely matching experimental results. In summary, the incorporation of CPG in CSA cement pastes influences the hydration process, hydration products, and compressive strength. Higher curing temperatures accelerate the hydration process and the consumption of CPG and ye'elinite. The addition of CPG improves the compressive strength at elevated temperatures, but excessive AFt formation can lead to cracking. The study also highlights the importance of thermodynamic modeling in predicting the phase assemblages of CSA cement mixed with CPG.

Effects of glass bubbles on the radiative cooling performance of cementitious cooling composites and its carbonation behavior: the role of content, size, and pre-crush

Daoru Liu, Department of the Built Environment, Eindhoven University of Technology, Eindhoven 5600 MB, the Netherlands

H.J.H. Brouwers, Department of the Built Environment, Eindhoven University of Technology, Eindhoven 5600 MB, the Netherlands.

Qingliang Yu, ¹School of Civil Engineering, Wuhan University, Wuhan 430072, China; ²Department of the Built Environment, Eindhoven University of Technology, Eindhoven 5600 MB, the Netherlands

Email of the corresponding author: q.yu@bwk.tue.nl (Q. Yu)

Keywords: refractive interface, scattering, surface topology, optical properties,

Cement, being the most widely used artificial material, contributes significantly to energy consumption and carbon emissions, contradicting the United Nations' sustainable development goals. In addition to exploring low-carbon alternative binders, another promising approach to reducing the life-cycle embodied energy consumption and carbon emissions is through the functionalization of cementitious materials. For example, designing cementitious coolers to combat heatwaves and reduce building cooling energy consumption can contribute to the sustainability of the cement industry.

Radiative cooling, an energy-free and carbon-neutral cooling method, has emerged as a potential solution to address climate change and achieve carbon neutrality. Effective radiative cooling requires high solar spectral reflectivity (R_{sun} , $\lambda \sim 0.3\text{-}2.5 \mu\text{m}$) and spectral emissivity at the atmospheric window (ϵ_{atm} , $\lambda \sim 8\text{-}13 \mu\text{m}$). Organic polymers such as PTFE, P(VdF-HFP), and cellulose are commonly used in the preparation of organic radiative coolers due to their controllable microstructure (particularly pore structure) and the presence of strong mid-infrared absorption-capable C-C, C-O, and C-F bonds. Additionally, various nano/micro refractive indexes, such as humps, gullies (fibers), pores, and their combinations, are incorporated to enhance scattering and achieve high R_{sun} . In contrast to polymer-based radiative coolers (coatings, films, and textiles), the preparation of inorganic cementitious cooling composites eliminates the need for toxic organic solvents and sophisticated facilities. Furthermore, inorganic coolers exhibit enhanced durability compared to organic ones, particularly in terms of ultraviolet resistance.

While the role of glass bubbles as an important component in enhancing the cooling performance of coatings/paints/films has been investigated, their impact on the cooling performance of cementitious materials remains unexplored. The high alkalinity of cementitious systems could potentially decompose soda-lime-borosilicate ($\text{Na}_2\text{O}/\text{CaO}/\text{K}_2\text{O}-\text{B}_2\text{O}_3-\text{SiO}_2$) glass bubbles, unlike the natural environment of these composites. This decomposition could affect the properties of both cementitious materials and glass bubbles, subsequently influencing the cooling performance of cementitious coolers. According to the Mie theory, the size of glass bubbles can also influence the scattering efficiency and radiative cooling performance. Additionally, a study by Yu et al. demonstrated that broken glass bubbles can improve the solar reflectivity of glass bubble-P(VdF-HFP)-based paints from approximately 93% to over 97% by enhancing scattering performance. However, crushed glass bubbles are expected to exhibit higher reactivity due to increased surface area. Moreover, the significant density differences between glass bubbles and cement constituents may cause stratification during mixing, casting, and early-stage hydration, resulting in anisotropy, particularly on the top and bottom surfaces of the final cementitious coolers. The behavior of crushed glass bubble fragments in cementitious systems may differ from that of intact glass bubbles. Lastly, the high-volume addition of glass

ICSBM 2023

3rd International Conference of Sustainable Building Materials

25-27 September, Wuhan, China

bubbles could potentially affect evaporative cooling performance due to the compact structure of glass bubbles.

In summary, several knowledge gaps exist regarding the engineering practice of glass bubbles in cementitious coolers. Therefore, to advance the sustainability of the cement industry and buildings, this study aims to investigate the impact of glass bubbles (size, content, and pre-crushing) on the cooling performance (radiative + evaporative) of cementitious coolers. UV-VIS-NIR spectrophotometer and FTIR spectroscopy equipped with integrating spheres are used to obtain the solar reflection spectra and mid-infrared emissivity spectra. 3D microtomography (μ CT) and scanning electron microscopy (SEM) are used to characterize the microstructure. Finite-difference time-domain (FDTD) simulation is conducted to investigate the scattering behaviors of different surface topologies obtained by the 3D Optical Profiler. Finally, outdoor measurement is performed to validate the on-site cooling performance of as-prepared inorganic coolers.

Influences of carbonate sources on the performance of calcium carbonate-metakaolin- cement composites

Gang Liu, School of Human Settlements and Civil Engineering, Xi'an Jiaotong University, Xi'an, 710049, P.R. China

Keywords: blended cement, calcium carbonate, wet carbonation, performance evaluation, sustainability

Limestone powder is a traditional natural calcium carbonate source, and it has been used in various cement concrete production. The role of limestone on hydration properties, fresh behaviour and engineering performances of OPC-based composites has been intensively investigated. For the purpose of CO₂ sequestration and calcium silicate base wastes valorization, pre-carbonation treatment can effectively improve the properties of related solid wastes. The produced carbonated powder could be the promising alternative to limestone powder in ternary binder systems. Four different carbonated powders were prepared from waste cement pastes, BOF slag, magnetically separated steel slag, and magnesium slag by wet-carbonation, respectively. The carbonated powder was applied as a calcium carbonate source in calcium carbonate (15%)-metakaolin (30%)-cement (55%) composites to fully replace natural limestone powder. The fresh behaviour, reaction kinetics, reaction products, mechanical performance, and microstructure properties of composites were tested and the influences of carbonate sources were discussed. The results will contribute to the high-end application of calcium silicate-based wastes in sustainable building materials.

The Mechanism of Microwave Curing for Ultra-high Performance Concrete

Yidi Liu, School of Civil Engineering and Transportation, Northeast Forestry University, Harbin 150060, China

Shuangxin Li*, School of Civil Engineering and Transportation, Northeast Forestry University, Harbin 150060, China

Email of the corresponding author: lxs190034@nefu.edu.cn

Keywords: response surface method; microwave curing; ultra-high performance concrete; compressive strength; microstructural characteristics;

Ultra-high performance concrete (UHPC) has high strength and high durability, the application of which benefits for extending the service life of building structures and promoting the sustainability development of whole construction industry. However, basic UHPC demands a high cement content, and the hydration extent of cement lower than 50%, and the tremendous residential cementitious materials only play a filling role. In order to make full use of cement and further improve the performance of UHPC, it is necessary to promote the full hydration of residential cement. Microwave curing has a significant accelerating effect on cement hydration, and it has been found that a proper microwave curing system can improve the utilization of cementitious materials in UHPC, therefore, the application of microwave curing on producing UHPC can decarbonize UHPC through reducing the energy demand and cement usage. But many findings on the effects of microwave curing on concrete are not consistent because there is a lack of the knowledge on microwave curing regimes on curing effects. Then, it is difficult to clarify the role of microwaves in the stages of cement hydration and concrete hardening, so that the microwave curing regimes used in the various studies vary widely and lack systematic rules. The view that microwave curing has the effect of enhancing the early strength of concrete has been supported by different scholars, but whether microwave curing affects the long-term strength of concrete is a controversial issue among different scholars. In this study, after a detailed literature research and preliminary studies, it is summarized that three single-factor preferred ranges of heating power, microwave curing duration, and curing temperature under microwave curing conditions have an effect on the strength of concrete. This study selected the range of values for the curing temperature from 40 to 100 °C, the range of values for the heating power from 300 to 2000 W, and the range of values for the microwave curing duration from 30 to 180 min. Using the Box-Benhen design method with heating power, microwave curing duration and curing temperature as independent variables, and 1 d compressive strength, 7 d compressive strength and 28 d compressive strength as dependent variables, a response surface regression model was set up to investigate the effects of the three factors and their interactions on the indicators of 1 d, 7 d and 28 d compressive strength of concrete, respectively. The optimal concrete curing system was determined by the response surface method and the reliability of the model was verified by experiments. The microstructural properties of the specimens under standard curing conditions and under the optimal microwave curing regime were investigated by nanoindentation, and the internal densities and products of the concrete at 28 d under the optimal curing regime were further investigated by using the SEM method in combination with the XRD method. Response surface method was used in this study to seek the optimal parameters and optimal parameter combinations based on the regression equations of the functional relationship between the three fitting factors of curing temperature, heating power and microwave curing duration and the compressive strength response values using experimental data. The data show that, among the microwave process parameters, the effect of microwave curing time is significant, and the effect of heating power and curing temperature is less significant. The optimum heating power was found to better not exceed 1850 W, the compressive

ICSBM 2023

3rd International Conference of Sustainable Building Materials

25-27 September, Wuhan, China

strength increases with the increase of microwave curing time, but when the microwave curing time reaches about 120 min, the compressive strength no longer increases with the extension of microwave curing time. The effect of curing temperature is small and must not be higher than 100 °C, but in the case of curing time and heating power fixed, the compressive strength increases with the rise of curing temperature. The 28 d compressive strength of microwave cured specimens under the optimal microwave curing system was slightly higher than the 28 d compressive strength of standard cured specimens, which proved that microwave curing under reasonable curing conditions would not affect the late strength development of UHPC. According to the nanoindentation technique, under the optimal curing regime, the internal part of UHPC is denser and the microstructure is better developed, and the hydration products fill the initial microcracks to a certain extent; under the standard curing regime, the hydration products are not sufficient to fill the microcracks resulting in relatively loose specimens, and thus the mechanical properties are affected. According to the analysis of SEM and XRD method, the hydration reaction of 28 d UHPC under the optimal curing condition was more sufficient, and the large amount of C-S-H gel generated filled the internal microcracks to make the structure denser, and the macroscopic results were consistent.

Assessing the feasibility of partially replacing Portland cement with calcined Dutch clay

Z. Liu, Department of the Built Environment, Eindhoven University of Technology, De Zaale 11, 5600 MB, Eindhoven, the Netherlands

K. Schollbach, Department of the Built Environment, Eindhoven University of Technology, De Zaale 11, 5600 MB, Eindhoven, the Netherlands

H.J.H. Brouwers, Department of the Built Environment, Eindhoven University of Technology, De Zaale 11, 5600 MB, Eindhoven, the Netherlands

Email of the corresponding author: K.Schollbach@tue.nl

Keywords: low-grade Dutch clays; economic efficiency; pozzolanic activity; supplementary cementitious material; pozzolan.

Portland cement is a widely used construction material with high embodied CO₂. A considerable amount of CO₂ emission during the cement production process is associated with the calcination of calcium carbonate, which could be reduced by replacing clinker with supplementary cementing materials (SCMs) in blended cement. Commonly used SCMs such as fly ash, silica fume, and blast furnace slag have limitations in their production and availability and cannot meet the growing demands of the construction industry. As a result, the need for new sources of SCMs to reduce CO₂ emissions from concrete is great. Clays are abundantly available sources that could extend the use of SCMs in blended cement. Generally, clays are classified according to their internal structure as 1:1 (e.g., kaolinite; halloysite) or 2:1 (e.g., illite; montmorillonite; pyrophyllite) clay minerals and consist primarily of mineral particles with a particle size of fewer than 20 μm. Calcined clays are thermally activated clays that had been dehydroxylated in the temperature range of 650–850 °C, it is possible to obtain pozzolanic reactivity. The reactivity of calcined clay is strongly related to its metakaolin content. There have been numerous previous studies on the use of pure metakaolin, but moderate and low-grade kaolinitic clays have great economic and engineering potential to produce calcined clays with proper pozzolanic activity. Clay is a common lithology in the Dutch shallow subsurface. It is used in earth constructions such as dikes and as raw material for the fabrication of bricks, roof tiles, etc. In addition, clay with pure kaolinite in the Netherlands is not available, and there is almost no medium or low-grade kaolinitic clays. In recent years, researchers have made some explorations on the application of low-grade clay in cement-based materials. Although most studies define the quality of clay based on the content of kaolinite, there is no clear definition of the boundaries between “high-grade” and “low-grade” clays. It is clear to show that clay with a kaolinite content of less than 40% is usually considered “low-grade clay”, and the calcination temperature used is basically between 700 and 900 °C. Up to now, only a few studies have explored the feasibility of using clay with a kaolinite content of around 30% as SCMs. Therefore, it is worthwhile to explore the suitable cement replacement level with low-grade clay. In this work, the suitability of several low-kaolinitic Dutch clays as SCMs is investigated. X-Ray Fluorescence (XRF), Thermogravimetric analysis (TGA), Particle Size Distribution (PSD), BET nitrogen adsorption analysis (BET), X-ray diffraction (XRD), and Fourier transform infrared spectrometer (FT-IR) was used to analyse the characterization of raw clays. The pozzolanic reactivity of the activated clays was determined using the bound water method specified in the ASTM C1897 (also known as the R³ test). And the strength activity index (SAI) method and the relative strength index (RSI) method were used to determine the effective replacement level. To get a clearer picture of the real benefits of using mortar with low-grade calcined Dutch clays, a classical method called TOPSIS (a technique for order performance by similarity to ideal solution) is used to consider the compressive strength, strength activity index, kaolinite content, CO₂ emission, and cost of

ICSBM 2023

3rd International Conference of Sustainable Building Materials

25-27 September, Wuhan, China

the samples. The results show that the optimal cement replacement level is 20 wt.%. Iron oxide is the main colorant in the clay materials. The color development of calcined Dutch clays is mostly depending on the oxidation state of the iron oxide present in the original clay and the phases in which iron occurs in the clay and its susceptibility to oxidation and reduction reactions. In addition, it seems possible to partially replace Portland cement with calcined Dutch clay with 20 wt.%, which would be very beneficial in reducing the production costs of using low-grade Dutch clay for applications in large scale construction projects.

Enhancing Mechanical Properties of Portland Cement with Blending CO₂-intermixed High Belite Calcium Sulfoaluminate Cement

Shuang Luo¹, Tung-Chai Ling^{1,*}

¹College of Civil Engineering, Hunan University, Changsha 410082, China

Email of the corresponding author: tcling@hnu.edu.cn; tcling611@yahoo.com

Keywords: Intermixing of CO₂, high belite calcium sulfoaluminate cement, compressive strength, reaction mechanism

Intermixing CO₂ during the mixing process (CO₂-intermixed) of ordinary Portland cement (OPC) is a feasible way in enhancing its early mechanical properties by promoting the hydration reaction of calcium silicate phases. However, the intermixed CO₂ dose is generally limited to less than 0.3% by weight of cement due to the slow reaction rate between CO₂ and tricalcium silicate (C₃S) during the short mixing process. Moreover, excessive carbonation products, such as calcium carbonate (CaCO₃), precipitated on the cement clinker's surface can reduce the active area, leading to a significant reduction in long-term strength. High belite sulfoaluminate cement (BCSA), one of the low-carbon alternative binders to cement, possesses more rapid hydration reaction rate and highly reactive with CO₂, is expected to exhibit more advantages in both CO₂ sequestration capacity and long-term mechanical properties.

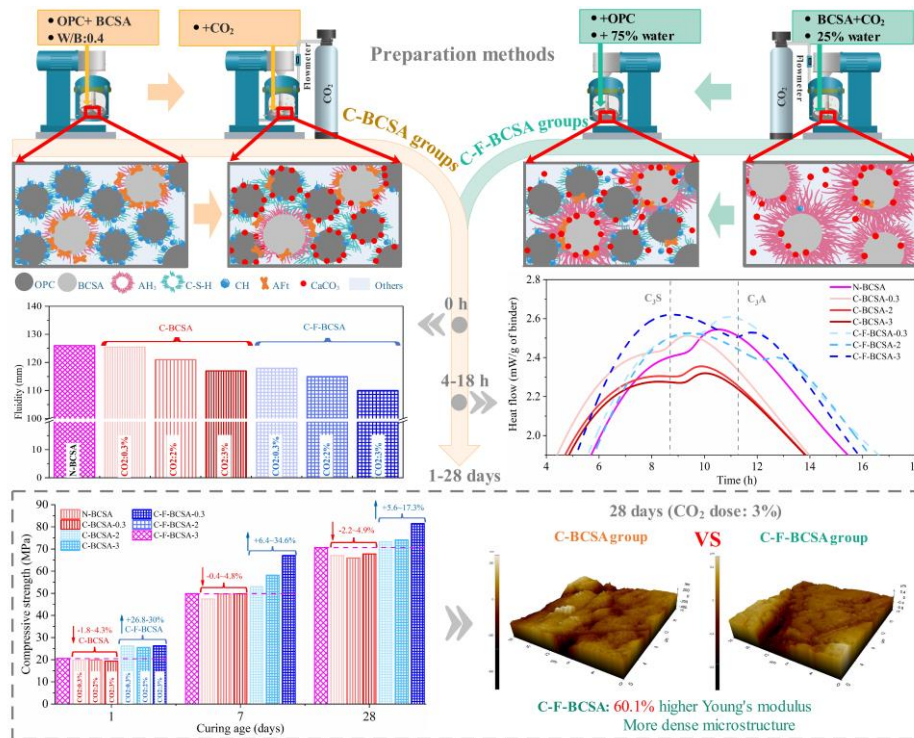
This study aims to propose a novel CO₂ intermixing approach by incorporating CO₂-intermixed BCSA paste with OPC paste. The BCSA/OPC ratio and final water-to-binder (W/B) ratio were fixed at 1/9 and 0.4 respectively. Two preparation methods were investigated in this study. The first method comprised the initial mixing of all binders (BCSA and OPC) with water, followed by the intermixing of CO₂ during mixing process. Samples prepared by this method were denoted as C-BCSA. In the second method, BCSA was initially mixed with a portion of water and then intermixed with CO₂. Subsequently, OPC and the remaining water were added and mixed to result in carbonated blended mixtures (C-F-BCSA). For comparison, non-carbonated BCSA blended OPC paste with W/B 0.4 were also prepared (denoted as N-BCSA). The characteristics of reaction products and hydration development of BCSA blended OPC paste were analysed using particle size distribution (PSD) analysis, Fourier transform infrared spectroscopy (FTIR), X-ray diffraction (XRD), isothermal calorimetry, and atomic force microscope (AFM). Additionally, the flowability and compressive strength of BCSA blended OPC pastes were examined.

The results show a significant amount of CaCO₃ formed in the C-BCSA groups due to the reaction between CO₂ and ettringite. This facilitated the generation of more aluminum hydroxide (AH₃) gel, which increased the specific surface area of the cement particles and viscosity of the mixture. The flowability of the C-F-BCSA groups was also found to be lower than that of C-BCSA groups. After 4-18 hours, all C-BCSA groups exhibited a similar exothermic pattern to that of N-BCSA groups, with the peak of C₃A being higher than that of C₃S but at lower values. However, the peak exothermic intensity decreased with the increase of CO₂ doses, attributed to the reduction of the reactive surface area of calcium silicate minerals. In contrast, the C-F-BCSA groups, especially at high CO₂ doses significantly promoted the exothermic reaction of C₃S, illustrated by a higher peak of C₃S compared to that of C₃A. As a result, after curing for 1 day, the compressive strength of the C-F-BCSA group intermixed with 3% CO₂ was 30% higher than N-BCSA, while the C-BCSA group experienced 4.3% lower compressive strength.

During the subsequent 7-28 days of the reaction, XRD and FTIR analyses revealed that the content of calcium silicate hydrate (C-S-H) and AH₃ gel in the C-F-BCSA groups was higher than that in the C-BCSA groups. This superiority was attributed to the accelerated hydration reaction of calcium silicate phases (C₂S and C₃S) and calcium sulphoaluminate (C₄A₃S) in the

C-F-BCSA groups. Moreover, in C-F-BCSA groups, the presented C-S-H can absorption of aluminium ions in the blended cement paste to form a significant amount of calcium aluminium silicate hydrate (C-A-S-H) gel and thereby densifies the microstructure of the blended cement paste. On the other hand, the C-F-BCSA groups displayed a substantial CO₂ sequestration capacity, with a substantial CO₂ uptake of 8.8% at 28 days as the intermixed CO₂ dose was 3%. Consequently, the C-F-BCSA group intermixed 3% CO₂ dose exhibited 20.2% improved strength and 60.1% increased Young's modulus (from AFM analysis) compared to C-BCSA group at 28 days. In summary, blending 10% CO₂-intermixed BCSA with 90% OPC can overcome the inhibitory effect of extensive CO₂ dose on the reactivity of calcium silicate and achieves higher long-term strength characteristics.

Graphical Abstract



The role of mineral wool waste in geopolymer: the cementing properties and environmental impact

Yan Luo, M.Sc. Department of the Built Environment, Eindhoven University of Technology

H.J.H. Brouwers, Ph.D., Prof., Department of the Built Environment, Eindhoven University of Technology

Qingliang Yu, Ph.D., Prof., School of Civil Engineering, Wuhan University; Associate Prof., Department of the Built Environment, Eindhoven University of Technology

Email of the corresponding author: q.yu@bwk.tue.nl

Keywords: Mineral wool waste; Geopolymer; Reaction kinetics, Fiber, Leaching

Mineral wool is known as the most used building insulating material in the world, the mineral wool waste (MWW) generated from mineral wool manufacturing as well as the construction and demolition (C&D) industry is estimated to be over 2.5 Mt annually in Europe. Up till now, the reutilization of MWW is extremely low as it is always considered unrecyclable materials, and mostly disposed in the landfill. However, owing to its low density and the fibrous nature of MWW, there is a growing conflict between the non-recyclable nature of MWW and the limited landfill spaces. Therefore, developing alternative ways to reutilize MWW is urgently needed, especially taking sustainability and eco-friendly into consideration. Nowadays, despite increasing attention has been devoted to the alkali activation of MWW, the investigation on joint-activation of MWW with Class F fly ash remains scarce.

This work aims to experimentally investigate the possibility of utilizing MWW in the geopolymer system as a supplementary cementitious material, with a focus on the cementing properties and environmental impact. The MWW was recycled from the Rockwool manufacturing lines and after drying, the MWW was milled to obtain a comparable particle size to Class F fly ash. The potential geopolymerization reactivity of MWW was determined by an alkaline dissolution test. Afterward, by using an activator with a mixing of NaOH and water glass, MWW/Class F fly ash geopolymer blends were prepared with different MWW substitutions. The reaction kinetics, product assemblage, and gel composition were studied by using isothermal calorimetry, X-ray diffraction (XRD), Fourier transform infrared spectroscopy (FT-IR), and energy-dispersive spectroscopy (EDX). The microstructural formation was characterized using multiple techniques, including scanning electron microscope (SEM) and microtomography (Micro-CT). The reaction kinetics, product assemblage, and microstructural formation were further correlated to the cementing properties with regard to drying shrinkage and mechanical strength evolution. Furthermore, a one-batch leaching test was performed on the final blended geopolymers in order to evaluate the environmental impact during the service life of MWW-incorporated geopolymers.

The results reveal that MWW shows a certain reactivity of geopolymerization with significant Al and Si ion dissolution under an alkaline environment. It is observed that the incorporation of MWW into the geopolymeric system has a limited influence on the reaction product assemblage. However, the dissolution of MWW and its fibrous nature not only impacts the gel composition but also alters the microstructural formation with a coarser pore structure, which poses a synergetic influence on drying shrinkage and mechanical strength of the blended system. In addition, the MWW used in this study contains several environmentally sensitive elements, including Arsenic (As), Cobalt (Co), Molybdenum (Mo), Antimony (Sb), Zinc (Zn), chromium (Cr), and vanadium (V). According to inductively coupled plasma-optical emission spectrometry (ICP-OES) analysis, the leaching of these elements from raw MWW is within the limits in civil applications according to the Dutch Soil Quality Decree (SQD). Nevertheless, after alkali activation, higher leaching of As, Cr, Mo, and V is observed in the hybrid geopolymer with increasing MWW substitution, especially the leaching value of V exceeds 30 mg/kg in 12 wt.% MWW incorporated geopolymer as compared to the limit of 1.8 mg/kg in SQD.

ICSBM 2023

3rd International Conference of Sustainable Building Materials

25-27 September, Wuhan, China

This work comprehensively investigates the potential for reutilizing MWW by alkali activation and clarifies the role of MWW in geopolymer systems as supplementary cementitious material. MWW shows a certain enhancement in the geopolymerization process and cementing performance. While notably, heavy metal leaching is noticed after alkali activation, which can be an environmental risk for its future application in alkali-activated materials. In this case, further study to improve the immobilization of heavy metals is required in MWW-incorporated geopolymer systems.

Effect of metakaolin and superplasticizer on drying shrinkage of hardened Portland cement pastes

Nataliya Lushnikova, ¹Postdoctoral researcher, Department of the Built Environment, Eindhoven University of Technology, P.O. Box 513, 5600 MB Eindhoven, The Netherlands;

²Associate Professor, Department of Architecture and Environmental Design, National University of Water and Environmental Engineering, Soborna st. 11, Rivne, 33028, Ukraine

Oleksandr Bezusyak, Associate Professor, Department of Building Products Technology and Materials Science, National University of Water and Environmental Engineering, Soborna st. 11, Rivne, 33028, Ukraine

Email of the corresponding author: n.lushnikova@tue.nl

Keywords: cement paste, drying shrinkage, metakaolin, superplasticizer

The paper covers the results of determination of mutual influence of superplasticizer (SP) and metakaolin (MK) on drying shrinkage of hardened Portland cement paste as this parameter has significant effect on durability and mechanical properties of concrete, in particular self-compacting concrete. There was investigated the influence of type of superplasticizer (naphthalene formaldehyde type NF and polycarboxylate PC type), its dosage (depending on recommendations of manufacturers), metakaolin dosage (5-15% as a partial replacement of cement), specific surface of metakaolin on the. To avoid the direct impact of water dosage on the shrinkage deformations, all the tests had been held at equal water binder ratio: water to cement + metakaolin $W/(C+MK)=0.3$. The dosage of SP was calculated as the percentage of binder content (cement+metakaolin).

For cement pastes there had been determined flowability by flow spread diameter using Vicat apparatus mould (cone), cm. For determination the shrinkage deformations the prism specimens had been tested 40×40×160 mm. The specimens were cured 1 day after casting at relative humidity 95=98% and temperature (20 ± 2) °C. The initial value of the specimens length was measured at the day of 1 day instantly after demoulding. The drying shrinkage was determined by linear comparator. The shrinkage had been measured during 90 days of hardening. The specimens had been cured at ambient temperature (20 ± 2) °C and relative humidity $(50 \pm 10)\%$. There were 3 stages of the experiments for determination the following factors effects on hardened cement paste shrinkage:

- 1) Effect of type (NF, PC type) and dosage of superplasticizer);
- 2) Effect of dosage of MK (5-15%);
- 3) Effect of specific surface of MK (1,400-1,800 m²/kg).

The experimental results prove that the increase in SP dosage at constant MK content and water binder ratio leads to linear increasing of drying shrinkage. The raise of SP above the dosages recommended by manufacturers lead to setting and hardening time retarding with subsequent intensification of shrinkage. There is no strict correlation between specific surface of metakaolin and drying shrinkage.

There are many researches stated the positive effect of MK on drying shrinkage of cement paste and concrete []

It was determined, that optimum content of MK from the point of minimization drying shrinkage is about 10% by total cement and MK.

It can be explained by high water retention of metakaolin that prevents intensive drying of the specimens and reduction of the specimens volume. The decreasing the open porosity of hardened cement paste, demonstrated in our previous experiments, stated the decreasing the intensity of moisture exchange with environment of specimens containing metakaolin. Such cement pastes can serve as the models of the cement matrix in high-strength self-compacting concrete and can be applied for manufacturing self-compacting architectural concrete mixtures

ICSBM 2023

3rd International Conference of Sustainable Building Materials
25-27 September, Wuhan, China

due to high aesthetical properties of metakaolin.

Effect of CO₂ curing on carbonation products and subsequent hydration of cementitious materials

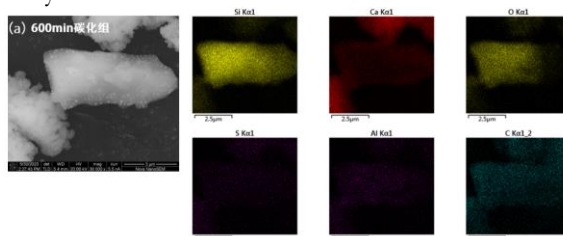
Congcong Ma, College of Materials Science and Engineering, Chongqing University, Chongqing 400045, PR China

Linwen Yu, College of Materials Science and Engineering, Chongqing University, Chongqing 400045, PR China

Email of the corresponding author: linwen.yu@cqu.edu.cn

Keywords: CO₂ curing; carbonation products; subsequent hydration; cementitious materials.

CO₂ curing is a hot research topic in recent years, but the morphology and inter-binding mode of carbonation products such as silica gel, alumina gel, silica-alumina gel and decalcified C-S-H gel are still unclear. Moreover, the effect of CO₂ curing on the subsequent hydration still needs further investigation. For cementitious materials, it is difficult to distinguish the carbonation products and hydration products after setting and hardening because they are closely intertwined. Therefore, paste slurry with a water-cement ratio (W/C) of 2 was used to inject CO₂ at different hydration ages and quantified the reaction heat after CO₂ curing based on the results of QXRD, TGA and cumulated heat release. According to the exothermic curve of the paste slurry with a W/C of 2, the start time of CO₂ injection was determined as 8 min (peak of the induction period), 43 min (end of the induction period), 400 min (middle of the accelerated hydration period) and 600 min (peak of the accelerated hydration period). The duration of CO₂ injection was decided depending on the pH value of the paste slurry.



The results showed that regardless of the pre-hydration age, semi-transparent mist products with CaCO₃ particles embedded in the gel were clearly visible after CO₂ curing. From EDS mapping results, it could be inferred that the mist-like gel is silica gel or silica gel with slight amount of alumina gel. Due to the large W/C and the low density of gel, which lead to the distribution of gel at the outside of the clinker particles and its poor connection with the matrix. In addition to the CaCO₃ particles embedded in the gel, there were a large number of net-like decalcified C-S-H, shuttle-like aragonite, cubic calcite, and a small amount of spherical vaterite. Aragonite appeared to intersperse in the product, while calcite mostly covered on the surface of the clinker particles. After subsequent 28 days (d) hydration, a large number of rod-like CaCO₃ or carbonated ettringite with lengths ranging from a few microns to more than 10 microns were scattered around or interspersed in the product. Based on the exothermic curves of the paste after CO₂ curing at different pre-hydration ages, the rate of heat liberation was accelerated compared with the control group. It was due to the fact that the CaCO₃ formed by carbonation act as crystal seeds provided more nucleation sites and promote the hydration rate. However, the cumulated heat release was lower than that of the control group, partially attributed to the consumption of some clinker by carbonation. From the results of QXRD and TGA, the amount of CaCO₃ produced was calculated, and then the amount of clinker consumed by carbonation was estimated. After elaborate calculations, it could be concluded that CO₂ curing partially prevents the subsequent hydration. After 28 d subsequent hydration, hexagonal plates of Ca(OH)₂ were

ICSBM 2023

3rd International Conference of Sustainable Building Materials

25-27 September, Wuhan, China

found. The silica gel arising by carbonation can react with Ca(OH)_2 to form C-S-H gel, which affect the development of strength at a later time.

The following conclusions were obtained:

(1) The cementitious materials with different pre-hydration age cured by CO_2 produced mist-like silica gel or silica gel with slight amount of alumina gel, and these gels were not tightly linked to the matrix.

(2) Different crystalline types of CaCO_3 were produced, with aragonite interspersed between the products and vaterite and calcite covered on the product surface.

(3) CO_2 curing enhanced the hydration reaction in the early stage but partially hindered the subsequent hydration.

Mechanism and Properties of Solidification of Simulated Intermediate and Low Level Radioactive High Concentration Borate Solution by Portland Cement

Haosen Ma^{1,2}, 1. State Key Laboratory of Silicate Materials for architectures, Wuhan University of Technology, 430070 Wuhan, Hubei, PR China; 2. School of Materials Science and Engineering, Wuhan University of Technology, 430070 Wuhan, Hubei, PR China

Wei Chen¹, 1. State Key Laboratory of Silicate Materials for architectures, Wuhan University of Technology, 430070 Wuhan, Hubei, PR China

Qiu Li^{1*}, affiliation and addresses: 1. State Key Laboratory of Silicate Materials for architectures, Wuhan University of Technology, 430070 Wuhan, Hubei, PR China

Email of the corresponding author: Qiu-Li@whut.edu.cn

Keywords: Boron calcium mineral; Cement hydration inhibition; Boron occurrence state; B-AFt; Gowerite

Cement is commonly used for the solidification of low and medium level radioactive waste. High concentration borate waste liquid is the most difficult type. The treatment of high concentration borate waste liquid has become a difficulty and challenge. At present, the common way of high concentration borate waste liquid solidification is the addition of calcium hydroxide, but the formation of calcium borate is unstable in cement paste. Phase transformation of calcium borate will be occurred in the elderly stage, resulting in volume expansion and reduced the volume stability of specimen. Besides, the inhibition mechanism of high concentration borate waste liquid on the hydration process of cement is not clear. In this paper, the inhibition mechanism of borate solution on the hydration process of cement was studied. At the same time, the effects of sodium hydroxide and sodium aluminate on the process of simulated high borate waste liquid and the performance of cement waste form were studied through hydration kinetics, mechanical properties and durability, phase assemblage, and microstructure. The mechanism of high concentration borate waste liquid inhibition and the mechanism of improvement the performance of cement waste form by the addition of solidification agent were revealed.

The retardation mechanism of simulated high concentration borate waste liquid on cement hydration has been studied. The results show that: the occurrence of boron element in borate solution is mainly related to the pH value of boron solution. With the increment of the pH value, boron mainly exists in the form of $B(OH)_4^-$ instead of $B(OH)_3$. The simulation experiment results show that, when the pH value is low (pH value is about 7), the retardation product of borate solution is ulexite, which covered the whole surface of cement powder and leads to the inhibition of cement hydration process. When the pH value increases, the main hydration product of cement and borate solution is calcium metaborate. In the actual experiment, only ulexite is formed, which indicates that the appearance of ulexite will greatly inhibit the hydration process of cement and hinder the appearance of other borate minerals. It shows that the inhibition degree of borate solution on cement hydration increases with the increasement of concentration and decreases with the increase of pH value of borate solution.

The combined effect of $NaAlO_2$ and $NaOH$ on the early hydration of Portland cement with high concentration borate solution was studied. Through the analysis of hydration kinetics, mechanical properties, durability, microphases, micro-morphology and other aspects. The retardation mechanism of cement hydration under the participation of high concentration borate solution and the mechanism of restart hydration by adding $NaOH$ and $NaAlO_2$ has been researched. The results show that amorphous ulexite as a retarder is formed on the surface of cement particles, which prevents the further dissolution of cement particles. The combined

ICSBM 2023

3rd International Conference of Sustainable Building Materials

25-27 September, Wuhan, China

effect of NaAlO₂ and NaOH can overcome the inhibition of borate solution on cement hydration and restart the cement hydration process. The products such as boron-contained ettringite (B-AFt) and gowerite can be produced instead of ulexite. By adding NaOH to improve the pH value, by adding NaAlO₂ to introduce aluminate source. The formation of sufficient boron-containing ettringite, curing boron ions in the structure of boron-containing ettringite, reducing the concentration of borate solution. The ionic environment and thermodynamics of the hydration process has been changed with the formation of gowerite.

Self-sensing properties of alkali-activated materials

Yuwei Ma¹, Wind engineering and Engineering Vibration Research Center of Guangzhou University:

Fangjie Li², Wind engineering and Engineering Vibration Research Center of Guangzhou University:

Email of the corresponding author: 187354872@qq.com

Keywords: alkali-activated materials, carbon fiber, electrical conductivity, piezoresistive properties, slag, activator.

Self-sensing concrete is a novel construction material that possesses both structural and sensing capabilities, allowing it to monitor its own stress, strain, and damage. In this study, we focused on the self-sensing properties of carbon fiber-reinforced alkali-activated composites (CFAAC). We examined the impact of various factors, including carbon fiber content, raw material composition, and conductive aggregates, on the mechanical, electrical, and piezoresistive properties of alkali-activated materials. Our findings demonstrate that alkali-activated materials exhibit exceptional electrical conductivity and self-sensing properties even with a low carbon fiber content. Compared to cement-based materials with equivalent carbon fiber content, alkali-activated materials exhibited significantly lower electrical resistivity. The use of slag reduced the electrical resistivity and enhanced the piezoresistive properties of alkali-activated conductive mortars. However, an excessive sodium oxide content in alkali-activated mortars had a detrimental effect on the piezoresistive properties. Furthermore, silica addition is beneficial to the stability of piezoresistive behavior. Additionally, we explored the utilization of fly ash microsphere in CFAAC, which significantly improved the electrical conductivity and piezoresistive properties.

Machine learning based strength prediction model for cement clinker

Zhongcheng Ma¹, Ziqiang Li², Suping Cui^{2,*}, Hongtao Xu³, Jiayuan Ye¹

1 State Key Laboratory of Green Building Materials, China Building Materials Academy, Beijing 100024, China

2 Faculty of Materials and Manufacturing, Beijing University of Technology, Beijing, 100124, China

3 Faculty of Information, Beijing University of Technology, Beijing, 100124, China

Email of the corresponding author: Suping Cui, cuisuping@bjut.edu.cn

Key words: Clinker strength, Big data analysis, Machine learning, Prediction model.

Cement clinker is a semi-finished product of cement, and clinker strength is an important parameter for quality control of cement production. At present, clinker strength testing in cement enterprises mainly relies on manual sampling and determination at regular intervals, which has a lag and cannot meet the requirements of enterprises for real-time control of cement production and quality monitoring, and is not conducive to the stable operation of production. Therefore, it is important to explore and further improve the method of predicting clinker strength to adapt to the actual production of enterprises and establish a reasonable prediction model.

With the development of artificial intelligence technology and big data analysis technology, machine learning has become the frontier direction and hot area of materials research, and big data analysis technology combined with machine learning and other intelligent computing technology has become the first major research hotspot and development trend in the field of big data. The production process of cement and other process industries can provide a large amount of multidimensional production data such as process parameters, inspection data and structure images for big data analysis. Many scholars have adopted machine learning-based big data analytics to establish cement strength prediction models, but these cement clinker strength prediction models only use clinker chemical composition, mineral composition, and laboratory inspection data such as free calcium oxide and alkali content as influencing parameters, which have a certain time lag.

In this study, from the purpose of guiding and adjusting the clinker production process in real time, numerous production process parameters in the actual production of cement plants and machine learning methods are combined, and the physical and chemical characteristics parameters of raw fuels, the operating parameters of the thermal system and clinker quality parameters, which are related to the strength of cement clinker, are selected through the analysis of the process mechanism of cement production and the production experience of the operators in the central control room and laboratory of cement plants. The input features were determined by the method of maximum information relevance analysis, and the prediction model was established by combining the common machine learning methods of BP neural network (BPNN), support vector regression (SVR), random forest (RF), gradient boosting decision tree (GBDT), extreme gradient boosting (XGBoost), and LightGBM, and the results showed that: the MSE of the model using neural network model has the best MSE of 0.6872, RMSE of 0.8290, and MAE of 0.655. It is effective and promising to explore the clinker strength prediction model by combining physical and chemical characteristic parameters of raw fuel, operating parameters of thermal system and clinker quality parameters and other relevant process parameters in cement clinker strength production as the input features of the model. The cement clinker strength prediction model based on process parameters can not only effectively solve the problem of hysteresis in cement clinker strength measurement, but also identify and solve the quality problems of cement clinker in a timely manner by regulating the process parameters that have

ICSBM 2023

3rd International Conference of Sustainable Building Materials

25-27 September, Wuhan, China

the greatest impact on clinker strength early in the clinker production process, so as to keep the cement production process in a state of scientific control and promote the high-quality development of the cement industry.

Effect of steel slag powder on the properties of magnesium phosphate cement

Xiangrui Meng^{1,2}, Bin Li^{1,2}, Bing Chen^{1,2*}

1. State Key Laboratory of Ocean Engineering, Shanghai Jiao Tong University, Shanghai, 200240, P. R. China.

2. Department of Civil Engineering, Shanghai Jiao tong University, Shanghai, 200240, P. R. China.

Email of the corresponding author: hntchen@sjtu.edu.cn (B. Chen)

Keywords: Magnesium phosphate cement, Steel slag powder, Ground granulated blast furnace slag, reaction mechanism, mechanical properties.

This paper focuses on the effects of mixtures of steel slag (SS) and ground granulated blast furnace slag (GGBS) mixtures on the workability, compressive strength, water resistance, and pore structure of magnesium phosphate cement (MPC). The results showed that a certain amount of mineral admixture could optimise the fluidity of MPC. The 28d compressive strength of modified MPC did not change obviously, and the water resistance was significantly enhanced. The microstructure and hydration products of MPC were investigated by scanning electron microscopy (SEM) and X-ray diffraction (XRD), a large amount of unreacted MgO was found, and the main hydration product was struvite. In addition, SS and GBFS reacted with ADP to generate a new material phase, and at the same time, there was a synergistic effect between the steel slag and slag. Mercury intrusion porosimetry (MIP) and Electrochemical Impedance Spectroscopy (EIS) results showed that the porosity of the structure increased with the increase of mineral admixture. This study provides new ideas for reducing the cost of MPC, developing new directions for MPC applications and resource utilization of SS and GGBS.

Mechanisms of Steel Corrosion and Chloride Binding in Cement-Based Materials

Xing Ming ¹, Zongjin Li ¹

¹ Faculty of Innovation Engineering, Macau University of Science and Technology, Avenida Wai Long, Taipa, Macao SAR, China.

Email of the corresponding author: zjli@must.edu.mo

Keywords: steel corrosion; chloride binding; ab-initio molecular dynamics; density functional theory; nano alumina

Chloride-induced steel corrosion is the primary durability issue for reinforced concrete structures (RC) serviced in the marine environment and sub-zero areas. Understanding the mechanisms of steel corrosion and chloride binding in cement-based materials is thus crucial to tackle the above issue and prolong the service life of RC structures in harsh environments. Here, we combined multiple experimental and simulation methods to investigate the insightful interaction mechanisms among chloride ions, cement hydrates and steel surface. Based on the revealed mechanisms and processes, the high chloride binding capacity and favorable corrosion resistance are finally realized towards the design of high-durable cement-based materials. The detailed content can be below:

(1) The nature of steel depassivation and corrosion induced by chloride (Cl) at atomic scale was revealed through the density functional theory (DFT) calculations to better understand the Cl induced corrosion mechanism. The results indicated that Cl species weakened the bonding of oxygen (O) with outer iron (Fe) atoms while enhanced the hybridization of O with inner Fe atoms, thus induced the breakdown of passive films. Besides, Cl facilitated the charge loss of outer Fe atoms and improved the interactions of water molecular (H₂O) with these Fe atoms. When co-adsorption with O atom, hydroxyl (OH) generated by dissociative adsorption of H₂O enhanced the charge loss of outer Fe atoms. Then OH strongly bonded with the neighboring Fe atoms to form the initial corrosion products, iron hydroxides (Fe-OH).

(2) Concerning the interactions between Cl and cement hydrates, the most reactive component of ordinary Portland cement (OPC), tricalcium aluminate (C₃A), was investigated on its hydration kinetics, chloride binding behaviors and hydrated phase assemblages through multiple ex-situ and in-situ methods. The hydrated phases of C₃A demonstrated different chloride binding isotherms in NaCl and CaCl₂ solutions at different ages. Chloride ions can suppress the formation of calcium aluminate hydrates (OH-AFm and C₃AH₆) while calcium ions were favorable to increase the content of hydrocalumite (Cl-AFm) and regulate its crystal structure. The carbonation process deteriorated the chloride binding capacity of C₃A pastes through producing more calcium mono/hemi-carboaluminate phases (Mc/Hc) or forming a solid solution between Mc and Cl-AFm.

(3) The atomistic chloride binding mechanisms were further uncovered through the ab-initio molecular dynamics (AIMD) simulation on interfacial activities of chlorides. Chloride ions mainly distributed in the electric double layer (EDL) of positively charged surface ([Ca₂Al(OH)₆]⁺) through electrostatic interactions with calcium ions and protons, while sodium ions were mainly confined within the interface region between the negatively charged surface ([Cl·2H₂O]⁻) and hydrocalumite main layer, forming various ionic complexes. The above interactions are driven from the nucleophilic nature of bound chlorides and electrophilic nature of water hydrogens and calcium ions.

(4) Based on the above complex interactions among chlorides, C₃A hydrates and iron surface, the alumina nano particles (ANPs) were incorporated to improve the chloride binding capacity of cement pastes in chloride solutions and the anti-corrosion performance of mortars under accelerated corrosion process. The ANPs facilitated the formation of alumino-ferrite-mono

ICSBM 2023

3rd International Conference of Sustainable Building Materials

25-27 September, Wuhan, China

(AFm)-type phases, thereby improved the content of chemically bound chlorides. Solution calcium (Ca) ions benefited the chloride captured by calcium-(alumino)silicate-hydrates (C-(A-)S-H) in the assistance of ANPs, especially at high initial chloride concentrations, and further evoked a pH-related chloride binding response. Moreover, the enhanced corrosion resistance was finally realized by incorporating appropriate amount of ANPs because of the filling and chemical effects induced low permeability of mortars. In general, the ANPs possess dual functions in the aspects of chloride binding and corrosion inhibition.

Compatibility evaluation on phosphogypsum-based cementitious binder and cold-bonded aggregates to conventional cements and concretes

Gaoshang Ouyang^{a,c}, Tao Sun^{b,c,*}, Lin Tang^a, Shiwei Long^a, Dong Xu^d

a. School of Materials Science and Engineering, Wuhan University of Technology, Wuhan, 430070, Hubei Province, China

b. State Key Laboratory of Silicate Materials for Architectures, Wuhan University of Technology, Wuhan, 430070, Hubei Province, China

c. Wuhan University of Technology Advanced Engineering Technology Research Institute of Zhongshan City, Zhongshan, 528400, Guangdong Province, China

d. School of Civil Engineering and Architecture, Wuhan University of Technology, Wuhan, 430070, Hubei Province, China

Keywords: Excess-sulfate Phosphogypsum Slag Cement; ordinary Portland cement; calcium sulfoaluminate cement; contact use; compatibility

In response to serious environmental issues brought by large-scale phosphogypsum landfilling, Excess-sulfate Phosphogypsum Slag Cement (EPSC) and phosphogypsum-based cold bonded aggregates (PCBAs) have witnessed their rapid development in recent years. EPSC and PCBAs are known of extremely eco-efficient and economical with acceptable properties. However, due to the presence of excessive sulfate, the phosphogypsum-based materials are suspected to be incompatible with conventional cements, which greatly limits the application prospects. In addition, the complexity of construction environment invites inevitable contact or joint use of different cements composites, which may impact the services of facilities. Therefore, it is of great significance to evaluate the compatibility of EPSC and PCBAs to various types of cements and concretes.

In this work, several methods are employed to systematically estimate the consistency between EPSC and the other two typical cements. Firstly, EPSC paste are molded with ordinary Portland cement (OPC) and calcium sulfoaluminate cement (CSA) pastes to record the early and long-term volume deformation behaviors. Then, EPSC mortar (EPSCM) is series (-S) and parallel (-P) connected to OPCM and CSAM respectively via fresh molding, and mechanical strengths of the hardened mortars are determined. Besides, the tensile bonding strengths between mortars are tested. Thirdly, the coarse PCBAs is manufactured by granulating and curing, which afterwards is mixed with CSA and OPC to prepare concretes (marked as CSAC and OPCC, individually), in comparison with EPSCC; compressive strength of concretes is examined with crushing principles discussed. At last, the interface between the two phases (cements; mortars; aggregates and cement) is analyzed by means of Vickers-hardness and Morphology detection technologies, and the probable mechanisms are proposed.

Results found, given EPSC the largest expansion, EPSC and CSA in contact show coordinated volume deformation behavior, while macro cracks was spotted at the interface of OPC-EPSC due to unbalanced expansions. Similarly, the recognized porous interface in series-connected mortar OPCM-EPSCM-S allows easier bending failure, which therefore reduces the flexure strength from 6.66 MPa of OPCM to 4.36 MPa. In contrast, CSAM-EPSCM-S has ease transition and faint interface between the two mortars, so the strength remains better. Contact use has less influence on parallel-connected mortars in mechanical strengths. Further, the adherence of EPSCM on OPCM and CSAM perform better than reverse adhesion (OPCM and CSAM on EPSCM), and that of OPCM on EPSCM is relative the worst. All the tensile

ICSBM 2023

3rd International Conference of Sustainable Building Materials
25-27 September, Wuhan, China

bonding strengths are larger than 0.6 MPa, meeting the standard (GB/T 25181-2019) requirement for construction mortar. The 28 and 90 d compressive strength of PCBAs based concrete EPSCC is higher than 40 MPa, while CSAC is about 37 MPa and OPCC is approximately 30 MPa. Concrete fragments after compressive tests exhibit that EPSCC and OPCC present both aggregate fracture and interfacial failure, and PCBAs in EPSCC is integrating into the substrate with ambiguous boundaries. Instead, CSAC failure occurs chiefly along with the fracture of PCBAs. It reminds that the crashing characteristics of concrete principally subject to the relative stiffness and interface properties between the substrate matrix and aggregates. Microhardness indicates: CSA > EPSC > OPC > PCBAs > interfaces. The microstructure detected the interface of OPCC is the weakest, like a rift valley wide hundreds of microns, where needle-like ettringite grows in abundance, speculated aroused from concentrations of sulfate and water during the fresh state. In comparison, PCBAs are more affinitive to CSA and EPSC, and CSAC and EPSCC have much fewer defects in their interfaces.

Based on above results, it is suggested that the similarity in hydrates makes EPSC more compatible to CSA, and they can accessibly be used in contact. However, it is not recommended for fresh EPSC paste or mortar to directly contact EPSC composites, since a weak interface will form. The incorporation of PCBAs into EPSC gives concrete the highest mechanical properties. Compared with EPSCC, CSAC has a better interface between aggregates and cements, which achieves maximum utilization of the mechanical properties of PCBAs. But the embedment of PCBAs in OPC will generate internal sulfate attack, resulting in obvious interfacial defects, and thereby significant strength loss. Nevertheless, concerning the largest market of OPC, modification on PCBAs surface is needed, in the future research, to prevent leakage of sulfate and to improve the interface properties, so as to enhance the compatibility of PCBAs to OPC and eventually extend the application perspectives.

Silica-aerogel composites for thermal insulation application: Characteristics and reinforcement evaluation

S.Pantaleo¹, F. Gauvin¹, K. Schollbach¹, and H.J.H. Brouwers¹

¹Department of the Built Environment, Eindhoven University of Technology

Email of the corresponding author: s.m.pantaleo@tue.nl

Keywords: Silica-aerogel; latex; composites; thermal insulation; building materials

The development of new insulation materials is nowadays a matter of high importance regarding the need for the decrease of GHG and CO₂ emissions¹. Considering the building field, better insulation materials imply smaller temperature losses. A better-controlled temperature implies less energy needed and, therefore, smaller energy consumption. Among all the insulators, silica-aerogels exhibit the lowest thermal conductivity on the market² and exist in different shapes such as monolith, nano-powder, or granulates. This material was, for a long time, too expensive, but it is now considered because it meets the criteria now required to help reduce energy consumption.

Wall cavity filling via direct pumping is targeted for the use of silica-aerogel granulates, especially in the Netherlands, where most of the targeted houses or installations possess or can easily have this specific type of construction. This very efficient process also has the advantage of impacting as less as possible the current installation. Only small holes need to be made and can be refilled easily afterward.

For wall cavities purposes, silica-aerogels granulates can not be used alone most of the time. The main reasons are that it could deteriorate over time, and the addition of extra chemicals, based on the application, is often needed. Therefore, it needs to be combined with a binder. To deal with this problem, latexes come as a promising candidate. Largely used in paint or adhesive industries for mixing and formulations³, latexes allow the mixing of different components while maintaining a sufficient viscosity level, which is important for both the pumping step and. In addition, most of the latexes are nowadays water-based, which is an important point regarding sustainability. Finally, latexes meet the need for binding because they form a lattice and trap the different components while drying. Therefore, everything stays together, and water is removed via evaporation.

But because water-based latex and silica aerogels do not present specific compatibility, mixing them could lower the properties of the composite in the final application. Previous studies investigated the interface of latex with nano-silica and its improvement applied to thin film applications. But looking at thermal insulation purposes, silica-aerogel granulates are chosen, and the efficiency of the bonding considering bigger particles, but also when the quantity of silica-aerogel overcomes the binding, need to be evaluated. This work focuses on the mitigation of this negative effect by adding a chemical at the interface of latex/silica aerogel. So, the evolution of the strength will be measured based on the different compositions. Looking at the final application, the evolution of thermal conductivity remains important. Other properties, such as the efficiency of the bonding and moisture absorption, will also be studied.

Analysis on Influencing Factors of Field Test Results of Resistance to Chloride Ion Penetration

Mingqiang Qin^{1,2}, Jun HU^{1,2}, Kuangyi LIU^{1,2}, Baobao YAN^{1,2}

1. CCCC Wuhan Harbor Engineering Design & Research Institute Co., LTD, Wuhan, Hubei 430040

2. Key lab of large-span Bridge Construction Technology, Ministry of Communication, Wuhan, Hubei 430040

Email of the corresponding author: dzqinmq@tom.com, hujun12@ccccltd.cn, 368992173@qq.com, 550673001@qq.com

Keywords: chloride ion penetration; PERMIT; surface moisture; permeable formwork cloth; silane coating

The patterns of the effects of the water retention status of concrete surfaces, the coating of silanes and the use of permeable formwork cloth on the test values of the PERMIT method in the marine environment were investigated. The results showed that the stable peak current of PERMIT ion migration meter had a good linear relationship with the measured value of RCM method; through grinding treatment within a certain range, the influence of silane coating and permeable formwork cloth on the penetration resistance test value of surface concrete could be eliminated; based on the linear relationship between the modified peak current of PERMIT ion migration meter in the stable stage and the value measured by RCM method, the chloride ion diffusion coefficient of solid concrete structure at the age of 56 d was deduced to be in the range of $1.9 \sim 2.6 \times 10^{-12} \text{ m}^2/\text{s}$, with good penetration resistance.

The Influence of nano silica on the Carbonation Resistance of Supersulfated Cement

Zhongxu Song , Shandong Provincial Key Lab for the Preparation & Measurement of Building Materials, University of Jinan, Jinan, Shandong, 250022, China

Email of the corresponding author: mse_chenh@ujn.edu.cn (Heng Chen)

Keywords: Supersulfated cement; Nano silica; Carbonation; Microstructure

The energy-intensive manufacturing process of Portland cement and its significant CO₂ emissions, estimated to contribute 7-10% of global CO₂ emissions, emphasize the need for low-carbon cementitious materials. Supersulfated cement (SSC) is one such environmentally friendly alternative, comprising 1 to 5 wt.% alkaline activator(usually Ordinary Portland cement (OPC)), 65 to 85 wt.% ground granulated blast furnace slag(GBFS), and 10 to 25 wt.% calcium sulfates. SSC offers numerous advantages, including significantly lower CO₂ emissions, high long-term strength, low heat of hydration, and exceptional durability in harsh chemical environments. These properties make SSC a versatile and sustainable material for various applications.

However, its slow hydration process results in a porous structure and a lack of carbonation-resistant compounds(such as calcium hydroxide(CH)) in the hydration products, which greatly affects its practical application in construction. Nano silica (NS) not only regulate the reaction between silica phase and alumina phase during the hydration process of supersulfated cement, accelerating the hydration process, but also enhance compactness through the tight packing of nanoscale particles.

This study investigated the mechanical properties of different proportions influenced by NS, and employed techniques such as XRD, SEM, TGA(Thermogravimetric analysis), and LF NMR (low-field nuclear magnetic resonance) to analyze the pore structure, phase composition, hydration degree, and microstructure of supersulfated cement before and after carbonation. The results have revealed that in the pre-carbonation stage, the group with NS significantly enhances compressive strength and improves the hydration of slag. Simultaneously, the active siliceous particles increase the total amount of C-(A)-S-H hydration products and suppress the early formation of ettringite (AFt). Interestingly, this does not have an impact on the final total AFt content after hydration. Additionally, LF NMR testing indicates that the increased content of C-(A)-S-H contributes to a denser microstructure. Moreover, the experimental findings demonstrate that the siliceous particles delay the decline in compressive strength and reduce the penetration depth of CO₂ during carbonation. Compared to the control group, the group with siliceous particles maintains a higher AFt content even after 7 days of carbonation, with less formation of calcium carbonate. In conclusion, the data from this study indicate that a lower volume ratio of AFt to C-(A)-S-H in SSC leads to better resistance against carbonation. Hence, this research reveals the mechanism by which NS influence the carbonation resistance of supersulfated cement, offering valuable insights for the practical application of this material.

水化硅酸钙的粘弹性研究

Glassy materials with ubiquitous long-range disorder and short-range order always present viscoelastic features (i.e., creep and stress relaxation). Calcium silicate hydrate (C-S-H) gels inside the cement concrete perhaps are the largest amounts of glassy materials in the world. Viscoelastic features of cement concrete have a great impact on the durability of concrete structure. For example, it has been reported that concrete creep is partly responsible for an estimated 78.8 billion dollars required annually for highway and bridge maintenance in United State alone. It is widely accepted that viscoelastic features of cement concrete are strongly affected by C-S-H gels, the debate over viscoelastic behavior of C-S-H gels remains unresolved. Here we report the synthetic C-S-H powder and thin film, and their viscoelastic characteristics. With the increase of Ca/Si ratios, mean chain length of silicate chain in glassy C-S-H gels decreases. From surface chemical bonds (Si-O and Ca-O), hydrogen content and density, synthetic C-S-H thin film seems to a dried gel with little structural water. Macroscopic short-range order and long-range disorder for glassy C-S-H gels is verified by mapping of intensity ratios of Ca and Si laser spectral lines. The phenomenological behavior of viscoelasticity of C-S-H gels is related to the change of lattice constants of nano-crystals inside C-S-H gels, bond breakage and reformation. In conclusion, under external small stress or strain for long time, the polyamorphism transformation of C-S-H gels with energy decreasing leads to obvious viscoelastic behavior. These discoveries in this work may enable to deepen fundamental understanding of microstructure of cement-based materials, guaranteeing the safe of infrastructure. Besides, the findings in this work reveal some viscoelastic mechanisms of glassy gel materials.

ICSBM 2023

3rd International Conference of Sustainable Building Materials
25-27 September, Wuhan, China

Nanoscale Mechanisms of C-S-H Decalcification in Seawater

Yong Tao¹, Yanjie Sun¹, Roland J.-M. Pellenq^{2,*}, Chi Sun Poon^{1,*}

¹ Department of Civil and Environmental Engineering, The Hong Kong Polytechnic University, Hung Hom, Kowloon, Hong Kong

² EPIDAPO, IRL2006, The Joint CNRS/George Washington University laboratory, Washington-DC, US

* Roland J.-M. Pellenq; Chi Sun Poon

Email of the corresponding author: roland.pellenq@cnr.fr (R.J.M.Pellenq);
cecspon@polyu.edu.hk (C.S.Poon)

Keywords: Thermodynamics; Dissolution; Calcium silicate hydrates; Seawater; Molecular dynamics.

Ca leaching is one of the cementitious materials' most important issues concerning cement-based infrastructure's long-term safety performance. However, the decalcification of main hydration products under aggressive solution attacks is rarely investigated from a thermodynamic perspective. This work compared the Ca dissolution free energy of crystalline and amorphous calcium silicate hydrates (C-S-H) in pure water and seawater. It is found that C-S-H with a higher Ca/Si ratio features lower dissolution free energy. For a given C-S-H, the Ca dissolution free energy highly depends on its initial coordination structure, i.e., the more coordination numbers of Ca ions with the surface atoms at the initial site, the higher the dissolution free energy barrier. Amorphous C-S-H possesses a lower Ca dissolution free energy than crystalline C-S-H due to its higher Ca/Si ratio and poorer coordination numbers of surface Ca ions. Unlike most experimental studies that attribute the accelerated C-S-H decalcification to the pH value and ionic solubility in the solution, we found that seawater significantly lowered the Ca dissolution free energy by forming an electrical double layer structure on the C-S-H surfaces. The adsorbed cations within the stern layer timely compensated for the surface charge mismatch during the formation of Ca vacancy, which induced the "ionic exchange" between the Ca ion and adsorbed cations. This study provides insights into the cementitious materials' degradation mechanism concerning Ca leaching and inspires relevant mitigation strategies.

Pre-wet-carbonated 10% cement in the production of CO₂-mixed cement pastes

Wang Minlu¹, Ba Tung Pham¹, Shuang Luo¹, Tung-Chai Ling^{1,*}

¹College of Civil Engineering, Hunan University, Changsha 410082, China

Email of the corresponding author: tcling@hnu.edu.cn; tcling611@yahoo.com

Keywords: CO₂-mixing, aqueous carbonation, fresh cement pastes, compressive strength, CO₂ uptake

The intermixing of an appropriate CO₂ amount with cement-based materials can effectively improve the compressive strength and provide environmentally benefit. However, a direct intermixing CO₂ with fresh cement paste faces a major challenge regarding the limited CO₂ uptake, dramatic loss of workability, short setting time and poor in long-term performance.

This study aims to propose a new approach to pre-mixing CO₂ with a small amount of the cement used in a slurry condition, to promote the CO₂ absorption and minimize the loss of workability. In this method, 10% of the total cement was initially mixed with the total designed water. The slurry was then subjected to the aqueous carbonation with specific CO₂ dose to produce carbonated slurries. Finally, the remaining 90% of cement was mixed with the whole carbonated slurries to produce CO₂-mixed cement pastes. The water-to-cement ratio (W/C) was fixed at 0.5 and four different CO₂ doses (0.06, 0.6, 6 and 12% per weight of 10% cement carbonated) were studied. Samples were denoted as C-0 to C-12 based on CO₂ doses applied. After aqueous carbonation, the effect of aqueous carbonation on characteristics of carbonated slurries such as sedimentation behaviour and pH value of carbonated slurries was investigated. The morphological change of carbonated particles (solid part of carbonated slurries) was examined using Fourier transform infrared (FTIR) and scanning electron microscopy (SEM) method while CO₂ uptake and amount of generated CaCO₃ were determined using thermogravimetric analysis (TGA). Regarding CO₂-mixed cement pastes, the effect of CO₂ doses on the flowability, compressive strength, pore structure development and hydration was examined.

The results show that carbonated slurries subjected to CO₂ dose possessed high amount of CaCO₃ (4.78% of CaCO₃ in case of 12% of CO₂) and the carbonated particles' surface was covered with numerous needle-like and flocculent hydration products such as AFt and C-S-H gel at very early age. This led to the increase in particles' specific surface area and interparticle frictional force, thereby decreased the sedimentation rate as CO₂ doses increased. Besides, the decrease of pH value with the increase of CO₂ dose was insignificant (about 0.6 before and after carbonation). As for CO₂-mixed cement pastes, similar flowability between CO₂-mixed cement pastes and control pastes was observed. Compared to the control sample, the compressive strength of all CO₂-mixed samples at 1 d increased by about 7-18% and achieved higher or similar values at 28 d. The slight improvement of later strength was attributed to the structure densification caused by CaCO₃, which was illustrated by the lower porosity of the CO₂-mixed cement pastes matrix. However, for high CO₂ doses (6 and 12%) the compressive strength followed the trend observed in conventional direct CO₂ mixing method, attributed to numerous micro cracks observed in carbonated samples. In conclusion, this modified approach allows relative higher CO₂ dose used and uptake (up to 1.2% of total cement weight) in ready-mixed cement-based materials while maintaining or improving the flowability and mechanical performance, which was hardly achieved using conventional direct CO₂ mixing method.

Experimental and numerical investigation on thermal properties of alkali-activated concrete at elevated temperatures

Tan Wang^a, Min Yu^{a,b}, Hanjie Lin^a, Feiyu Shi^b, Dawang Li^{b,c}, Yin Chi^a, Long-yuan Li^{b,*}

a) School of Civil Engineering, Wuhan University, Wuhan 430072, China

b) School of Engineering, Computing and Mathematics, University of Plymouth, Plymouth PL4 8AA, UK

c) Guangdong Provincial Key Laboratory of Durability for Marine Civil Engineering, Shenzhen University, Shenzhen 518060, China

Keywords: Alkali-activated concrete; Steel fibre; Elevated temperatures; Thermal properties; Experiment; Modelling.

This paper presents the experimental and numerical investigation on the thermal properties of steel fibre-reinforced alkali-activated concrete (AAC) made by using multiple precursors at elevated temperatures. The temperature-dependent thermal properties such as mass change, thermal conductivity, density, specific heat, and thermal expansion are reported. The effects of temperature heating AAC, coarse aggregate, and steel fibre on the thermal performance of AAC are evaluated quantitatively. Experimental results show that high temperature greatly affects the thermal properties of AAC. Coarse aggregate and steel fibre also have a considerable influence on the thermal properties. Based on the test results, a multi-phase mesoscale model is developed to predict the thermal properties considering volume fractions of steel fibre and coarse aggregate, which can be used in the fire safety design of AAC structures.

Enhancing the early performance of BOFS-blended cement pastes by internal carbonation with 13X zeolite

Wang Zhikai, Wang Xiaoli, Ling Tung-Chai*

College of Civil Engineering, Hunan University, Changsha, 410082, Hunan, China

Email of the corresponding author: tcling@hnu.edu.cn; tcling611@yahoo.com

Keywords: 13X Zeolite, Basic oxygen furnace slag, Compressive strength, CO₂ uptake, Internal carbonation

The CO₂ curing of BOFS binder can improve the material's performance and offer environmental benefit. However, the application of this method in BOFS faces a major challenge of the limited CO₂ uptake. This limitation is primarily caused by the dense structure of BOFS blocks prepared using dry-mixed method. This study proposes a novel approach on the carbonation of BOFS binder by combining the internal carbonation and the CO₂ curing. The objective of this approach is to improve early mechanical properties and CO₂ uptake. 13X-zeolite particles, a synthesized products of high-alumina fly ash, which is believed to provide better CO₂ uptake capacity thanks to its porous structure were chosen. Zeolite particles can physically absorb CO₂ before preparing the pastes and subsequently release CO₂ during mixing process. Moreover, the nanopores characteristics of 13X zeolite particles facilitate the diffusion of CO₂ during the curing stage.

In this study, 13X zeolite particles were initially absorbed CO₂ under a pressure of 0.2 bar. Subsequently, CO₂-13X zeolite particles were mixed with cement and BOFS powder. After that, water and water reducer agent were added for mixing. The water-to-solid (W/S) ratio of all samples was fixed at 0.4 with cement occupying 30% of the solid phase by weight, for the purpose of achieving instant which was used to make sure the samples could be demolding featured. BOFS was replaced by a certain proportion of pure 13X zeolite (denoted as PZ) and CO₂-13X zeolite (denoted as CZ). For comparison, a control group comprising only BOFS and cement was prepared. After demolded, all samples were subjected to CO₂ curing with 65% RH and 20° C for 1 d, followed by standard curing with 20° C and 95% RH until testing day. The mineral phases and morphology changes of the paste were characterized using Quantitative X-ray Diffraction (QXRD), Scanning Electron Microscope (SEM) and Thermogravimetry Analysis (TGA), and their mechanical properties of were determined by hydration heat measurement, compressive strength, fluidity and pore structure development.

The results showed that the 13X zeolite can capture 15 wt.% CO₂ upon initial carbonation for 2 h. The fluidity of the CZ samples possessed about 30% reduction, attributed to the internal carbonation of cement and BOFS powder generating CaCO₃, which increased the particles' specific surface area. At 1 d, both PZ and CZ samples achieved significant enhancement in strength compared to control sample. This is supported by the results of hydration heat showing the superior values of C₃S peak. CZ group achieved about 28% higher of calcite formation and CO₂ uptake than PZ group. The CZ group enhanced the CO₂ uptake by 1.2% and increased the calcite content by 2.3%, indicating that 80% of the CO₂ absorbed in the zeolite was utilized for internal carbonation (curing) in BOFS-blended cement pastes. At 3 d (1 d of CO₂ curing and 1 d further standard curing), the compressive strength of group CZ was the highest, about 40% higher than that of the PZ group, indicating that CO₂-13X zeolite can provide an internal carbonation curing function to improve the early mechanical properties of the BOFS-blended cement pastes. In conclusion, it is feasible to utilize 13X zeolite as carrier for CO₂ so as to improve the early performance and carbonation development over time of BOFS-blended cement pastes.

Effects of Pre-curing and Water-cement Ratios on the Carbonation Curing of Cement-based Materials

Shengkun Wu^{1,2}, Qi Liu^{1,*}, Tianyong Huang², Michelle Tiong¹

¹Beijing Key Laboratory for Greenhouse Gas Storage and CO₂-EOR, Unconventional Petroleum Research Institute, China University of Petroleum, Beijing 102249, China

²Beijing Building Materials Academy of Sciences Research, State Key Laboratory of Solid Waste Reuse for Building Materials, Beijing 100041, China

Email of the corresponding author: liuqi@cup.edu.cn (Q. Liu)

Keywords: Carbonation curing; Pre-curing; Water-cement ratios; Cement-based materials

Recently, carbonation curing has attracted extensive attention as an effective method for carbon capture, utilization and storage (CCUS), as well as for improving the mechanical properties of cement-based materials. However, pore structure and pore water saturation which can control the diffusion of CO₂ and the leaching of Ca²⁺, are found to be the key factors restricting the carbonation reaction rate. To understand its influence mechanism, this paper investigates the effects of pre-curing age (standard curing of 0, 1, 3, 5, 7 days) and water-cement ratios (w/c of 0.4, 0.5 and 0.6) on the microstructure and mechanical properties of cement-based materials. The cement mortars (cement-sand ratio of 1:3) and cement pastes under the same water-cement ratios and curing conditions were used. Compressive strength and phenolphthalein test were applied to characterize the mechanical properties and carbonation depth of cement mortars. Mercury intrusion porosimeter (MIP) was used to characterize the pore structure of cement mortars. X-ray diffractometer (XRD), Fourier transform infrared spectroscopy (FTIR) and Thermogravimetric analysis (TGA) were employed to analyze the phase changes of cement pastes. Scanning electron microscope (SEM) with energy dispersive X-ray spectroscopy (EDX) was adopted to examine the changes of morphologies of cement pastes. The experimental results demonstrated that the compressive strength decreased with the increase of w/c, and there was a maximum compressive strength at different pre-curing ages for different w/c. Specifically, when w/c was 0.4, 0.5 and 0.6 respectively, the highest compressive strength of cement mortars after pre-curing for 1 day, 3 days and 5 days, which were 62.6 MPa, 58.8 MPa and 44.1 MPa, respectively. Besides, based on the carbonation reaction, the evolution model of strength was established, and it was found that the compressive strength after carbonation curing and the carbonation degree are positively related. XRD and SEM results revealed that calcium carbonate (CaCO₃) was the main carbonation product, and the consumption of unhydrated cement clinker phases (C₃S and C₂S) during the carbonation enhanced the calcite precipitation in the pores of cement mortars. According to TG/DTG curves, there was an obvious exothermic peak between 500°C and 950°C, confirming the formation of CaCO₃. In addition, as the w/c increased, the temperature corresponding to the peak also increased, indicating the increment of CaCO₃ crystallinity. Based on the FTIR results, the position of SiO₄⁴⁻ stretching bond of the carbonated cement pastes changed from Q² to Q³ with increasing w/c, which confirmed the formation of amorphous low-Ca C-S-H. This was supported by the EDX results, revealing the Ca/Si was in range of 0.8~1.5. On the other hand, the appearance of CO₃²⁻ characteristic bonds at 875 cm⁻¹ and 714 cm⁻¹ indicated calcite. The MIP results showed that the porosity was increased with increasing w/c. Yet, the pore water saturation varied with different pre-curing ages, which ultimately affected the rate of carbonation reaction and thus, changed the compressive strength. Overall, an appropriate pre-curing age can significantly improve the mechanical properties of carbonated cement-based materials, while the refinement of pore structure due to carbonation also can decrease the negative impact of large pores formed in the cement-based materials prepared with high w/c.

Experimental and numerical investigation on thermal properties of alkali-activated concrete at elevated temperatures

Min Yu^{a,b}, Hanjie Lin^b, Tan Wang^b, Feiyu Shi^a, Dawang Li^{a,c}, Yin Chi^b, Long-yuan Li^{a,*}

a) School of Engineering, Computing and Mathematics, University of Plymouth, Plymouth PL4 8AA, UK

b) School of Civil Engineering, Wuhan University, Wuhan 430072, China

c) Guangdong Provincial Key Laboratory of Durability for Marine Civil Engineering, Shenzhen University, Shenzhen 518060, China

Keywords: Alkali-activated concrete; Steel fibre; Elevated temperatures; Thermal properties; Experiment; Modelling.

This paper presents the experimental and numerical investigation on the thermal properties of steel fibre-reinforced alkali-activated concrete (AAC) made by using multiple precursors at elevated temperatures. The temperature-dependent thermal properties such as mass change, thermal conductivity, density, specific heat, and thermal expansion are reported. The effects of temperature heating AAC, coarse aggregate, and steel fibre on the thermal performance of AAC are evaluated quantitatively. Experimental results show that high temperature greatly affects the thermal properties of AAC. Coarse aggregate and steel fibre also have a considerable influence on the thermal properties. Based on the test results, a multi-phase mesoscale model is developed to predict the thermal properties considering volume fractions of steel fibre and coarse aggregate, which can be used in the fire safety design of AAC structures.

Study of the rheological properties and flocculation mechanism of PAM on underwater non-dispersible slag/fly ash-based alkali-activated cementitious materials

Ze Yu, School of Civil Engineering, Dalian University of Technology, Dalian 116024, PR China

Baomin Wang, Dalian University of Technology, Dalian 116024, PR China

Email of the corresponding author: yuze@mail.dlut.edu.cn

Keywords: Underwater non-dispersion; Alkali-activated slag/fly ash base cementitious material; Polyacrylamide; Rheological properties; Dispersion resistance.

With the continuous development of the economy and society, the resources required by mankind are increasing, leading to a gradual reduction in the resources available for exploitation of land. The ocean has received a great deal of attention from society due to the richness of its resources, and the construction of marine engineering is an important prerequisite for the expansion of marine space and the exploitation of marine resources. With the increasing number of underwater projects, the concrete used for underwater projects has also increased. Concrete that has been in seawater for a long period of time is prone to corrosion leading to deterioration in performance, which adversely affects the development of marine engineering. At the same time, the concrete used for underwater pouring also has the problem of large liquidity loss, when the liquidity loss is large, the slurry can not be evenly and densely filled into the mould, so that the slurry is not dense enough to lead to the quality of concrete is not guaranteed. Therefore, there was a need to find a new material that would reduce flow losses when pouring underwater concrete. Alkali-Activated cementitious materials have received widespread attention due to their excellent durability in seawater, and they also have the advantage of fast setting times and high strength, but their poor resistance to dispersion also limits their use in the development of pouring underwater concrete. In this paper, polyacrylamide (PAM) was incorporated to improve the resistance to the dispersion of underwater non-dispersible alkali-activated slag/fly ash base cementitious material (UNDAASF). The flow rate and rheological parameters of UNDAASF slurry were tested, and the flocculation mechanism of PAM on UNDAASF was investigated in combination with Zeta potential test, electrical conductivity test and XPS test. The results show that when the amount of PAM is small, the different molecular weight of PAM has a certain improvement effect on the flow of the slurry, and as the amount of PAM continues to increase, the flow of the slurry gradually decreases. The rheological test results show that the Herschel-Bulkey model can better describe the workability of the fresh slurry than the Bingham model and the power-law model, and that the viscosity of the slurry decreases to a certain extent when the PAM dose is small, resulting in poor dispersion resistance. As the PAM dosage increases, the shear stress and viscosity of the slurry increase, the dispersion resistance increases and the flowability decreases, resulting in a viscous slurry with reduced flowability, which is not conducive to construction. The results of the Zeta potential, electrical conductivity and XPS tests show that the potential of PAM in alkaline solutions is higher than in aqueous solutions, and both increase with doping and molecular weight. That the carboxyl groups of the PAM side chains complex with Ca^{2+} and Al^{3+} and lead to changes in conductivity, and that the binding of the carboxyl groups to Ca^{2+} and Al^{3+} increases with increasing molecular weight and doping of PAM, ultimately improving the dispersion resistance of the UNDAASF slurry.

Influence of different chain transfer agents on properties of polycarboxylate superplasticizers

Zhengkang Yu¹, Zhonghe Shui¹, Huoming Zhu^{2*}

¹State Key Laboratory of Silicate Materials for Architectures, Wuhan University of Technology, Wuhan 430070, China

²Foshan Huaxuan New Material Co., Ltd., Foshan 528143, China

Email of the corresponding author: 2937703365@qq.com

Keywords: Polycarboxylate superplasticizer; Chain transfer agent; Dispersion; Adsorption

Polycarboxylate superplasticizer (PCEs), as an important type of concrete admixture, have widely applied in cementitious materials due to its advantages of high water-reducing ratio at low dosages, excellent dispersion and dispersion retention ability. In the freshly mixed cementitious materials, the carboxylic group on the backbone provides electrostatic repulsion by adsorption on particle surface, and polyethylene oxide (PEO) as the side chain provides steric hindrance to prevent the agglomeration of particles, which greatly improves the dispersion and dispersion retention of cement particles. The molecular structure of PCEs has strong designability, which can be used for dispersing cement paste, retarding cement hydration, reducing the crystal size, improving the strength and durability of concrete by modification of PCEs. The molecular structure of PCEs is affected by the types of synthetic materials and synthesis methods, which determines the workability, mechanical properties and durability of concrete. Currently, to enhance the performance of PCEs by manipulating the composition of monomers, the role of chain transfer agents in the synthesis and properties of PCEs have received inadequate consideration, and the chain transfer agents are typically employed in low quantities during the polymerization process to adjust the molecular weight of PCEs. In this study, four kinds of PCEs with the same average molecular weight were synthesized by using acrylic acid (AA), industry-grade methallyl ether (HPEG) as monomers under the action of different chain transfer agents including 3-mercaptopropionic acid (MPA), 2-mercaptoethanol (ME), sodium hypophosphite (SHP) and sodium methallyl sulfonate (SMAS), namely PCE-MPA, PCE-ME, PCE-SHP and PCE-SMAS, with molar ratios of AA to MPA, ME, SHP, and SMAS as 1:0.04, 1:0.035, 1:0.12, and 1:0.16, respectively. The synthesized products were characterized using various analytical techniques, including ¹H Nuclear Magnetic Resonance (¹H NMR), Infrared Spectroscopy (IR), Gel Permeation Chromatography (GPC) and dynamic light scattering (DLS) to investigate the effects of different chain transfer agents on the molecular structure of PCEs. The results verified the successful synthesis of PCEs and the molecular structure met the expected design. PCE-MPA and PCE-ME had larger number average molecular weight (M_n) and smaller polydispersity index (PDI) than PCE-SMAS and PCE-SHP. In order to quantify the interaction of four kinds of synthesized PCEs on cement particles, the adsorption behavior of PCEs with different concentrations on cement and Zeta potentials were studied. Compared with PCE-ME and PCE-MPA, the adsorption capacity of PCE-SHP possessing a large number of low molecular weight PCEs with high degree of freedom and the stronger complexation ability of hypophosphite with Ca²⁺ than the carboxyl group was higher. The order of zeta potentials (absolute value) of cement pastes containing synthesized PCEs was PCE-SHP > PCE-ME > PCE-MPA > PCE-SMAS, owning a similar order with the adsorption behavior. Meanwhile, the effects of PCEs on the dispersion ability, rheological properties, mechanical properties of cement paste containing synthesized PCEs were also disclosed. PCE-SHP had the highest adsorption capacity and the highest Zeta potential (absolute value) of cement paste, which makes it have excellent working performance in cement paste. The results showed PCE-SHP significantly increased the fluidity of cement paste, reduced the plastic viscosity of cement paste,

ICSBM 2023

3rd International Conference of Sustainable Building Materials

25-27 September, Wuhan, China

prolonged the setting time of cement paste, and improved strength of cement paste. Then, the hydration products were also analyzed using X-ray diffraction analysis (XRD). It was found that PCEs can retard cement hydration by its dispersing effect and adsorption behavior. PCE-SHP ultimately inhibited nucleation and growth of calcium hydroxide (CH) crystals. This study revealed the mechanism of chain transfer agents on PCEs and provided a new idea for the modification of PCEs.

Effect of the activation agents on the properties of the obtained geopolymers from high-calcium fly ash

Katarzyna Zarębska¹, ¹Faculty of Energy and Fuels, AGH University of Krakow, Al. Mickiewicza 30, 30-059 Krakow, Poland;

Jakub Szczurowski¹, ¹Faculty of Energy and Fuels, AGH University of Krakow, Al. Mickiewicza 30, 30-059 Krakow, Poland;

Jakub Mokrzycki¹, ¹Faculty of Energy and Fuels, AGH University of Krakow, Al. Mickiewicza 30, 30-059 Krakow, Poland;

Email of the corresponding author: zarebska@agh.edu.pl

Keywords: fly ash, geopolymers, activation

Fly ashes are being produced worldwide to the greatest extent from coal, lignite, and biomass combustion. The main components of FA include: SiO₂, Al₂O₃, CaO, Na₂O, K₂O, MgO, SO₃, and Cl (chlorine). Depending on the origin of the fuel, the chemical composition of fly ash (FA) may vary significantly. FA can also origin from municipal waste incineration plants. As the amount of municipal solid waste incineration (MSWI) fly ashes generated worldwide increases, the problem of thermal waste conversion byproducts is becoming an environmental threat. What more, MSWI fly ashes contain high contents of CaO (often >15%), which makes it further processing and utilization more difficult. Therefore, it is extremely important to try to manage them and search for potential utilization pathways. FA's were intensively investigated in recent years as additives to cements, raw materials for zeolites, mesoporous silicates and geopolymers syntheses, and as source of rare earth elements. Production of geopolymers is gaining attention, as these materials can be treated as a replacement to commercially used Portland Cement. Also, due to high compressive strength values (>50 MPa), fire resistance, and stability of mechanical properties, geopolymers are a promising novel construction materials. Also, the CO₂ emissions from geopolymers production are much smaller, than those from Portland Cement.

Ash from a Polish thermal waste conversion plant was selected for the study. Due to the high content of free CaO, the use of fly ash from MSWI directly in the production of cements would be limited due to standards for construction materials. The ashes could become additives for the synthesis of geopolymers. A non-standard synthesis procedure was used in the study. Briefly, 8M KOH, 8M NaOH or 8M H₃PO₄ were used as activation agents. Fly ash was weighed and mixed with the activator, keeping a constant solid/activator ratio of 0.68 for base activation, and 1.10 for acid activation, respectively. After 5 minutes of mixing, the mixture was transferred into 40×40×160 mm³ metal molds and left at room temperature for 24 hours. The molds were then placed in an electric oven at 60 ± 2 °C for 24 hours to cure the materials. The aim of the study was to manage fly ash by obtaining geopolymers characterized by high mechanical properties, thermal conductivity and refractoriness. The produced materials were characterized in detail by means of XRD, XRF and FTIR. To gain a better knowledge on the mechanical properties and the effect of fly ash alkali or acid activation, geopolymers were evaluated by means of their mechanical properties by testing their compressive strength after 7 and 28 days. Geopolymers obtained on the basis of fly ash alkali activation had compressive strengths comparable to corresponding materials obtained in the literature. Acid activation did not yield the expected results of increased mechanical strength. The type of activator chosen had a significant effect on the results obtained.

The results may become a useful background for further studies on the utilization of high-calcium fly ash (HCFA) as a problematic waste for production of value added materials. MSWI fly ash derived alkali activated materials can become an additives to geopolymers synthesis also due to their sufficient CO₂ capture abilities. In such composite materials, MSWI fly ash can

ICSBM 2023

3rd International Conference of Sustainable Building Materials

25-27 September, Wuhan, China

serve as an adsorbent of green house gas, while being used as construction material (geopolymer). Such class of novel materials can become a promising direction for so called “intelligent buildings”.

Funding: This research was funded by National Science Centre, Poland grant number OPUS-22 UMO-2021/43/B/ST8/1636.

Feasibility of preparing carbonated fly ash as supplementary cementitious material

Hongzhi Zhang, School of Qilu Transportation, Shandong University, 250002, Jinan, PR China

Yingxuan Shao, School of Qilu Transportation, Shandong University, 250002, Jinan, PR China

Xiangpeng Zhao, School of Qilu Transportation, Shandong University, 250002, Jinan, PR China

Yifeng Ling, School of Qilu Transportation, Shandong University, 250002, Jinan, PR China

Zhi Ge, School of Qilu Transportation, Shandong University, 250002, Jinan, PR China

Email of the corresponding author: hzzhang@sdu.edu.cn

Keywords: CO₂ mineralization; carbonated fly ash; carbide slag; supplementary cementitious materials; blended cement paste

The aim of the current study is to investigate the feasibility of preparing carbonated fly ash (FA) as supplementary cementitious material for partial cement replacement. Class F FA (with low calcium content) and Class C FA (with high calcium content) were used for mineral CO₂ sequestration. Calcium carbide residue (CS) was blended with FA containing low calcium content (LFA) to improve its CO₂ uptake capacity. Investigations on the carbonated FA and its feasibility as a SCM to (partly) substitute OPC were carried out. It is expected that the current study paves an efficient way to reduce the carbon footprint of concrete industry.

In this study, HFA, LFA, and blends of LFA and CS were carbonated using the so-called direct aqueous carbonation method at a room temperature of 20 °C. In terms of the blends, LFA was mixed with 10 wt.% and 20 wt.% CS to improve its CO₂ uptake capacity and termed as LCS-10 and LCS-20, respectively. The carbonation treated HFA, LFA, LCS-10 and LCS-20 were termed as CHFA, CLFA, CLCS-10 and CLCS-20, respectively. In the direct aqueous carbonation method, the liquid-to-solid ratio of 7.5 mL g⁻¹ was chosen to improve the carbonation efficiency. The injection of CO₂ was stopped when the pH value of slurries reached 7.0. Morphology, particle size distribution, and chemical phases of the carbonated FA were characterized and its performance as SCMs was investigated.

It is found that the CO₂ uptake capacity of FA is governed by its calcium content. The addition of CS can significantly promote the CO₂ sequestration and lead to a higher crystallinity of the formed calcium carbonate. After carbonation treatment, FA loses its alkalinity. The mineralization product mainly consists of calcite. Calcium carbonate particles with cubic shape nucleate on the FA surfaces and cluster further with the mineralization. This leads to the increased SSA. Additionally, the carbonation treatment shifts the particle size distribution of FAs towards smaller sizes. When used as supplementary cementitious materials, the carbonation treatment does not significantly increase the water requirement of FA but does effectively mitigate the set retardation in OPC/FA blends. For LFA, the addition of CS for the carbonation treatment significantly increases the 3d and 28d SAIs by 37.2% and 24.3%, respectively. However, limited increment of SAI for HFA is observed as the hydraulic nature of HFA is inhibited by the carbonation treatment. The mineralized calcium carbonate alters the early hydration kinetics of binders from both physical and chemical mechanism. The CHFA, CLCS-10 and CLCS-20 can accelerate the cement hydration by reducing the induction period. Evidence from the XRD, TGA and SEM observations confirms that the dosage of mineralized calcium carbonate governs the ettringite preservation, carboaluminate formation and increase in hydration degree of cement clinker phases. The results indicate that a high-volume cement replacement can be achieved using synergy CO₂ mineralization of LFA and CS under normal temperatures and pressures.

ICSBM 2023

3rd International Conference of Sustainable Building Materials

25-27 September, Wuhan, China

Nevertheless, further research on the influence of carbonated FA on the durability and volume stability of blended cement is required for the popularization of the synergy carbonation technique.

Effects of the electrical double layer on nanoscale chloride transport in alkali-activated slag materials

Yong Zhang, Xianqiang Xu, Yuchi Fang, Zhengxian Yang

College of Civil Engineering, Fuzhou University, Fuzhou, 350116, China

Email of the corresponding author: y.zhang@fzu.edu.cn (Yong Zhang)

Keywords: Alkali-activated slag; Electrical double layer; Chloride transport; Nano pores; Zeta potential

Reliable cognition of chloride transport is a prerequisite to characterize and improve the durability of marine concrete structures. Percolation theory, where pore connectivity is the key factor, has been predominantly adopted to correlate the pore structure and chloride transport in the capillary pores of traditional Portland cement concrete. It is worthwhile to note that the electrical double layer present on the pore surface turns out to be essentially important in the chloride penetrability especially when nanoscale pores govern the connectivity of transport channels. Alkali-activated materials, typically with more gel pores while less capillary pores in the microstructure, have nowadays achieved widespread popularity. Increasing awareness should be placed on the fierce interactions between chloride ions and the electrical double layer. Such interactions become increasingly pronounced with decrease of pore sizes and need to be taken into account when using Fick's law of diffusion for chloride transport description. However, previous research regarding electrokinetic transport of chloride ions in nanoscale pore structure of alkali-activated materials can hardly be found.

This paper aims to emphasize and quantify the critical role of the electrical double layer in the nanoscale chloride transport properties of alkali-activated slag materials. Mathematical descriptions and systematic experiments were combined to analyse the structure and physiochemical property of the electrical double layer. The potential distribution within the electrical double layer was characterized with the Poisson-Boltzmann approach. The zeta potential as a function of slag hydration and chloride concentration was analysed by electrophoresis method. Natural diffusion tests were carried out to determine chloride diffusion coefficient and oxygen diffusion coefficient of alkali-activated slag mortar specimens with different activators and different water/binder ratios. Results show that the alkali-activated slag system possesses a more negatively charged pore surface than the Portland cement system and the zeta potential of both systems is reduced with age. Chloride peaks exist within the surface layers especially for specimens exposed to chloride ions of low concentrations, a result of chloride accumulation caused by electrical double layer adsorption. High chloride concentrations compress the thickness of electrical double layer and thus weakening the chloride peak. By exposing solution with higher chloride concentration, the chloride diffusion coefficient calculated from Fick's law is obviously increased for low water/binder specimens while changes insignificantly for high water/binder specimens. An increase of water/binder ratio enlarges the transport channels and the electrical double layer effect on chloride ions is impaired consequently. The effect of electrical double layer on chloride transport is negligible for pores above 1000 nm while becomes substantially pronounced for pores below 10 nm, as indicated by the Poisson-Boltzmann analysis. The ratio of oxygen to chloride diffusion coefficient (D_{O_2}/D_{Cl}) can be regarded an effective index to quantify the electrical double layer effect on chloride diffusion behaviour. Such ratio shows an exponentially increasing trend as the decrease of water/binder ratio. Chloride transport in the alkali-activated slag materials is significantly affected by the electrical double layer. It is suggested that the effect of electrical double layer should be included in the modelling and quantification of chloride diffusion behaviour in the specimens with $D_{Cl} < 5 \times 10^{-12} \text{ m}^2/\text{s}$ based on natural diffusion tests.

Mechanical property, microstructure and anti-acid rain erosion performance of red mud-slag-based geopolymer

Tianyi Zhi ¹, Mengxiao Ge ¹, Mingkang Gao ¹, Yifan Yang ¹, Zhongtao Luo ^{1,*}, Xiaohai Liu ^{1,*}, Lei liu ^{1,*}

¹ School of Materials Science and Engineering, Zhengzhou University, Zhengzhou 450001, China

Email of the corresponding author: luozhongtao@126.com; liuxiaohai@zzu.edu.cn; liulei_cbma@163.com

Keywords: red mud; slag; geopolymer; acid rain erosion; pH;

Geopolymer is a promising and sustainable cementitious material with high mechanical strength, low energy consumption and low CO₂ emissions. As a bauxite residue, the inert content of red mud resulted in low utilization and large reserves. Granulated blast furnace slag is a solid waste produced during the industrial iron smelting process. It has a large amount of amorphous aluminosilicate glass phase, which has good reactivity. Therefore, adding slag powder to red mud can effectively improve the activity of red mud powder. In this study, red mud-slag based geopolymer was prepared, and the compressive strength, microstructure and acid rain erosion resistance of red mud-slag based geopolymer were investigated.

For the preparation of geopolymer, the composite powder and the activator were fully mixed at a mass ratio of 1:0.70. For the simulated acid rain erosion experiment, the samples were leached with the prepared acid rain solution with pH of 2.0 and pH of 4.5. The frequency of acid rain spraying was 3 h, and each spraying time was 1 min. After leaching to a certain age, the weight loss and compressive strength of the samples were tested. The hydration product and the morphology were tested by X-ray diffraction (XRD, Panalytical, X'Pert PRO MPD, Holland) and scanning electron microscope (SEM, TENSOR II, Germany), respectively.

As shown in Table 1, at the slag content of 10-50 wt%, the compressive strength of the red mud-slag geopolymer increased with the increasing slag content. When the slag content was 70 wt%, the 28-day compressive strength reduced by 2.47% compared to the slag content of 50%.

Table 1 Effect of slag proportion on the compressive strength of the samples.

Slag (%)	Red mud (%)	Modulus	Solid content (%)	Compressive strength (MPa)	
				7 d	28d
10	90			8.56	13.20
20	80			12.03	22.97
30	70			22.52	32.20
40	60	1.6	30	28.16	51.30
50	50			39.64	65.06
70	30			56.78	63.45

The SEM test results indicated that the microstructure of the polymerization product of the red mud slag based geopolymers was composed of a lamellar structure at 7 d, and the microstructure had two forms. One is rolled and connected with each other to form a honeycomb structure; the other is the lamellae exist independently, and the lamellae have different sizes and are staggered with each other to form a dense structure. At 28 d, the product was mainly composed of a three-dimensional network structure formed by a lamellar network structure.

The mass loss rate of red mud-slag based geopolymers increases with the age of acid rain erosion and the acidity of acid rain. When the pH of the simulated acid rain is 2.0 and the erosion age was 84 days, the mass loss rate of the geopolymer is 4.40%. At this time, the compressive strength of the geopolymer is reduced by 13.5% compared with that when it is not.

ICSBM 2023

3rd International Conference of Sustainable Building Materials

25-27 September, Wuhan, China

When the acid rain pH was 4.5 and the erosion age was 84 d, the mass loss rate of the geopolymer was only 3.33%. However, the compressive strength of the geopolymer was basically unchanged from that before the erosion.

Based on the results of the experiment, the following conclusions can be drawn:

- (1) When the content of slag was 10-50%, the compressive strength of red mud-slag geopolymer increased with the increase of slag content. When the slag content was 70%, the 28-d compressive strength of the geopolymer was reduced by 2.47% compared with the slag content was 50%.
- (2) The morphology of the red mud-slag based geopolymer was different at different ages. The EDS data showed that the products with different morphologies are a mixture of N-A-S-H and C-A-S-H.
- (3) The mass loss rate of red mud-slag based geopolymers increases with the age of acid rain erosion and the acidity of acid rain. In addition, the mass loss of the geopolymer was basically unchanged from that before the erosion.

Characterization and Hydrophobic Surface Study of Gypsum based Composite by Modified Reduced Graphene Oxide

Zhi Zhenzhen¹, Guo Yanfei^{1*}, Wang Liting², Tan Hongbo², Liu Bo¹, Dong Binbin¹, Zhang Hua¹

1-Luoyang Institute of Science and Technology, School of Materials Science and Engineering, Luoyang, 471023, P. R. China;

2-Wuhan University of Technology, State Key Laboratory of Silicate Materials for Architectures, Wuhan, 430070, P. R. China

Email of the corresponding author: guoyfvip@163.com

Keywords: Beta-hemihydrate desulfurization gypsum, Hydrophobic surfaces, Surface contact angle analysis, Mechanical properties, Softening coefficient.

As one of the green and low-carbon building materials, beta-hemihydrate desulfurization gypsum (β -HDG) has many excellent properties and have been widely used in the fields of building materials and decoration. However, its inherent poor water resistance and other defects seriously restrict its application scope. In this work, the β -HDG based composite materials with hydrophobic surfaces were prepared. Surface contact angle analysis was used to study the surface hydrophobic characteristics of β -HDG based composite materials. The compressive strength, flexural strength, ratio of compressive to flexural strength, water absorption rate and softening coefficient of hardened specimens were measured to determine mechanical properties. The pore structure and microstructure of hardened specimens were characterized to evaluate the effect of hydrophobically modified reduced graphene oxide (H@rGO). With the content of 0.15wt% H@rGO, the surface hydrophobicity of the hardened sample was significantly improved, surface contact angle and softening coefficient were up to 113° and 0.77, the compressive strength was increased by less than 60%. The pore size and total porosity of the hardened samples decreased, resulting in the improvement of the softening coefficient and mechanical properties of gypsum based composite.

Preparation and Properties of the Alite-modified Calcium Sulfoaluminate Clinker by Using High Magnisum Limestone

Chao Zhu, affiliation and addresses: College of Materials Science and Engineering, Nanjing Tech University, Nanjing, PR China

Tao Lu, affiliation and addresses: College of Materials Science and Engineering, Nanjing Tech University, Nanjing, PR China

Zhuqing Yu^{1,2}, affiliation and addresses: ¹College of Materials Science and Engineering, Nanjing Tech University, Nanjing, PR China; ²State Key Laboratory of Materials-Oriented Chemical Engineering, Nanjing, P. R. China

Xiaodong Shen^{1,2}, affiliation and addresses: ¹College of Materials Science and Engineering, Nanjing Tech University, Nanjing, PR China; ²State Key Laboratory of Materials-Oriented Chemical Engineering, Nanjing, P. R. China

Email of the corresponding author: zyu@njtech.edu.cn

Keywords: Alite, Calcium sulfoaluminate cement; High magnisum limestone.

Cement is one of the most commonly used materials in the construction field. The production of Portland cement clinker requires high calcination temperature (1450°C) and consumes huge energy and large amounts of raw materials. The development of cement industry is limited to carbon emissions and resource shortages. Meanwhile, Portland cement has poor resistance against aggressive environment. At present, many researches are carrying out to develop high performance and low carbon emission cements.

Alite-modified calcium sulfoaluminate (AMCSA) cement is a kind of eco-friendly cement. AMCSA cement is calcined at 1250 °C~1350 °C by adding appropriate calcium sulfate to the raw material produced for Portland cement. Meanwhile, mineralizer is used. AMCSA cement has the favourable characteristics of Portland cement and sulfoaluminate cement. The calcination temperature of AMCSA cement is lower than that of Portland cement. Less limestone is required and less carbon dioxide is produced. In the AMCSA cement, the main mineral compositions are calcium sulphoaluminate C_4A_3S and tricalcium silicate (alite). The presence of C_4A_3S is beneficial to the property of hardening, early strength and micro-expansion of cement. The presence of alite is conducive to the late strength and the bonding performance of cement.

It is well known that the formation temperature of C_4A_3S is lower than that of alite. During the production of AMCSA clinker, the first key issue is to keep stable coexistence of alite and C_4A_3S . Early studies found that the coexistence of alite and C_4A_3S can be achieved by adding a certain amount of mineralizer to the raw material to reduce the formation temperature of alite to 1300 °C. Magnesium oxide (MgO) and calcium fluoride (CaF₂) can be used as mineralizer to achieve the coexistence of alite and C_4A_3S . Some studies found that an appropriate amount of MgO can not only reduce the calcination temperature of clinker and promote the formation of alite and C_4A_3S , but weaken the effect of sulfur trioxide on alite. Because the addition of sulfur trioxide will increase the formation temperature of alite by about 100 °C, and excessive sulfur trioxide will result in the formation of a large amount of f-CaO and dicalcium silicate, thus inhibiting the formation of tricalcium silicate. Increasing the content of magnesium oxide is an effective way to keep stable coexistence of alite and C_4A_3S . However, more MgO can form periclase and influence the stability of cement. Therefore, it is expected to use some raw materials containing magnesium oxide to control the calcination of clinker.

At present, the storage of high grade limestone is decreasing year by year. By using low grade limestone raw materials to replace high quality raw materials is an effective way to resolve

ICSBM 2023

3rd International Conference of Sustainable Building Materials

25-27 September, Wuhan, China

this problem. The aim of this study is to prepare AMCSA clinker by using high magnesium limestone. By changing the content of high-magnesium limestone and the calcination temperature, the properties of the AMCSA clinker is investigated. Then, the properties of the AMCSA cement is determined.

Mechanism of Ba ion solution in LCCSB and its influence on carbonation reaction

Jianping, Zhu, Henan Polytechnic University School of Materials Science and Engineering
Jiaozuo, China¹

Haole, Wang, Henan Polytechnic University School of Materials Science and Engineering
Jiaozuo, China.

Xuema, Guan, Henan Polytechnic University School of Materials Science and Engineering
Jiaozuo, China.

Email of the corresponding author: jianpingzhu@hpu.edu.cn

Keywords: Barium slag, Low calcium CO₂ sequestration binber, First principles calculations, Ion doping, Carbonation reaction

At present, a new Low Calcium CO₂ Sequestration Binber (LCCSB) has been reported, in which CS, C₃S₂ and C₂AS are the main minerals. LCCSB is a promising carbonizing activated cementing material with good carbon fixation ability. It is of great significance to improve the carbonizing reactivity of LCCSB for its practical application. In this paper, the solution mechanism of barium (Ba) doping in LCCSB and its effects on its mineral composition, microstructure and other properties were studied, and the influence mechanism of BA doping on LCCSB mineral structure and carbonation activity was further revealed. In addition, the carbonation reactivity, carbonation hardening properties, carbonation products and microstructure of LCCSB under different barium doping conditions were characterized by XRD, TGA, FT-IR and SEM-EDS. The results of density functional theory simulations, backscattered electron diffraction and X-ray diffraction show that Ba ions are more inclined to enter the mineral CS by substituting Ca atoms, followed by Ca sites in C₂AS minerals. Further analysis from partial density of states, electron density difference and local distortions show that the doping preference of Ba in CS is due to the efficiency of newly formed bonds, while the electronic structure matching and small local distortion enhance the efficiency of newly formed bonds. The carbonization strength of Ba ions increases after solid solution into LCCSB, and the leaching rule of Ca ions in the carbonization process shows that Ba ions have an effect on the dissolution rate of Ca ions in LCCSB, which is confirmed by first-principle calculation. Before and after Ba ion doping, the total bond order density (TBOD) of Ca-O bond decreases, and the smaller the TBOD, the weaker the overall bond strength of the system, the easier it is to be decomposed by impurity ions, and the more easily Ca ions are dissolved, indicating the potential high carbonization reactivity. The above results provide a potential application prospect for the preparation of highly carbonized LCCSB by sintering barium-containing solid waste, research results are expected to further clarify the carbonization mechanism based on solid waste ions doping LCCSB, and bring better environmental benefits for CO₂ storage.

Thermal responsive clay-hydrogel composite for additive construction

Haidong Zhuang^{1, 2}, Zhenbang Guo¹, Zhengyao Qu^{1,*}

¹State Key Laboratory of Silicate Materials for Architectures, Wuhan University of Technology

²School of Materials Science and Engineering, Wuhan University of Technology

Email of the corresponding author: quzhengyao@whut.edu.cn

Keywords: 3D printing, clay, gelatin, temperature response

3D printing technology has broad application prospects in the traditional construction field, which can greatly shorten the construction period and improve the design of building structures, and it is also a construction technology with great potential in extreme environments. When clay is applied in the 3D printing process, the printed object is usually vulnerable to external damage or deformation, relatively low strength compared to other 3D printing materials, and does not have enough stability to maintain complex shapes. In this study, a temperature-stimulating responsive intelligent clay 3D printing formula was innovatively proposed by combining clay and gelatin. The combination of these two materials overcomes the limitations of traditional materials. Gelatin can enhance the bonding strength between layers of the clay system, improve the printable performance and mechanical strength of the clay, and increase its early bearing capacity. During the experiment, the gelatin is cross-linked first by adjusting the temperature, which achieves higher design flexibility and printing accuracy in the 3D printing process. Make the printing process more fine and stable. At the same time, the plastic properties of clay and the adjustable pore structure of gelatin combine to provide the necessary support and deformation ability for printing, ensuring the stability and structural integrity of the printed object, and making the printed structure more stable.

Coupled thermodynamic modelling and experimental study of alkali-activated slag cement under combined attack of chloride and sulfate salts

Yibing Zuo

School of Civil and Hydraulic Engineering, Huazhong University of Science and Technology,
Wuhan, China

Email of the corresponding author: zuoyibing@hust.edu.cn

Keywords: alkali-activated slag cement; combined attack; sodium chloride; magnesium sulfate; thermodynamic modelling

Alkali-activated materials (AAMs) are a family of existing alternative construction materials that could reduce the current environmental impact of Portland cement (PC) production and utilization. While there is a general consensus about the strength and CO₂ footprint advantages of AAMs over PC, a widespread debate still exists pertaining to the durability of AAMs, which thereby hinders their bulk application and commercialization. Currently, the existing researches usually focus on the durability of AAMs under the action of a single factor such as sulfate attack, chloride ingress, drying–wetting cycles, etc. Thus, the researched outcomes and proposed models cannot be used to guide the durability design of AAMs under multi-factor coupling action. Against this background, the present study aims to investigate the durability of alkali-activated slag cement under combined attack of sodium chloride and magnesium sulfate by using thermodynamic modelling and experimental techniques. The thermodynamic modelling results were benchmarked with the experimental data, showing a good agreement. The phase evolution as well as physical adsorption and chemical binding of chloride ions would be presented and discussed. The preliminary results show that the combined attack of sodium chloride and magnesium sulfate exhibits not only characteristics by single attack of those two salts but also coupling effects. It promoted the formation of chloride intercalated hydrotalcite while inhibited the formation of Friedel's salt and magnesium silicate hydrate. Besides, an increase of the magnesium sulfate proportion led to lower capacity of chemically binding chloride.

TOPIC B: Waste recovery, treatments and valorizations

**Lightweight, deformable, and water-resistant cement mortars
with recycled plastics enabled by in-situ polymerization**

Ahmed Al-Mansour, Chengji Xu, Qiang Zeng*

College of Civil Engineering and Architecture, Zhejiang University, 310058, Hangzhou, China
Second author, affiliation and addresses:

Email of the corresponding author: cengq14@zju.edu.cn

Keywords: Waste plastic, upcycling, lightweight concrete, in-situ polymerization.

Traditional concrete has been the primary building material used in the construction industry. Typically, two-thirds of the total volume in concrete are constituted by natural aggregates, which has caused significant environmental issues and ecosystem disturbances. Meanwhile, the steady proliferation of plastics usage and its expanded applications has further strained the environment due to its slow biodegradability. The accumulated amount of plastic on Earth has surpassed other fabricated materials, and so has its waste. As a result, the concept of incorporating recycled waste plastic (RWP) into concrete to partially or fully replace natural aggregates has gained increasing attention.

The incorporation of RWP in concrete as a replacement for natural aggregates often results in reduced compressive and flexural strengths, largely due to the weak bond between RWP aggregates and the cement matrix. Thus, this research employs in-situ polymerization to develop stronger interaction between RWP aggregates and the cement matrix. The primary monomer used for this process was sodium acrylate (SA) at concentrations of 0%, 1%, and 2% to fabricate in-situ polymerization modified mortars (iPMM) with RWP aggregates. The microstructural changes of the mixtures were observed using scanning electron microscopy (SEM). Mass gain was utilized to evaluate sorptivity of the specimens, while the porosities were determined by mercury intrusion porosimetry (MIP). Finally, a full replacement of sand by RWP aggregates was assessed ecologically and economically.

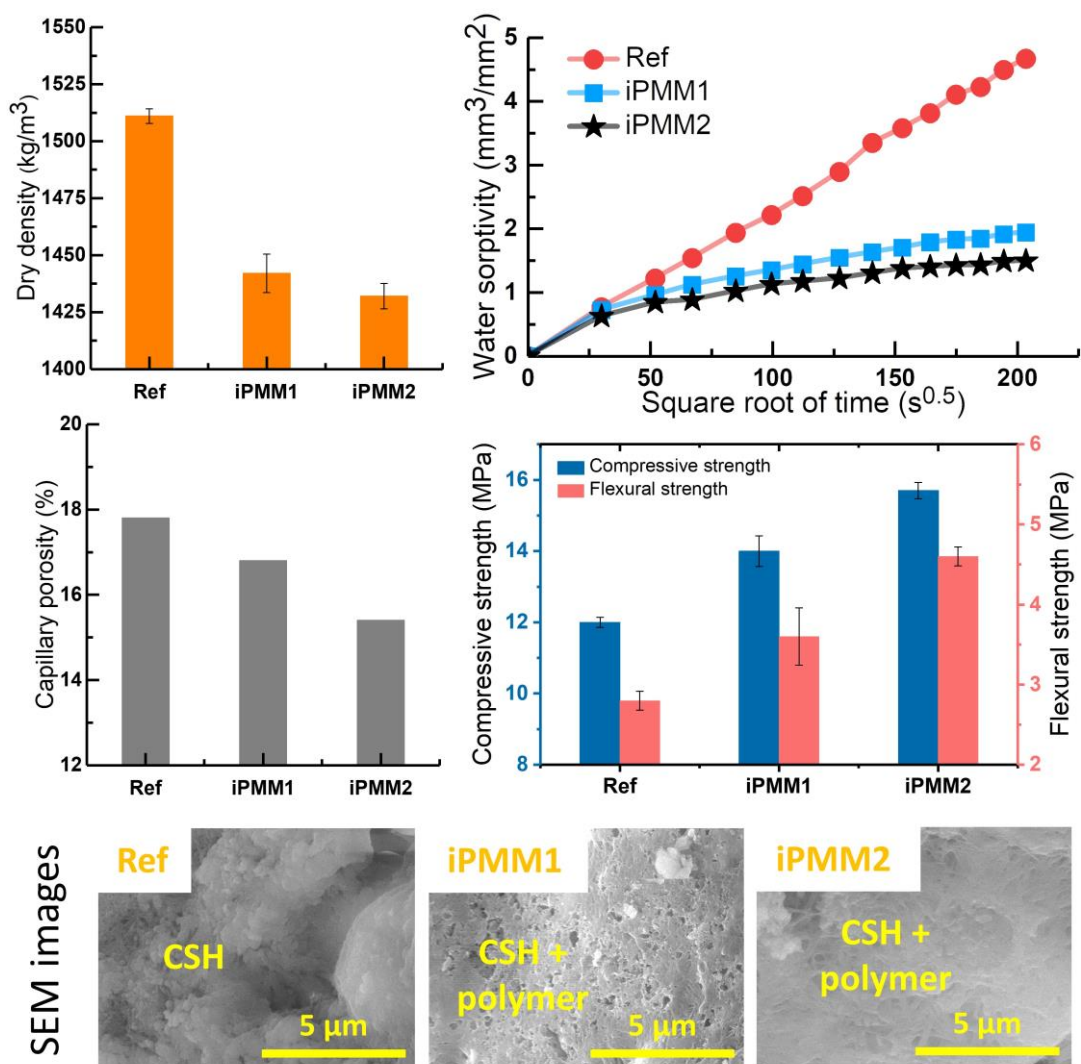
The load-displacement figures revealed that iPMM2 exhibits over 70% increase in deformability compared with the reference sample under compression and flexure loads. Polymer-modified cement-based materials usually show such increase in ductility, which is enabled by the polymeric networks that are capable to absorb more energy. Notably, the higher strength of iPMM mixtures compared with the reference specimens indicated that utilizing RWP aggregates without modifying the cement matrix yield significant drops in the mechanical performances. In contrast, iPMM2 specimens were found to have compressive and flexural strengths that were approximately 29% and 76% higher, respectively, than those of the reference specimens.

Compared with typical cement mortars, the average dry density results indicate substantial reductions, which may be ascribed to using 100% RWP aggregates in addition to the presence of polymers in the cement mixtures. The waterproof performance of the iPMM specimens differed for different SA concentrations. For instance, iPMM1 and iPMM2 displayed two separate phases before being fully saturated, with an initial rapid sorptivity phase characterized by a linear relationship between mass gain and time, lasting for a short duration of around 27 minutes. Then, a slower phase with reduced water uptake was noticed. In contrast, the reference specimens displayed a single-phase linear relationship with a relatively lower waterproof performance. Meanwhile, the MIP results revealed that the addition of SA to the cement mixtures led to a decrease (i.e., 14%) in total porosity, where the reference sample had a porosity just below 18%, iPMM2 possessed nearly 15% total porosity of the sample. These results indicate that the porous structure of the samples can be considerably refined through the concurrent processes of

cement hydration and polymerization.

The SEM samples provided more detailed microstructural changes of the iPMM mixtures. Typical C-S-H gel was observed in the reference sample binding and reducing interparticle voids. In contrast, the creation of dense polymeric networks, as well as typical C-S-H gel, was noted in the SA mixtures. The typical products of cement hydration, combined with inter-connected 3D polymer chains, formed the material's microstructure and improved its ability to withstand more loads. Detecting the polymer-like films and gel-like structures verified the synchronous in-situ polymerization and cement hydration.

This study concludes that in-situ polymerization in cement mixtures with RWP aggregates results in improved compatibility and, therefore, higher load-bearing performances and ductility. Furthermore, the sorptivity of the polymer-modified samples (i.e., iPMM2 > iPMM1 > Ref) was substantially enhanced. Finally, from the economic and ecologic analysis, fully replacing sand with RWPs in cement mixtures to fabricate non-structural elements such as blocks for partition walls resulted in substantial decreases in the amount of sand and CO₂-eq emissions, owing to the decrease in density of mixtures with RWP aggregates compared with a typical mixture. The results obtained from this research hold noteworthy findings for the construction sector, particularly concerning the advancement of sustainable design approaches for cement-based materials.



Evaluation of chloride diffusion in recycled aggregate concrete including slag using PSO-BP and GA-BP neural network

Xixuan Bai^{1,2,*}, Xuan Liu¹, Cheng Liu¹

¹School of Civil Engineering and Architecture, Wuhan Institute of Technology, Wuhan, 430073, China

² Hubei Provincial Engineering Research Center for Green Civil Engineering Materials and Structures, Wuhan, 430073, China

Email of the corresponding author: baixx87@wit.edu.cn (X. Bai).

Keywords: Recycled aggregate concrete, Artificial neural network, optimization algorithm, Recycled aggregate concrete, Slag

Abstract: Chloride ingress is one of the major contributing factors to the corrosion of reinforced concrete structures. Additionally, the utilization of recycled aggregates diminishes the resistance of recycled concrete against chloride ion attack. The addition of moderate amount of slag powder has an enhanced benefit on the chloride ion attack resistance of recycled concrete. High applicability of artificial neural networks in predicting chloride diffusion rates in recycled concrete containing slag. To enhance the prediction accuracy of the neural network-based durability model for recycled concrete, in this paper, the optimizing of particle swarm algorithm (PSO) and genetic algorithm (GA) on BP neural network were adopted to predict the chloride ion diffusion rate of recycled concrete mixed with slag powder and containing different coarse aggregate replacement rates. Based on 340 sets of experimental data from different literatures, the proposed neural network models were trained and validated by using 8 parameters, namely, curing age of RAC, water, cement, sand, coarse aggregate water absorption, slag fines content, coarse aggregate substitution rate, and water-cement ratio as input parameters of the hybrid neural network models, and using chloride ion diffusion rate as output parameter. Evaluation indices, including Mean Squared Error (MSE), Root Mean Squared Error (RMSE), Mean Absolute Error (MAE), and Coefficient of Determination (R²), were employed to assess the prediction performance and generalization capability of the models. By the comparative analysis of models, the results demonstrated that both the PSO-BP and GA-BP models achieved high prediction accuracy and exhibited strong generalization ability. Overall, the PSO-BP neural network model exhibited slightly higher accuracy compared to the GA-BP model, and both outperformed the conventional BP model. Furthermore, the results suggested that the proposed hybrid algorithmic neural network was helpful to find the best RAC mating ratio design, so as to predict the RAC service life, and to develop effective structural maintenance plans.

Ambiently dried silica aerogel from waste glass, production and sustainability analysis

Marina Borzova, Valerie Lenigk, Katrin Schollbach, Florent Gauvin, Jos Brouwers.

Department of the Built Environment, Eindhoven University of Technology, P.O. Box 513, 5600 MB Eindhoven, The Netherlands.

Email of the corresponding author: m.borzova@tue.nl

Keywords: silica aerogel, waste recycling, life cycle assessment, insulation material, sustainability.

To make the building materials industry more circular recycling of waste glass has been investigated in the past. Researchers have used it as a supplementary cementitious material or added it to geopolymers. This work describes a new protocol for complete synthesis of silica aerogel via ambient pressure drying method from mixed fine glass waste as a starting material.

Silica aerogel is a ultra-light highly porous material with extremely low density and high specific surface area, which makes it an outstanding insulation material with the lowest thermal conductivity when compared to all other existing products including air. The production of aerogels has been of significant interest due to their unique properties making them useful in a variety of applications. In particular, aerogels in this research are produced for the purpose of being an insulation material for buildings.

However, the traditional method of producing aerogels, high-temperature supercritical drying (HTSCD), has proven to be expensive and energy-intensive, resulting in significant carbon emissions. As an alternative, the study investigates the use of ambient pressure drying (APD) as an alternative production process for aerogels. APD is of particular interest since the supercritical drying step is the most energy-intensive component of the aerogel production process. Additionally, the use of waste glass as a replacement for commercial silica will be investigated. By combining waste raw materials with this alternative process, the research aims to reduce the negative environmental impact of aerogel production.

The study describes a novel protocol for extraction of silica from waste glass, its purification, synthesis of sodium silicate which is then used for the silica aerogel synthesis. Next, a life cycle assessment of the APD aerogel production process to determine the overall environmental impact is conducted using SimaPro database. This will help determine how much more sustainable the APD process compared to the HTSCD process actually is, as well as giving insights as to which the biggest emission producing steps are. Surprisingly, there is limited literature on the lifecycle assessments of aerogels, which underscores the need for further research in this area. By conducting a comprehensive lifecycle assessment, this study aims to identify areas for improvement and guide future research in the field.

Firstly, parameters for optimal silica extraction were optimized to maximize the extraction efficiency, with special attention towards the potential future upscaling of the process. The summary of the results can be seen in table 1. Next, silica aerogel produced via APD method was analyzed to assess its quality compared with commercially available silica aerogel. The produced silica aerogel particles obtained super hydrophobic property (149.5°), sufficiently low thermal conductivity (0.027 W/m·K), high specific surface area (608 m/g²) with pore volume of 2.02 cm³/g, porosity of 90.1%, and bulk density of 0.137 g/cm³. Potential for solvent recycling, and unreacted residue repurposing as a supplementary cementitious material are currently being developed.

ICSBM 2023

3rd International Conference of Sustainable Building Materials
25-27 September, Wuhan, China

Table 1. Summary of waste glass silica dissolution in base parameter optimization.

Parameter	Reaction time, hours			Solid to liquid ratio			Base	
Parameter value	6	24	48	1:10	1:50	1:100	NaOH	NaOH/Na ₂ CO ₃
Silica dissolved	34.4%	51.5%	57.6%	45.1%	51.5%	59.6%	51.5%	73.7%

Life cycle assessment was conducted on a laboratory scale, taking into account all resources consumed such as electricity to operate equipment, chemicals and water, and others. The goal is to conduct a complete, “cradle to grave” analysis, including the considerations for the end of life for this material or potential recycling or reusing paths. Since silica aerogels are relatively new and are not yet widely applied in the building industry, it is not possible to determine the ageing and end of life process with high precision.

In conclusion, this study shows a detailed synthesis route for sodium silicate from waste glass, followed by silica aerogel, and the sustainability evaluation of this process.

Real-time Sensor-based Characterization of Recycled Coarse Aggregates (RCA)

Cheng Chang ¹, ¹Resource & Recycling, Department of Engineering Structures, Faculty of Civil Engineering and Geosciences, Delft University of Technology, Stevinweg 1, 2628 CN, Delft, The Netherlands

Francesco Di Maio ¹, ¹Resource & Recycling, Department of Engineering Structures, Faculty of Civil Engineering and Geosciences, Delft University of Technology, Stevinweg 1, 2628 CN, Delft, The Netherlands

Abraham T. Gebremariam ¹, ¹Resource & Recycling, Department of Engineering Structures, Faculty of Civil Engineering and Geosciences, Delft University of Technology, Stevinweg 1, 2628 CN, Delft, The Netherlands

Peter Rem ¹, ¹Resource & Recycling, Department of Engineering Structures, Faculty of Civil Engineering and Geosciences, Delft University of Technology, Stevinweg 1, 2628 CN, Delft, The Netherlands

Email of the corresponding author: C.Chang-1@tudelft.nl

Keywords: Recycled coarse aggregates; Quality measurement; Concrete recycling; Gocator; LIBS

Preserving material value over extended periods is crucial to ensure effective management of End-of-Life (EoL) concrete. Nevertheless, the industry often hesitates to substitute natural aggregates with recycled aggregates due to concerns about the variability in recycled aggregate quality and the substantial costs and time required to assess their quality. Addressing these concerns becomes imperative to ensure that recycled aggregates meet industry requirements. This can be achieved by conducting comprehensive material quality measurements and demonstrating their quality clearly. A key objective of assessing the quality of recycled aggregates is to provide users with timely information on optimal utilization. By cost-effectively measuring the quality of recycled aggregates and making this information readily accessible online, the industry can address concerns about variability, quality, and trust along the value chain. This approach allows users to make informed decisions and confidently incorporate recycled aggregates into their projects. In this context, innovative recycling technologies that enable efficient characterization of recycled aggregates play a pivotal role. These technologies facilitate the upcycling of EoL concrete and contribute to implementing a circular economy. By embracing these technologies and promoting recycled aggregates, the industry can achieve sustainable resource management, reduce environmental impact, and contribute to a more sustainable construction sector while making profits.

Implementing C2CA (Concrete to Cement and Aggregate) technologies enables the acquisition of recycled coarse aggregates (RCA) from EoL concrete, specifically within the 4~16 mm range. These RCA are subsequently transported onto a conveyor belt and subjected to inspection using the 3D scanner Gocator and laser-induced breakdown spectroscopy (LIBS) to assess their particle size distribution (PSD) and composition in terms of contaminants. A feeding system is employed to ensure a consistent flow of RCA, resulting in triangular-shaped piles on the conveyor belt. A single conveyor belt can handle more than 50 tons of RCA per hour. The Gocator captures high-resolution point clouds, simultaneously allowing uninterrupted conveyor belt operations. The obtained point clouds are processed using the FastScape algorithm, which segments them into individual particles. Through statistical analysis of the segmented particles, the PSD is calculated and compared with the results of manual sieving. Experimental results demonstrate the feasibility and effectiveness of this method in real-time characterizing the PSD of RCA piles on the conveyor belt. LIBS is then used to identify and classify potential

ICSBM 2023

3rd International Conference of Sustainable Building Materials
25-27 September, Wuhan, China

contaminants in the streams of RCA, providing timely warnings regarding the presence of hazardous substances. A total of eight potential contaminants are considered as target contaminant materials within the RCA streams. Such contaminants are bricks, cement paste, foam, glass, gypsum, mineral fibers, plastics, and wood. An efficient method with minimal influence from the surrounding environment is proposed to identify and classify EoL concrete waste and RCA on the conveyor belt via a clustering-based identification algorithm. The algorithm combines principal component analysis and chi-square distribution to generate its database for each material from the spectra resulting from the LIBS. These spectra are applied to train and validate the classification model. The number of particles per second for which the material identification is done by LIBS: is 40/s. In addition, the effects of different pre-processing methods and parameter selection are investigated and discussed. The model is verified with an accuracy of 0.97, a precision (weighted average) of 0.98, a recall (weighted average) of 0.97, and an F1-score (weighted average) of 0.98 for the validation set under the optimal conditions.

The proposed procedure presents several notable advantages, including hazardous substance warning, real-time feedback, minimal data processing, and automated processing, all of which collectively contribute to RCA's efficient and accurate characterization. Combining these advantages offers a novel approach for accurately assessing the quality of RCA derived from EoL concrete on the conveyor belt. By integrating Gocator and LIBS technologies, industrial applications of RCA can experience significant benefits, as it provides precise, efficient, and real-time results. This timely information empowers decision-makers with the necessary knowledge to make informed choices regarding RCA utilization, processing, and management in concrete aggregate recycling. This innovative approach, therefore, holds significant potential for enhancing the processing and high-end utilization of EoL concrete. Ultimately, this study highlights the potential for sustainable resource utilization and waste reduction in the construction industry.

Evaluation of Graphene Oxide on Microstructure and Micromechanical Properties of Ultra-high Performance Concrete with Recycled Fine Aggregate

Chen Kang¹, School of Civil Engineering and Architecture, Wuhan Institute of Technology, Wuhan 430074, China

Wu Ziyang¹, School of Civil Engineering and Architecture, Wuhan Institute of Technology, Wuhan 430074, China

You Xiao¹, School of Civil Engineering and Architecture, Wuhan Institute of Technology, Wuhan 430074, China

Ye Ziqian¹, School of Civil Engineering and Architecture, Wuhan Institute of Technology, Wuhan 430074, China

Cheng Shukai^{1,2,*}, School of Civil Engineering and Architecture, Wuhan Institute of Technology, Wuhan 430074, China; Hubei Provincial Engineering Research Center for Green Civil Engineering Materials and Structures, Wuhan Institute of Technology, Wuhan 430074, China

Email of the corresponding author: chengsk@wit.edu.cn

Keywords: Ultra-high-performance concrete, Recycled fine aggregate, Graphene oxide, Microstructure, Interfacial transition zone (ITZ)

To compensate the defects of recycled aggregate concrete (RAC) prepared by recycled aggregates, the application of nano-materials has been proved as an innovative and high-efficiency strategy. This study aims to use the graphene oxide (GO) to enhance the properties of ultra-high performance concrete (UHPC) with recycled fine aggregate (RFA). The effects of GO on the mechanical properties, autogenous shrinkage, penetrability, microstructure, interfacial transition zone (ITZ) and micromechanical properties of UHPC are investigated, so as to fully understand the mesoscopic and macroscopic mechanical behaviours of GO reinforced UHPC with RFA. It was found that the incorporated of RFA significant decreased on the early compressive strength and increased the water and chloride permeability, while it had remarkable mitigation on autogenous shrinkage of UHPC. Moreover, with the increase of GO content, the compressive strength and transport properties of UHPC with RFA were increased. The addition of GO further reduced the autogenous shrinkage and enhanced the micro-hardness of ITZ in UHPC with RFA. The incorporated of GO caused more calcium silicate hydrate generation and promoted the homogenization of the microstructure, leading to decrease of the porosity in ITZ. Furthermore, when the critical content of GO was 0.06%, the microscale fracture toughness in ITZ was also increased due to the reduction of porosity and the bridge effect of GO, which was contributed to the improvement of the interface bonding between steel fibers and matrix. This study reveals that the synergy between GO and RFA in UHPC is a new approach for producing environment-friendly sustainable construction materials.

Preparation of low calcium cement clinker based on solid waste

Wei Chen, Wuhan University of Technology

Siye Wang, Wuhan University of Technology

Bo Li, Wuhan University of Technology

Email of the corresponding author: lipt712@163.com

Keywords: clinkerization temperature; Solid waste recycling; Low carbon clinker.

A large amount of CO₂ emissions is one of the problems that need to be solved urgently, the impact on the global climate has begun to emerge. Cement industry is one of the industries with concentrated energy consumption, its CO₂ emission has accounted for 7% of the total, which will be 12% in China. The decomposition of raw materials and the provision of high temperature fossil fuels are the main factors of high CO₂ emissions in the cement industry. At the same time, amount of solid waste is increasing year by year and the generated solid waste is still difficult to use, which has become a common problem worldwide. Solid waste as raw material for cement production has been proved feasible in many studies. The research challenge of this part lies in the diversity and fluctuation of the chemical composition of solid waste. For cement production, there are some harmful components affect the quality of cement clinker in solid waste. Some of the solid wastes have strict quantity restrictions in resource recycling due to their high content of Al₂O₃, Fe₂O₃ and MgO which affected the amount of solid waste used for recycling in cement production.

Portland cement clinker contains more than 60% tri-calcium silicate (C₃S) and is produced at 1450°C, which releases about 850 kg CO₂ per ton of clinker. The CaO content of low calcium cement clinker composed of C₂S, C₃S₂, and CS is more than 10% lower than that of ordinary Portland cement clinker. Low calcium cement has obvious low-carbon advantages in raw material composition, sintering temperature, phase composition, and other aspects. The use of carbonization curing can further reduce the total carbon dioxide emissions of the clinker.

In order to improve the resource utilization of solid waste and reduce carbon emissions during cement production. A low calcium carbon mineralized cement clinker with high mass fraction of solid waste (67 mass%) was synthesized from copper tailing and phosphorus tailing. Because CS phase can not be formed under the condition of low temperature and short soaking time. Combine with phase diagram simulation and pre-experiment results, C₂S and C₃S₂ were taken as the main phases in this clinker design. The optimum composition range of clinker was 45-50% CaO, 35-39% SiO₂, 5-8% Fe₂O₃, 5-8% Al₂O₃. The Ca/Si of this low calcium cement clinker is between 1.25 and 1.40. Based on the guidance of the CaO-SiO₂-Al₂O₃ ternary phase diagram, multiple composition points within the above ratio range were selected for clinker preparation, and their mechanical properties, microstructure, etc. were tested. Result display, the optimum clinkerization temperature range for clinker preparation was 1200-1220 °C. The compressive strength of clinker prepared at 1215 °C after being carbonated with CO₂ for 72 hours reached 53.9 MPa. In obvious lamellar Calcite structure can be observed in the electron microscope test. According to the experimental and calculation results, compared with Portland cement clinker, this low calcium cement clinker can reduce carbon dioxide emissions by about 40%. All the results show that the clinkers have competent properties and achieve the resource utilization of solid waste and reduces CO₂ emissions.

Preparation of polypropylene-encapsulated toluene diisocyanate microcapsules for self-healing concrete cracks

DU Fei¹, LIU Bo², JIANG Lu², GUO Hongyang¹, LI Jing¹, ZUO Danying^{2*}, DU Wei^{2*}

¹ Central & Southern China Municipal Engineering Design and Research Institute Co. Ltd.

²School of Materials Science and Engineering, Wuhan Textile University.

Email of the corresponding author: zdy@wtu.edu.cn (D.Z.); duwei@wtu.edu.cn (W.D.)

Keywords: Microcapsule; Concrete; Self-healing; Polypropylene; TDI

The cracks will occur during the use of concrete, and the post-repair methods can no longer meet the requirements. Compared to manual post repair methods, self-healing technology can efficiently repair cracks and has long-term significance in ensuring the safety and durability of engineering. This paper used melting dispersion condensation method to prepare polypropylene-encapsulated toluene diisocyanate (TDI) microcapsules, and characterize the particle size distribution, mechanical properties, morphology and structure of microcapsules by particle size analyzer, nanoindentation tester, optical microscope and Fourier Transform Infrared Spectrometer. When the mass ratio of polypropylene and TDI is 1:2, the stirring speed is 600rpm, and the preparation temperature is 140°C, the average particle size of microcapsules is 70μm, and the coating rate is 67.2%. The FTIR spectrum of microcapsules shows that there is an asymmetric stretching vibration peak of TDI isocyanate group (2270 cm⁻¹), which proves that TDI has been successfully encapsulated into polypropylene microcapsules. TG shows that the microcapsule has excellent thermal stability. The mechanical properties of microcapsules are good, it is not easy to break during concrete mixing process. When the content of microcapsules is 2.5%, it has a good self-healing ability on concrete cracks and can effectively improve the service life of concrete.

Effect of lightweight aggregate (LWA) and superabsorbent polymers (SAP) on autogenous shrinkage, hydration and properties of UHPC

Shuo Feng, ¹ School of Civil Engineering, Shandong University, Jinan, Shandong Province 250061, China; ² School of Civil Engineering, Harbin Institute of Technology, Harbin, Heilongjiang Province 150090, China

Qingsong Zhang, ¹ Geotechnical and Structural Engineering Research Center, Shandong University, Jinan 250061, Shandong, China

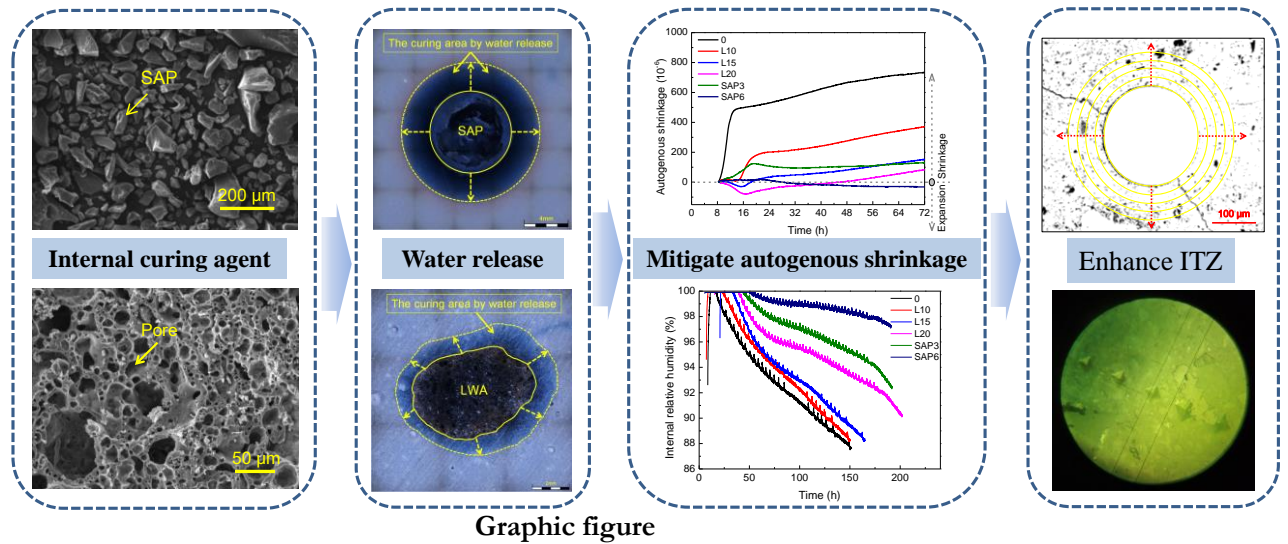
Huigang Xiao, ¹ School of Civil Engineering, Harbin Institute of Technology, Harbin, Heilongjiang Province 150090, China; ² Key Lab of Structures Dynamic Behavior and Control of the Ministry of Education and Key Lab of Smart Prevention and Mitigation of Civil Engineering Disasters of the Ministry of Industry and Information Technology, Harbin Institute of Technology, Harbin 150090, China

Email of the corresponding author: xiaohg@hit.edu.cn

Keywords: Ultra-high performance concrete, lightweight aggregate, superabsorbent polymers, autogenous shrinkage, relative humidity

Ultra-high performance concrete has a large risk to cracking at an early age due to high content of cement and silica fume and the low water to binder ratio bringing high autogenous shrinkage, which severely weakens the mechanical and durability of concrete structure. Internal curing is one of the effective methods to mitigate autogenous shrinkage. The internal curing behavior of saturated lightweight aggregate (LWA) and super absorbent polymer (SAP) was systemically investigated using autogenous shrinkage, isothermal calorimetry, relative humidity (RH), mercury intrusion porosimetry, X-ray microtomography methods, etc. The results indicated that LWA and SAP improve compressive strength by 10% and 5.5%, respectively. High dosage of SAP and LWA has an adverse effect on the mechanical properties of UHPC. The LWA dosage of 10%, 15%, and 20% reduce autogenous shrinkage by 49.4%, 79.2%, and 88.8%, respectively. The SAP dosage of 0.3% reduces autogenous shrinkage by 82%. The content of 0.6% SAP can eliminate autogenous shrinkage at 3 d, and even slightly expand. Internal curing agent slowly releases water to maintain high relative humidity inside, thus reducing capillary tension to inhibit autogenous shrinkage. SAP decreases the rate of early hydration, and LWA retards early hydration. The dosage of LWA at 10% increased the $\text{Ca}(\text{OH})_2$ content of cement matrix by 6.4%, with the increase of LWA dosage to 20%, the $\text{Ca}(\text{OH})_2$ content of the cement matrix increased by 10.1% at 28 d. SAP dosage of 0.3% increased the $\text{Ca}(\text{OH})_2$ content of the cement matrix by 33.5%, and with the further increase of SAP dosage, the $\text{Ca}(\text{OH})_2$ content of the cement matrix increased by 38.0% at 28 d. content in cementite increased by 38.0% with a further increase in SAP dosage. The internal curing agent increases the content of $\text{Ca}(\text{OH})_2$, which is the result of promoting hydration. The addition of LWA at 15% and 20% increased the porosity by 33.9% and 62.4%, and the addition of SAP at 0.3% and 0.6% increased the porosity by 44.4% and 55.9%. The addition of LWA and SAP reduced the total proportion of non-hazardous and less hazardous pores but increased the proportion of hazardous pores, and the proportion of multi-hazardous pores was increased by 37.4%-49.8% with the addition of SAP, and this negative effect on the strength could not offset the positive effect of SAP on the strength. The microhardness decreases with the increase of the distance between LWA and SAP hole walls. The interface between LWA and the matrix is dense. This is due to the connectivity of the holes in the LWA and the good occlusion between the LWA and the cement matrix. Holes were formed around the SAP separated from the cement matrix, micro-cracks existed around the holes, and the edges of the holes formed by the collapse of the SAP were filled with $\text{Ca}(\text{OH})_2$

due to the high affinity of SAP for calcium and other divalent and trivalent ions. The porosity around the steel fibers decreased significantly with increasing distance porosity regardless of the presence of conditioner in the UHPC, and the porosity stabilized when the distance increased from 60 μm to 80 μm . The addition of 15% LWA and 0.3% SAP reduced the steel fiber interface porosity by 17.1%-29.4% and 12.7%-20.8%, respectively.



Graphic figure

The immobilization of Pb, Zn and Cd by spontaneous combustion gangue geopolymer and the depolymerization and reconstruction mechanism

Xiao Han¹, School of Civil Engineering, ¹Dalian University of Technology, Dalian 116024, PR China

Baomin Wang, Dalian University of Technology, Dalian 116024, PR China

Email of the corresponding author: han_xiao@mail.dlut.edu.cn

Keywords: Geopolymer; Spontaneous combustion gangue; Immobilization; Depolymerization and reconstruction.

Extended Abstract:

1. Introduction

MSWI fly ash is classified as hazardous wastes (HW18) in the National Hazardous Waste List, because it is rich in heavy metals (such as Cd, Pb, Cr and Zn etc.), and requires proper treatment before further landfill disposal. In addition, Coal gangue (CG) is one of the largest amounts of industrial wastes in the world, and spontaneous combustion is likely to occur when it reaches an ignition point. This produces a large number of toxic and harmful gases such as CO, CO₂, SO₂ and NO_x, which are discharged into the atmospheric environment, and heavy metal elements such as arsenic, mercury, fluorine, lead and selenium are released into the soil and groundwater. Both MSWI fly ash and spontaneous coal gangue causes serious environmental and ecological pollution problems, and seriously threatens the production safety and the health of surrounding personnel. Therefore, in this study, heavy metals in MSWI fly ash were solidified by geopolymer prepared by spontaneous combustion gangue. The optimum ratio of spontaneous combustion gangue geopolymer were determined. And the deterioration mechanism and action mechanism of heavy metals in MSWI fly ash on the solidified body of spontaneous combustion gangue geopolymer were comprehensively analysed, explored the immobilization mechanism of heavy metals in MSWI fly ash from the perspectives of physical sealing, chemical bonding and adsorption effect, which provides scientific theoretical support for the popularization, application and safety evaluation of solidified body.

2. Methodologies

Firstly, the physical properties (including density, moisture content, particle size distribution, microstructure, water demand ratio, strength activity index, stability, etc.) and chemical properties (including pH value, chemical composition, mineral composition, etc.) of spontaneous combustion gangue and MSWI fly ash were tested and analyzed. And the types, contents, leaching toxicity, occurrence forms and chemical valence of heavy metals in MSWI fly ash were analyzed.

Then, the central composite design experiment of response surface was carried out under the two chemical activators of $K_2O \cdot nSiO_2 + KOH$ and $Na_2O \cdot nSiO_2 + NaOH$ with the setting time, fluidity and compressive strength as the objective function, and the optimum ratio was determined. On the basis of the optimum mix ratio, the depolymerization and repolymerization process and the spatial coordination form and bonding state of Si-Al phase in spontaneous combustion gangue geopolymer with different alkali-cement ratio, water glass modulus and W/C were studied by means of XRD, TG-DTA, FTIR, RAMAN, XPS, MIP, SEM.

Ultimately, according to the total content of Pb²⁺, Zn²⁺ and Cd²⁺ in MSWI fly ash, Pb²⁺ (0.06%-3%), Zn²⁺ (0.25%-3%) and Cd²⁺ (0.01%-1.5%) were added to the geopolymer of

spontaneous combustion gangue in proportion. The physical sealing and chemisorption of N-A-S-H and C-A-S-H for Pb, Zn and Cd, the effects of Pb, Zn and Cd on the micro-morphology, hydration products, pore distribution and mechanical properties of geopolymers, and the phase formation and chemical morphology distribution of Pb, Zn and Cd in spontaneous combustion gangue geopolymer were analyzed using XRD, TG-DTA, FT-IR, RAMAN, XPS, MIP, SEM, ICP.

3. Results and conclusion

Table 1 The optimum ratio and compressive strength of spontaneous combustion gangue geopolymer

	Sodium silicate modulus	Alkali /CG	W/CG	3d	7d	28d	90d	180d	360d
$K_2O \cdot nSiO_2 + KOH$	1	0.14	0.22	8.73	29.46	41.00	55.95	51.53	76.50
$Na_2O \cdot nSiO_2 + NaOH$	2	0.1	0.36	8.23	29.18	39.60	48.33	35.26	59.84

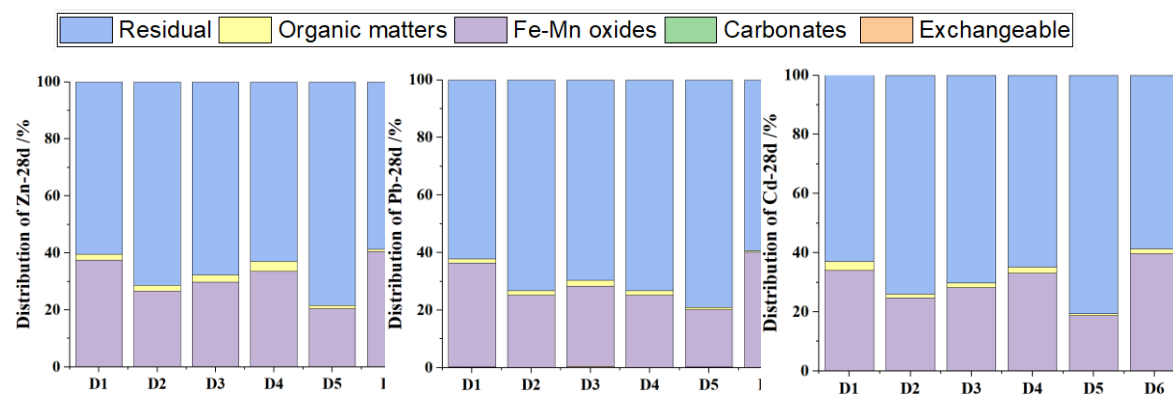


Fig.1 The chemical form of Pb, Zn and Cd in spontaneous combustion gangue geopolymer

The compressive strength of spontaneous combustion gangue geopolymer prepared with $K_2O \cdot nSiO_2 + KOH$ were higher that of $Na_2O \cdot nSiO_2 + NaOH$. And The significance of the influencing factors both were Sodium silicate modulus $>$ Alkali/ CG $>$ W/CG. The best when the content of Pb, Zn and Cd is 0.18%, 1.22% and 0.09%, and the curing rate of 90 d reaches 92.13%, 96.96% and 99.81% respectively. In addition, the chemical form of heavy metals is dominated by bound to carbonate at 3d, and gradually concentrated in bound to Fe-Mn oxides and residue with the increase of age. The crystal peak in the geopolymer of spontaneous combustion coal gangue is mainly SiO_2 , amorphous peak appeared in the range of $20^\circ \sim 40^\circ$ (2 θ), and the flocculent amorphous gel was also observed in SEM. The higher the compressive strength, the wider the stretching vibration peaks of Si-O and Al-O at $1200-950cm^{-1}$. And Na^+ and K^+ have a synergistic effect, and it is difficult for K^+ to move out because of its large radius, which can continuously and effectively promote the Polycondensation between SiO_4 and AlO_4 tetrahedron.

Compressive strength and hydration kinetics of phosphate slag-cement materials under varied curing temperature

Lingling Hu^{1,2,3}, Xianqiang Zhu^{1,2,3*}, Wenjing Wang^{1,2,3}, Guoyi He^{1,2,3}

1. State Key Laboratory of Precision Blasting, Jiangnan University, People's Republic of China
2. Hubei Province Key Laboratory of Engineering Blasting, Jiangnan University, People's Republic of China
3. School of Digital Construction and Blasting Engineering, Jiangnan University, People's Republic of China

Email of the corresponding author: 1163989372@qq.com

Keywords: Phosphate slag, Variable temperature, Macroscopic mechanical properties, Hydration kinetic

Effective usage of industrial waste in concrete is a prominent research direction of renewable building materials; many academics have conducted extensive research on it over the years, and it is possible that renewable building materials have achieved significant progress. With the advancement of industrialization, for example, the new toxic and hazardous industrial waste, renewable building materials have a new era of mission, focusing on this new type of hazardous waste— phosphate slag renewable building materials development is also imminent. However, due to its retardation effect, the application of phosphate slag in concrete has been at a bottleneck for a long time, and research on its macro-performance and micro-mechanism under diverse dose and temperature is insufficient. In this study, the static mechanical properties and hydration kinetic of cementitious materials with different dosages of phosphorite slag (10%, 20, and 30%) and varied w/b ratios of 0.3, 0.4, and 0.5 under variable temperature curing 20 °C, 40 °C, and 60 °C were investigated by static mechanical experiments and hydration kinetic experiments, which were combined with X-ray Computed Tomograph(X-ray CT) and Thermogravimetry analysis /Differential thermogravimetry (TG/DTG) to investigate the relationship among the hydration kinetic, macroscopic mechanical properties, and the microstructural evolution of cementitious materials. From the results, when the temperature was increased from 20 °C to 60 °C (w/b ratios of 0.4) at 2 d, the compressive strength of the pure cement control sample diminished by -1%, while the compressive strength of the cement sample with 20% phosphorous slag increased by 50%, meaning that this high-temperature circumstances showing a positive influence on its early compressive strength. As the temperature was raised to 40 °C (w/b ratios of 0.3), the normalized heat flow of the phosphate slag-cement sample gradually increased from 33% to 56% with the contents of phosphate slag from 10% to 30%, which was significantly greater than that of the pure cement sample (increment of 31%). Furthermore, it was discovered that the porosity of the phosphorus slag sample appeared to be obviously reduced after the increasing the curing temperature, and the internal Ca(OH)₂ content was also significantly increased using X-ray CT scan and TG/DTG experiments on phosphorus slag-cement specimens. Overall, high-temperature curing overcomes the problems caused by the retardation effect of phosphate slag, resulting in a new development in its application in concrete. With further research, there will be a new understanding about the incorporation of phosphate slag, and there will be a significant development for renewable building materials. With the advancement of research, high-temperature phosphate slag maintenance for the macro-performance and micro-mechanisms will be further revealed for the application of phosphate slag in concrete will be more significant development, phosphate slag retarding effect caused by the problem may have a new solution (such as the mixing of silica

ICSBM 2023

3rd International Conference of Sustainable Building Materials

25-27 September, Wuhan, China

fume or fly ash and other active admixtures to improve its early strength). Of course, it is also possible to guide the retardation of phosphate slag, which is used to reduce the early strength of some specific concrete, enhance its mobility and plasticity, in the field of making complex structural designs simpler to execute, or in the manufacturing of prefabricated components.

Effect of MgO content on high-temperature phase transformation of coal gangue

Jintao Li, School of Geoscience and Surveying Engineering, China University of Mining and Technology-Beijing, Beijing 100083, China

Qinfu Liu*, School of Geoscience and Surveying Engineering, China University of Mining and Technology-Beijing, Beijing 100083, China

Email of the corresponding author: lqf@cumtb.edu.cn

Keywords: Coal gangue; Phase transformation; Cordierite; Magnesia silicate mineral.

Coal gangue (CG) is an industrial solid waste generated during coal mining, accounting for about 10-20% of coal output. According to the source of CG, it can be divided into two types: excavation gangue and washing gangue. The washed gangue has the characteristics of a more stable chemical composition and provides a good basis for industrial utilization. CG is a sedimentary rock associated with coal seam in the process of coal formation, its main inorganic chemical composition is Si and Al, which can also be called aluminosilicate solid waste. Therefore, the building materials industry has the potential to become a major consumer area for large-scale utilization of CG. In recent years, the research on the preparation of glass ceramics and mullite ceramics from coal gangue has been carried out gradually, but the research focus is on the practical application properties of the target products. There is not much attention paid to the high-temperature (above 1000°C) phase transformation process of CG or CG with different additives. In this study, CG samples from the Pingshuo mining area of Ningwu Coalfield of Shanxi province were used to study the phase transformation characteristics at high temperatures, and the effect of MgO on the phase transformation of coal gangue at high temperatures was explored by adding different contents of MgO, as well as the phase transition law and mechanism.

The high-temperature calcination experiment is divided into two groups, one is the high-temperature calcination of coal gangue (CG), and the other is the high-temperature calcination of coal gangue mixed with different contents of MgO samples (CM). The heat treatment was performed in a Muffle furnace at temperatures between 400° C and 1400° C with calcination at intervals of 100° C at a warming rate of 10° C/min and held for 2 hours. Subsequently, the samples were cooled to room temperature in the furnace. Characterization of the original and calcined samples using testing methods such as XRD, FTIR, TG/DSC, SEM-EDS, XRF, ICP-MS, etc.

The mineralogical and geochemical analysis of CG shows that its mineral composition is mainly kaolinite and a small amount of boehmite and quartz, and the material composition is relatively single, which can be used as a raw material for the comprehensive utilization of solid waste. The SiO₂/Al₂O₃ mass ratio of CG is 1.14, which can be used as a SiO₂-Al₂O₃ raw material for glass-ceramic or ceramics.

The phase transition of CG after calcination can be roughly divided into two stages, medium and high-temperature phase transition below 1000°C and high-temperature phase transition above 1000°C. In the previous stage, the original minerals kaolinite and boehmite were calcined to remove the hydroxyl groups in the crystal structure, thus forming metakaolinite and alumina in an amorphous state, and anatase mineral phase appears in the stage. The latter stage is mainly manifested as metakaolinite to mullite, and amorphous silica and quartz will be transformed into cristobalite phase, and anatase can not be detected at 1200°C, Ti atoms enter the mineral lattice of mullite.

The mass ratio of SiO₂/MgO in CG is 298, and with the addition of MgO, the mass ratio of SiO₂/MgO ranges from 1.72-7.99. The analysis found that the theoretical mass ratio of SiO₂/MgO of iolite was 3.72 as the cut-off point, and when it was greater than this value, with

ICSBM 2023

3rd International Conference of Sustainable Building Materials

25-27 September, Wuhan, China

the increase of temperature, the Mg-containing mineral was eventually cordierite, but when it was less than this value, the Mg-containing minerals were cordierite, spinel, and enstatite, that is, too high Mg content would inhibit the formation of iolite. During the calcination process at 1000-1400 °C, the phase detected by the experiment is different from the phase simulated by thermodynamics. It may be caused by amorphous silica and alumina formed by the thermal decomposition of the original mineral gangue, which preferentially forms spinel and forsterite with MgO. With 1400°C as the final temperature, when 10w% magnesium oxide is added to CG, the mineral phase of cordierite formed works best. In addition, when the added MgO is less than this value, the phase transition of Mg-containing minerals follows the transformation law of island-chain-cyclic silicate minerals, that is, forsterite-enstatite-cordierite.

Intelligent Grasping Planning of Decoration Waste Using Generative Grasping Convolutional Neural Network

Zuohua LI ^{1,2,*}, Quanxue DENG ^{1,2}, Peicheng LIU ^{1,2}, Jiafei NING ^{1,2}, Yunxuan GONG ^{1,2}
and Qitao YANG ^{1,2}

1 School of Civil and Environmental Engineering, Harbin Institute of Technology, Shenzhen, Shenzhen 518055, China

2 Guangdong Provincial Key Laboratory of Intelligent and Resilient Structures for Civil Engineering, Shenzhen 518055, China

Email of the corresponding author: lizuohua@hit.edu.cn

Keywords: waste recovery; grasping system; intelligent sorting; real-time grasping; decoration waste recycling.

Intelligent sorting robots have the potential to replace manual labor in the sorting of decoration waste in harsh environments. The grasping planning of robots plays a crucial role in achieving intelligent sorting of decoration waste. However, challenges such as unstable grasping accuracy and slow convergence during training persist in intelligent grasping for decoration waste. In this research, we propose a novel approach for intelligent grasping planning of decoration waste, utilizing the Generative Grasping Convolutional Neural Network (GGCNN). This method aims to guide the robot in accurately and efficiently grasping decoration waste items. The proposed method involves preprocessing the collected depth images by applying image binarization to filter out irrelevant information while retaining the depth information of the target objects. To further enhance the training quality of the network, we introduce the Focal Loss function as the algorithm's loss function. Compared to the traditional Mean Square Error (MSE) loss function, the Focal Loss function effectively addresses the issue of imbalanced positive and negative samples. The research results demonstrate that our proposed method achieves a prediction error range of -2.72° to 7.38° for the grasping angles of decoration waste targets, meeting the requirements for robotic arm grasping. Moreover, the predicted grasping widths consistently exceed the actual widths of the target objects, effectively avoiding collisions between the end effector of the robotic arm and the decoration waste caused by excessively narrow width predictions. Compared to the original network GGCNN, our proposed method shows a 5% improvement in the success rate of grasping decoration waste. This improvement highlights the effectiveness of our approach in enhancing grasping accuracy and efficiency.

In conclusion, our research proposes a more efficient strategy for the intelligent recycling and utilization of decoration waste, thereby driving the advancement of waste recovery practices. By implementing intelligent sorting robots and the proposed grasping planning method, we can enhance the efficiency of decoration waste recycling while reducing the risks associated with human workers operating in challenging conditions. Moreover, the accurate and efficient grasping of decoration waste items contributes to the effective recovery and recycling of valuable materials, promoting resource sustainability and minimizing the environmental impact of waste disposal. To enhance the robustness and reliability of the grasping planning capability for decoration waste, we expanded our custom dataset by incorporating the Cornell dataset. This integration allowed us to enrich our dataset with diverse samples from the Cornell dataset, thus improving the overall performance and accuracy of the grasping planning system. By combining these datasets, we ensured a more comprehensive and representative training experience, enabling our system to handle various scenarios and object variations effectively when grasping decoration waste. Through the combination of the GGCNN network and advanced deep learning techniques, our proposed method successfully achieves the grasping of decoration waste in dynamic scenarios. The experimental results validate the feasibility of our approach. Overall, our

ICSBM 2023

3rd International Conference of Sustainable Building Materials

25-27 September, Wuhan, China

research contributes to the development of intelligent waste sorting and recycling systems, offering promising prospects for optimizing resource recovery, reducing environmental pollution, and propelling advancements in the field of waste recovery.

Recycle of contaminated-gypsum in BOF slag system

Xuan Ling, Department of the Built Environment, Eindhoven University of Technology, P.O. Box 513, 5600 MB Eindhoven, The Netherlands

Katrin Schollbach, Department of the Built Environment, Eindhoven University of Technology, P.O. Box 513, 5600 MB Eindhoven, The Netherlands

H.J.H Brouwers, Department of the Built Environment, Eindhoven University of Technology, P.O. Box 513, 5600 MB Eindhoven, The Netherlands

Email of the corresponding author: X.ling@tue.nl

Keywords: Contaminated-gypsum, Heavy metals, BOF slag, Ettringite

The extensive use of sulfuric acid in chemical and metal industries results in a substantial generation of spent sulfuric acid. Neutralizing this spent acid with lime-containing industrial waste products is an efficient disposal method, but it leads to the formation of heavy gypsum-containing precipitates. In NOAH, Norway, nearly 100,000 tons of such precipitates are produced annually, posing a challenge due to the increasing need for landfills to store them. Additionally, these precipitates have a high leachable heavy metal content, hindering their further use.

Basic Oxygen Furnace (BOF) slag, a by-product of steelmaking with an annual production about 10.4 million tons in Europe, primarily consists of dicalcium (C_2S) and tricalcium silicate (C_3S), RO phase, and free lime, making it a potential cementitious material. Previous studies have investigated the combination of steel slag and commercial gypsum, achieving optimal compressive strength with a steel slag to gypsum ratio of 1/16 under carbonation curing. However, the compaction process used in those studies limits practical engineering applications. The desirable mechanical properties of the such blends system is partially attributed to the utilization of steel slag with relatively higher content of CaO and some C_3S . Nonetheless, the phase composition of BOF slag is a complex and dynamic system influenced by multiple factors such as the chemical composition adjustments, steelmaking process parameters. BOF slag generated in the Netherlands, with an annual production of 0.7 million tons, is rich in C_2S and $C_2(A,F)$ but lacks C_3S , resulting in low hydraulic activity and hindering its application as a binder constituent.

This study aims to develop the recycling of contaminated gypsum in BOF slag without C_3S , using a traditional casting method. The addition of potassium-citrate is employed for accelerated reaction and the carbonation curing is adopted. The associated hydration mechanism, mechanical properties, and solidification of heavy metals derived from the CG and BOF slag are investigated. This work contributes to recycling new streams of contaminated gypsum, while developing cement-free building materials. Furthermore, the blends of CG and BOF slag have the potential to capture CO_2 with an enhanced mechanical properties.

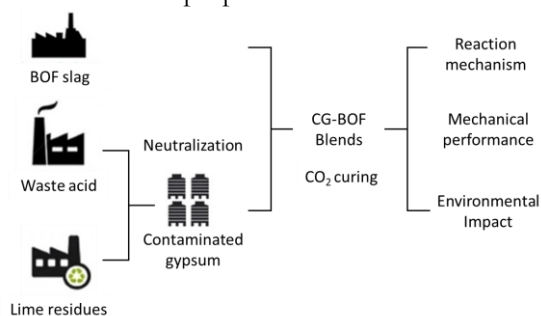


Figure 1: Research programme of the present work.

Mechanical and self-sensing properties of ultra high performance fiber reinforced concrete (UHPFRC) with steel slags

Liu Zhijie ^{1,2}, Qi Xibo ², Shui Zhonghe ^{2,*}

1 International School of Materials Science and Engineering, Wuhan University of Technology, Wuhan, 430070, China

2 State Key Laboratory of Silicate Materials for Architectures, Wuhan University of Technology, Wuhan, 430070, China

Email of the corresponding author: lzjqx@outlook.com

Keywords: UHPFRC, Steel slags, smart concrete, structural health monitoring, self-sensing

Ultra-high performance fiber-reinforced concrete (UHPFRC) has emerged as an advanced cement-based material with superior mechanical properties and durability. However, real-time monitoring of the health status of UHPFRC structures during their service life remains a challenge. Self-sensing cementitious composites, which can sense their own strain/stress and damage by measuring electrical resistance changes, have shown promise for continuous structural health monitoring. Most research has focused on developing self-sensing capabilities in normal concrete by incorporating conductive fillers. It is unclear whether these findings can be extended to UHPFRC, which has very different mechanical properties. This study investigated the effects of incorporating steel slag powder on the mechanical properties, electrical conductivity, and self-sensing capacity of UHPFRC under compression and flexural loading.

UHPFRC typically contains high binder content, low water-to-binder ratio, steel fibers, and superplasticizer. The mix proportions in this study were designed using a modified Andreasen and Andersen particle packing model to optimize particle distribution and minimize porosity. P.II 52.5 cement, silica fume, fly ash, and fine steel slag powder (<10 μm) were used as binders. Sand with particle sizes of 0.075-0.6 mm was used as aggregate. Straight brass-coated steel fibers 13 mm in length and 0.2 mm in diameter were added at 2% by volume. A polycarboxylate-based superplasticizer was incorporated to adjust workability. The control UHPFRC without steel slag was prepared along with mixtures containing 10%, 20%, 30% and 40% cement replacement by steel slag.

The workability, compressive strength, flexural strength, resistance responses under loading, hydration heat, and microstructures of the UHPFRC mixtures were tested. Workability was assessed by slump flow test. Compressive strength was measured on cubic specimens at 1, 7, and 28 days according to EN 196-1. Four-point bending tests were conducted on prism specimens to obtain load-deflection curves and flexural strengths. The fractional change in resistivity (FCR) under compressive or flexural loading was monitored in real-time by a four-probe DC method to evaluate self-sensing capacity. Hydration heat was monitored by isothermal calorimetry over 72 hours. The pore size distribution and connectivity of steel fibers were examined by X-ray computed tomography.

Results showed that the addition of steel slag powder increased the slump flow, indicating improved workability. Compressive strength was reduced at early ages with increasing slag content due to delayed hydration, but the 28-day strengths remained similar up to 20% slag replacement. The first-peak flexural strength increased by up to 48% with slag addition, and deflection at peak load was increased, indicating improved ductility. Under compressive loading, the maximum FCR values were 37.6% for 10% slag and 28.2% for 20% slag, significantly higher

ICSBM 2023

3rd International Conference of Sustainable Building Materials

25-27 September, Wuhan, China

than 19.6% for the control UHPFRC. The FCR increased linearly with stress ratio in these mixtures. Under flexural loading, the maximum FCR increased from 25% for the control to 54.1% with 40% slag. Analysis of X-ray CT images showed the addition of 10-20% slag resulted in well-distributed pores and optimized connectivity of steel fibers.

In conclusion, the partial replacement of cement by fine steel slag powder improved the workability, flexural strength and self-sensing capacity of UHPFRC. Slag content of 10-20% was optimal for enhancing the sensitivity of electrical resistance to applied load, by modifying the pore structure and connectivity of conductive networks in the matrix. The study demonstrates that tailored design of UHPFRC microstructure with steel slag enables real-time monitoring of damage and stress conditions through self-sensing functionality. This electrically conductive UHPFRC has promise for integrated sensing and structural health monitoring of concrete infrastructures. Further work is needed to investigate long-term self-sensing performance and applications in reinforced UHPFRC structures.

Design, Preparation, and Performance of Sustainable Concrete Incorporating Solid Waste of Manganese Residue

LONG Guangcheng, WANG Fan, Bai Min, TANG Zhuo, MA Kunlin, ZENG Xiaohui, XIE Youjun

Central South University, The National Engineering Technology Center for High-speed Railway Construction Technology, Changsha, 410075

The potential environmental risks associated with electrolytic manganese residue (EMR), as well as its complex and inert mineral composition, pose limitations on its direct utilization as a resource. However, the abundant presence of oxide components in electrolytic manganese residue offers new possibilities for the preparation of clinker, mineral admixtures, and ceramic aggregates. This study aims to design and prepare a sustainable concrete system using solid waste derived from EMR. The system consists of EMR-based clinker, EMR-based mineral admixtures, and EMR-based ceramic aggregates, thereby achieving a cradle-to-grave lifecycle approach in a circular economy. By utilizing EMR as main raw material and additional CaO and Al₂O₃, a high-performance clinker system is synthesized at 1200 °C. This clinker system is composed of belite, iron phase solid solution, calcium sulfoaluminate, and anhydrite. The mineral admixtures, which exhibit an activity index exceeding 85%, are obtained by activating the EMR through calcination at temperatures ranging from 800 to 850 °C. The ceramic aggregates are successfully fabricated at 1050 °C using a composition comprising 90% EMR and admixtures. These aggregates exhibit a remarkable barrel compressive strength of 13.1 MPa. The ultimate objective of this research is to employ the aforementioned EMR-based products in the design and production of sustainable concrete. Furthermore, comprehensive testing and evaluation are conducted to investigate the performance and environmental risks associated with the resulting concrete. This study provides novel insights into the high-value utilization of solid waste materials and offers significant contributions to the advancement of sustainable concrete concepts.

Role and Immobilization of cerium(IV) in Portland cement: A chemical analog of plutonium(IV)

Haosen Ma, State Key Laboratory of Silicate Materials for architectures, Wuhan University of Technology, 430070 Wuhan, Hubei, PR China¹

Yanjie Tang, State Key Laboratory of Silicate Materials for architectures, Wuhan University of Technology, 430070 Wuhan, Hubei, PR China¹

Wei Chen, State Key Laboratory of Silicate Materials for architectures, Wuhan University of Technology, 430070 Wuhan, Hubei, PR China¹

Qiu Li*, State Key Laboratory of Silicate Materials for architectures, Wuhan University of Technology, 430070 Wuhan, Hubei, PR China¹

Email of the corresponding author: qiu-li@whut.edu.cn.

Keywords: Plutonium, Cerium, Solidification, Cement, C-(Ce)-S-H gel

The common solidification material for intermediate-level waste (ILW) and low-level waste (LLW) is cementitious materials which has been used for dozens of years on a global scale. ILW and LLW blended with cement, and properly solidified and encapsulated in the cement waste form for the further disposal or storage. The challenge part for ILW and LLW solidification by cementitious materials is the radionuclides immobilization and radiation damage, which mainly comes from the occurrence of isotope Cs, Sr, Co, U, and Pu et al.

In the ILW and LLW, the radionuclides like Cs, Sr and Co were generated in the operation of nuclear power plant and wildly spread in the liquid radioactive waste. Additionally, the isotope U, Pu and Np were usually existing at tetravalent ions in the liquid effluents generated the plutonium-uranium extraction (PUREX) process. These radionuclides released into soil, water body, forest, animals, and ocean after nuclear power plant accident in Chernobyl and Fukushima, even after ten years there still contains large amount radionuclides in the environment of Fukushima nuclear power plant. These isotopes need to be solidified safely and properly for the protection of human health and environment.

In this study, the solidification ability and immobilization mechanism of Ce⁴⁺ with Portland cement and C-S-H were investigated. Leaching test was used to evaluate the Ce⁴⁺ solidification ability of cement paste. Hydration kinetic, microstructure and coordination environment of silicon were used to investigate the effect of Ce(NO₃)₄ to paste. Phase assemblage, chemical binding energy, coordination environment of silicon and microstructure were used to reveal the immobilization mechanism of Ce⁴⁺ by C-S-H gels.

With the increment addition of Ce(NO₃)₄, the free calcium increased suggest the real Ca/Si molar ratio decreased, resulted in the intensity decrease of the (002) reflection of C-S-H. The average coordination number of Ce with O was 4.3, and average coordination number of Si with Ce-O shell was 1.6. Part of Cerium replaced the bridging portion of silicon in the drierketten structure of the silica chains and entered the structure of C-S-H gels, other cerium occurred in CeO₂ crystalline grains intermixed with C-(Ce)-S-H gels. After the entrance process of Ce⁴⁺ into C-S-H structure, the MCL of C-(Ce)-S-H increased, the interlayer spacing of C-S-H decreased, and the binding energy of cerium increased. The cerium has the concentration distribution phenomenon in C-S-H and distributed in the whole sample, and the distribution of cerium transformed form uniform to nonuniform with the cerium content increased.

The solidification mechanism of Cerium by cement material is transformed the free Ce⁴⁺ into CeO₂ crystalline grand and C-(Ce)-S-H gels. The occurrence of Ce in C-Ce-S-H inhibited the entrance process of Al into the structure of C-S-H. CeO₂ crystalline grand and C-(Ce)-S-H gels is stable in the high alkali environment inside the cement paste so that decreased the

ICSBM 2023

3rd International Conference of Sustainable Building Materials

25-27 September, Wuhan, China

leachability of Ce^{4+} . This paper provides a theoretical support for immobilization and solidification of plutonium(IV) in ILW with Portland cement-based materials.

Effect of Geometric Morphology of Recycled Fine Aggregate on the Rheology and Strength of Cement Mortar

Juntao Ma, North China University of Water Resources and Electric Power, School of Civil Engineering and Communication, Zhengzhou, 450045, China

Yunlei Wang, North China University of Water Resources and Electric Power, School of Civil Engineering and Communication, Zhengzhou, 450045, China

Luobing Zhang, North China University of Water Resources and Electric Power, School of Civil Engineering and Communication, Zhengzhou, 450045, China

Juntao Dang, North China University of Water Resources and Electric Power, School of Civil Engineering and Communication, Zhengzhou, 450045, China

Email of the corresponding author: majuntao@ncwu.edu.cn

Keywords: Recycled fine aggregate, Particle shape, Water absorption, Rheological properties, Compressive strength

The rheological properties and mechanical properties of recycled fine aggregate are affected due to its irregular particle shape and high water absorption, which limits its application in cement concrete. In this experiment, the porosity and particle shape of recycled fine aggregate, sodium silicate modified recycled fine aggregate and natural river sand were tested, and the water absorption and bulk density of the particles were analyzed. On this basis, the fluidity, yield stress, plastic viscosity and strength of mortar prepared with different fine aggregate were analyzed, and the mechanism of action was texted. Results revealed that the water absorption and bulk density of the recycled fine aggregate were significantly reduced by the mortar attached to the surface, and the fluidity of the mortar prepared by the recycled fine aggregate was worse than that of the mortar prepared by natural river sand, and the yield stress and plastic viscosity reach 181.09Pa and 24.09Pa·s. Moreover, The rheological properties of recycled fine aggregate mortar were improved by sodium silicate, and its plastic viscosity was equivalent to that of mortar replaced by 60% recycled fine aggregate. When the replacement amount of recycled aggregate was less than 30%, the compressive strength could be increased by about 13%, while the improvement of the strength was not obvious by sodium silicate modification

Mechanical and Thermal Performance of Electric Arc Furnace Slag-based Alkali Activated Mortar

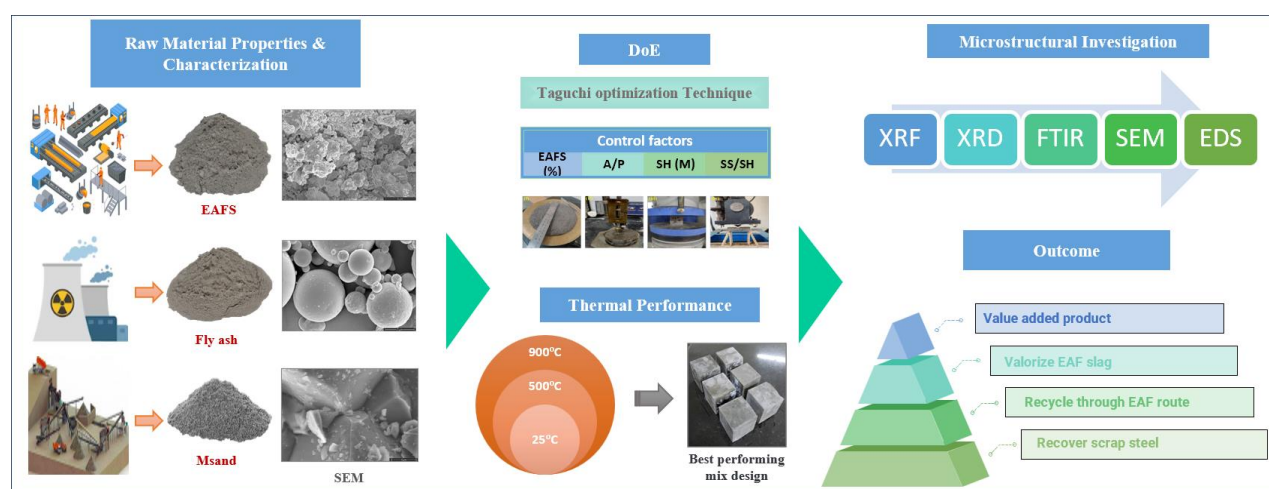
Anant Mishra¹, Pragyana Upadhyaya¹, Mukund Lahoti^{1*}

¹Department of Civil Engineering, BITS-Pilani, Pilani

Email of the corresponding author: mukund.lahoti@pilani.bits-pilani.ac.in

Keywords: Electric arc furnace steel slag; alkali-activated material; Supplementary cementitious materials; Fire-resistance.

Graphical abstract



The greenhouse gases have emerged as a significant environmental concern, with infrastructure development recognized as a major contributing factor. Additionally, the rapid expansion of industrialization has necessitated the use of materials that are durable, sustainable, economical, and fire-resistant. Steel, a highly demanded material for infrastructure projects, is primarily manufactured using two methods: the Blast Furnace (BF) route and the Electric Arc Furnace (EAF) route. The BF route is a traditional method of steel production and relies on iron ore, coke, and limestone, while EAF route mainly uses scrap steel. Additionally, BF route is energy-intensive due to the high temperature requirement, while EAF route is generally more energy efficient by using electricity for melting scrap steel. To effectively address the urgent need for achieving net zero emissions and lower down the environmental burden, a paradigm shift from the conventional Blast Furnace (BF) route to the Electric Arc Furnace (EAF) route is essential. However, this transition leads to an increased production of EAF slag (by-product from EAF route), which is often disposed of in landfills. Despite its potential, the presence of free lime hinders its use as an additive in the cementitious products. However, it is a promising precursor for alkali-activated materials (AAMs) due to high calcium content and silica. These materials exhibit comparable physio-mechanical properties to cementitious materials. This article emphasizes the utilization of EAF slag as a precursor for AAMs that presents an opportunity to reduce waste, promote circular economy principles, and offers a greener alternative material to mitigate greenhouse gas emissions associated with cement production. Additionally, by examining the thermal behaviour and performance of alkali-activated materials derived from EAF slag, this research contributes to the advancement and practical application of fire-resistant construction materials. The integration of EAFS based AAMs into the construction industry not only facilitates a greener and more sustainable future but also enhances the resilience and safety of built environments.

EAFS was sourced and subjected to comprehensive characterization, including analysis of chemical composition, particle size, and mineralogical properties. The Class F Fly ash modifier was replaced incrementally from 0% to 75% (by weight) in steps of 25%. The activator to precursor content ratio was varied from 0.5 to 0.65 (by weight). The combination of activators, specifically the sodium silicate to hydroxide ratio, was adjusted between 1.5 to 3.0. Additionally, the sodium hydroxide molarity ranged from 8 to 14M. To explore the effects of these mix design parameters, Taguchi design of experiment (DoE) methodology was employed. The experimental procedure commenced by dry mixing the precursor and modifier in a Hobart mixer to achieve homogeneity, followed by the addition of manufacturing sand at a fixed ratio of 1:3. To form uniform slurry, an activator was added. The resulting samples were then subjected to ambient curing for duration of 28 days. The samples were then subjected to the elevated temperatures of 500°C and 900°C in a furnace. The heating rate was 5°C/min with a rest time of one hour. Various tests and analyses were conducted to evaluate the fresh, hardened, and residual properties, as well as the durability and microstructural characteristics of the AAMs.

The compressive strength was observed for L16 trial mixes at 25°C, 500°C and 900°C. The mix composed of 75% EAFS and 25% fly ash shows the best results at ambient temperature. All the mix shows a significant decrease in the compressive strength at 500°C due to the unequal thermal stresses, material anisotropy, and crack damage by dehydration of residual physical water in the matrix. Interestingly, the mix composed of 100% EAF slag and 75% EAF slag demonstrated better residual strength at 900°C. This increased strength can be attributed to condensation reactions and chemical changes within the matrix, resulting in the release of chemically bound water and strengthening of the overall matrix. At 900°C, the matrix underwent melting and significant chemical changes, including sintering, which transformed amorphous phases into semicrystalline and ultimately crystalline ceramic phases. Visual observation and analysis supported the formation of Akermanite (impart residual strength) and Gehlenite (highly stable at elevated temperature), contributing to the observed residual strength. Analyses using Fourier transform infrared spectroscopy revealed the low reactivity of EAF slag at room temperature, indicating the presence of unreacted material. However, at elevated temperatures, alkaline activation of the precursors was evident. Microstructural characterization showed the transformation of unreacted EAF slag particles, cracks, and voids into a more homogeneous matrix with fewer microcracks and voids at 900°C. In conclusion, the utilization of EAF slag offers a way to reduce land accumulation, promote a waste-to-wealth approach, mitigate environmental burdens, and provide a sustainable alternative for fire-resistant construction materials.

Synergistic Valorization of Hazardous Nickel-Chrome Plating Sludge in Alkali-Activated Electric Arc Furnace Slag-Fly Ash Blended Bricks: A Waste to Wealth Approach

Anant Mishra¹, Gaurav Tyagi¹, Mukund Lahoti^{1*}, Anupam Singhal¹, Srikanta Routroy¹, Dipendu Bhunia¹

¹Department of Civil Engineering, BITS-Pilani, Pilani

Email of the corresponding author: mukund.lahoti@pilani.bits-pilani.ac.in

Keywords: Nickel-chromium plating sludge; electric arc furnace steel slag; alkali-activated material; Supplementary cementitious materials; sludge re-utilization

Nickel-chromium (Ni-Cr) Plating Sludge (NCPS) is the by-product generated during the chrome-electroplating of steel, which imparts mirror-like silver shine, enhanced durability, and hardness to steel. Unfortunately, NCPS is hazardous as it contains high content (25%~30%) of heavy metals such as nickel and chromium. Landfilling is the only prevalent legitimate method of sludge disposal. But, landfilling is risky, expensive, and increasingly unfeasible due to a shortage of urban land space. Electric arc furnace slag (EAFS)- is another unexplored industrial waste. It is the by-product of secondary steel manufacturing through the electric arc furnace route. Its reutilization efforts in concrete and alkali-activated material have limitations of volume expansion and flash setting, respectively. This paper is a pioneering attempt that adopts a multi-pronged strategy of synergistic waste utilization. We report the valorization of NCPS in a novel, ambiently cured alkali-activated EAFS- fly ash binder (AEFB). The raw materials were dry mixed in a Hobart mixer to attain homogenization. A uniform slurry was then made by adding a combination of activators (sodium silicate and sodium hydroxide). Around 90 bricks and cube specimens were cast and ambiently cured for 28 and 56 days. The fresh and hardened properties were analyzed using tests for flowability, setting time, and compressive strength. The durability was assessed using water absorption and acid resistance tests. Efflorescence tests were conducted with a visual examination. Furthermore, microstructural characteristics were analysed. To analyze the environmental safety of bricks, the United States Environmental Protection Agency (USEPA)-based Toxicity Characteristic Leaching Procedure (TCLP) Method 1311 was used. The heavy metals concentration in the leachate was analyzed using Inductively Coupled Plasma Optical Emission Spectroscopy (ICP-OES). With progressive NCPS incorporation, the binder flowability was slightly reduced (10%-15%), and the setting time remained almost unaffected. Initially, as NCPS substituted increasing percentages of binder content, NCPS addition prevented the compressive strength degradation in proportion to binder content reduction by acting as a micro-filler in the binder matrix and contributing to the compressive strength. However, after 10% replacement, compressive strength reduced significantly due to the major replacement of calcium-sodium aluminate silicate hydrate ((C,N)-A-S-H) gel by the non-reactive NCPS particles. Nevertheless, the strength of all the mixes averaged 30MPa, thus well-exceeded the standard building codes' provisions. Water absorption values of AEFB bricks was found to be around 3%-7%, and were well below the permissible limit of 20%. Minimal deterioration of brick texture was observed after six months of acid-resistance tests performed with H₂SO₄ (5% w/w) and MgSO₄ (2.5% w/w). Nil efflorescence was detected indicating negligible salt percolation on the brick surface. XRD tests revealed presence of calcite, mullite, quartz, gehlenite, and merwinite. FTIR spectra depicted shifting of T-O-T (T=Si/Al) bond towards a longer wave number indicating alkaline activation of the precursors. The microstructural characterization results indicated that gel formation remains unaffected by the addition of NCPS. SEM-EDS images confirmed the filling of micro-pores of the binder matrix by sludge particles and the effective immobilization of heavy metals of sludge within the binder matrix. TCLP test results indicated the concentration of heavy metals in the leachate to be well below the permissible

ICSBM 2023

3rd International Conference of Sustainable Building Materials
25-27 September, Wuhan, China

limits.

Influence of Temperature in Accelerated Dry Carbonation of Recycled Concrete Fines

L.N. Sousa¹, K. Schollbach¹, and H.J.H. Brouwers¹

¹ Department of the Built Environment, Eindhoven University of Technology

Email of the corresponding author: l.nobrega.sousa@tue.nl

Keywords: accelerated carbonation; concrete fines waste; temperature.

The recycling of concrete from construction and demolition (C&D) wastes has gained significant attention as a way to mitigate the negative environmental consequences associated with its production. C&D waste is typically collected from demolition sites and undergoes a process of crushing and sieving to separate the aggregate fraction for reuse. However, this process also generates a fine fraction of concrete that contains a high concentration of cement paste. Incorporating this fine fraction directly into new cement-based mixtures has challenges due to its high water absorption capacity and low reactivity.

To address this issue, researchers have explored the concept of accelerated semi-dry carbonation of concrete waste, also called recycled concrete fines (RCf). This technique involves a direct gas-solid reaction in a CO₂-rich environment with the presence of water vapor. In general, the underlying principle is the reaction of CO₂ with hydrated cement phases, leading to the formation of calcium carbonate (CaCO₃) and silica gel. This transformation allows the concrete waste fines to be reincorporated into building materials while simultaneously CO₂ uptake.

Temperature plays a critical role in achieving optimal efficiency in the accelerated carbonation process. Therefore, this study aims to investigate the effects of temperature on the accelerated carbonation of recycled concrete fines. The RCf used in this study was provided by industry partners (Circular Mineraal, Netherlands). Experimental investigations were conducted at different temperatures, 20, 35, and 50°C, during 3h, 1 day, and 3 days of carbonation. Then, after analysis of phase composition (XRD), SSA by BET method, and thermogravimetric analysis of samples before and after carbonation, it was observed that increasing the temperature affected the generation of calcium carbonate, the main product of carbonation. Thus, this study aims to contribute to our understanding of the accelerated carbonation of recycled concrete fines provided by industry and its potential as a CO₂ uptake. Additionally, the findings provide valuable insights into optimizing process parameters of semi-dry carbonation of recycled concrete fines.

Assessment of mechanical and durability properties of concrete containing waste ceramic tiles as coarse aggregates

Suvash Chandra Paul¹, Department of Civil Engineering, International University of Business Agriculture and Technology, Dhaka 1230, Bangladesh

Samrat Ashek Ullah Faruky², Department of Civil Engineering, International University of Business Agriculture and Technology, Dhaka 1230, Bangladesh

Noor Md. Sadiqul Hasan³, Department of Civil Engineering, International University of Business Agriculture and Technology, Dhaka 1230, Bangladesh

Md Abdul Basit⁴, Department of Civil Engineering, International University of Business Agriculture and Technology, Dhaka 1230, Bangladesh

Md Jihad Miah⁵, Department of Civil and Architectural Engineering, Aarhus University, Aarhus 8000, Denmark

Adewumi John Babafemi⁶, Department of Civil Engineering, Stellenbosch University, Stellenbosch 7602, South Africa

Email of the corresponding author: ajbabafemi@sun.ac.za

Keywords: Ceramic tiles waste, mechanical strength, water absorption, pores, microstructure in tiles concrete.

Due to the lack of proper recycling technology and knowledge, the demolished waste generated from various construction projects and old structures is a major concern in many countries. Landfilling sites with demolished waste also seems to be an issue in some countries. Conversely, the growing demand for modern infrastructures requires a vast amount of aggregates as it is one of the major constituents of concrete. Generally, aggregates are collected from the quarry or breaking the mountains, which are limited in nature. In many countries, construction industries import natural aggregates to meet their demand which may increase the cost of concrete. Therefore, alternative sources such as recycling the demolished concrete or aggregates like byproducts generated from different sources could play an important role in smooth concrete production. Using recycled materials like aggregates in concrete production has numerous benefits in reducing CO₂ emissions, saving landfill space, preserving natural resources, reducing the cost of new concrete, etc. Generally, recycled aggregates are cheaper than natural or virgin aggregates as they are abundant and often do not meet the requirements in many applications.

Tile waste generated from the ceramic industry, demolished buildings or even during the construction process and setting of a building is also a challenging issue and recycling them could be one way to solve this waste generation. This research work aimed to utilize the waste ceramic tiles in concrete production that may finally minimize the environmental impact and create a new recycling business. Therefore, for the purpose of the research work, ceramic tiles as coarse aggregates in concrete were used at a replacement level of 0%, 10%, 20%, 30%, 50%, and 100%, respectively, of natural coarse aggregates. The concrete cylinder was cast and tested for compressive and split tensile strength after curing for 7, 14 and 28 days. For determining the water absorption and pores in the concrete, 50 mm thickness and 100 mm diameter disc-shaped samples were also prepared for all mixes according to ASTM C642. Microstructural studies were also performed using scan electron microscopy (SEM) image analysis for selected mixes. Different relations among strength, water absorption and pores are also developed for the prediction of concrete properties using tiles aggregates.

ICSBM 2023

3rd International Conference of Sustainable Building Materials

25-27 September, Wuhan, China

The experimental results indicate that compared to the reference concrete, both compressive and split tensile strength of concrete decreased as the percentages of tiles aggregates increased. However, 10% aggregate replacement still seems acceptable as in the replacement level, the strength reduction was relatively low. Generally, the smooth surface and flat shape of waste tiles aggregates might form less bonding among the aggregates and cement paste and, thus, strength reduced. Water absorption and the percentages of total pores in the concrete samples for all mixes were also higher when compared with the reference concrete. A linear relationship is also found among compressive strength to water absorption and pores. As the absorption and pores in concrete increased, compressive strength decreased gradually. Microstructural analysis shows a weak interfacial transition zone (ITZ) form between the tile aggregate and cement paste, which could be the main reason for the lower performance of concrete mixes with tiles aggregates. Nevertheless, the successful application of the appropriate amount of tile aggregate can not only reduce the cost of concrete but could also preserve the environment.

Limitation of Innovation and Sustainability - Example of Industrial Floors in Germany

Chris Straub, ¹CSH CONCEPT GmbH i.G., Tannenkrugstraße 22-28, D-26180 Rastede, Germany, cs@aii-boden.de

Ralf Rosener, ¹, rr@gruppe-industrieboden.de

Jan Martens, ¹, jm@aii-boden.de

Email of the corresponding author: cs@aii-boden.de

Keywords: industrial floor, problems, state-of-the-art, real-life-application

The industrial or real-life application of scientific results is often difficult and time intensive. As well the combination of various approaches that (at the first glance) have nothing in common may result in undesired side effects. As well the changing needs and regulations need to be accounted for. Sometimes it is said that the transition from the laboratory to the real world takes 20-30 years. Long term studies under real conditions may take another 10-20 years, and only thereafter it might have a change to be widely applied. Within this time frame the laws and the scientific knowledge may have changed considerably so the “new” technology might be already outdated.

Sustainability can be achieved by various means. One way is to apply sustainable materials with a sustainable technology, another is the usage of (maybe not so sustainable) materials and technology, but to have the result long lasting and maintenance free. Because the real sustainability of something can only be determined at the end of its life and after it has been recycled. An optimal solution would be to combine both mentioned approaches.

Industrial floors are exposed to different loads (static/dynamic), whereas the surface smoothness should be kept for years. The typical weathering of concrete surfaces over time (chemical attack, mechanical abrasion, freeze-thaw stress, ...) apply as well. And while it is quite common to change the interior of a production hall, the floor can hardly be changed without a major time loss (time = money) and high investment costs. In most cases it is cheaper to build a new hall.

Depending on the economical area or the purpose of the industrial building, the floor needs to fulfil different demands. In most cases it is a concrete floor, in some cases with a surface layer. And because a floor is something that needs to function perfectly for the whole time, owners are not inclined to “try something new and innovative”, they want certainty. Especially if the “new and innovative” system has neither been field-tested nor been in service for more than 10 years. Strangely enough new technology can be implemented easier than new chemistry (i.e. new binder).

For example: If a company can offer a joint-less industrial floor with the traditional concrete from the concrete-mixing-plant nearby, that is ok. But if the same technology as usual should be applied but with a new innovative binder (or improved aggregates, or whatever), then there is no way that any customer want to have this kind of “experimentation” on his floor.

Another point worth mentioning are the standards. Luckily (?) there are no specific standards for industrial floors in Germany. However, there are standards for the cement (e.g., DIN EN 197), the concrete (e.g., DIN 1045), the surface roughness (EN 16165) of the floor and much more. They must be applied if any of the materials are to be used or if people are walking over the floor. Most gaps in between are covered by industrial guidelines, which are basically as mandatory as “real” standards.

ICSBM 2023

3rd International Conference of Sustainable Building Materials

25-27 September, Wuhan, China

For example: The application of polymer-fibres in concrete is very limited, because there are no “official” guidelines how to calculate the static/dynamic load or the internal stress (calculation of the crack width).

With these limitations it is very hard to be innovative in industrial flooring in Germany.

The state of the art is currently:

- Reinforced concrete (because there is hardly anybody anymore who dares to calculate not-reinforced concrete, whereas in most cases the CO₂-output of the floor could be significantly lowered without the usage of steel, but with a sufficiently thicker concrete layer).
- The reinforcement could be a steel mesh or steel fibres or combination of both.
- In most cases the concrete is monolithic, whereas screeds are common as well.
- Nearly all concrete surfaces are power-trowelled. Very few are smoothed by other means.
- It is cheaper (during the construction) to keep the bare concrete surface, whereas for some applications an additional top-coating (epoxy, PU, tiles, etc.) is necessary.

Developing Sustainable Building Materials through Utilization of Steel Industrial Solid Waste: A Case Study of Sintering Flue Gas Desulphurization Ash and Steel Slag Composite Cementitious Material

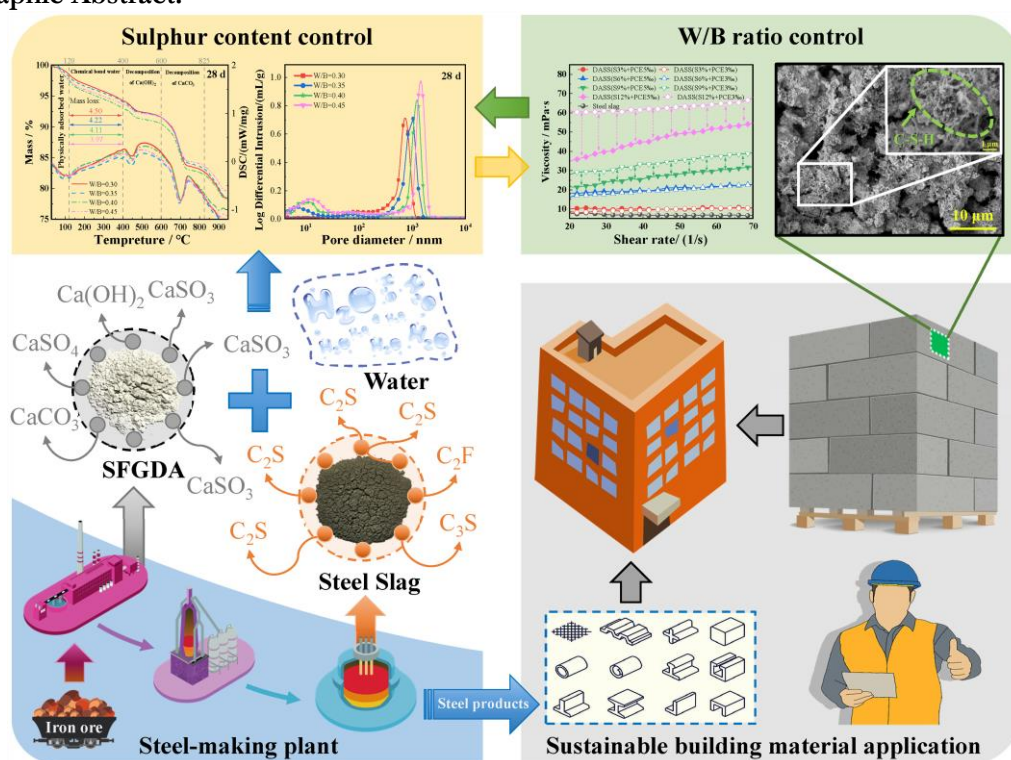
Rui Sun^{1,2}, ¹School of chemical and environmental engineering, China University of Mining and Technology-Beijing, Beijing 100083, China; ² Department of Civil and Environmental Engineering, The Hong Kong Polytechnic University, Hung Hom, Kowloon, Hong Kong, China

Dongmin Wang^{1*}, ¹School of chemical and environmental engineering, China University of Mining and Technology-Beijing, Beijing 100083, China

Email of the corresponding author: wangdongmin@cumtb.edu.cn

Keywords: sintering flue-gas desulphurization ash, steel slag, hydration mechanism, sulphur content

Graphic Abstract:



Abstract:

Producing sustainable building materials using industrial solid waste can reduce dependence on cement and promote resource recycling. The sintering flue gas desulphurization ash (SFGDA) has become the largest solid waste except granulated blast furnace slag (GBFS) and steel slag (SS) discharged by steel-making plant, and is difficult to reuse due to its high CaSO₃ content. In recent years, a significant increase in accumulated SFGDA stock, driven by stringent flue gas emission policies, has created new environmental issues. This paper investigates the hydration behavior of a low-carbon cementitious material named DASS, consisting of SFGDA and SS, under different water/binder (W/B) ratios (0.30, 0.35, 0.40, 0.45) and sulphur contents (3.14%, 6.28%, 9.42%, 12.56%). The study aims to reveal the hydration mechanism of the DASS composite cementitious material, examining both the properties of fresh paste (fluidity, rheological properties, and setting time) and hardened paste (mechanical strength). The hydration process of the DASS composite

cementitious material is clarified through the analysis of heat release, hydrate assembly, and microstructure evolution. Furthermore, the compatibility between the DASS composite cementitious material and three types of fine aggregates is compared, providing a basis for its use as a building material. The hardening of the DASS composite cementitious material is mainly attributed to the hydration of SS, promoted by the anions dissolved from SFGDA, such as SO_3^{2-} and OH^- . The hydration products of the DASS composite cementitious material include C-S-H, C-A-S-H, $\text{Ca}(\text{OH})_2$, and $\text{K}_2\text{Ca}_5(\text{SO}_4)_6 \cdot \text{H}_2\text{O}$. The SO_3^{2-} and OH^- dissolved from SFGDA destroy the dense surface of steel slag, accelerating the dissolution of C_2S , C_2F , and other minerals, leading to the formation of C-S-H and more $\text{Ca}(\text{OH})_2$. While a high W/B ratio provides good workability, excessive water only leads to a short-term improvement in heat release during dissolution without contributing to the hydration reaction. A loose matrix structure with numerous unhydrated particles is formed at a W/B ratio of 0.45. Conversely, reducing the W/B ratio to 0.35 significantly shortens the setting time and increases the compressive strength at 28 days from 4.49 MPa to 9.40 MPa for the DASS cementitious material. The sulphur phase introduced by SFGDA clearly influences the hydration of the DASS composite cementitious material in the following three aspects. First, in the fresh paste, both setting time and fluidity decrease with increasing sulphur content, beside the rheological properties can be improved notably by superplasticizer, especially at high sulphur content. Second, heat release analysis shows that for sulphur content up to 3%, similar to the sulphur content requirement of Portland cement, the hydration exothermic peak appears at 3 hours, 2 hours earlier than pure steel slag paste. The cumulative heat release at 72 hours decreases with increasing sulphur content, ranging from 38.61 J/g to 41.27 J/g. Third, the compressive strength of hardened DASS paste increases gradually with sulphur content from 3.14% to 9.42% up to 28 days, but drops with further increases in sulphur content. After 28 days, the mechanical properties suffer severe damage when the sulphur content reaches 12%. In the DASS paste with a W/B ratio of 0.35 and a sulphur content of 9.42%, a large amount of newly formed $\text{Ca}(\text{OH})_2$ is consumed by the pozzolanic reaction of steel slag after 60 days, generating more C-S-H to fill the pores between raw material particles. According to chemical reaction equilibrium, a quick and continued accumulation of hydrates supporting strength development only occurs with a suitable OH^- concentration in the liquid phase, thus the dosage of SFGDA should be controlled. In summary, the recommended proportioning of the DASS cementitious material includes approximately 6%~9% sulphur supplied by SFGDA, and higher mechanical properties can be achieved by lowering the W/B ratio as much as possible. This innovative low-carbon cementitious material can be easily and conveniently produced by steel-making plants, making it a viable option for sustainable building materials in constructions.

Effect of different heat treatment conditions on the activity of recycled powder

The effects of different calcination temperature, heating rate and holding time on the activity of recycled powder (RP) were studied. The mechanical property, mineral component, reaction products and microstructure of modified RP were analyzed by compressive strength, X-ray diffraction, infrared spectroscopy and scanning electron microscopy. The results show that the order of influence on the activity of RP is calcination temperature, holding time and heating rate. Under the optimal heat treatment condition (600 °C calcination temperature + 60 min holding time + 5 °C/min heating rate), the 28d compressive strength of the specimen can reach 40.8 MPa, which is 480% of the strength of original specimen. RP prepared at different heat treatment conditions have various compositions and structures, which is the essential reason for the change of their hydration reactivity.

Future fossil-free steelmaking slags – prospect for sustainable use in building materials

Van der Laan, Sieger R^{1,2, 1)} Dept. PDM, Tata Steel R&D, Netherlands

Schollbach, K., ²⁾Building materials, Dept. Built Environment, Eindhoven University of Technology.

Email of the corresponding author: sieger.van-der-laan@tatasteelurope.com

Keywords: Basic Oxygen Furnace slags, Electric Furnace Slags, Supplementary Cementitious Materials

Introduction

As mandated by the European Green Deal (European Commission, 2021), in the next seven years the iron & steel industry, as well as the cement industry in Europe will need to drastically transform their production processes to achieve major reductions in CO₂-emissions and a circular economy. As part of this process steel production will change from carbothermic to hydrogen based which will lead to significantly different slags with consequences for the cement industry. Currently Blast Furnace (BF) slag, a white slag from carbothermic iron-production is an important SCM used to replace up to 85% of Ordinary Portland cement (OPC) (EN 197-1 Cement - Part 1) resulting in a high-quality binder with much lower embodied carbon than Portland cement. Global Annual BF-slag production is around 380 Million ton/y [1], compared to 3.8 Billion ton/y of Portland Cement clinker [2], and can fulfil about 10% of the cement demand. Furthermore, Steel industry produces large amounts black slags, the Basic Oxygen Furnace slags from BF-metal refining (165 million ton/y) and the Electric Arc Furnace slags from iron-scrap recycling (120 Mton) [3, 4]. These latter two slags contain high amounts of iron-oxide components and have found no large scale sustainable application, specifically because of heavy metal leaching risks. There is a dual challenge, can steelmaking from iron-ore by hydrogen reduction produce white slags that are suitable as SCM's like BF slag, and can current and future ferrous-rich black slags become fully sustainable with circular use in building materials?

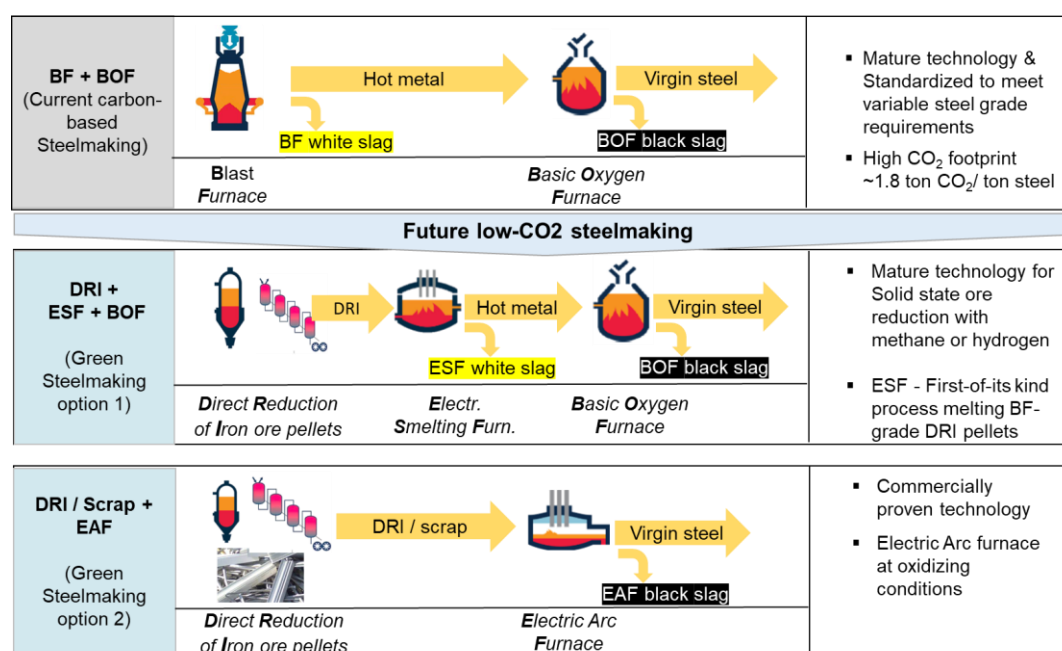


Figure 1: Predominant current and future steelmaking production routes.

Current and near-future processes

Solid state hydrogen-based reduction of iron ore (DRI) will replace the blast furnace (BF) process and therefore the production of BF slag in its current form will stop. In the BF route, reduction and melting are both achieved inside the BF itself, and refining is performed in a separate Basic Oxygen Furnace (BOF) (Fig 1). For the new DRI-based process route, the DRI-unit only performs reduction and all impurities from the ore remain in the solid DRI. Subsequently the impurities are removed during melting in an Electric Furnace forming a slag. There are two furnace options that represent two fundamentally different process options for DRI melting, oxidizing or reducing conditions. Under oxidizing conditions in an Electric Arc Furnace (EAF), a ferrous black slags will form (DRI-EAF). The EAF directly yields virgin steel, requiring only secondary metallurgical modifications to achieve the desired end-product. Melting under reducing conditions in an Electric Smelting Furnace (ESF) would produce an iron-free white slag (DRI-ESF). The latter process would require a further refinement step of the metal in a Basic Oxygen Furnace (BOF) with yet another slag as by-product (Figure 1). The first choice of oxidizing conditions (EAF) Has fully mature technology at industrial scale (TRL9) facilitating the immediate transformation towards “green” steelmaking, however, for the long-term the process development under reducing conditions for DRI melting (ESF) are preferable.

Future slag amounts and compositions

The produced slag amounts vary with the production route. In the carbon-based route (BF-BOF) 400 kg of slag is produced per ton of steel of which 275 kg (BF slag) can be valorized as SCM. In the green routes, the outlook is bleaker, only white slag forms in the DRI-ESF route and at about half the rate of the BF-route.

Table 1: Slag rates for the “green” steel transition (in kg / ton liquid steel)

Slag type	BF	BOF	Scrap - EAF	DRI-EAF	DRI-ESF
current	275 ^[3]	126 ^[3]	169 ^[3]	130-300	130-200

The suitability of slags for the cement industry depends on several factors. These are: predictable stable composition, grindability, reactivity & workability, environmental safety, long term volume stability and durability. Starting point are the phases present. This is determined by the ratio of major elements and the cooling speed of the slag. Minor and trace elements are also strongly influential. Once they become solubilized they form aqueous oxy anions (silicate, phosphate, carbonate, vanadate, chromate, etc) and their concentration controls the formation of hydrated phases, which in turn determines the strength, leaching and durability of a cementitious material.

In the Reducing Furnace (ESF) process route, a CMAS-rich slag is produced of which the minor element and trace element content is subject of ongoing investigations. Since conditions in the ESF are expected to be slightly less reducing than in the Blast Furnace, the slag will take up more phosphorous, titanium, vanadium, manganese and chromium (in oxide form). However, the exact concentrations these element-oxides are dependent on the process itself and the DRI composition, in turn dependent on the ore and fluxes used for DRI-pellet making. Hence, a range of compositions need to be investigated for building material application.

Conclusions

The prospective slags from hydrogen-steelmaking routes will pose a serious challenge to the cement industry for use. Amounts of white slag will be less than half and the EAF slags will be difficult to activate for use as SCM, and likely can only serve as aggregate. BOF slags will remain to be produced and will remain to have an unfulfilled potential as binder.

Reactivity and Microstructure of De-chlorinated Ti-Extracted Residues

Shuping Wang^{1*}, Jingxiong Zhong¹, Yuntao Xin¹, Xuwei Lv¹, Guanwu Zeng²

¹ College of Materials Science and Engineering, Chongqing University, Chongqing, China

² State Key Laboratory of Vanadium and Titanium Resources Comprehensive Utilization, Panzhihua, Sichuan, China

Email of the corresponding author: shuping@cqu.edu.cn

Keywords: Ti-extracted Residue, De-chlorination, Reactivity, Microstructure

De-chlorinated Ti-extracted residue was a by-product when the titanium was extracted from blastfurnace slag by “high temperature carbonization and low temperature selective chlorination” method and a de-chlorination process subsequently. However, after this special treatment, the potential application of the residue as a supplementary cementitious material is unclear. This study aims to investigate the reactivity of the residues with three different de-chlorinated degrees. Grinding was conducted on the residues to increase their specific surface and consequently to improve its reactivity. The pozzolanic reactivity of the residues were evaluated by the compressive strength ratio, and meanwhile, the mechanism of reactivity improvement by grinding was discussed according to the microstructure analysis. Results showed that the residues had similar chemical compositions to those of ground blastfurnace slag (GGBS), but the reactivity of the residues decreased with increasing degree of de-chlorination. Only the residue without de-chlorination treatment showed a similar reactivity to that of GGBS. It was because the residues exhibited increased polymerization of silicate tetrahedra and decreased glassy structure content after de-chlorination. Grinding the material to a specific surface area higher than 500 kg/m² was greatly beneficial to the reactivity improvement of the residues. The optimum values of pozzolanic reactivity were 136.7%, 91.6% and 81.5% for the originally Ti-extracted residue, low and high de-chlorinated degree of Ti-extracted residues, respectively. It was attributed to that the Si-O bonding of the residues would be broken by mechanical grinding, leading to an increasing amount of glassy structure. Consequently, the reactivity of the residues was improved. This investigation demonstrated that the residues can be used as supplementary cementitious materials in cement and concrete.

A novel method of co-disposal of steel slag and municipal solid waste incineration fly ash under alkali activation

Yunqing Xing¹, Baomin Wang²

¹Doctor in Materials Science, School of Civil Engineering, Dalian University of Technology, Dalian city, Liaoning Province, 116024, China.

²Professor, School of Civil Engineering, Dalian University of Technology, Dalian city, Liaoning Province, 116024, China.

Email of the corresponding author: wangbm@dlut.edu.cn

Keywords: chemical form, heavy metal, steel slag; MSWI FA; C-(A)-S-H

Municipal solid waste incineration fly ash (MSWI FA) is a by-product of municipal solid waste incineration and regarded as hazardous waste in many countries because of high content of heavy metals, chloride salts, sulfate, and dioxin. The harmless and efficient disposal of MSWI FA has become an urgent problem to be solved. Alkali-activated cement as an alternative material to ordinary Portland cement have superior durability under aggressive environments. Alkali-activated binders can effectively solidify heavy metals of MSWI FA due to its special silicon-oxygen tetrahedral and aluminum-oxygen tetrahedral structure. Due to the low content of silicon and aluminum, it is not enough to use alkali-activated MSWI FA alone to fix its heavy metals, and additional materials with the pozzolanic activity or latent hydraulicity. Steel slag is an industrial by-product of the steel manufacturing process and large amount of steel slag is piled up and discarded and causes series of environmental pollution. Steel slag contains silicate, aluminate, and ferric aluminate phases like cement clinker and the cementitious properties of steel slag can be improved by alkaline activation. This makes it possible for steel slag to be used as a complementary precursor to immobilize heavy metals in MSWI FA. The key to solidification treatment is to convert high migration active heavy metals from MSWI FA into stable and insoluble chemical forms and reduce their contact with the external environment. This study aimed to solidify the harmful components in MSWI FA by alkali activation and explore the influence of steel slag on the phase evolution and solidification mechanism of heavy metals with curing time. X-ray diffraction (XRD), Fourier transform infrared spectrometer (FTIR), thermogravimetry (TG) and scanning electron microscope (SEM) were carried out to characterize the microstructure and composition of solidified body and explore the solidification mechanism. X-ray photoelectron spectroscopy (XPS) and improved Tessier method were performed to determine the chemical forms of heavy metals. The leaching toxicity of MSWI FA and all specimens was tested according to the Chinese Standard HJ/T 299-2007. The leaching concentrations of heavy metal in leachates were measured by Inductive Coupled Plasma Emission Spectrometer (ICP). Compared with untreated MSWI FA, the leaching concentration of Pb and Zn in alkali-activated solidified bodies with the addition of steel slag was greatly reduced. The leaching behaviour of heavy metals was closely related to the proportion of exchangeable and carbonates form. Pb and Zn on the MSWI FA surface existed in the form of PbCl₂, PbCO₃, PbSO₄, ZnO and ZnCl₂, equivalent to exchangeable and carbonates fraction in sequential extraction process. Under alkali-activation, the chemical forms of Pb and Zn in solidified body were converted into stable and insoluble precipitation, which reduced the leaching toxicity of heavy metals. The negative charge generated due to the substitution of aluminum for silicon in C-(A)-S-H gel provided binding sites for heavy metal cations. With the addition of steel slag, more C-A-S-H gel formation and C-(A)-S-H gel with larger Al/Si ratio and smaller Ca/Si ratio showed higher degree of polymerization and crosslinking than alkali-activated MSWI FA matrix, further reducing the migration activity of Pb and Zn. The compressive strength of the solidified body with steel slag increased significantly, which enhanced the physical encapsulation for Pb and Zn. Moreover, the electrostatic adsorption of chloride ions by C-(A)-S-H gel and the

ICSBM 2023

3rd International Conference of Sustainable Building Materials

25-27 September, Wuhan, China

formation of Friedel' salt reduced the chloride salt content adhering to the solidified body surface and reduced their migration activity.

A novel power ultrasonic-assisted mixing technology to prepare cement paste: dispersion, hydration dynamics and products evolution of Portland cement paste

Guangqi Xiong^{1,2}, College of Materials Science and Engineering, Chongqing University, Chongqing, 400045, China; Department of Civil and Environmental Engineering, The Hong Kong Polytechnic University, Hung Hom, Kowloon, Hong Kong, China

Yuanliang Ren¹, College of Materials Science and Engineering, Chongqing University, Chongqing, 400045, China

Zheng Fang¹, College of Materials Science and Engineering, Chongqing University, Chongqing, 400045, China

Xiaolong Jia¹, College of Materials Science and Engineering, Chongqing University, Chongqing, 400045, China

Chong Wang^{1*}, College of Materials Science and Engineering, Chongqing University, Chongqing, 400045, China

Shuai Zhou^{1*}, College of Materials Science and Engineering, Chongqing University, Chongqing, 400045, China

Email of the corresponding author: chongwang@cqu.edu.cn; shuaizhou@cqu.edu.cn

Keywords: Power ultrasound assisted mixing; Dispersion; Hydration dynamics; Products evolution

This paper developed a novel power ultrasonic-assisted mixing technology to prepare cement paste at a water-to-cement ratio of 0.40. Three ultrasonic power levels (0 W, 480 W and 912 W) were adopted. Rheology, sedimentary stability experiments and compressive strength were tested. The hydration process was determined by means of inductively coupled plasma-optical emission spectrometry (ICP-OES), isothermal calorimetry, X-ray diffraction (XRD) with the Rietveld method, Fourier transform infrared spectroscopy (FTIR) and Thermogravimetric analysis (TGA). The results indicated that high-intensity power ultrasound (e.g., 912 W) decreased the apparent viscosity of fresh cement paste. The time required to reach 250 ml precipitation volume was increased by 76.4%, which indicated that the PUS acted on the particles in the form of vibration, combined with the mechanical shear energy generated by mechanical mixing, weakening the agglomeration energy and dispersing the particles. The rapid formation of calcium hydroxide (CH), ettringite and C-S-H gels was promoted by power ultrasound, which accelerated the crystallization nucleation process. The CH content of the 480 W and 912 W groups increased 5.27% and 3.79% at 1 day and 2.86% and 1.57% at 28 days, respectively. The hydration exothermic results showed that the hydration kinetic process of cement paste prepared by the PUS-assisted mixing process can be described by the nucleation and crystal growth (NG), phase boundary reaction (I) and diffusion (D) stages. The transition time from NG to D in the ultrasound group was faster than that in the reference group. Moreover, power ultrasound shortened the induction period and increased the accumulated heat release of cement paste at early hydration ages. The total heat release of the 480 W and 912 W groups increased by 7.83% and 11.89%, respectively, compared with that of 0 W when the cement paste was hydrated for 36 h. The capillary pores and gel pores were both reduced at 28 days hydration ages by applying high intensity power ultrasound (e.g., 912 W) treatment. The porosity, including middle and large capillary pores, decreased with increasing ultrasonic power from 2.25% in the 0 W group to 0.62%

ICSBM 2023

3rd International Conference of Sustainable Building Materials

25-27 September, Wuhan, China

in the 912 W group. The small capillary porosity increased from 8.20% to 8.79%. The changes in capillary pores that were closely related to the permeability indicated that high intensity power ultrasound may improve the resistance to ion attack or gas penetration in cement paste. Moreover, the gel porosity of the 912 W group decreased 35.17% and 31.87% compared with that of the 0 W and 480 W groups, respectively. The power ultrasound also enhanced the early age strength and ensured the strength increment rate at late hydration ages. The compressive strength of the 912 W group increased by 26.1% at 1 day and 18.3% at 28 days compared with that of the control group. This study also found that ultrasonic irradiation increased the gel-space ratio of the cement matrix, which had a linear correlation with the increase in the compressive strength of the matrix. The model performance was also the motivation to present predictions for the compressive strength of cement pastes under different power ultrasound irradiation. Furthermore, considering the pore refinement effect of power ultrasound, it is worth noting that power ultrasound may also have a positive impact on the durability of cement paste, which is worthy of further study.

Preparation and Performance Optimization of C₂S-C₄A₃\$/Q Phase Cement with High Volume of Mixed Solid Wastes

Jinghua Yan, State Key Laboratory of Silicate Materials for Architectures & School of Material Science and Engineering, Wuhan University of Technology, Wuhan, 430070, China

Shoude Wang Shandong Provincial Key Laboratory of Preparation and Measurement of Building Materials, University of Jinan, Jinan 250022, China

Wei Chen, State Key Laboratory of Silicate Materials for Architectures, Wuhan University of Technology, Wuhan, 430070, China

Email of the corresponding author: yanjh@whut.edu.cn, chen.wei@whut.edu.cn

Keywords: solid waste; high magnesium limestone; belite cement; Q phase; mechanical performance

Carbon neutralization in cement industry and effective utilization of solid waste play important role in ensuring the goal of that peak carbon dioxide emissions before 2030 and achieve carbon neutrality before 2060. To this end, east China's Shandong Province is taking more forceful measures and policies. One of the important measures is economical, efficient and environmentally friendly method to consume gold and aluminum industrial solid wastes such as gold tailings and red mud. Portland cement production technology using cement kiln to co-dispose gold and aluminum industrial solid waste has many problems, such as high carbon dioxide emission, large high-quality limestone consumption and so on. While high belite cement has been paid attention due to low sintering temperature, wider adaptability to raw materials, immobilized harmful ions and so on. In this thesis, C₂S-C₄A₃\$/Q phase cement was successfully synthesized using low grade raw materials (high magnesium limestone and medium- and low-grade bauxite) and industrial solid waste by analyzing the minerals and components of gold tailings, red mud and desulfurized gypsum, combining with the characteristics of cement industrial production, and through the design and optimization of composition and process of new high belite cement clinker, the harmlessness and activation of excess magnesium oxide were realized. Based on the new definition of three modulus conforming to C₂S-C₄A₃\$/Q phase system, the effects of Al/Si ratio, firing temperature and sintering soaking time on the compressive strength of C₂S-C₄A₃\$/Q phase cement were explored by using the response surface method. Finally, a new type of belite cement with outstanding mechanical performance was obtained. The main research contents are as follows:

Belite sulphoaluminate cement containing MgAl₂O₄ was prepared from gold and aluminum industrial solid waste, and the excess MgO that introduced by high magnesium limestone was formed stable minerals and realized harmless treatment. The main mineral phases of the new type of cement clinker were dicalcium silicate (C₂S), calcium sulphoaluminate (C₄A₃\$), magnesium aluminum-spinel (MgAl₂O₄) and tetracalcium ferroaluminate (C₄AF). The effects of sintering temperature, holding time, MgO overdosage and SO₃ overdosage on mineral formation and growth were significant. The optimal calcination system was 1300 ± 50 °C and soaking for about 60min. The shift of XRD peak confirmed the solid solution ions of C₂S and C₄A₃\$. The excess MgO was converted into MgAl₂O₄, which made cement soundness was still acceptable when MgO content reached 5.3%. The excess SO₃ could not only make up for the loss of gypsum decomposition, but also increase the solid solubility of MgO in minerals. The high-belite sulphoaluminate containing MgAl₂O₄ cement based on gold and aluminum industrial solid waste had unique performance such as high early strength and short setting time. The compressive strength cured 7d was more than 50MPa, and the total heat release of hydration for 50 days was only about 158J/g. It was expected to be applied in large concrete structures. The hydration products of this cement were AFm, AFt and AH₃, etc. And it was confirmed that MgAl₂O₄

ICSBM 2023

3rd International Conference of Sustainable Building Materials
25-27 September, Wuhan, China

did not participate in the hydration reaction and effectively solidify MgO. The heavy metal leaching concentration of cement products after curing for 14 days was only 0.01 ppm, far lower than the national standard leaching limit, and the heavy metal ions were effectively stabilized.

C₂S-C₄A₃S/Q phase cement was prepared from gold and aluminum industrial solid waste, and the excess MgO that introduced by high magnesium limestone was formed Q phase which could promote the improvement of material performance. By exploring the factors affecting the synthesis of Q phase single ore and the coexistence of Q-phase and C₄A₃S, C₂S-C₄A₃S/Q phase cement was prepared at 1300 °C to realize the functionalization of MgO, which was expected to further improve the solid solution of MgO in the cement industry and enhance the application of high magnesium limestone in cement preparation. C₂S-C₄A₃S/Q phase cement clinker was CaO-Al₂O₃-SiO₂-SO₃-MgO-Fe₂O₃ six-element system. By defining new three modulus (C_q, A/S, M/\$), the preparation scheme was optimized and verified by response surface method. It was found that the mechanical strength of C₂S-C₄A₃S/Q phase cement was outstanding when the aluminum-silicon ratio was 1.3~1.44, the sintering temperature was 1200°C~1250°C, and the holding time was 60min~75min. The strength of C₂S-C₄A₃S/Q phase cement was 57.01MPa after 7 days.

Synthesis of Novel Shrinkage-reducing Polycarboxylate Superplasticiser and its Performance on the workability and Shrinkage of Alkali-Activated Slag

Shuo Yan, Urban Construction and Digital City Teaching Experiment Center, School of Architecture and Planning, Yunnan University, Kunming, 650500, P R. China

Jinyi Guo, Urban Construction and Digital City Teaching Experiment Center, School of Architecture and Planning, Yunnan University, Kunming, 650500, P R. China

Yunhui Fang, KZJ New Materials Group Co., Ltd, Xiamen 361199, P R. China.

Jun Ren, Urban Construction and Digital City Teaching Experiment Center, School of Architecture and Planning, Yunnan University, Kunming, 650500, P R. China

Email of the corresponding author: renjun@ynu.edu.cn

Keywords: Alkali-activated slag; Shrinkage-reducing polycarboxylate superplasticiser; Shrinkage; Rheology; Hydration;

Alkali-activated slag (AAS), a low carbon cementitious materials, possess several sustainability and performance advantages such as low hydration heat of hydration, low carbon footprint, early high strength, etc., which makes them as an potential alternative building materials. However, comparing to Portland cement (PC), AAS displays a high shrinkage and poor workability, which limits its further engineering applications. Therefore, the addition of chemical admixture could be one of the most efficient way to solve those issues. Since the incorporation of shrinkage-reducing agents (SRAs) can partially solve the high shrinkage issue, it may potentially lower the compressive strength or lead to compatibility issues. Similarly, although the addition polycarboxylate superplasticisers (PCE) can somehow increase the workability, its compatibility with cementitious materials, as well as the other admixture, should be noticed. Therefore, the synthesis of shrinkage-reducing polycarboxylate superplasticizers (SR-PCE) could be a promising approaches to tackle the compatibility issues of the different admixture and solve the poor workability with high shrinkage issue of AAS. Unfortunately, the investigation on the performance of SR-PCE in AAS has not been extensively conducted.

The aim of this study is to propose a novel type of shrinkage-reducing polycarboxylate superplasticiser (SR-PCE) and investigate its performance in alkali-activated slag (AAS). For preparing the SR-PCE, a shrinkage-reducing monomer, in terms of 1,6-hexanediol diacrylate (HDDA), was applied and co-polymerised with isopentyl polyoxyethylene ether (TPEG) macromonomers. Moreover, its performance was investigated in AAS activated by waterglass with a modulus of 1.5 under the Na₂O equivalent of 4 wt%. The resulting SR-PCE polymer was characterised by using Fourier transform infrared spectroscopy (FTIR) and size exclusion chromatography (SEC). The shrinkage reducing effect was evaluated by surface tension measurement. Moreover, the workability of the AAS incorporating SR-PCE was assessed through slump tests and the rheological behavior was analysed as well. Finally, the effect of SR-PCE on the drying shrinkage of alkali-activated slag was investigated.

The results demonstrated that the synthesised SR-PCE exhibited a high monomer conversion rate and relatively low molecular weight and polydispersity index (PDI). The addition of SR-PCE decreased the surface tension of the AAS pore solution to 36.78 mN/m. Moreover, the synthesised SR-PCE in this study effectively increased the workability and reduced the dynamic yield stress of AAS. After a curing period of 28 days, the addition of 0.4% SR-PCE reduced the drying shrinkage of alkali-activated slag specimens by 26%. Microstructural analysis indicated that SR-PCE refined the distribution of pores in AAS, and reduced capillary tension.

Composition design of a low-carbon emission clinker using Phosphogypsum instead of limestone

Bo Yuan, Wuhan University of Technology

Jiwen Xu, Wuhan University of Technology

Bo Li, Wuhan University of Technology

Wei Chen, Wuhan University of Technology

Email of the corresponding author: lipt712@163.com

Keywords: Phosphogypsum; Carbothermal reduction; Ternesite; Low-carbon clinker

Phosphogypsum is a kind of industrial by-product gypsum precipitated by reaction of sulfuric acid and phosphate rock when phosphoric acid is prepared by wet method. Phosphogypsum has a large output, and about 4.5 ~ 5t phosphogypsum is produced for every 1t phosphoric acid produced. Due to the low grade of phosphate rock, phosphogypsum contains impurities such as fluoride and phosphorus pentoxide. The adhesion of residual sulfuric acid leads to the strong acidity of phosphogypsum. The residual acid and impurities of phosphogypsum deposited in rainwater leaching will cause serious pollution to soil and water source. Phosphogypsum preparation of sulfuric acid co-production of ordinary Portland cement clinker as early as the last century in China has been proposed and used in industrial production, but due to the high calcine temperature of C_3S , the firing atmosphere is not compatible, and phosphogypsum contains melting impurities, so that there are many problems in industrial production, in the firing process is easy to make the kiln blocked, and the output is very low.

The cement industry is energy and carbon emission intensive industry, the use of phosphogypsum instead of limestone firing low calcium clinker, not only reduces the firing temperature, but also can absorb phosphogypsum during firing, absorb carbon dioxide during maintenance, so that it is possible to achieve real negative carbon, the key to the use of phosphogypsum as calcium raw materials lies in the temperature, the choice of reducing substances, In industry, coke is generally used as a reducing agent, which is accompanied by solid reaction and gas reaction in the process of firing.

In this experiment, phosphogypsum was used as the whole calcium raw material, and a new type of clinker with high carbonization activity was successfully designed. The clinker mainly consisted of β - C_2S and auxiliary C_5S_2S . It was observed that the calcium oxide decomposed by phosphogypsum had higher reactivity than that produced by calcium carbonate. The optimal carbon sulfur molar ratio of phosphogypsum is 2.0, and the suitable composition range of clinker is CaO 45 ~ 50%, SiO₂ 35 ~ 39%, Fe₂O₃ 3~ 5%, Al₂O₃ 3~ 10%. The carbonization properties of the clinker were measured by pressing molding and carbonizing curing. After carbonizing for 1d, the compressive strength of the test block reached 81MPa. The carbonized products were mainly calcite and amorphous silica gel, and the weight percentage of CO₂ in the sample was 19%. The overall results show that the clinker with phosphogypsum as the total calcium source has good carbonization activity, and has a good application prospect in solid waste utilization.

Effective iron removal method for coal gangue applied in cement industry

Kenan Zhang, School of Geoscience and Survey Engineering, China University of Mining and Technology -Beijing, Beijing 100083, China

Xingjian Kang, School of Geoscience and Survey Engineering, China University of Mining and Technology -Beijing, Beijing 100083, China

Qinfu Liu (corresponding author), School of Geoscience and Survey Engineering, China University of Mining and Technology -Beijing, Beijing 100083, China

Email of the corresponding author: lqf@cumtb.edu.cn

Keywords: coal gangue; calcination; magnetic; removal; iron

Coal gangue (CG), a concomitant product of coal seam sedimentation that makes up 10% to 15% of the entire amount of coal produced, is a kind of industrial waste separated during coal mining and washing. Being the largest industrial waste in China, CG has produced more than 700 million tons of emissions overall, and more than 70 million tons annually in this country. In addition to taking up a lot of lands, the storage of CG also pollutes the environment. Water pollution, soil quality decline, ecosystem degradation, and biodiversity loss are much severe in CG storage region. After a long period of accumulation, the structure of gangue mountain becomes loose and susceptible to cause natural disasters such as mudslides and landslides. Additionally, the CG piles' spontaneous combustion will release toxic gases such as SO₂, CO, H₂S, and NO_x, which will pollute the air and potentially result in acid rain. The effective use of this industrial solid waste, converting the waste into available resources and minimising environmental pollution, is urgent.

The comprehensive utilization of CG is mainly focused on power generation, backfilling the mine void, and production of construction materials. In context of building materials, some researches have been carried out on the mechanical properties of cement and coarse and fine aggregates prepared from CG. The main component of CG is coal series kaolinite, and its main chemical components are SiO₂ and Al₂O₃. The kaolinite would be transformed into metakaolinite with high pozzolanic activity after activation process. Thus, CG with high kaolin content has the potential to replace part of cement as a supplementary cementitious material after calcination. The use of calcined coal gangue (CCG) would reduce cement consumption, the relevant energy consumption, and environmental pollution. The existence of iron phase (usually siderite and pyrite), albeit in small amount, prompt the color of CCG turning into red when calcining, owing to the decomposition and oxidization of iron phase to form hematite. The addition of red CCG into cement-based materials would affect the overall color of cement-based materials and limit the high-volume application of CCG powder in cement industry.

Traditional beneficiation methods for the removal of iron from CG always have some problems. For example, chemical methods involve a lot of reagents. Bioleaching for iron extraction is time-consuming. Flotation requires the selection of a suitable flotation reagent regime, and if pyrite is mixed with sulphidic ores or oxidized on the surface, its flotation is usually depressed. Magnetic separation is one of the main methods of separating iron-bearing minerals from gangue with low cost. However, pyrite is reported to be diamagnetic or weakly paramagnetic with a very small and positive susceptibility. As a result, the separation of pyrite from CG is difficult by industrial magnetic separation processes tending to work in the range of 0.5 to 1 T. One way to improve the magnetic separation of pyrite is to apply an equipment with higher background magnetic field and magnetic field gradient, while another is to convert the pyrite into a strongly magnetic mineral. The latter might be more advantageous in that enlarging the magnetic

ICSBM 2023

3rd International Conference of Sustainable Building Materials
25-27 September, Wuhan, China

difference between the target product and the other components leads to higher separating selectivity and lower separating difficulty.

Herein, a method of calcination in the air to enhance the magnetic properties of pyrite followed magnetic separation was adopted. An experimental procedure about calcinating CG at the temperature range of 300 to 1000°C and held for 30 to 180 min under isothermal conditions has been implemented. The magnetic susceptibility of the samples determined by vibrating sample magnetometer after being calcined at 400°C for 60 to 120 min was greater than 16 times that of the raw gangue. The samples were magnetically separated after oxidizing calcination at 400 °C for 60, 90 and 120 min, respectively. The recovery of Fe reached more than 83.17% and the Fe₂O₃ content (loss on ignition deducted) of their non-magnetic products were less than 1.02%, down from 5.58% for raw coal gangue. The main mineral of CG used in the experiment was kaolinite, and the iron in the gangue existed predominantly in the form of pyrite. The organic matter in the gangue burned and consumed oxygen in the furnace, thus generating a weak oxidizing environment. The enhanced magnetism of the gangue after calcination in this slight oxidizing atmosphere was attributed to the formation of strongly magnetic magnetite, an intermediate product of pyrite to hematite.

Through this research, we hope to provide a practical method for the industrialization, large-scale, and high value utilization of CG waste by removing iron from CG with high content of kaolinite before using it in cement industry.

Heavy metal solidification and reaction mechanism in alkali-activated MSWI fly ash specimens with natural zeolite

Xiong Zhang ¹, Baomin Wang ^{1*}, Jun Chang ¹.

¹ School of Civil Engineering, Dalian University of Technology, Dalian 116024, Liaoning, China

Email of the corresponding author: wangbm@dlut.edu.cn

Keywords: Alkali-activation, MSWI fly ash, Zeolite, C-(A)-S-H, Heavy metal

As the lives of individuals improve, the amount of municipal solid waste (MSW) generated increases annually. Because of the benefits of volume reduction, sterilization, and heat recovery, incineration is the dominant option for MSW disposal. MSWI fly ash is produced during the MSW incineration (MSWI) process. Because of its high heavy metal concentration, MSWI fly ash has a lower utilization ratio than other solid waste. A large number of researchers are investigating various strategies to increase the disposal ratio of MSWI fly ash, such as high-temperature heat treatment, separation and extraction, and solidification and stabilization technology. Solidification and stabilization technology is attracting the interest of various academics owing to its lowered CO₂ emissions and economics.

MSWI fly ash has a high CaO percentage and a low SiO₂ content. Zeolite, a new siliceous material, was used in this study to increase the compressive strength and heavy metal solidification ratios of the alkali-activated MSWI fly ash matrix. The mechanism of alkali-activated MSWI fly ash reactivity with zeolite (FZ) specimens is also investigated. The 3 d compressive strength of alkali-activated MSWI fly ash with 40% zeolite substitution (FZ40-3d, similar abbreviations are used in later iterations) is 1.28 times greater than that of FZ0-3d in this study. The inclusion of zeolite can significantly increase the early compressive strength of FZ specimens.

X-ray diffraction (XRD) results reveal that the wide peak at 28.5°-30.5° emerges clearly in FZ40 specimens, indicating that the addition of zeolite increases the gel phase amount in the FZ specimens. Due to the air carbonation of the gel phase surface, a new mineral peak of tilleyite is also detected. According to the fourier transform infrared spectroscopy (FTIR) and magic angle spinning nuclear magnetic resonance (MAS NMR) data, the gel phase was primarily in the form of (Ca, Na)-(A)-S-H. The zeolite vibration peak is dramatically attenuated in the Si MAS NMR spectrum, indicating that zeolite is involved in the alkali-activated process. Simultaneously, zeolite can raise the polymerization degree of the C-S-H gel phase from Q¹ to Q². Meanwhile, the Al MAS NMR spectrum shows that aluminum in zeolites participates in the polymerization process, forming C-A-S-H (Q₃(1Al)). According to the hydration heat data, zeolite addition increases the total heat quantity by 14-34%. Simultaneously, the heat peak of FZ specimens containing zeolite is later than that of pure alkali-activated MSWI fly ash specimens (FZ0). Because the three-dimensional network skeleton structure of the zeolite must be depolymerized before it can participate in the alkali-activated reaction. The pozzolanic reactivity of [SiO(OH)₃]⁻ and [AlO(OH)₃]⁻ resulting from zeolite depolymerization enhances the overall quantity of heat release in FZ specimens. The total heavy metal leaching concentration in FZ specimens has achieved the treatment standard. Meanwhile, with zeolite addition, the amounts of Pb, Zn, and Cd leaching concentrations are lowered much more when compared to FZ0 specimens. The use of zeolite contributes even more to MSWIFA's safety.

Zeolite increases the amount of the C-(A)-S-H gel phase and the degree of polymerization. Meanwhile, the porous characteristics of zeolite perform heavy metal adsorption, which decreases the amount of heavy metal leaching concentration in FZ specimens. The inclusion of zeolite enhances the compressive strength and heavy metal solidification ratio. The considerable early compressive strength of FZ specimens reduces curing times and the risk of heavy metal release during transportation. And the extremely small leaching quantity of heavy metal in FZ

ICSBM 2023

3rd International Conference of Sustainable Building Materials
25-27 September, Wuhan, China

specimens improves the utilization possibility of MSWI fly ash as a resource.

Solidification mechanisms of lead in high ferrite cement clinker

Zhuoyang, Zhang, ¹Jiangsu Key Laboratory for Construction Materials, Southeast University, Nanjing, CHINA

Yunsheng, Zhang*, ¹Jiangsu Key Laboratory for Construction Materials, Southeast University, Nanjing, CHINA; ² School of Civil Engineering, Lanzhou University of Technology, Lanzhou, CHINA

Email of the corresponding author: zhangys278@163.com

Keywords: High ferrite cement clinker, solidification, hydration, lead, solidification.

The use of solid waste to produce low carbon, high ferrite cement clinker with favorable durability delivers potential application prospects. However, the existence of lead in lead-containing solid waste not only restricts its utilization ratio but also causes potential environmental pollution, which eventually restricts its application in high ferrite cement clinker production. The work at hand explores the migration mechanisms of lead in high ferrite cement clinker and evaluates the influence of lead on hydration properties of high ferrite cement by free lime test, X-ray diffraction (XRD), inductively coupled plasma-optical emission spectroscopy (ICP-OES), as well as hydration heat-evolution test.

In this study, the analytical grade reagents were used as cement raw materials to eliminate the interference of other trace elements. And lead was added in the form of oxide. The free lime test result indicates that the free lime content will be increased slightly with the rising dosage of PbO content. However, when the content of PbO increased to 3 wt.%, the free lime content increased by 125% in comparison with the sample without lead addition. It implies that the excessive addition of lead in raw material has an adverse effect on the formation of C₃S phase.

Then from the overall variation trend of the solidification ratio, it can be seen that the solidification ratio decreases gradually with the reduction of PbO content. With a PbO content of 0.5 wt.%, the solidification is the highest, which is 36.77%. However, when the addition of PbO in raw materials increases from 0.5 wt.% to 2 wt.%, the solidification ratio in clinker gradually reduces to 13.20%. This indicates that the main migration behavior of Pb during the calcination process of high ferrite cement clinker is volatilization. Moreover, the increasing dosage of PbO tends to promote its volatilization to a certain extent, which is related to the increase of the initial concentration during the reflection.

From the lead distribution analysis, it can be seen that the majority of lead elements tend to be solidified in the clinker mineral phases in the form of solid solutions. The lead was nearly uniformly distributed in C₃S, C₂S, and C₄AF phases, which does not show obvious solidification priority. Without considering the loss of Pb due to solidification, the average solidification ratio of lead in the silicate phases to the total solidification ratio is 71.32%, while that in the interstitial phases is 28.68%. It means that the difference in solidification ratios in different mineral phases mainly depends on the content of the mineral phase in the clinker.

The XRD analysis shows that for the semi-volatile heavy metal element Pb, its addition in raw material shows no impact on the mineral phase composition of high ferrite cement clinker. And no lead-contained new phases will be generated even with a relatively high PbO dosage.

Finally, the hydration heat evolution results show that the solidification of lead in the mineral phases of high ferrite cement clinker has no significant effect on the induction period. While for the acceleration period, it can be seen that compared with the control group sample, when the lead content in raw material increases by 2 wt.%, the second heat release peak increases from 1.66 to 1.79 mW/g. This indicates that the lead solidified in the C₃S phase will promote hydration heat release in the acceleration stage to a certain extent.

Study on the effect of sewage sludge ash on the properties of cement paste and its water film thickness

Zunrui Zheng ^{1,2}, Shuang Liu ¹, XiaoLi Xie ³, Weiwei Zhu ¹, Xixiang Liu ¹, Lang Liu ¹, Kao Chen ¹, Cixin Chen ¹, Jinguo Peng ², Shanfeng Wu ², Nan Li ⁴, Zheng Zhou ⁴

¹Colleges and Universities Key Laboratory of Environmental-Friendly Materials and New Technology for Carbon Neutralization, Guangxi Key Laboratory of Advanced Structural Materials and Carbon Neutralization, School of Materials and Environment, Guangxi Minzu University, Nanning 530105, China

²Guangxi Guo Biao Environmental Technology Co., Ltd. Nanning 530021, China

³College of Civil Engineering, Guangxi Polytechnic of Construction, Nanning, Guangxi 530007, China;

⁴Guangxi Huahong Water Group Co., Ltd. Nanning 530105, China 530000, China

Email of the corresponding author: zhuww1230@163.com (W.Z.)

Keywords: sewage sludge ash; water film thickness; cement paste; workability; compressive strength

To dispose of sewage sludge generated from municipal wastewater treatment plants, incineration has emerged as one of the most environmentally friendly and safe disposal options, and sewage sludge ashes (SSA) as the ultimate by-product have been produced in large quantities. Some published literature points out that cement pastes prepared with a small amount of SSA as a substitute for cement exhibit comparable strength but a reduction in workability. However, limited information is available on how SSA affects the properties of cement paste. This study explores the effects of SSA on both the fresh and hardened properties of cement paste. Additionally, the concept of water film thickness (WFT) was extended to cement paste with SSA. A total of 30 sets of cement pastes with different SSA contents and different water/cementitious materials (W/CM) ratios were made, and their flowability (flow spread and flow rate), cohesiveness, compressive strength, packing density, and WFT were measured. The results showed that the addition of SSA would enhance the cohesiveness of cement paste but reduce the flowability and compressive strength. In addition, the WFT is the most important factor influencing the flow rate of cement paste, and the flow rate increases with the increase of WFT. However, the flow spread, cohesiveness, and compressive strength of cement paste are jointly controlled by WFT and SSA content. It turns out that the WFT theory is also applicable to SSA cement paste.

Understanding the microstructural evolution of 3D printing steel slag-cement with low-field NMR relaxation

Lingli, Zhu, Henan Polytechnic University School of Materials Science and Engineering Jiaozuo, China¹

Wanting, Zhao, Henan Polytechnic University School of Materials Science and Engineering Jiaozuo, China.

Yu, Zhao, Henan Polytechnic University School of School of Civil Engineering Jiaozuo, China.

Xuema, Guan, Henan Polytechnic University School of Materials Science and Engineering Jiaozuo, China.

Email of the corresponding author: zhaoyu@hpu.edu.cn

Keywords: 3D printing steel, low-field NMR relaxation, the rheological properties, steel slag, hydration microstructure

3D printed steel slag cementitious materials are 3D printed composites made of steel slag as a supplementary cementitious material instead of cement. Due to the special process of 3D printing, it must have pumpable, printable and buildable workability. The early workability of 3D printed materials is significantly affected by their microstructural characteristics, so the development of new test tools can better understand the microstructure of the early materials and establish a link with rheology. This study reports on the application of low-field nuclear magnetic resonance (NMR) relaxation time measurements to characterize the microstructural evolution of 3D printed steel slag cementitious materials during the early 6h period, exploring the effect of steel slag properties on the early hydration microstructure. The link between the rheological properties and the pore microstructure of 3D printed steel slag cementitious materials over time was investigated. Compared with low alkalinity steel slag, high alkalinity steel slag of 10-20 μm can effectively promote the formation of capillary pores and reduce the porosity. Time-dependent relaxation measurements effectively characterized the time-dependent rheological properties, where (0~0.1 μm) pore throat distribution was correlated with the static yield stress. The low-field NMR relaxation characteristics can characterize the early properties of 3D printed cementitious materials, which can help to perform early nondestructive and rapid testing of 3D printed cementitious materials and contribute to building intelligence.

TOPIC C: Alternative reinforcements for concrete structures

Effect of Accelerated Aging on the Bond Behavior of TRM Composites Through Single-lap Shear Tests

N. Azimi, Ph.D. student, University of Minho, ISISE, ARISE, Department of Civil Engineering, Guimarães, Portugal.

D.V. Oliveira, Associate Professor, University of Minho, ISISE, ARISE, Department of Civil Engineering, Guimarães, Portugal.

Katrin Schollbach, Assistant Prof, Department of the Built Environment, Eindhoven University of Technology, Eindhoven 5600 MB, the Netherlands.

P. B. Lourenço, Professor, University of Minho, ISISE, ARISE, Department of Civil Engineering, Guimarães, Portugal.

Email of the corresponding author: nimaa32@gmail.com.

Keywords: Textile reinforced mortar; TRM; Fiber Reinforced Cementitious Matrix; FRM; Tensile testing; Mechanical properties.

Textile Reinforced Mortars (TRM) have emerged as a sustainable solution for strengthening existing masonry structures and are gaining significant popularity in contemporary construction practices. This system entails embedding textile fibers within an inorganic matrix, typically cement or lime-based mortars, and applying it over the surface of the substrate. While extensive research has been conducted on the mechanical properties of these composite systems, there remains a dearth of knowledge concerning their long-term performance and durability. Thus, the objective of the present study is to enhance our understanding in this field by investigating the bond behavior of TRM composites comprising basalt textiles and a lime-based mortar after exposure to acidic and alkaline attacks using a single lap shear test. To achieve this objective, a clay brick as the substrate has been employed, and constructed single-lap shear specimens using a lime-based mortar and a basalt fabric. These specimens were subjected to accelerated aging conditions simulating acidic and alkaline environments. The temperature and pH of the solutions were maintained at constant levels throughout the exposure period. Specifically, the specimens were tested after 1000, 3000, and 5000 hours of exposure to evaluate their bond behavior in comparison to control specimens of the same age. Furthermore, the effect of acidic and alkaline environments was investigated on the material properties of the constituent materials. Elastic modulus tests were also conducted on cylindrical mortar samples and compared against reference samples. Moreover, optical microscopy was utilized for a better understanding of the deterioration.

The results obtained from our study reveal compelling insights into the behavior of TRM composites over extended durations of exposure. As the exposure time increased, the mortar exhibited significant deterioration, leading to a notable change in the failure mode of the TRM composite. By identifying the strength, stiffness, and failure mode of each specimen and comparing them to the reference stage, it was possible to derive essential design parameters for various field applications. The findings of this research contribute to the existing body of knowledge on TRM systems by shedding light on their long-term performance and durability under acidic and alkaline environments. The characterization of bond behavior and the identification of material property changes provide valuable information for engineers and practitioners involved in designing and applying TRM solutions for masonry structures. Understanding the behavior of TRM composites in chemical attacks is crucial for ensuring their

ICSBM 2023

3rd International Conference of Sustainable Building Materials

25-27 September, Wuhan, China

reliable and effective implementation in real-world scenarios as well as an initial understanding of durability modeling.

Future research directions in this domain may include exploring additional environmental conditions, investigating the influence of different types of textile fibers, and evaluating the performance of TRM composites in varying temperature and moisture conditions. Such investigations will further enhance understanding of such a sustainable strengthening solutions and aid in the development of guidelines and design recommendations for their optimal utilization. Finally, each specimen's strength, stiffness, and failure mode have been identified and compared to the reference stage to derive design parameters for various field applications. These results showed the sensitivity and major reduction in the material properties of basalt-TRM over the acidic medium and draw a good understanding of its aging behavior and alteration of the failure mechanism.

A comparative study of the composition and corrosion of concrete sewer pipes in the Netherlands

Beatrice, Cerrai, M.Sc. Department of the Built Environment, Eindhoven University of Technology¹

Katrin, Schollbach, Ph.D., Assistant Prof., Department of the Built Environment, Eindhoven University of Technology¹

H.J.H., Brouwers, Ph.D., Prof., Department of the Built Environment, Eindhoven University of Technology¹

Email of the corresponding author: b.cerrai@tue.nl

Keywords: concrete, corrosion, degradation, sewer systems, sulphate attack

The primary deterioration process in concrete sewerage systems is microbiologically induced concrete corrosion (MICC). Bacterial activity in sewers initiates a cyclical process that results in the production of sulfuric acid (H_2SO_4), which reacts with the cement paste of the concrete. Microorganism activity promotes the creation of hydrogen sulphide (H_2S) gas and the metabolization of sulphur present in the pipe environment into sulfuric acid, causing damage to the concrete. Sulphur-oxidising bacteria that live on the moistened surface of the pipe produce sulfuric acid at the concrete surface, converting the cementitious material to ettringite and gypsum. Both have a higher volume than the original cement compounds, which promotes cracking; they offer no structural support to the concrete pipe and may be eliminated by the sewage flow, thus increasing the continual corrosion cycle.

The corrosion process understanding and its product identification are critical to designing solutions to the problem, for example, specifically developed coatings applied as corrosion-resistant treatments for sewerage systems maintenance and to formulate a more efficient concrete mixture, appropriate for the circumstances of this peculiar environment.

The present study evaluates different concrete pipe samples from the Netherlands' sewer systems spanning from the 1920s to the present and from the cities of Arnhem and The Hague.

Thus, the samples from The Hague were taken from pipes placed in 1924 and 1951, respectively, whereas those from Arnhem were set in 1997. In this case, the primary goal of the research is to analyse the products of this peculiar degradation mechanism and then relate them to the composition of the various types of cement, which is unknown due to a lack of data on the materials used in the construction of pipes. The joint goal would be to define the composition of the unknown material in detail, compare the samples in terms of components according to production time, and assess the differences in terms of quality, characteristics, durability, and susceptibility to degradation. The purpose is to characterise the concrete composition in detail and assess the degradation of the material on a microscopic scale through a petrographic study with optical microscope imagery in reflected light. The present investigation utilises both qualitative and quantitative X-ray Diffraction (XRD) analysis, as well as other complementary analysis techniques such as Scanning Electron Microscopy imaging for morphology study in core drillings with Energy Dispersive Systems for element identification and Thermal Gravimetric Analysis (TGA), Fourier-transform Infrared Spectroscopy (FT-IR) and X-ray Fluorescence (XRF) for elemental analysis.

The XRD and TGA results reveal the presence of gypsum, ettringite and calcite as major MICC products, present in proportionally greater quantities depending on the sewer pipe installation date. Following investigations will include detailed characterization of the cement matrix extracted from concrete and analysed using other techniques such as X-ray Fluorescence (XRF), elemental spectroscopic analysis, and observation of additional samples with the naked eye and

ICSBM 2023

3rd International Conference of Sustainable Building Materials

25-27 September, Wuhan, China

under the microscope to detect compositional differences in the mixture constituting the concrete. The intent is to assess the existence of any additives to the mix, such as differences in aggregate nature or cement types employed, and how these might affect concrete deterioration due to sulphate attack. The primary goal is to correlate the identified corrosion products to the concrete design mix, which is defined as a combination of cement, aggregates, and the amount of water used to produce concrete pipes.

The findings highlight the association between corrosion products and damaged concrete composition.

Effect of polymer fibres recycled from waste tyres on impact resistance of concrete after heat exposure

Meng Chen, School of Resources and Civil Engineering, Northeastern University, Shenyang, 110819, China

Xiu-Wen Cui, School of Resources and Civil Engineering, Northeastern University, Shenyang, 110819, China

Tong Zhang, School of Resources and Civil Engineering, Northeastern University, Shenyang, 110819, China

Email of the corresponding author: zhangtong@mail.neu.edu.cn

Keywords: Fibre reinforced cementitious composites; Recycled tyre polymer fibre; Dynamic compressive properties; Coupled effects; Damage evolution

Recycled tyre polymer (RTP) fibre obtained by recycling and separating scrap tyres has been applied to enhance the dynamic and thermal properties of cement-based materials. The main purpose of this work is to systematically explore the role of RTP fibres in enhancing the dynamic compressive behaviour of concrete after heating exposure. The optimal RTP fibre volume of 0.1% was adopted following the previous study on high-temperature properties of concrete with the same raw materials and mix proportion. RTP fibre reinforced concrete was first exposed to elevated temperatures (including 20, 105, 250, 400 and 600 °C) and then naturally cooled down to room temperature. After that, the residual dynamic compressive properties in terms of failure mode, dynamic compressive strength, dynamic increase factor, peak strain and energy dissipation capacity under various strain rates (i.e., 40, 60, 80, 100 and 120 s⁻¹) were measured by split Hopkinson pressure bar test. Following the obtained experimental results, the underlying mechanisms were discussed with the assistance of microscopic characterisations.

The results reveal that the failure pattern of RTP fibre reinforced concrete under dynamic compression is mainly dominated by the strain rate effect, while the increase in heating temperatures has no significant influence on the failure pattern. In contrast, the failure mode changes from splitting failure (38.5–41.8 s⁻¹) to core failure (58.7–82.1 s⁻¹), and finally to pulverization failure (99.2–120.6 s⁻¹) with the increase in strain rate. Moreover, the dynamic compressive strength increases by 17.35%–25.86% with the increasing strain rates from 38.5 s⁻¹ to 120.6 s⁻¹, as the cracks can develop across the coarse aggregates and RTP fibres at higher strain rates. There exists a decreasing trend of residual dynamic compressive strength with elevated temperatures (up to 56.11% reduction at 600 °C), which can be mainly ascribed to the evaporation of moisture and decomposition of hydration products in concrete. By incorporating the temperature-related functions into logarithmic equations, a new model is proposed to predict the dynamic increase factor considering the coupled effects of strain rate and elevated temperatures with a high correlation coefficient of 0.9915. The strain rate effect leads to the increase of peak strain at a higher strain rate regardless of the temperatures. Although the peak strain also increases with elevated temperatures at under 400 °C, a sudden drop of peak strain occurs at a higher temperature because of the further dehydration of cement hydrates. Similarly, the fracture energy also reaches the maximum value between 20 °C and 250 °C, which is ascribed to the increase of peak strain at relatively low temperatures. The bridging effect of RTP fibres at lower strain rates and rupture of RTP fibres at higher strain rates contribute to the dynamic properties of concrete when the temperature is lower than the melting point of RTP fibres. The pore-crack network within the concrete matrix formed by the thermal expansion of RTP fibres can eliminate the explosive spalling and thus ensure the residual dynamic properties of concrete after heating.

Enhancing the dynamic splitting tensile behaviour of ultra-high performance concrete using waste tyre steel fibres

Meng Chen, School of Resources and Civil Engineering, Northeastern University, Shenyang, 110819, China

Jun-Qi Sun, School of Resources and Civil Engineering, Northeastern University, Shenyang, 110819, China

Tong Zhang, School of Resources and Civil Engineering, Northeastern University, Shenyang, 110819, China

Email of the corresponding author: zhangtong@mail.neu.edu.cn (T. Zhang)

Keywords: Ultra-high performance concrete; Waste tyre steel fibre; Split Hopkinson pressure bar; Dynamic splitting tensile properties; Sustainable analysis

The application of waste tyre fibres in ultra-high performance concrete (UHPC) can not only reduce the total material cost of UHPC but also ease the pressure to decompose waste tyres. However, there are few insights into how waste tyre fibres affect the dynamic properties of UHPC, and it is still unclear whether industrial fibres can be replaced by waste tyre fibres in terms of the impact resistance. Therefore, this study investigates the feasibility of enhancing the dynamic splitting behaviours of UHPC with waste tyre steel (WTS) fibres, and comparisons with industrial straight steel (ISS) fibre reinforced UHPC is conducted. To be more specific, a series of experiments were carried out to investigate the effects of various WTS fibre volume fractions (i.e., 1.0%, 2.0%, 3.0%, 4.0%, expressed as WTS1.0, WTS 2.0, WTS 3.0, WTS 4.0, respectively) on the workability, compressive strength, elastic modulus, flexural strength, and static splitting strength of UHPC, and the dynamic failure pattern, dynamic splitting strength, dynamic increase factor (DIF), and dissipation energy were investigated by means of a splitting Hopkinson pressure bar (SHPB) test. For the sake of comparison, the conventional UHPC containing 2.0% ISS fibres (namely, ISS2.0) was also prepared as the reference.

The results show that the slump of UHPC is reduced with the increasing WTS fibre content, but the static compressive strength, elastic modulus, flexural strength, and static splitting tensile strength of WTS4.0 are improved by 8.9%, 9.8%, 4.4%, and 19.8%, respectively, as compared with WTS1.0. It can be attributed to the fibre skeleton of three-dimensional disordered distributed WTS fibres in the UHPC matrix, which increases the bonding and anchoring forces and inhibits crack propagation. The dynamic splitting behaviour, including dynamic splitting strength, DIF and energy dissipation capacity, were highly sensitive to the strain rate for all the mixtures. The failure pattern of all mixtures under dynamic loading is similar, which are fracture initiation under the strain rate of 2.11~2.36 s⁻¹, fracture expansion under the strain rate of 3.45~4.91 s⁻¹ and fracture splitting under the strain rate of 6.33~6.64 s⁻¹. The dynamic properties of UHPC are improved when the WTS fibre content reached 3.0% and decreased after exceeding

ICSBM 2023

3rd International Conference of Sustainable Building Materials

25-27 September, Wuhan, China

fibre fraction of 3%. For example, the dynamic splitting strength, DIF, energy dissipation capacity of UHPC increases by 17.2-25.0%, 2.4-11.6% and 23.0-31.8%, respectively, while the content of WTS fibres increases from 1% to 3%, but decreased by 1.7-5.4%, 7.7-11.5%, and 5.5-10.1%, respectively, when the content of WTS fibres reaches 4%. The reason for this phenomenon may be that with the further increase in WTS fibre content, the fibres tend to agglomerate during the mixing process, which reduces the bonding efficacy between the fibres and the UHPC mixture. Compared with the reference ISS2.0, WTS3.0 has better dynamic performance, and the DIF of WTS3.0 is 15.1% higher than that of ISS2.02.0 under the strain rate of 3.45~4.91 s⁻¹. In addition, an up to 30.0% reduction in carbon content can be achieved by using WTS fibres instead of ISS fibres in UHPC. The optimal WTS content of UHPC was regarded as 234 kg/m³ considering static mechanical properties, dynamic splitting tensile behaviour, material cost and environmental impact.

Mixture design theory of ultra-high performance concrete (UHPC): From particle packing model to artificial intelligence techniques

Dingqiang Fan: Department of Civil and Environmental Engineering & Research Centre for Resources Engineering Towards Carbon Neutrality (RCRE), The Hong Kong Polytechnic University, Kowloon, Hong Kong, China

Jian-Xin Lu: Department of Civil and Environmental Engineering & Research Centre for Resources Engineering Towards Carbon Neutrality (RCRE), The Hong Kong Polytechnic University, Kowloon, Hong Kong, China

Rui Yu: State Key Laboratory of Silicate Materials for Architectures, Wuhan University of Technology, Wuhan, 430070, China

Chi Sun Poon: Department of Civil and Environmental Engineering & Research Centre for Resources Engineering Towards Carbon Neutrality (RCRE), The Hong Kong Polytechnic University, Kowloon, Hong Kong, China

Email of the corresponding author: dingqiangfan@foxmail.com

Keywords: Ultra-high performance concrete (UHPC); Mixture design; Particle packing model; Artificial intelligence.

This study proposed a novel method for the mixture design of ultra-high performance concrete composites by using particle packing model and artificial intelligence techniques. Firstly, a novel multi-scale design method for UHPC composites that combined the particle packing model and centropiasm theory. This design method can be briefly summarized by the following steps: Firstly, the micro centropiasm loop (MCL)/water film was incorporated into the modified Andreasen and Andersen (MAA) model to optimize the mixture of UHPC paste; then, the designed UHPC paste was integrated into MAA model through sub centropiasm loop (SCL)/paste film to further design UHPC mortar; finally, the steel fibres were incorporated the designed UHPC mortar to further improve its mechanical properties. To demonstrate the superior performance of the designed UHPC pastes, mortars and composites, their micro-meso-macro properties were evaluated in detail. The results showed that increasing MCL can promote the cement hydration degree. At an MCL thickness of 0.2 μm , the average packing density of the C-S-H gel of the UHPC pastes was the highest at 0.846. Moreover, the increase in SCL led to the improvement of workability and compressive strength of UHPC mortar, as well as a reduction in porosity of all scales. In addition, it was demonstrated that as the steel fiber contents was 2.0 vol.% and the preset SCLT was 30 μm , the comprehensive performance of UHPC was better (workability: 230 mm, compressive strength: 168.91 MPa). After that, an approach for characteristics prediction of UHPC by employing Genetic algorithm based artificial neural network (GA-ANN) technique was proposed. Herein, 80 mixtures in total were conducted as a training dataset, and then a GA-ANN model is created for characteristics prediction of UHPC, which exhibits significant superiorities in fitting goodness and prediction accuracy compared to other classical prediction models. Furthermore, a prediction software based on GA-ANN technology with an efficient Graphical User Interface (GUI) is developed. Finally, a novel framework for precise mix-design of UHPC was proposed by combining the MAA and GA-ANN models as follows: at first, conduct the preliminary mix-design by the MAA model, and then further adjust the mixture by GA-ANN technique according to objectives and requirements. In addition, a mixture towards an advanced particle packing structure (a higher wet packing density) was developed by this new design method, which verified the feasibility and practicability of this new design method. This research proposed a method for the application of

ICSBM 2023

3rd International Conference of Sustainable Building Materials

25-27 September, Wuhan, China

AI technique in the UHPC field, which realizes the precise design and characteristics prediction of UHPC. By this way, it made full use of the advantages of computer science, which can promote the informationization process of the UHPC industry. Moreover, as an emerging technique, there is a need for depth investigation of GA-ANN technique in the future, such as function expansion, algorithm optimization and novel mix-design method. Overall, the mixture design plays a vital role in concrete materials, and its scientific and intelligent development holds great significance.

Study on the deterioration of interfacial bond strength between LWAC and OC under the coupling effect of sulfate erosion and dry-wet cycles

Zhenghao Fu, Wuhan University of Science and Technology, No.2, West Huangjiahu Road, Hongshan District, Wuhan, China (School of Urban Construction)¹

Hongbing Zhu, Wuhan University of Science and Technology, No.2, West Huangjiahu Road, Hongshan District, Wuhan, China (School of Urban Construction)¹

Jingyi Chen, Wuhan University of Science and Technology, No.2, West Huangjiahu Road, Hongshan District, Wuhan, China (School of Urban Construction)¹

Email of the corresponding author: zhuhongbing@wust.edu.cn.

Keywords: Sulfate dry-wet cycles, LWAC, Interfacial bond strength, Microstructure, Micro-hardness

After reviewing the existing studies, it has been found that the coupling effect of sulfate erosion and dry-wet cycle can cause significant damage to concrete materials. Moreover, because of the existence of the interface, composite concrete structures are more susceptible to being attacked by this action than monolithic poured concrete structures. In fact, it can even lead to debonding separation between the two types of concrete. However, at present, the evolution of the interfacial bond strength between lightweight aggregate concrete (LWAC) and ordinary concrete (OC) during this durability damage process is unclear. This would pose a significant obstacle to the application of LWAC as a repair and reinforcement material in coastal areas. Therefore, the dry-wet cycle test of 5 % sodium sulfate solution for 225 days (a total of 15 rounds) was carried out on the new and old concrete composite specimens by using the dry-wet cycle method of completely soaking for seven days + natural drying for eight days. Furthermore, splitting tensile, direct shear, scanning electron microscope, and microhardness tests were performed on the old and new concrete interfaces at different numbers of dry-wet cycles. As results of this study, firstly, with the increase of dry-wet cycles, the interfacial splitting tensile and shear failure modes all changed from mixed cohesive failure to interfacial bonding failure. Based on the failure mode, this was a bad sign. Secondly, the interfacial splitting tensile strength, the direct shear strength, and the corrosion resistance coefficients (K_T and K_S) increased slightly during the first two cycles. Their increases were about 5.03 %, 5.36 %, 2.56 %, and 2.83 %, respectively. However, from the beginning of the third cycle, the above four indicators would decline significantly. For the sample after 15 cycles of dry-wet cycles, these four indicators were only 53.08 %, 34.60 %, 50.27 %, and 33.19 % of the undamaged interface, respectively. Besides, the degree of influence of dry-wet cycle times on splitting tensile strength and shear strength F_T and F_S are 329.74 and 330.09, respectively. They are much larger than $F_{0.025}$. These undoubtedly proved this coupling effect was very aggressive on the interface between LWAC and OC. Thirdly, the conversion relationship between the direct shear strength of the interface and the interfacial splitting tensile strength would evolve during the dry-wet cycle. The ratio of shear strength to splitting tensile strength first stabilized at about 1.55 and then declined rapidly from the 12th cycle. After 15 cycles, it was only about 1.00. This indicated that the conversion relationship for interfacial shear-tensile strength in the conventional state in existing studies might not be applicable to interfaces during durability damage. Finally, microscopic experiments found that in the early stage of the dry-wet cycle test, the products of sulfate attack (ettringite and gypsum) filled the pores. The interfacial transition zone (ITZ) was denser, and the micro-hardness rose. In the middle and late stages of the dry-wet cycle test, many microcracks appeared in the ITZ, and the microhardness declined significantly. These also explained why the mechanical strength of the interface first increased and then decreased under the coupling effect of sulfate erosion and dry-wet cycles. In summary,

ICSBM 2023

3rd International Conference of Sustainable Building Materials

25-27 September, Wuhan, China

the coupling effect of sulfate erosion and dry-wet cycles on the mechanical strength and microstructure of the interface between LWAC and OC was serious. It should be given sufficient attention.

Influence of SCMs on the resistance to chloride penetration of ultra-high performance fiber reinforced concrete

Jia He, M.Sc., Department of the Built Environment, Eindhoven University of Technology, P.O. Box 513, 5600 MB Eindhoven, The Netherlands, e- mail: j.he@tue.nl

Qingliang Yu, Ph.D., Prof., School of Civil Engineering, Wuhan University, 430072, P.R. China;
Associate Prof., Department of the Built Environment, Eindhoven University of Technology, P.O. Box 513, 5600 MB Eindhoven, The Netherlands, Tel: +31 (0)40 247 2371, e- mail:
q.yu@bwk.tue.nl

Jos Brouwers, Ph.D., Prof., Department of the Built Environment, Eindhoven University of Technology, P.O. Box 513, 5600 MB Eindhoven, The Netherlands, Tel: +31 (0)40 247 2371, e- mail: jos.brouwers@tue.nl

Due to the large consumption of cement and high CO₂ emission, the further widespread and sustainable development of ultra-high performance fiber reinforced concrete (UHPFRC) has been severely restricted. Replacing cement with supplementary cementitious materials (SCMs) is a feasible way to promote the development of the eco-friendly UHPFRC. This study is to investigate the optimal critical value for maximum replacement level of limestone powder (LSP) and ground granulated blast furnace slag (GGBS) without compromising the superior flowability, hydration kinetics, pore structure, mechanical properties and durability of UHPFRC. Moreover, the distinct mechanisms of GGBS-cement and LS-cement binder systems for UHPFRC at various GGBS and limestone replacement levels are clarified in this study. The critical values for the cement replacement by GGBS and Limestone are 285 kg/m³ and 142 kg/m³, respectively. As optimal replacement levels for cement, 30 wt% GGBS and 15 wt% LSP are suggested in order to develop the eco-friendly and efficient UHPFRC with maximum binder efficiency.

Two-dimensional concrete meso-aggregate modeling method based on voronoi method

Jinyang Li, Department of the Built Environment, Eindhoven University of Technology, P.O. Box 513, 5600 MB Eindhoven, The Netherlands:

Renjun Yan, School of Naval Architecture, Ocean and Energy Power Engineering, Wuhan University of Technology, Wuhan 430063, P.R. China:

H.J.H. Brouwers, Department of the Built Environment, Eindhoven University of Technology, P.O. Box 513, 5600 MB Eindhoven, The Netherlands:

Qingliang Yu*, School of Civil Engineering, Wuhan University, 430072, P.R. China; Department of the Built Environment, Eindhoven University of Technology, P.O. Box 513, 5600 MB Eindhoven, The Netherlands:

Email of the corresponding author: q.yu@bwk.tue.nl

Keywords: Voronoi; crushed stone aggregate; pebble aggregate; aggregate grading; B-spline

The meso-mechanics of concrete involves the study and analysis of concrete at the meso-scale level, which is an intermediate scale between the micro-scale and macro-scale. It aims to understand the mechanical behavior and properties of concrete by examining its constituent materials and their interactions at this level. At the meso-scale, concrete is considered as a composite material comprising various components, such as aggregates, cement paste, the interfacial transition zone, and additional reinforcements or fibers. The process of meso-scale numerical simulation of concrete consists of two steps. Firstly, it involves generating two-dimensional and three-dimensional aggregate particles, taking into account their shape, spatial distribution, and volume fraction. Secondly, meso-scale numerical simulations are conducted, considering the influence of material properties of each phase component on concrete. Aggregates and fibers exhibit a random distribution in the meso-structure of concrete. Moreover, their spatial random arrangement determines the location of the interfacial transition zone surrounding the aggregates and fibers, leading to different damage development modes and failure strengths. Therefore, accurately representing the meso-geometry model of concrete is crucial for numerous numerical studies. However, achieving accurate replication of the natural characteristics of aggregates and fibers poses challenges in the meso-scale numerical simulation of concrete.

Voronoi diagrams have been extensively used in modeling various material structures, including polycrystalline materials and particulate composites. The versatility of Voronoi diagrams has demonstrated their potential in accurately representing aggregates with different morphologies. Moreover, their simplicity makes them easy to implement through a straightforward algorithm. While applying Voronoi diagrams for establishing concrete aggregate models is feasible based on these advantages, there are some limitations in the random generation of aggregates. Firstly, Voronoi-based aggregate modeling methods have not effectively addressed the aggregate grading problem, which refers to achieving the desired distribution of aggregate sizes. Secondly, ellipsoidal and circular aggregates differ significantly from the actual shape of pebble aggregates, introducing deviations in the representation of realistic aggregate shapes.

This paper is organized as follows: Firstly, it provides a detailed explanation of the Voronoi method and aggregate grading theory. Secondly, it presents the simulation of random generation of convex polygonal aggregates using the Voronoi graph partitioning technique in computer graphics. To meet the requirements of aggregate grading theory for aggregate area distribution, a convex polygonal aggregate model algorithm is proposed, which satisfies the grading requirements by randomly scaling the aggregate shape. To approximate the shape of pebble

ICSBM 2023

3rd International Conference of Sustainable Building Materials

25-27 September, Wuhan, China

aggregates, the B-spline curve interpolation method is applied to simulate the rounding process of the aggregate based on the random generation algorithm for convex polygon aggregates. The study further investigates the algorithm for generating the interfacial transition zone, building upon the random generation algorithms for convex polygons and ellipsoid-like aggregates. Finally, the paper examines the method of importing the aggregate model into finite element software. The results demonstrate that the proposed concrete meso-aggregate modeling method based on the Voronoi method not only effectively simulates the geometric shapes of crushed stone and pebble aggregates but also overcomes the aggregate grading problem. In particular, the generated elliptical aggregates closely resemble the shape of pebble aggregates while retaining the geometric features of convex polygonal aggregates.

Study on the design of alkali-activated concrete and its bonding properties with steel rebar

Li Qi^{1,2}, Li Peipeng^{1,2}, Ren Zhigang^{1,2*}

1. Hainan Institute, Wuhan University of Technology, Sanya 572019, PR China

2. School of Civil Engineering and Architecture, Wuhan University of Technology, Wuhan 430070, PR China

Email of the corresponding author: renzg@whut.edu.cn (Z. Ren)

Keywords: Alkali-activated concrete, chloride permeating, sulphate erosion, bond-slip

Improving the durability of building materials in the marine environment is an important factor in achieving building sustainability. In this study, the effects of fly ash, metakaolin, and limestone powder contents on the resistance of alkali-activated slag concrete to chloride and sulphate erosion and binding capacity were investigated by means of accelerated erosion, long-term immersion, and microscopic characterization. The results show that these mineral admixtures negatively affected the compressive strength of alkali-activated concrete while increasing chloride ion penetration. However, the specimens mixed with limestone powder had the lowest impact due to the filling effect. The addition of metakaolin significantly increased the chloride binding capacity of the concrete, which was the contribution of the N-A-S-H gel. Moreover, among the specimens immersed in chlorine salt for 30d, only pure slag and specimens mixed with 15% metakaolin were found to have Friedel's salt. In the accelerated erosion test with magnesium sulphate solution, two kinds of specimens mentioned have high resistance to sulphate. Through XRD, it can be seen that a large amount of gypsum was produced in each specimen, which is the main reason for the decrease in strength of the specimens in the later stage. In addition, the production of hydrotalcite was observed in SEM, which may contribute to the ability of alkali-stimulated concrete to collect chloride ions and deserves further investigation. The above tests show that fly ash has more negative than positive effects on alkali-activated concrete, while both metakaolin and limestone powder should not be mixed in amounts greater than 15%, although they are helpful for alkali-inspired concrete durability. Alkali-activated concrete reinforced with copper-plated microfilament steel fibers was prepared by an improved mix ratio and its bonding properties to steel rebars before and after electrochemically accelerated corrosion were investigated. The results of the rebar pull-out tests showed that: Rebar pullout is the dominant damage mode, followed by a small amount of brittle concrete or rebar damage. Accelerated corrosion specimens were split after testing, and large amounts of iron oxide and ferrous oxide were observed at the bond interface. At a corrosion rate of 2%, a small amount of corrosion products filled the interface between the concrete and the rebar, improving the bond strength between the two. Continuing to increase the corrosion rate to 4%, the corrosion products will produce volume expansion, destroying the bond between reinforcement and concrete, resulting in a reduction of bond strength. Higher bond strength between reinforcement and alkali-activated concrete than with normal concrete was found. In addition, increasing the fiber volume rate does not always improve the bond strength, but it reduces the brittle damage of the concrete and is expected to have an improvement in structural integrity. The optimum fiber volume rate was 0.5%.

Enhancing Chloride Migration Resistance of Cement Mortar with Fly Ash Through the Addition of Nano-Metakaolin

Qiuchao Li¹, Yingfang Fan^{*1}, Yanzi Qi¹, Shiyi Zhang^{1,2}, Surendra P. Shah^{3,4}

1 Institute of Road and Bridge Engineering, Dalian Maritime University, Dalian, Liaoning 116026, China;

2 School of Civil Engineering and Architecture, Shandong University of Technology, Zibo 255000, China

3 Department of Civil and Environmental Engineering, Northwestern University, Evanston, IL 60208, USA

4 Civil Engineering, University of Texas at Arlington, Arlington, TX 76010, USA

Email of the corresponding author: fanyf@dlmu.edu.cn

Keywords: Fly ash; Nano-metakaolin; Cement mortar; Chloride migration; Chloride concentration

Fly ash (FA) is an industrial waste that can contaminate the environment and soil if not properly managed. Fortunately, FA exhibits high pozzolanic activity and can be used to partially replace cement in the preparation of sustainable concrete. This not only reduces pollution caused by cement production and lowers carbon emissions, but also enhances the long-age mechanical properties and durability of cement-based materials. Nevertheless, when FA replaces cement, the reduced amount of cement available for hydration in the early stages leads to inadequate strength and a deterioration in chloride migration resistance in cement-based materials. This is highly detrimental to concrete structures under construction in marine environments, as the migration of chloride ions into the concrete can cause steel reinforcement corrosion, which impacts the durability of concrete structures. This article aims to investigate the improvement of nano-metakaolin (NMK) on the chloride migration resistance of FA cement-based materials. The rapid chloride migration (RCM) method was employed to compare the effects of various nanomaterials, including nano SiO₂, nano CaCO₃, nano Al₂O₃, nano attapulgite clay, and nano metakaolin, on the chloride migration resistance of cement mortar. The objective was to identify the most cost-effective nanomaterial i.e., nano-metakaolin. Subsequently, the influence of NMK on the chloride migration resistance of FA cement mortar at different curing ages was examined. The compressive and flexural strengths of NMK/FA cement mortar were obtained through strength testing. The mechanism behind the impact of NMK on the chloride migration resistance was explored using scanning electron microscopy. Furthermore, through automatic potentiometric titration of chloride ions, the chloride ion concentration in NMK/FA cement paste under simulated chloride environment was determined. The results reveal that among all nanomaterials tested, NMK exhibited the highest cost-effectiveness in enhancing chloride migration resistance of cement mortar; the optimum content of NMK in improving the chloride migration resistance of cement mortar is determined to be 5wt.%. NMK demonstrated a significant improvement in the chloride migration resistance of FA cement mortar, particularly before reaching a curing age of 7 d. Incorporating 5wt.% NMK into 30wt.% FA cement mortar resulted in a 72.93% reduction in chloride migration coefficient compared to solely adding 30wt.% FA cement mortar at a curing age of 7d. NMK enhances the compressive and flexural strengths of FA cement mortar at different curing ages (3, 7, 14, 28 d). Specifically, when cured for 7 d, the addition of 5 wt.% NMK increased the flexural strength of cement mortar containing 30wt.% FA by 10.35%. NMK leads to a denser microstructure in FA cement mortar, promotes the formation of hydration products and improves its chloride migration resistance of FA cement

ICSBM 2023

3rd International Conference of Sustainable Building Materials

25-27 September, Wuhan, China

mortar. Additionally, NMK exhibited the most substantial reduction in chloride ion concentration within FA cement paste at a curing age of 7d. When 5wt.% NMK was added to 30wt.% FA cement paste, the chloride ion concentration was only 51.96% compared to that observed in solely adding 30wt.% FA cement mortar. In conclusion, the addition of NMK results in a significant enhancement of chloride migration resistance, compressive strength, and flexural strength in FA cement mortar, especially during the initial curing period of 7d. NMK provides an effective solution to improve early-age strength and chloride migration resistance of FA cement-based materials, making it a suitable choice for the production of high-performance and sustainable concrete.

Strength estimation of concrete model scale sections with FRP for floating wave energy converters

Xiaoteng, Li ^{1*}, School of Earth Sciences and Engineering, Hohai University, Nanjing, 210098, China;

Hongqiang Chu ², School of Mechanics and Material Engineering, Hohai University, Nanjing 210098, China;

Rod Jones ³, School of Science and Engineering, University of Dundee, Dundee, DD14HN, United Kingdom;

Li Zheng ³, School of Science and Engineering, University of Dundee, Dundee, DD14HN, United Kingdom.

Email of the corresponding author: xiaoteng.li@hhu.edu.cn

Keywords: Fire reinforced polymer, flexural strength, ultimate moment capacity, wave energy converter.

Wave energy can add to the renewable market in many coastal areas. However, its conversion to electricity is more expensive than other renewable techniques due to high capex of wave energy converters (WECs). There is interest in using reinforced concrete as a more economic option with reinforcement using fibre-reinforced polymer (FRP) composites such as glass-fibre-reinforced polymer (GFRP) and carbon-fibre-reinforced polymer (CFRP). Macro-synthetic fibres can be added in some mix to limit cracking and potentially prevent catastrophic inundation. It is inevitable given the very large scale of WECs that structural elements will require construction joints although some designs could potentially be continuously slip formed to avoid this. This research reported here focuses on the potential of concrete sections with FRP and fibres as the sole reinforcement for WECs based on laboratory-scale model element testing.

Internal GFRP rebars (8 mm diameter) and external CFRP wraps (28 mm² cross-sectional area applied with thixotropic epoxy resin) were used as the tensile reinforcement separately for C50 concrete mode beam sections. The mix with internal fibres where applicable had 2.2% fibre volume fraction of concrete (20 kg/m³) and fibres were added together with cementitious materials.

The test beams were designed with three different reinforcement conditions:

- (i) 2 × 8 mm dia GFRP tensile reinforcement, beam size 500 × 100 × 100 mm (GC1 & GC2);
- (ii) 1 ×, 2 × or 3 × 28 mm² CFRP tensile reinforcement with a central epoxy-glued joint, beam size (including joint) 1003 × 100 × 100 mm (CC2.1, 2.2 & 2.3)
- (iii) 1 × 28 mm² CFRP tensile reinforcement with 55 mm macro-synthetic fibres added in concrete mix at a dosage of 20 kg/m³, beam size 1000 × 100 × 100 mm (CC3).

CC2.1, 2.2 & 2.3 beams were produced by joining two 500 × 100 × 100 mm beams end-to-end with a 3 mm layer of epoxy resin adhesive. This represents the way in which concrete lever arm sections are attached to hydraulic actuators that, in turn, produce electrical power. Quasistatic four-point bending tests were carried out on all beams to examine load-deflection behaviour, crack formation and ultimate limit behaviour.

ICSBM 2023

3rd International Conference of Sustainable Building Materials
25-27 September, Wuhan, China

The experimental results and estimated ultimate moment capacity for concrete sections are given in the Table. As shown, both methods are to some degree inaccurate. Two potential causes could mainly be attributed to this difference:

(a) The bond-to-concrete mechanisms of tensile GFRP and CFRP reinforcement are different while the epoxy bonding significantly affected tensile strength, especially when concrete surface was not supplementarily treated.

(b) The calculation of balanced FRP reinforcement ratio adopted would be inaccurate due to the presence of FRP/epoxy/concrete bond line and joint, indicated by CC2.3 failure mode that ultimately no concrete crush observed, although calculated being over-reinforced.

Table Experimental results and calculated estimations for the ultimate moment capacity of concrete model scale sections with FRP.

Beam	Experimental	Estimation (ACI 440.1R-15)		Estimation (Pilakoutas et al., 2011)		Modified estimation	
	M_{exp} (kN m)	M_{est} (kN m)	M_{est}/M_{exp}	M_{est} (kN m)	M_{est}/M_{exp}	M_{est} (kN m)	M_{est}/M_{exp}
GC1	4.7	3.8	0.81	4.5	0.96	-	-
GC2	4.9	3.8	0.78	4.5	0.92	-	-
CC2.1	0.8	4.8	6.00	5.0	6.25	1.5	1.88
CC2.2	1.9	7.6	4.00	5.2	2.74	3.0	1.58
CC2.3	2.3	8.8	3.83	5.9	2.57	6.1	2.65
CC3	1.2	4.7	3.92	5.0	4.17	-	-

Since the epoxy resin bond to concrete or concrete/CFRP significantly affected the structure, the design stress of external tensile CFRP wrap reinforcement can be instead derived as $\min \{\text{design tensile strain of epoxy resin, ultimate tensile strain of CFRP wrap, } 0.003\}$.

0.003 is the maximum strain in tension of external tensile CFRP reinforcement calculated from CC3. Generally, full encapsulation and immersion of CFRP wraps in the epoxy resin would rather be achieved for best bonding. However, voids were observed being existed within the bonded CFRP from X-ray reconstructed images. Thus, for tensile CFRP cross-sectional area, a safety factor of 0.9 is proposed using volumetric fraction analysis of the detected voids. As shown in the Table, for jointed beam with CFRP, modified estimation gave closer results although still 1.5-2.7 times greater than test ones. This is probably due to the significant structure effect of the joint.

This research studied the strength behaviour and capacity estimation of concrete beams with FRP from model-scale sections. Driven by industry demands, the research here was aimed at determining the potential of a steel-free reinforcement solution used for WEC design to substantially reduce costs. Concrete beam sections with internal GFRP bars ultimately reached estimated strength but failed in brittle mode. For those sections with external tensile CFRP wraps, strength was limited by bond failure within the concrete/epoxy/CFRP line. This research compared two capacity calculation methods and modified determination of the CFRP reinforcement tensile strain and cross-sectional area, turned out being effective in ameliorating the estimation.

Formation of gradient interface in concrete repair and its durability under load and marine environment coupling effects

Hao Liu^{1,2}, Haoliang Huang^{*1,2}, Jiangxiong Wei^{1,2}, Qijun Yu^{1,2}

¹School of Materials Science and Engineering, South China University of Technology, Guangzhou, China

²Guangdong Low Carbon Technologies Engineering Center for Building Materials, Guangzhou, China

The concrete structures serving in marine environment is subjected to the synergistic effect of many factors such as ions and loads, which makes the repaired concrete structures more prone to interface failure due to the discontinuity of the interface microstructure. In this study, interface with gradient microstructure between cement-based repair and substrate was built up by using waterborne epoxy resin (WER) to modify the repair material, and the durability of the repair under load and marine environment coupling effects was investigated. Experimental results showed that a gradient microstructure at the interface zone between the repair and the substrate was successfully built up with low viscosity WER. Due to the formation of gradient microstructure at the interface zone, the porosity and the micromechanical properties were significantly improved. After experienced wet-dry cycles in marine environment for 2 months, the bonding strength of the repair specimens without WER significantly decreased by 11% under the stress levels of 0.5, while that of repair specimens with WER only decreased about 3%. The porosity of interface zone at the zone 10 mm away from the surface of the repair specimens without WER was increased about 17%, while that of the repair specimens with WER has almost no significant change. In addition, it was found that Mg element was enriched at the interface of the repair specimens with or without WER, while this phenomenon is relatively more obvious in the repair specimens without WER. It can be demonstrated that the formation of gradient microstructure at the interface zone can effectively improved the durability of the repair.

Alkalinity optimization and long-term life prediction for BFRP bars serving in simulated marine concrete environments

Xiang Liu¹, State Key Laboratory of Silicate Materials for Architectures, Wuhan University of Technology, 430070 Wuhan, Hubei, PR China

Wei Chen², State Key Laboratory of Silicate Materials for Architectures, Wuhan University of Technology, 430070 Wuhan, Hubei, PR China

Email of the corresponding author: chen.wei@whut.edu.cn

Keywords: BFRP bars; Optimal alkalinity; Marine concrete; Long-term life prediction

Fiber-reinforced polymer (FRP) composites have many advantages, such as light weight, high strength, fatigue resistance, corrosion resistance, designability, and easy processing, and can reasonably replace steel bars. Excellent corrosion resistance is the most common feature of FRP composites; nonetheless, with the deepening of this field, researchers are gradually realizing that these composites, especially those based on cost-effective basalt-fiber-reinforced polymer (BFRP), are not completely immune to the service environment in civil engineering applications. Their mechanical properties are seriously degraded under the long-term action of humid heat and alkaline environments, which is mainly due to the swelling and hydrolysis of the resin matrix by the OH⁻ and H₂O in the external environment, resulting in internal microscopic damage, including debonding of the fiber/resin interface and damage to the fiber molecular structure. Among them, the high alkalinity of concrete matrices limits the applicability of FRP bars, and solving this problem has become the goal of most researchers in this field. More research is required on the effect of the alkalinity gradient on the degradation of the mechanical properties of BFRP bars and whether there is an optimal alkalinity value that can minimize their degradation rate.

This study aims to explore the evolution of the relationship between degree of decrease in the service alkalinity of the BFRP bars and extended service degradation, as well as to experimentally verify the existence of optimal alkalinity that minimizes the rate of BFRP bar degradation. The tensile strength is measured to predict the long-term behavior of the BFRP bars. Furthermore, the moisture absorption and micromorphology of BFRP bars subjected to different simulated SWSSC pore solutions are investigated. The ionic dissolution of BFRP bars and the chemical structure of their surface resin are used to demonstrate their degradation mechanisms in various corrosive solutions.

According to the results obtained, the following conclusions can be drawn: (1) At low aging temperatures, the moisture absorption and tensile strength degradation rate of BFRP bars immersed in the S11 corrosive solution (pH= 11.07) are significantly lower compared with those in other solutions. At high aging temperatures, instead, the deterioration increases along with the solution alkalinity. (2) Apparent morphology, SEM, and X- μ CT analyses showed that the degradation of BFRP bars proceeds from the outside to the inside, mainly affecting the internal resin matrix. The content of fibers and resin is reduced considerably outside the BFRP bar compared to the inside (from 34.79% to 20.80% and 31.90% to 14.81%, respectively), and the external void content increases dramatically from 33.32% to 64.41% after exposure to the S13 corrosive solution (pH= 13.24). (3) The amount of Si element dissolved in the basalt fibers and the O-H/C-H ratio of the surface resin first decreases and then increases as the solution alkalinity is raised; they reach the smallest values for BFRP bars immersed in the S11 corrosive solution. (4) According to the long-term service life prediction, reducing the pH of the concrete pore solution from 13 to 11 can extend the service life of BFRP bars by up to 50 times.

ICSBM 2023

3rd International Conference of Sustainable Building Materials
25-27 September, Wuhan, China

Effect of gneiss rock powder on the performance of machine-made sand concrete

Qin Jiefa, Yu Songbai, Chen Chao, Yang Mo, Jin Sheng, Ren Zheng, Wei Yang, Zhang Heng

Huaxin cement Co., LTD. 430073

Effects of gneiss rock powder with different dosage and fineness on working performance, physical performance and long-term durability of concrete. Study found that the work performance and admixture content of gneiss rock powder concrete were equivalent to that of fly ash concrete. With the increase of the proportion of gneiss rock powder replacing the supplementary cementing material, the physical properties of concrete were decreased. The content of gneiss rock powder as the concrete supplementary cementing material should be less than 20%, and the fineness of gneiss rock powder had no influence on the mechanical properties of concrete. There were no obvious difference between gneiss rock powder concrete and fly ash concrete in durability. The chloride ion diffusion coefficient of gneiss rock powder concrete was slightly higher than fly ash concrete, The wear resistance and anti-water impermeability performance of gneiss rock powder concrete had no obvious difference with fly ash concrete.

Key words: gneiss powder, the working performance, physical performance; long-term durability of concrete

A widely applicable freeze–thaw damage model for concrete considering a nonuniform temperature field

Xian–Liang Rong¹, 1. College of Civil Engineering, Tongji University, Shanghai 200092, China

Qi–Yu Zhang², 2. School of Materials Science and Engineering, Tongji University, Shanghai 201804, China

Email of the corresponding author: rxl021@126.com

Keywords: freeze–thaw damage model; unevenly distributed temperature field; relative dynamic elastic modulus; maximum freezing rate; maximum hydrostatic pressure

Since the 1940s, concrete freezing damage in severe frosty regions has attracted the attention of many scholars. As a porous medium, concrete can absorb and retain water. When the temperature is lower than 0 °C, the water in concrete pores begins to freeze and gradually melts with the increasing temperature. After a large number of freeze–thaw cycles (NFTCs), frost heave microcracks appear inside concrete and gradually expand and increase, providing channels for the intrusion of external water molecules and harmful ions. This intrusion will lead to a continuous deterioration in the mechanical properties of concrete (e.g., elastic modulus, compressive strength, tensile strength, and bond strength) and eventually result in a degradation in the mechanical (e.g., bending and shearing) and seismic performances of reinforced concrete (RC) members and structures. Due to the immaturity of early design specifications, the freeze–thaw damage mechanism is more complex and involves several variables. Therefore, the effect of freeze–thaw cycle (FTC) action on the mechanical properties of concrete and the bond properties are neglected in actual design and analysis, leading to a deviation between the analysis results and the actual state. Establishing a damage model to characterize the degree of FTC action and quantitatively characterize the deterioration in the mechanical properties of concrete is a prerequisite for more accurate analysis of concrete structures in severely cold regions. However, the existing studies performed at the material and component levels simply use NFTC as a damage index, but ignore the effect of uneven distribution in the concrete specimen and the difference in the freeze–thaw environment of concrete. In fact, the temperature field inside the coagulation diagram structure is inhomogeneously distributed. In other words, under the same freeze–thaw conditions, the concrete inside the structure at different depths suffers freeze–thaw damage to different degrees, and gradually weakens from the surface to the inside. Therefore, the results from the evaluation cannot be used to accurately characterize the freeze–thaw damage, and the results from different studies cannot be analytically compared. Therefore, this study uses the loss of relative dynamic modulus of concrete D as a physical index to characterize the degree of freeze–thaw damage. Starting from the concrete freeze–thaw damage mechanism (see Fig.1), a widely applicable freeze–thaw damage model that considers the nonuniform temperature field distribution (see Fig.2) inside the concrete structure is established based on Cai’s model (see Equ.1), theoretical derivations and experimental research. The accuracy and reliability of the

model are verified through design tests. Finally, the application of the freeze–thaw damage model considering nonuniform temperature field distribution (see Equ.2) is determined for RC beam–column joints under FTC action. The results show that the value for D is sensitive to the material coefficient λ . The value of λ tends to be a constant according to hydrostatic pressure theory and damage mechanics. The water–cement ratio significantly affects the temperature of the maximum freezing rate for concrete under FTC action, and the freezing rate for concrete under FTC action shows a linearly related with the quadratic power of the water–cement ratio. The freeze–thaw damage model considering nonuniform temperature field distribution can be used to accurately quantify the freeze–thaw damage of RC structures and members.

$$D = 1 - \left[(1 - D_0)^{\beta+1} - \frac{\alpha(\beta+1)\sigma_{\max}^\beta}{E_0^\beta} N \right]^{\frac{1}{\beta+1}} \quad (1)$$

where D is the relative dynamic loss modulus; D_0 is the initial damage; α and β are material parameters; σ_{\max} is the maximum hydrostatic pressure; E_0 is the elastic modulus of concrete under freeze–thaw action; and N is the NFTC.

$$D = \frac{V_d}{V} \{ 1 - [1 - 0.014N \times f_{cu}^{-0.804} \left[\frac{\eta}{K} \times U_{\max} \times \frac{d\theta}{dt} \times \phi(\bar{L}) \right]^{1.205}]^{2.205} \} \quad (2)$$

where V is the volume of the concrete structure under freeze–thaw action and V_d is the volume of concrete affected by freeze–thaw action; f_{cu} is the concrete compressive strength; η (poise) is the dynamic viscosity coefficient of the pore solution; K (m^2) is the permeability parameter of the pore solution in the cement paste; U_{\max} is the maximum value of; U ($m^3/m^3/^\circ C$), namely, $d\omega_f/d\theta$, is the volume of pore solution frozen in a per cubic meter of cement paste when the temperature decreases by 1 $^\circ C$; $d\theta/dt$ ($^\circ C/s$) is the cooling rate.

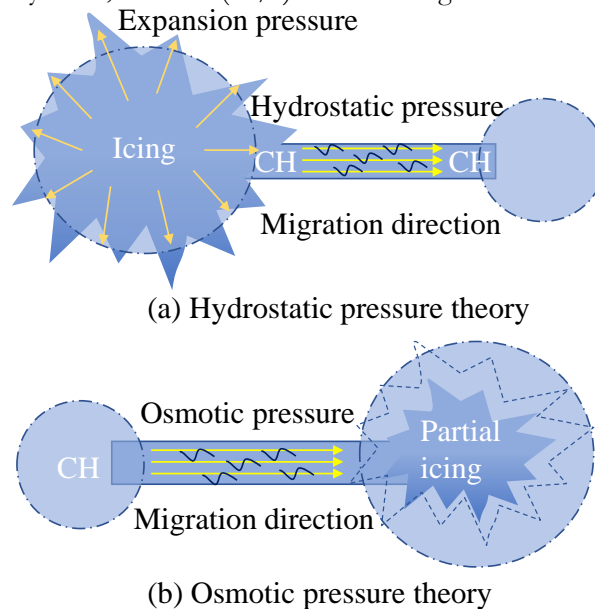
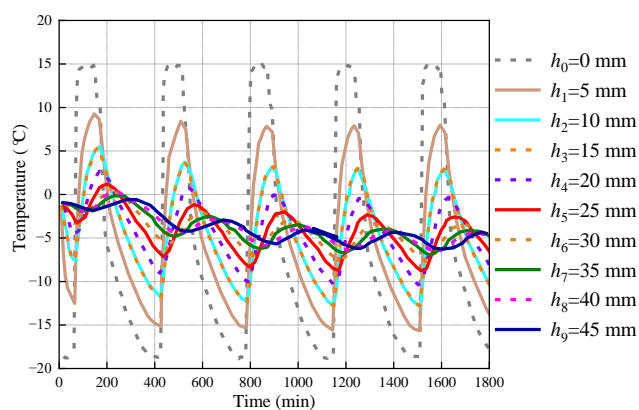
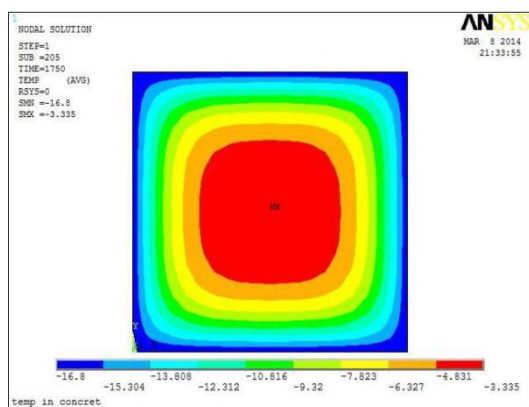


Fig. 1. Hydrostatic pressure and osmotic pressure theories.



(a) Temperature field distribution for S-1 at the end of the fifth cycle.

(b) Temperature variation at varying depths for S-1.

Fig. 2. Nonuniform temperature field distribution.

The potential use of Juncus plant fibers as reinforcement in compressed stabilized earth blocks

Reda SADOURI ^{1*}, Hocine KEBIR², Mustafa BENYUCEF ¹

Cadi Ayyad University¹, LRDDS Marrakech, Morocco

²Laboratoire Roberval, Université de Technologie de Compiègne, Centre de recherche Royallieu, Compiègne Cedex, France

Email of the corresponding author: r.sadouri@uca.ma

Keywords: Juncus fibers; ultrasonic test, mechanical strength; damage mode, thermal conductivity.

INTRODUCTION

Nowadays, there is a growing tendency to use natural fiber as reinforcement in earth blocks. Previous work [1-3] have shown the feasibility of producing building materials using local soil, and vegetable fibers, which are eco-friendly, regionally abundant with low cost, and interesting in terms of sustainable development. Earth has been used for thousands of years to build houses and shelters, where today about one 35 % of the world population still live [4, 5]. In most developing countries, houses are built using locally produced earth bricks because the presence of low environmental impact building materials contributes to reducing CO₂ emissions. Furthermore, up to 30 % of emissions could be reduced with a bioclimatic design and building structures that contain low environmental impact construction materials. In this context, the construction sector must change its building practices towards innovative and ecofriendly materials that meet the new requirement for users in terms of health impact, and comfort. Nevertheless, they are usually suffering from low strength and lack of durability. This is why it is recommended to stabilize earth blocks with low content of chemical binders (cement, lime, bitumen) in order to attain the minimum requirement in terms of strength and durability. This paper presents an experimental study on the effect of incorporating Juncus Fibers (JF) in compressed stabilized earth blocks (CSEB). Different destructive and non-destructive tests were carried out. Firstly, geotechnical characterization of soil has been conducted to assess its suitability to produce CSEB. The effect of JF on the apparent density, the dynamic elasticity modulus, the compressive strength, the damage mode, total water absorption capacity and thermal conductivity were discussed.

MATERIALS AND METHODS

In this work, we used raw earth material collected from the area of Ait Massoud next to Marrakesh to produce compressed earth blocks stabilized with low content of cement and reinforced with different percentage of juncus fibers from 0 to 0.2 % by weight. The geotechnical properties of the used soil were determined according to the standards to assess the suitability of the used earth to manufacture compressed blocks. The blocks were produced using hydraulic press with compaction pressure of 10 MPa. Then, the drying process of the samples took place in normal laboratory conditions for approximately 28 days until constant weight. Afterward, experimental test were carried out to study the influence of JF content on the properties of the composite materials.

MAIN RESULTS

The results indicated that the used soil is suitable to produce CSEB. Moreover, the finding noticed that an increase in JF content reduces apparent density, dynamic elasticity modulus, and thermal conductivity. For the total water absorption (TWA) test, the principal result is that all the composites remained unaffected and stable after a 4-day of immersion on water. While the increase of fiber content increase TWA.

ICSBM 2023

3rd International Conference of Sustainable Building Materials

25-27 September, Wuhan, China

CONCLUSION

Based on the results, the apparent density was reduced by approximately 12% in comparison with the unreinforced material. In terms of compressive strength the finding highlighted a reduction of about 14 % for 0.2% fibers weight replacement, compared to the composite material without fiber.

The evaluation of the dynamic modulus of elasticity shows a decrease from 3.832 GPa for non-filled blocks to 1.717 GPa for 0.2% fibers by wt. Moreover, it should be noted that the higher the juncus fibers content, the greater the thermal performances.

Investigations on the effect of surface treatment of hemp fibers on the mechanical and micro-performance of fiber-cement composites under accelerated aging

Helong Song, ¹ Tao Liu, ² Florent Gauvin, ^{1*} H.J.H Brouwers ¹

¹ Department of the Built Environment, Eindhoven University of Technology, PO Box 513, 5600 MB Eindhoven

² Department of Environmental and Resource Engineering, Technical University of Denmark, Brovej 118, Lyngby, Denmark

Email of the corresponding author: f.gauvin@tue.nl

Keywords: Hemp fibers; Hemp fiber-reinforced cement composites; Zirconium treatment; Alkaline degradation; Mechanical strength.

Nowadays, excellent-performance engineering materials made of biomass are dramatically advanced for the eco-friendly building field. Natural fibers reinforced cement composites have attracted much attraction and interest in the green and sustainable construction industry. This is due to the many advantages of natural fibers: low-cost, high Young's modulus, high availability, and renewability. However, the poor durability of natural fiber-reinforced cement composites is mostly due to the alkaline degradation of the embedded fibers in cement, which hinders the practical application of these materials in building and construction fields. To address this problem, this work aims to improve the alkali resistance of fibers by using zirconia to coat the fiber surface through a sol-gel technique. In this study, hemp fibers due to abundant availability in Europe were selected as the research objective. Three types of different treated fibers were incorporated into cement-based composites. The first type is the raw hemp fibers; the second type is the pretreated fiber after both acetone and alkali treatment; the third type is the zirconium-treated fibers. In addition, the amount of incorporated fiber is 2 % by weight of cement. After 28 d-curing, hemp fiber-reinforced cement composites were exposed to wetting/drying cycling conditions. The mechanical strength (compressive strength and flexural strength) of the investigated composites under different wetting/drying cycles were compared and analyzed. To deeply understand the reason behind the phenomenon, the interface compatibility index calculation between the fiber and the cement matrix, the thermostability of embedded fibers, and cement hydration products on the surfaces of the embedded fibers were studied. Furthermore, to compare alkali hydrolysis and mineralization, the different treated fibers were exposed to different simulated cement pore solutions for a period of time. The tensile strength of fibers was measured at different periods. The results show that the application of the zirconium treatment for the fibers did not provide a noticeable improvement in the mechanical strength of fiber-reinforced cement composites at 28 days of curing. By contrast, the zirconium-treated fiber-reinforced cement composites have the highest mechanical performances in terms of compressive strength and flexural strength regardless of the wetting/drying cycles. This confirmed that zirconium-treated fibers can benefit the improvement of hemp fiber-reinforced cement composites in durability. More amorphous phases (C-S-H) rather than crystallized phases such as portlandite and ettringites were precipitated on the surface of zirconium-treated fibers embedded in the cement-based composites. This is due to the hydration layer formed by the presence of zirconium on the fiber surface, which effectively prevent the cement hydration products from immigrating into the fiber surface and lumen, resulting in fiber degradation. Last but not least, the comparative results between alkali hydrolysis and mineralization indicated that zirconium treatment can effectively prevent fiber degradation in both aspects. Overall, the cement composites reinforced with zirconium-treated fibers presented improved durability, excellent interface compatibility between the fiber and the cement matrix, and higher alkaline resistance. The finding of this work provides an appropriate insight into the

ICSBM 2023

3rd International Conference of Sustainable Building Materials

25-27 September, Wuhan, China

development of industrial-scale, cost-effectively, and eco-friendly cement-based composites with hemp fibers. If this technique is successful, other natural fibers can be implemented in reinforcing the cement-based composites. Therefore, this technique of zirconium treatment employed on the fiber surface can accelerate the practical applications in the construction facilities such as structural layers in pavements and some building foundations.

Chloride induced mechanical degradation of ultra-high performance fiber-reinforced concrete: insights from corrosion evolution paths

Zhaoping Song^a, Shaohua Li^a, Qingliang Yu^{a,b,*}

^a School of Civil Engineering, Wuhan University, 430072, Wuhan, PR China

^b Department of the Built Environment, Eindhoven University of Technology, P.O. Box 513, 5600 MB Eindhoven, The Netherlands

Email of the corresponding author: q.yu@bwk.tue.nl

Keywords: Ultra-high Performance Fiber Reinforced Concrete; Chloride Induced Corrosion; Atomic Absorption Spectrometry; Nano-indentation; Corrosion Evolution Path; Mechanical Deterioration

Chloride-induced corrosion of ultra-high-performance fiber-reinforced concrete (UHPFRC) inevitably affects structural durability. However, the process of multi-fiber corrosion and mechanical deterioration still lacks sufficient understanding. This work aims to reveal the fiber corrosion degradation mechanism from a microscopic to macroscopic view, applying multiple analytical analyses of atomic absorption spectrometry, SEM-EDS, nano-indentation, polarization, and macroscopic mechanical testing. Results show that the flexural strength of specimens decreases significantly with the increase of corrosion degree, and a clear reduction of up to 47% is found at a high corrosion degree. Elastic modulus and nano-hardness of corroded samples vary in a wide range of 30 - 189 GPa and 0.16 - 6.41 GPa. With the increase in fiber content, two distinctive corrosion mechanisms are proposed. The corrosion path deteriorates from fiber edge to inner by the invasion of erosive solution through the matrix at low contents (< 2 vol.%). Considering impurities, greater interfacial defects and macro-cell potential differences at high contents (≥ 2 vol.%), another corrosion path originates from the fiber inner outward to the matrix. Fiber corrosion damages the fiber's structural integrity and induces matrix deterioration, the micromechanics of the matrix along the fiber edge 20 μm decreases at least 10% more than the concrete matrix. This work firstly sheds light on the mechanical deterioration of UHPFRC from the perspective of fiber corrosion paths considering different initiation scenarios.

Mesosopic numerical investigation on the bond behaviour between GFRP bar and UHPC

Donghua Tong, Yin Chi*, Le Huang*, Yaqi Li, Yanqin Zeng, Yinjie Yang, Lihua Xu

School of Civil Engineering, Wuhan University, Wuhan 430072, China

Email of the corresponding author: yin.chi@whu.edu.cn; huangle@whu.edu.cn

Keywords: Glass fibre-reinforced polymer (GFRP); Ultra-high-performance concrete (UHPC); Steel fibre; Bond mechanism; Mesoscale model

Ultra-high-performance concrete (UHPC) and fibre-reinforced polymer (FRP) have emerged as prominent high-performance materials that have gained substantial recognition in the construction industry in recent years. Structures made using UHPC generally include reinforcements such as Glass fibre-reinforced polymer (GFRP) bar to ensure reliable structural performance. The “strong alliance” strategy by combination of FRP bar and UHPC has become a promising approach to effectively improve the structure’s durability. Successful integration of GFRP bar and UHPC depends on their good bond for effective collaboration. The purpose of this paper is to analyse the nonlinear bond behaviour and failure mechanism at the bar/concrete interface by a three-dimensional mesoscopic numerical model. Considering the distinctive shape of helically wound GFRP bar, the geometric parameters of rib on the surface of GFRP bar were defined. Moreover, the random distribution of steel fibres within the matrix was taken into account, with specific emphasis on the surrounding region of GFRP bars at different steel fibre lengths. Particular attention is dedicated to the bond-slip relations of steel fibre-matrix interface to elucidate the mechanisms of fibre enhancement and toughening effects. The constitutive behaviour of the matrix is defined by employing the Concrete Damaged Plasticity (CDP) model, whereas the response of the GFRP bar is expounded using the sophisticated Hashin 3D UMAT (User Material). Interaction between GFRP bar and UHPC is provided as surface-to-surface standard contact with a hard interaction property and frictional coefficient of 0.3. A mesh non-conforming cohesive element insertion method was applied for modelling the behaviour of fibres within UHPC. The mechanical characteristics and failure modes of simulation were well-supported by existing experimental results, providing information unavailable from experimental investigation, including bond stress distribution and fracture evolution. Bond failure details and stress state within both the GFRP bar and UHPC can be reflected clearly. Influence of steel fibre (i.e., volume fraction and aspect ratio) as well as rib parameters (i.e., rib height, rib width, and inclination angle) on the bond performance was discussed. Results indicate that the length of steel fibre and the geometric shape of GFRP bar play a crucial role in determining fibre orientation within matrix near the bar/concrete interface, thereby affecting crack initiation and propagation. The abbreviated steel fibres demonstrate a heightened level of uniformity in their dispersion surrounding the GFRP bar, showcasing an increased frequency of permeating the gap between the ribs of the GFRP bar. The incorporation of steel fibres effectively inhibits the expansion of internal cracks in concrete, leading to a shift in the bond failure mode from splitting to pull-out. Increasing the steel fibre content and the height of surface ribs on GFRP bar can significantly improve the bond strength to a certain extent. However, further increases may be impeded by the shear resistance capacity of the ribs on the surface of GFRP bar. The proposed model presents a potent and economically alternative to laboratory testing methods. This paper makes a substantial contribution to the comprehension of the intricate interaction between GFRP bar and UHPC, providing invaluable guidance for practical implementation of FRP-reinforced UHPC structures in engineering applications.

TOPIC D: Functionalizing building materials

Long term development of mechanical properties of concretes with different water to cement ratio and internally cured concretes

Vlastimil Bilek¹, Faculty of Civil Engineering, VSB – TU Ostrava, Czech Republic

David Bujdos¹, Faculty of Civil Engineering, VSB – TU Ostrava, Czech Republic

Petr Miarka², Institute of Physics of Materials, Czech academy of Sciences, Brno, Czech Republic

Email of the corresponding author: vlastimil.bilek@vsb.cz

Keywords: bending strength, compressive strength, fracture properties, self-curing, water to cement ratio

As main difference between usual and high-performance concrete is considered low water to cement ratio and increasing importance autogenous shrinkage and microcracks formation in the case of HPC. Internal curing can enhance this situation but, from the other hand, it can reduce mechanical properties, as mechanical properties of porous soaked aggregates are lower.

Concretes with water to cement ratio $w/c = 0.50, 0.40$ and 0.30 were prepared. The dosage of ordinary Portland cement was kept constant – 450 kg for 1 m³ of concrete. Sand 0/4 mm and crushed granite 4/8 mm were used as aggregates. Polycarboxylate based superplasticizer were used for enhancing of workability of mixtures. Porous water-saturated aggregates (PSA) - expanded clay - were used for self-curing (internal curing) some of the concretes. The absorption of the PSA were measured and it was 33 %. 10% and 20 % of total volume of aggregates was replaced with PSA fraction 0/4 – it means, only sand was replaced. Some of specimens were wrapped with foil for avoiding of exchange water with environment and some of specimens were stored in water. Compressive and bending strength, modulus of elasticity and fracture toughness were measured at the age of 28, 91 and 365 days. Cubes 100 mm were used for compressive strength of concrete and prisms 80x80x480 mm for measurement of fracture properties and modulus of elasticity in accordance to Karihaloo and Nallathambi model of effective crack. Three-point bending strength was measured on fragments of beam after fracture test.

Compressive strengths increase as w/c decreases, but in accordance to Abrams law, more intensive increase can be expected for concrete with $w/c = 0.30$ in comparison with concrete with $w/c = 0.40$. This show deficiency of water in this concrete. Compressive strengths of water cured specimens were lower than that of foil cured. This is probably a consequence of pressure of water soaked in structure of concrete. This inner pressure helps to deteriorate the concrete during loading. Similarly, also bending strengths are better for foil cured specimens. This is a paradox because usually is water curing considered as the best way for avoiding of microcracking. Similar trends show also fracture toughness and modulus of elasticity. Probably, this is an effect of water between layers of CSH gel, but there is not strong evidence for this conclusion.

Presence of porous water-saturated aggregates reduces the compressive strength and bending strength of concrete with $w/c = 0.30$ at the age of 28 days. This was expected as strengths of grains of porous aggregate is worse than the strength of grains of sand. Later, at the age of 91 days and 1 year, the bending strengths of internally cured beams with 10 % of PSA are the same or even higher than that of without internal curing. This is a positive effect of PSA. Similar effect was recorded also in case of fracture toughness and modulus of elasticity.

Results are important for evaluation of effect of PSA on mechanical strength development. The

ICSBM 2023

3rd International Conference of Sustainable Building Materials

25-27 September, Wuhan, China

PSA can be not only expanded clay, as in this case, but also recycled concrete, recycled bricks or other secondary materials. Experiments with these recycled materials are performed and extended by fatigue tests.

Influence of expansive agent on the mechanical properties of steel-tube-confined high-performance concrete

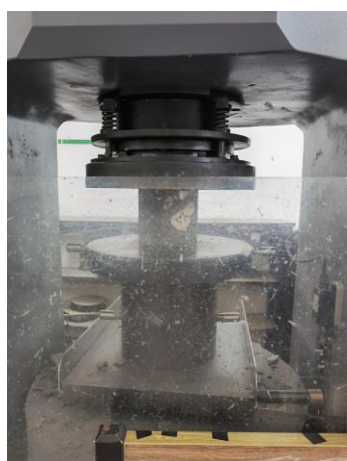
Yangyueye Cao¹, College of Basic Education, National University of Defense Technology, Changsha 410072, China;

Dianyi Song¹, College of Basic Education, National University of Defense Technology, Changsha 410072, China.

Email of the corresponding author: cy3yeah@163.com

Keywords: steel-tube-confined concrete, high-performance concrete, expansive agent, mechanical properties

Steel-tube-confined high-performance concrete (STCHPC) is a composite formed by filling steel tubes with high-performance concrete (HPC). Compared to normal concrete (NC), STCHPC has significant advantages in terms of load-bearing and deformation capacity; however, the shrinkage of HPC is much higher than that of NC. As a result, HPC tends to debond from the steel tube in STCHPC. Steel tube and HPC are only "mechanically" combined together, making it difficult to realize their joint work and hindering the high performance of STCHPC. In this study, expansive agent is added to HPC of C100 to reduce its shrinkage and thus improve the co-working properties of the tube and the HPC in the STCHPC specimen. The restrained shrinkages of the HPC with different dosages of expansive agent, namely 5%, 10% and 15%, are measured to assess the shrinkage reduction effect. Moreover, the influences of the expansive agent dosage on the compressive strengths of the HPC material and the STCHPC specimen are discussed respectively, using 100mm×100mm×100mm cubes and STCHPC specimens of two different dimensions. The test setups are given in Fig. 1. In order to evaluate the bond strength between the tube and the HPC, pushout tests are conducted, as shown in Fig. 2a. It should be noted that a rectangular steel block with a side length slightly smaller than the side length of the steel tube is placed on top of the STCHPC specimen to push the HPC. A 50 mm high space is left at the bottom of the tube to allow the HPC some room to move when it is pushed by the block. As illustrated in Fig. 2b, strain gauges are attached to the specimen to measure the circumferential strain around the specimen and the longitudinal strains along the height direction.

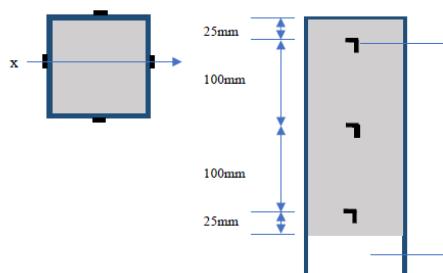
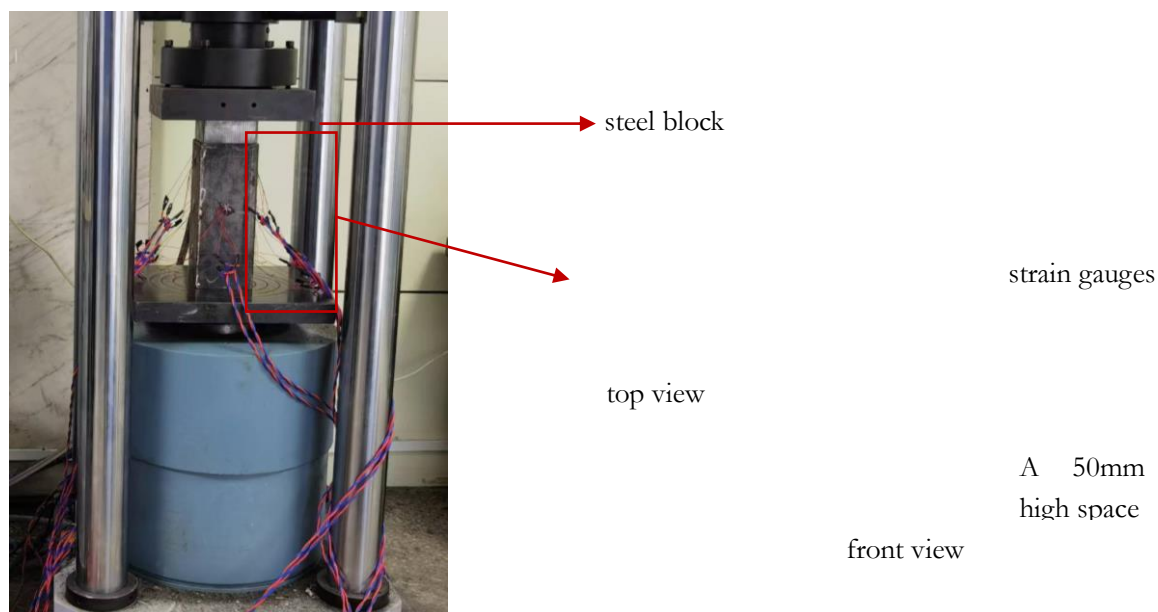


(a) HPC cube



(b) STCHPC specimen

Fig. 1 Compressive tests



(a) test setup

(b)

strain gauges arrangement

Fig. 2 Pushout test

The study show that the expansive agent can efficiently reduce the restrained shrinkage of the HPC. For instance, the 28d shrinkage of the HPC with 15% expansive agent is around 60% smaller than the one without the expansive agent. Moreover, the early strength of the HPC is slightly reduced, e.g., the 1d and 3d compressive strengths of the HPC cubes decrease by approximately 4.0% and 4.5%, respectively, when 15% expansive agent is added. In contrast, the 28d compressive strength increases by about 9.2%, indicating the positive effect of the expansive agent on the later strength of the HPC. The 28d compressive strength of the STCHPC specimen are also improved with the utilization of the expansive agent, and the influences are more remarkable with a higher dosage. This is due to the lower shrinkage of the HPC with more expansive agent, which makes the confinement of the steel tube on the HPC more significant. In terms of the pushout strength, the test results exhibit that the optimum dosage of the expansive agent varies with different STCHPC specimen dimensions. For example, the maximum pushout strength is observed when 15% expansive agent is used in the case of STCHPC specimen with a cross-sectional side length of 70mm; whereas the maximum pushout strength is achieved with 5% of expansive agent when the cross-sectional side length of the specimen increases to 116mm.

ICSBM 2023

3rd International Conference of Sustainable Building Materials

25-27 September, Wuhan, China

This observation suggests that the bonding of HPC to the steel tube is a synergistic effect of the tube confinement and the expansive agent, and that both influencing factors should be considered to achieve the optimum performance of STCHPC. The circumferential and longitudinal stresses in the tubes are calculated from the measured strains and they are used to quantitatively assess the effect of the expansive agent on the tube confinement. The study has important scientific significance and engineering application value.

Mechanism of inhibition of Temperature Rising Inhibitor on hydration of cement and supplementary cementitious materials

Weiyei Chen¹, Department of Civil Engineering, Tsinghua University¹, Beijing, China

Email of the corresponding author: yanpy@tsinghua.edu.cn

Keywords: Temperature Rising Inhibitor, hydration kinetics, supplementary cementitious materials, adsorption, precipitation

Temperature Rising Inhibitor (TRI) is a novel chemical additive used to reduce the early hydration heat of cementitious materials. A deep understanding of the mechanism by which TRI inhibits the hydration of cement and supplementary cementitious materials (SCMs) can help to understand the use of this additive. This study focused on the influence of β -cyclodextrin based TRI on the hydration kinetics of Portland cement and SCMs (slag, fly-ash, and silica fume), and the mechanism of action of TRI was explained by various analysis methods such as XRD-QPA, TG, ICP-OES, TOC, etc. The isothermal calorimetry results showed that within a 0.6% dosage, the decreases in peak values of heat releasing rates and total heat release in the first 3 days of the (blended) cement pastes were linearly related to the TRI dosage. When samples contained SCMs, the impacts of TRI on cement were more significant. The total organic carbon measurement of suspensions with TRI and different mineral particles showed that the phenomenon above was due to the different adsorption capabilities of mineral particles for TRI hydrolysis products. The isothermal calorimetry test of the hydration of pastes at different temperatures (25 °C, 35 °C, and 45 °C) showed that TRI was more effective on hydration inhibition at higher temperature than at lower temperature. XRD quantitative phase analysis on hardened (blended) cement pastes at different ages found that samples within 0.6% TRI added had significant differences in clinker mineral consumption and calcium hydroxide generation at early age compared to the blank sample, but they were basically same to blank sample when the age reached 28 days. The results of thermogravimetric analysis on samples cured at different ages corresponded to those of XRD quantitative phase analysis. The measurement of ion concentrations in pore solutions of (blended) cement pastes at various curing ages revealed that with the addition of TRI, the Ca concentration in pore solutions remained at a high level for a longer period of time compared to that of the blank sample, while the Si concentration and pH were lower than those of the blank sample. The synthesis of calcium hydroxide further indicated that the effect of TRI on prolonging the induction period was related to its inhibition of calcium hydroxide precipitation. And the synthesis experiment of calcium silicate hydrate (C-S-H) found that TRI was easily adsorbed on the C-S-H gel, which interfered with the further precipitation of C-S-H, explaining the role of TRI in decreasing the peak exothermic rate of cementitious materials hydration. The above results demonstrate that TRI inhibits the precipitation of calcium hydroxide and C-S-H through complexation and adsorption, respectively, thereby prolonging the induction period and decreasing the main exothermic peak of hydration of cementitious materials. Due to the fact that the TRI mainly affects cement in blended cement systems, the amount of TRI applied in composite cementitious material system should be based on the quality of cement as a reference.

Understanding the role of carbon nanotubes in low-carbon concrete: from experiment to molecular dynamics

Kai Cui, Dalian University of Technology, Dalian, China

Jun Chang, Dalian University of Technology, Dalian, China

Email of the corresponding author: mlchang@dlut.edu.cn

Keywords: Carbon nanotubes, Sulfoaluminate cement, Low-carbon, Hydration, MD simulation

Improving concrete's macro performance and durability is conducive to energy saving and emission reduction and is in line with the green and sustainable development concept. We innovatively proposed an effective method using dispersed CNTs to pre-saturated sand resulting in the dispersed CNTs distributed in the ITZ. We compared the methods of adding dispersed CNTs and dispersed CNTs pre-saturated sand. We also explored the macro performance, hydration process, and microstructure of low-carbon sulfoaluminate cement-based concrete through experiments and MD (molecular dynamics) simulations. The 28d compressive strength of CS2 (adding dispersed CNTs pre-saturated sand) compared with C0 (without adding CNTs) and C2 (adding dispersed CNTs) improved by 27.8% and 10.1%, respectively, while the 28d flexural strength enhanced by 16.7% and 6.3%, respectively. The primary mechanism is attributed to the adsorption and nucleation effect of CNTs; the CNTs promoted the generation of more AFt (ettringite) and AH3 (gibbsite), which improved the hydration degree. MD simulation also verified this mechanism, which modeled the change of Ca²⁺ mobility under the influence of CNTs addition. Ca²⁺ has a greater density distribution closer to the substrate under the effect of CNTs addition, indicating that substrate with CNTs addition has a stronger force on Ca²⁺. The stronger binding force between Ca²⁺ and substrate with the CNTs addition leads to a decrease in the density of Ca²⁺ in solution, which promotes further hydrolysis of the cement to release more Ca²⁺ for charge balance. The CNTs dispersed at the ITZ have a seeding effect; AFt and AH3 are generated around the CNTs, which reduces the width of the ITZ, dramatically promotes the combination of CNTs and the ITZ, and effectively improves the microscopic structure of the ITZ.

ICSBM 2023

3rd International Conference of Sustainable Building Materials
25-27 September, Wuhan, China

Salt scaling resistance of pre-cracked ultra-high performance concrete with the coupling of salt freeze-thaw and wet-dry cycles

Qian Deng ^a, Zixiao Wang ^a, Shaohua Li ^a, Qingliang Yu ^{a,b,*}

^a School of Civil Engineering, Wuhan University, 430072 Wuhan, PR China

^b Department of the Built Environment, Eindhoven University of Technology, P.O. Box 513, 5600 MB, Eindhoven, the Netherlands

Email of the corresponding author: q.yu@bwk.tue.nl).

Keywords: Ultra-high performance concrete; cracks; steel fiber content; salt freeze-thaw cycles; wet-dry cycles

Wet-dry cycles and cracking are unavoidable problems of concrete structures and reduce durability by enhancing the penetration of harmful ions and water, which may have a synergistic adverse influence with severe surface damage caused by salt freeze-thaw cycles. This study aims to investigate the salt scaling resistance of ultra-high performance concrete (UHPC) under multiple harsh environments including wet-dry cycles and pre-cracking. The workability of fresh concrete and the distribution of steel fibers are the key factors in determining the salt scaling resistance of UHPC. Pre-cracking and wet-dry cycles inhibit the rapid scaling damage of UHPC by accelerating chloride accumulation, which reduces the icing pressure of pore liquid and refining the micropores (<200 nm) capable of remaining non-frozen at low temperatures through the chemical binding of chloride. However, the combined effect of pre-cracking and wet-dry cycles can lead to the corrosion of internal steel fibers and more scaling damage, and the crack width should not be greater than 0.1 mm.

Research on Heat Resistance and Shielding Performance of Serpentine Shielded Concrete

Xueyu Gan¹ affiliation and addresses: WHUT

Email of the corresponding author: qiu-li@whut.edu.cn

Keywords: Serpentine aggregate Concrete Heat resistance Neutron shielding performance Radiation resistance

Neutrons are neutral particles with strong penetrating ability. When shielding neutrons, neutrons are usually slowed down with hydrogen-rich or low-atomic number materials, and then neutrons are absorbed with materials with large neutron absorption cross-sections. Serpentine contains a large amount of crystal water and has extremely high thermal stability, at 400 °C, the crystal water inside the serpentine will not be lost, so serpentine concrete is an ideal neutron shielding material. However, the high crushing value of serpentine and the serpentine associated mineral asbestos will have a great impact on the working performance of serpentine concrete.

Serpentine is used as coarse and fine aggregate to prepare serpentine shielding concrete. In order to solve the problem of poor working performance and poor mechanical properties of serpentine shielding concrete, river sand with a particle size below 0.6mm was selected to replace some serpentine fine aggregate. The water-to-adhesive ratio of serpentine shielded concrete prepared in this way can be reduced to 0.4, which has better mechanical properties and good working properties. In the preparation of serpentine shielding concrete, boron carbide particles of 1% serpentine shielding concrete mass are mixed with boron-containing minerals in situ in serpentine shielding concrete to increase the content of neutron ray absorption sections inside serpentine shielding concrete and improve the absorption capacity of serpentine shielding concrete to neutron rays.

The serpentine shielding concrete prepared according to the above method has good heat resistance, and the compressive strength increases by 15%-40% when baked to a constant mass at three temperature points of 300 °C, 350 °C and 400 °C, and the higher the compressive strength with the increase of temperature. When baked to constant at 300°C, 350°C and 400°C, the source of quality loss of serpentine shielding concrete and the loss of free water, bound water and CSH gel pore water inside the matrix is that serpentine aggregate does not lose water, so serpentine shielding concrete still has good shielding performance against neutron rays under high temperature conditions.

Formation of a layered structure porous glass-ceramics for neutron shielding

Kefeng Jiang¹, Wei Chen²

1.School of Materials Science Engineering, Wuhan University of Technology

2.State Key Laboratory of Silicate Materials for Architecture, Wuhan University of Technology.

Email of the corresponding author: chen.wei@whut.edu.cn

Keywords: neutron shielding, porous glass-ceramics, layered structure, B₄C

With the development of nuclear technologies, modern nuclear equipment trends to be more miniaturization and lightweight. The issue of nuclear safety has attracted more and more attention. Neutrons have stronger penetrating power than electrons and γ -rays and cause severer damage to human body than electrons, γ -rays and X-rays. Thus, the development of neutron shielding materials has attracted much attention.

The shielding of neutrons includes two process: scattering and deceleration of fast neutrons and absorption of thermal neutrons. The energy of fast neutrons can be transferred more effectively through neutron scattering to the target nucleus when the mass of a neutron is equal to the target nucleus. Thus, hydrogen with one neutron in its nucleus has the highest efficiency to slow down the fast neutrons. Materials containing much hydrogen like water, paraffin wax, polyethylene and etc. are suitable for slowing down the fast neutrons. The absorption efficiency of thermal neutrons depends on the neutron absorption cross-section. The elements like gadolinium (Gd), europium (Eu), cadmium (Cd), boron (B) and cobalt (Co) have rather high neutron absorption cross-section. Compounds of these elements can be used in neutron shielding materials. Among these elements, boron (B) has the advantages of chemical stability and low cost. And among the boron containing compounds, boron carbide (B₄C) has the highest content of boron and advantages of excellent mechanical strength, high melting point and relative low density. Boron carbide has been widely used in neutron shielding field.

Porous glass-ceramics is a kind of porous materials composed by glass phase and crystalline phase with gas inside. It has been used in thermal insulation, acoustic insulation, catalyst support and other fields due to its unique properties such as low density, low thermal and acoustic conductivity, excellent chemical resistance and excellent thermal stability. Compared with normal neutron shielding materials like concrete, metal foams, and boron-polymer composites, porous glass-ceramics have excellent comprehensive performances. Thus, porous glass-ceramics is suitable material for the neutron shielding of modern nuclear equipment. While the application of porous glass-ceramics in the neutron shielding hasn't been fully developed yet. Normal porous glass-ceramics have relatively low mechanical strength due to its low density and high porosity. Bulk glass-ceramics have rather high mechanical strength due to the dense structure and much crystalline. Thus, if the neutron shielding material can have a layered structure containing both porous structure and dense structure, it will possess both advantages of low density and excellent mechanical strength.

In this work, the influence of B₂O₃ on the foaming process and performances of porous glass-ceramics was investigated. And a "sandwich" structure neutron shielding porous glass-ceramics was prepared. The influence of B₂O₃ on the foaming process, pore structure, properties, performances, and neutron shielding rate was investigated. The addition of B₂O₃ can decrease the foaming rate of porous glass-ceramics. The incomplete foaming can help form a unique layered structure. The layered structure porous glass-ceramics with 5 wt.% B₂O₃ possess both advantages of light weight and high mechanical strength. This light weight and high mechanical strength neutron shielding porous glass-ceramics is potential to be applied in small nuclear equipment.

Fly ash as magneto-responsive additive for active rheology control of cementitious materials

Dengwu Jiao*, Assistant Professor, Department of Architecture and Civil Engineering, City University of Hong Kong, Kowloon Tong, Hong Kong SAR, China

Email of the corresponding author: dengjiao@cityu.edu.hk

Keywords: Active rheology control; Magnetic fly ash; Cement paste; Structural build-up; Magnetic field

Contradicting requirements of fresh properties exist in different casting operations of cement-based materials, e.g., the opposing requirements of structural build-up in reducing formwork pressure and improving multi-layer casting efficiency. 3D printing of concrete also needs to meet the contradicting requirements of rheological properties in pumping, extruding and layer-depositing process. Active rheology control is a potential approach to meet the contradicting requirements for the same concrete mixture, which can be achieved by activating an external magnetic field to a cementitious mixture containing magneto-responsive additives. As the main by-product of coal-fired power plants, fly ash particles are highly magnetic due to the presence of ferromagnetic spinel structures. It could be used as a potential responsive additive in the concept of active rheology control of cementitious materials, with the benefits of reducing the materials cost and increasing the sustainability of the binder materials.

This study presents the early magneto-responsive structural build-up of fly ash cement pastes by the means of small amplitude oscillatory shear (SAOS) technique, in which four different fly ashes with various particle sizes and magnetic properties are utilized. The correlations between the magneto-rheological (MR) effect and the magnetic properties of the incorporated fly ash are established. The magnetic force between fly ash particles in cement suspensions and the magnetic yield parameter, describing the relative magnitude of magnetic force to the resistance of the suspension, are then estimated. At last, the MR responses of fly ash and nano-Fe₃O₄ particles in cementitious suspensions are compared.

Results reveal that spherical fly ash with higher saturation magnetization and larger magnetic fraction generally shows higher MR response to an external magnetic field in cementitious suspension. Irregular fly ash with relatively low magnetic properties can show unexpectedly obvious MR response because of the morphological effect. By correlating the magnetic force, the magnetic yield parameter and the experimental parameters, when two neighbouring particles are both magnetic fly ash, the estimated magnetic yield parameter can be used as an indicator to describe whether the fly ash cement paste shows rheological response to a magnetic field. The intensity of MR response can be correlated to the average magnetic force calculated by considering the even distribution of magnetic fly ash particles in non-magnetic solid suspensions. Compared with cement paste with nano-Fe₃O₄ particles, fly ash cement paste shows a longer dominating period of liquid-like properties. It is concluded that fly ash can be used as a responsive additive to actively control the rheology and structural build-up of cement paste by applying magnetic field.

Design and Application Performance of Phase Change Heat Storage Aggregates and Concrete

Hui Li*, Fei Wang, Wukui Zheng, Zhigang Qiao, YongLe Qi

College of Materials Science and Engineering, Xi'an University of Architecture and Technology, Xi'an 710055, PR China

Ecological Cement Engineering Center of the Ministry of Education, Xi'an 710055, PR China

Shaanxi Ecological Cement & Concrete Engineering Technology Research Center, Xi'an 710055, PR China

Email of the corresponding author: lihui@xauat.edu.cn

As a potential thermal storage material, combined with building envelope, phase change materials (PCMs) can increase the thermal comfort of the building and reduce the space energy consumption.

A hollow structural carrier has been designed to encapsulate PCMs as aggregates to prepare phase change heat storage concrete (PCHSC). A systematic study was conducted on the granulation process and performance control of hollow structure ceramic particles (HSCPs), identifying the key factors affecting the performance of HSCPs. The absorption, encapsulation effect, and mechanism of HSCPs on PCMs were analyzed. The mechanical and thermal properties of the prepared PCHSC were studied. At the same time, based on environmental laboratory simulation experiments, the control effect of this PCHSC materials on indoor temperature was analyzed.

The results indicated that the macroscopic properties of HSCPs are mainly influenced by five factors: preheating time, preheating temperature, sintering time, sintering temperature, and shell thickness. By adjusting the sintering temperature and shell thickness, HSCPs with a compressive strength of 0.6-6.1 MPa, an effective porosity of 44.4% -69.69%, and a packing density of 435.26-678.20 Kg/m³ were prepared.

The absorption of PCMs by HSCPs is mainly affected by external forces, surface tension, and viscous resistance. Higher effective porosity usually leads to higher absorption, and a thinner shell is more conducive to PCMs entering the cavity of the ceramic particles under external forces. The leakage of PCMs is the result of the pressure generated by the thermal expansion of the gas sealed inside the pores on the ceramic shell wall being greater than the surface tension generated by the pores. To prevent the leakage of PCMs, a composite coating was applied to the surface of phase change aggregates. The leakage of wettable PCMs, such as paraffin, is the process of paraffin breaking through the capillary force at the end of the coating pores under the internal pressure difference, and increasing the coating thickness could reduce its leakage. The leakage of un-wettable PCMs, such as hydrated salts, is a process in which hydrated salts overcome energy barriers and work. It is related to the size of hydrated salt droplets, pore size, and internal pressure difference. The calculated phase boundary can be used to determine the encapsulation effect of coatings on hydrated PCMs.

When 8.1 wt.% PCMs is introduced into HSCPs, PCHSC with a compressive strength of 41.9 MPa at 28 days was prepared, which meets the requirements of concrete structural applications. Compared with ordinary concrete slabs, concrete slabs prepared using PCHSC could delay the occurrence of peak temperature, and the indoor peak temperature and temperature fluctuations were reduced by about 5.2 °C and 7.6 °C respectively.

The development of this new type of hollow structural carrier helps to encapsulate PCMs more conveniently and safely in concrete, providing a new approach for applying PCMs to building envelope structures.

Development of nano-enhanced composite phase change material for Trombe wall applications

Chukwumaobi Oluah^{1,2}, ¹Department of Mechanical Engineering Sciences, University of Johannesburg; ²Department of Mechanical Engineering, Northumbria University; ³Department of Mechanical Engineering, University of Nigeria Nsukka

Esther T. Akinlabi^{1,2}

Howard. O. Njoku³

Tien Chen Jen¹

Email of the corresponding author: coluah@uj.ac.za

Keywords: Phase change materials, trombe walls, nano particles, coal flyash

Trombe walls are green technology used to store and release thermal energy in buildings. They reduce the average electricity consumption meant for heating/cooling applications in buildings. Presented in this study is a sustainable material developed as a suitable alternative to conventional concretes/bricks used as massive wall materials in trombe wall systems. Coal flyash, calcium chloride hexahydrate, multiwall carbon nanotubes and sodium chloride were used to develop this new material. SEM, EDS, XRD, FTIR and a reduced scale thermal box experiments were conducted on the new material to prove its viability as a substitute to concretes as massive wall materials in trombe wall applications. The result of the thermal performance experiment revealed that the room with the composite phase change material absorbed more heat and regulated the ambient temperature more than the room without the composite phase change material hence making it suitable for use for thermal energy storage applications in buildings.

Surface Characterization of Carbonated Recycled Concrete Fines and Their Impact on Cement-Based, Lime-Based, and Alkali-Activated Materials

Xiaowei Ouyang *, Liquan Wang, Shida Xu, Yuwei Ma, Jiyang Fu

Research Center for Wind Engineering and Engineering Vibration, Guangzhou University,
Guangzhou 510006, China

Email of the corresponding author: xwouyang@gzhu.edu.cn

Keywords: Carbonation treatment; Recycled concrete fines; Cement paste; Lime-based materials; Alkali-activated materials.

In this study, an exploration into the surface characteristics of carbonated recycled concrete fines was undertaken utilizing techniques such as nuclear magnetic resonance (NMR), zeta potential analysis, and transmission electron microscopy (TEM). The investigation delved into the carbonation mechanism, shedding light on its intricate details. Concurrently, carbonated recycled concrete fines were employed to formulate cement-based, lime-based, and alkali-activated materials. These materials were subjected to meticulous evaluation at the micro-nano scale, enabling a thorough understanding of the mechanisms underlying their performance.

The efficacy of carbonation treatment in enhancing the properties of recycled concrete fines was substantiated, attributed to the interactions between CO₂ and the CH and C-S-H gel constituents of cement paste. To unravel the complexities of the performance enhancement mechanisms, a comprehensive analysis of the surface properties of carbonated recycled cement paste powder (CRP) was conducted. This analysis further elucidated the impact of CRP on the rheology, hydration kinetics, and strength development of cement paste.

The findings demonstrated that the carbonation process led to the formation of an amorphous silica gel layer enveloping the surface of CRP. CaCO₃ generated during carbonation was encapsulated within the silica gel matrix, limiting its exposure. The presence of the silica layer had a direct influence on the flowability of CRP-cement paste due to its strong affinity for water molecules. Initial stages of hydration witnessed the dissolution of the silica gel, thereby exposing the CaCO₃. Remarkably, CaCO₃ exhibited the ability to chemically absorb Ca²⁺, thereby facilitating the nucleation of C-S-H nuclei and stabilizing the C-S-H phase. Consequently, the growth of C-S-H was observed to be dense, uniform, and perpendicular on the CRP surface. The chemical bond formed between CaCO₃ and C-S-H further solidified the interface.

Notably, the enhanced interface between CRP and hydration products, attributed to the augmented C-S-H resulting from the reactions of silica gel with CH at the interface, was significantly stronger compared to the interface between recycled cement paste powder (RP) and

ICSBM 2023

3rd International Conference of Sustainable Building Materials

25-27 September, Wuhan, China

hydration products. This multifaceted understanding of the mechanisms at play highlights the transformative potential of carbonated recycled concrete fines in advancing the performance of cement-based, lime-based, and alkali-activated materials.

In conclusion, this study offers comprehensive insights into the surface properties of carbonated recycled concrete fines, their utilization in diverse material formulations, and their consequential impact on performance at the micro-nano scale. The findings pave the way for innovative approaches to enhance the sustainability and effectiveness of construction materials through informed material design and optimization.

Understanding the Generation and Evolution of Hydrophobicity of Silane Modified Fly Ash/Slag Based Geopolymers

Yuanshan She ^a, Yuxuan Chen ^{a,*}, Lijun Li ^c, Longjian Xue ^c, Qingliang Yu ^{a,b,*}

^a School of Civil Engineering, Wuhan University, Wuhan, 430072, PR China

^b Department of the Built Environment, Eindhoven University of Technology, P.O. Box 513, 5600 MB, Eindhoven, the Netherlands

^c School of Power and Mechanical Engineering, Wuhan University, Wuhan 430072, PR China

Email of the corresponding author: q.yu@bwk.tue.nl; Yuxuan.chen@whu.edu.cn

Keywords: Geopolymer; Hydrophobicity; Silane; Microstructure.

Silanes are widely used to enhance the corrosion resistance of cement-based materials by endowing the substrate with hydrophobicity. However, their applications in fly ash/slag based geopolymer (FSBG) are still rare. This study comprehensively investigates the hydrophobicity properties and reaction products of FSBG modified by isooctyltriethoxysilane admixture to reveal the mechanisms involved in the generation and evolution of hydrophobization effect. The hydration process and products are characterized by isothermal calorimetry, X-ray diffraction (XRD), Fourier transform infrared spectroscopy (FTIR), thermogravimetry and scanning electron microscopy (SEM) and energy dispersive X-ray (EDX). The porosity and pore structure is analyzed by gravimetry method and mercury intrusion porosimetry (MIP), respectively. Further, X-ray photoelectron spectroscopy (XPS) is applied to verify the modification by silane and detect the resultant change in chemical structure. The main conclusions can be made as follows: The coexistence of C-A-S-H and N-A-S-H gels is confirmed in the FSBG system according to the FTIR and EDX data. However, the formation of N-A-S-H gel is found to be restrained more intensely in the two gels with the use of silane, which is correlated with the higher amount of coupling sites located at the surface of fly ash particles and thus more silane adsorption. The addition of silane can effectively improve the erosion resistance of FSBG matrix with enabled hydrophobicity and lowered water absorption. Nevertheless, the mechanical strength in the long term is compromised. The increase of activator modulus has a negative impact over the strength and capillary absorption due to the higher porosity for the moduli range adopted in current research. The early compressive strength of FSBG at 1 day is found to slightly increase by introducing silane, which is consistent with the observed heat flow results. This can be mainly ascribed to the heat release along with the hydrolysis of silane, which completes within few hours after the mixing process and thus has a negligible effect for longer ages. With the application of silane, the reduction in porosity can be observed despite that the formation of hydration products is suppressed meanwhile, revealed from the FTIR, XRD and thermogravimetry results at 28 days. It may originate from the silane molecular layer occupying certain pore space, which is considered not to be incorporated into the gel skeleton and thus has less influence on the strength. This is why the porosity is actually not in accordance with the mechanical property. The evolution of contact angle on the surface of FSBG modified by silane is found to be closely dependent on its amount or more specifically its superficial density. However, the density has a maximum value caused by the restricted coupling sites, and thus excessive silane would not help but even worsen the hydrophobicity of the surface due to the reduced porosity. The contact angle evolution mode is revealed by proposing a formula, which can help to regulate and control the hydrophobicity properties of FSBG potentially. Moreover, due to the universal prerequisites adopted during the argumentation, they are also expected to be applicable for other geopolymer systems or cement-based materials with modification.

Biomimetic-Induced Hydroxyapatite for Autonomous Self-Healing in Cementitious Materials: Crack Repair and Rebar Corrosion Mitigation

Yanjie Tang, State Key Laboratory of Silicate Materials for Architectures, Wuhan University of Technology, Wuhan 430070, China; Department of the Built Environment, Eindhoven University of Technology, 5612 AP Eindhoven, The Netherlands

Yue Li, State Key Laboratory of Silicate Materials for Architectures, Wuhan University of Technology, Wuhan 430070, China

Katrin Schollbach, Department of the Built Environment, Eindhoven University of Technology, 5612 AP Eindhoven, The Netherlands

Wei Chen, State Key Laboratory of Silicate Materials for Architectures, Wuhan University of Technology, Wuhan 430070, China

H.J.H. Brouwers, State Key Laboratory of Silicate Materials for Architectures, Wuhan University of Technology, Wuhan 430070, China; Department of the Built Environment, Eindhoven University of Technology, 5612 AP Eindhoven, The Netherlands

Email of the corresponding author: chen.wei@whut.edu.cn

Keywords: self-healing cementitious materials; hydroxyapatite; supramolecular hydrogel; rebar corrosion; X-CT

Cement-based materials offer high strength, durability, and versatility, making them widely used in construction. However, they are prone to cracking from temperature changes, shrinkage stress, and cyclic loads during service. Cracks allow chloride ions and water to penetrate, increasing the risk of reinforcement corrosion. This compromises durability and shortens the service life of reinforced concrete. The development of self-healing cementitious materials plays a vital role in enhancing the durability of cement and concrete structures. Emulating the regenerative mechanisms observed in teeth and bones, the incorporation of hydroxyapatite products within the concrete matrix to address matrix defects represents a novel approach in the realm of self-healing technologies for cementitious materials.

This study focuses on utilizing biomimetic-induced hydroxyapatite as a means of achieving autonomous self-healing to address issues associated with crack repair and rebar corrosion in cement and concrete structures. A supramolecular hydrogel, specifically 2,6-bis[N-(carboxyethylcarbonyl)amino] pyridine (DAP), was employed as a carrier due to its high loading capacity and intelligent response following cracking, enabling the release of the repair agent and enhancing the healing efficiency of the matrix. In this study, $\text{NH}_4\text{H}_2\text{PO}_4$ was utilized as the repairing agent. The feasibility of combining DAP with $\text{NH}_4\text{H}_2\text{PO}_4$ for self-healing purposes was verified through the preparation of hydrogel-driven self-healing cementitious materials. Furthermore, the chemical stability of the simulated healing products after undergoing carbonation and exposure to chloride aggression was investigated. Subsequently, a comprehensive evaluation of the differences in reinforcement corrosion behavior between self-healing mortar and upscaled beams was conducted.

The findings indicate that the DAP supramolecular hydrogel relies on hydrogen bonding among gel molecular groups to establish a three-dimensional network structure, creating a space for the restorative agent. Moreover, successful loading of 1 mol/L $\text{NH}_4\text{H}_2\text{PO}_4$ within the DAP hydrogel was achieved. During the heating and cooling process, the supramolecular hydrogel undergoes dynamic reversible transformation from sol to gel state, enabling rapid encapsulation of the healing agent. Within a 24-hour period, the hydrogel gradually and continuously releases

ICSBM 2023

3rd International Conference of Sustainable Building Materials
25-27 September, Wuhan, China

phosphate in an alkaline solution, with a release amount reaching 76%. This sustained release provides ample time for the reaction between phosphate and calcium, facilitating the formation of self-healing products such as hydroxyapatite.

The designed self-healing system demonstrated successful repair of a 0.592 mm wide crack, resulting in the formation of hydroxyapatite as the primary healing product, accompanied by a minor presence of calcium hydrogen phosphate dihydrate and calcium carbonate. Carbonation exhibited minimal impact on hydroxyapatite within a dry environment, whereas in a wet environment, the effects of carbonation were more pronounced. In the presence of moisture, hydroxyapatite readily transformed into calcium hydrogen phosphate dihydrate or calcium carbonate. Notably, the introduction of chloride ions did not influence the nucleation and growth of hydroxyapatite.

Through X-ray computed tomography (X-CT) analysis of the reinforced specimens, it was observed that after 84 days of exposure to chloride salt erosion, the average thickness of the corrosion product layer for the blank control was within the range of 70-100 μm , with local regions exhibiting thicknesses exceeding 200 μm . In contrast, the repaired specimens displayed an average corrosion thickness of 40 μm , indicating effective mitigation of the corrosion rate through the integration of the self-healing agent.

Mechanical properties and underlying mechanisms of nickel coated carbon nanotubes reinforced ultra-high performance cementitious composite

Danna Wang ¹, Sufen Dong ², Xinyue Wang ¹, Baoguo Han ^{1,*}

¹ School of Civil Engineering, Dalian University of Technology, Dalian 116024 China

² School of Transportation & Logistics, Dalian University of Technology, Dalian 116024 China

Email of the corresponding author: hithanbaoguo@163.com (Baoguo Han).

Keywords: Ultra-high performance cementitious composites, nickel coated multi-walled carbon nanotubes, mechanical properties, microstructure, modification mechanisms

Ultra-high performance cementitious composite (UHPCC) with exceptional mechanical and durability properties is one of the most sought-after high-performing construction materials for high-rise buildings, long-span bridges, long tunnel, among others. It features low porosity and high compactness of the matrix by removing coarse aggregate, refining the fine aggregate particle gradation and introducing ultrafine mineral admixtures. The development of nanoscience and nanotechnology provides new possibilities for the optimization of UHPCC, taking into account the nano-core effect of nanofillers can modify the microstructures of UHPCC. Nickel coated multi-walled carbon nanotubes (Ni-MWCNTs) possessing extraordinary mechanical properties and thermal conductivity, are a promising nano reinforcement. Compared with ordinary carbon nanotubes (CNTs), the surface energy of Ni-MWCNTs treated with nickel plating is greatly reduced, and their wettability and dispersion in the matrix are modified. That is, Ni-MWCNTs combine the high mechanical strength of CNTs with the good wetting characteristics of nanoscale nickel particle, which show great potential in increasing their dispersion and composite efficiency in UHPCC. Therefore, researches on Ni-MWCNTs reinforced UHPCC are meaningful for the development of high-performance concrete.

This paper studies the mechanical properties of UHPCC reinforced by different aspect ratios of Ni-MWCNTs, including flexural strength, compressive strength, prismatic compressive strength, Young's modulus and Poisson's ratio. Besides, the thermocouples are arranged at the centre point of UHPCC specimens and the equidistant points around it, to monitor the temperature changes caused by the cement hydration heat inside UHPCC. As well, the modification mechanism of Ni-MWCNTs is also investigated through the Mercury Intrusion Porosimetry (MIP), Scanning Electron Microscope (SEM), energy dispersive x-ray spectrometry and ²⁹Si Nuclear Magnetic Resonance (NMR) tests of Ni-MWCNTs reinforced UHPCC.

The research results show that incorporating Ni-MWCNTs significantly improve the mechanical properties of UHPCC. The flexural strength, compressive strength and prismatic compressive strength of UHPCC with Ni-MWCNTs can be separately enhanced by 20–30%, 20–25% and 6–20%. Moreover, it is concluded that the mechanical strength of UHPCC generally increases with increasing doping of Ni-MWCNTs from 0.25 wt.% to 0.50 wt.%. The incorporation of 0.50 wt.% Ni-MWCNTs with an aspect ratio of 125 maximally increases the flexural strength and compressive strength of UHPCC by 34.0%/1.94 MPa and 25.2%/21.71 MPa, respectively. The prismatic compressive strength of UHPCC obtains a maximal increase of 20.2%/20.39 MPa when 0.50 wt.% Ni-MWCNTs with an aspect ratio of 1500 is incorporated. However, the Young's modulus and Poisson's ratio improvement degree of adding Ni-MWCNTs to UHPCC in this study are limited. In general, Ni-MWCNTs with small aspect ratios at 0.50 wt.%, as well as with large aspect ratios at 0.25 wt.% are beneficial to improve the Young's modulus and Poisson's ratio of UHPCC. The introduction of 0.25 wt.% Ni-MWCNTs with an aspect ratio of 3333/0.50 wt.% Ni-MWCNTs with an aspect ratio of 200 reinforces the Young's modulus to 34.56 GPa/ 34.94 GPa, which is 9.4%/10.6% greater than that of the control UHPCC. Additionally,

ICSBM 2023

3rd International Conference of Sustainable Building Materials
25-27 September, Wuhan, China

the Poisson's ratio of UHPCC mixed with 0.25 wt.% Ni-MWCNTs with an aspect ratio of 1500 or 0.50 wt.% Ni-MWCNTs with an aspect ratio of 125 increases by 8.5% or 9.4%, respectively. It is considered to be related to two reasons: one possibility is that Ni-MWCNTs with large aspect ratios are unevenly dispersed in cementitious matrix, especially at a high content; the other is thanks to the low probability of overlap between Ni-MWCNTs with small aspect ratios under the elastic ultimate load, which is not beneficial to the formation of a reinforced network structure. The mechanism of Ni-MWCNTs enhancing the mechanical strength of UHPCC can be explained as follows. First, the thermal conductive network formed by Ni-MWCNTs in matrix reduces the temperature difference and improves the temperature uniformity inside UHPCC, thereby decreasing thermal stresses, primary cracks and defects of composites. Then, it is observed that the incorporation of Ni-MWCNTs can reduce the porosity, improve the pore structure of the composites and make the microstructures dense by MIP test and SEM analysis. Furthermore, Ni-MWCNTs are conducive to promoting the transition of the silicate tetrahedral structure from dimer to dimer short chain and improving the polymerization degree of calcium silicate hydrate gel, according to the results of ²⁹Si NMR. Thereby, the introduction of Ni-MWCNTs contributes to optimizing the microstructure of matrix and achieving effective enhancement to UHPCC.

Preparing energy conservation self-levelling mortar via fly ash cenospheres/paraffin using in floor radiant heating

Fei Wang, College of Materials Science and Engineering, Xi'an University of Architecture and Technology, Xi'an, Shaanxi, China, 710055

Wukui Zheng, Materials Science and Engineering, Xi'an University of Architecture and Technology, Xi'an, Shaanxi, China, 710055

Yujin Gou, Materials Science and Engineering, Xi'an University of Architecture and Technology, Xi'an, Shaanxi, China, 710055

Zhigang Qiao, Materials Science and Engineering, Xi'an University of Architecture and Technology, Xi'an, Shaanxi, China, 710055

Yongle Qi, Materials Science and Engineering, Xi'an University of Architecture and Technology, Xi'an, Shaanxi, China, 710055

Hui Li, Materials Science and Engineering, Xi'an University of Architecture and Technology, Xi'an, Shaanxi, China, 710055

Email of the corresponding author: sunshine_lihui@126.com

Keywords: Gypsum, self-levelling mortar, fly ash cenospheres, phase change materials, floor radiant heating.

With the development of economy and the improvement of people's living standard, people requires more comfort of life, which will inevitably increase the consumption of energy. Data shows that building energy consumption has accounted for more than one third of the world's total energy consumption, in which nearly half of the energy consumption is used for space heating and cooling control. In the heating system, radiant floor heating system (RFHS) has the advantages of large heat exchange area, high space utilization efficiency, uniform indoor temperature distribution, etc. However, RFHS contribute negatively to global energy consumption and greenhouse gas emissions, it is necessary to develop new energy-saving technologies to reduce the energy consumption. Gypsum is a kind of green and environment-friendly cementitious material, which has excellent performance of ecology, low carbon, environmental protection and health. Gypsum-based self-leveling mortar made of gypsum is used as the ground leveling layer. After pouring on the ground, the ground will not produce cracks, drum and other phenomena. Gypsum-based self-leveling mortar has the social and economic benefits of energy saving and emission reduction, and can promote the comprehensive utilization of industrial solid waste. It is an environment-friendly green leveling mortar for the ground. In addition, phase change materials (PCM) are considered as potential candidates for RFHS because of their high enthalpy and relatively constant temperature during phase change as an effective heat storage technique. A growing literature has investigated RFHS integrated with PCMs in dry and wet construction. However, few scholars use gypsum self-leveling material and phase change material together for RFHS, so as to simplify the construction process and increase the heat storage capacity of the RFHS.

In this paper, the feasibility of preparing self-levelling energy storage mortar by incorporating fly ash cenospheres/paraffin (FACP) into gypsum-based materials. An experiment was designed to assess the effects of FACP on the flowability, microstructure, mechanical and thermal properties of gypsum based self-leveling mortar. The result shows that that the particle size, pre-treated method of FACP and sand replacement ratio affects many properties, by comprehensive thinking of strength, fluidity and thermal property as well as possible economic and environmental

ICSBM 2023

3rd International Conference of Sustainable Building Materials

25-27 September, Wuhan, China

impacts, and the medium size fly ash is considered to be a suitable particle size for making self-leveling mortar. Compared with untreated FACP and treated with silica fume, FACP treated with hardened cement could decrease the leakage of paraffin and increase the flowability of the mortar, increase the mechanical strength and fluidity of mortar. A radiant floor system proved that self-leveling energy storage mortar can prolong the indoor temperature within the comfortable range and improve the thermal comfort. In the application prospect, the research results provide a reference basis for using electricity to solve the problem of winter heating in hot summer and cold winter areas.

Design of Core-Shell Aggregates and Research on the Mechanism of Heavy Metal Stabilization in Red Mud

Di Wu¹, affiliation and addresses: Department of Civil Engineering, Qingdao University of Technology, Qingdao

Qingqing Xu¹, affiliation and addresses: Department of Civil Engineering, Qingdao University of Technology, Qingdao

Dongshuai Hou¹, affiliation and addresses: Department of Civil Engineering, Qingdao University of Technology

Xinpeng Wang¹, affiliation and addresses: Department of Civil Engineering, Qingdao University of Technology, Qingdao

Email of the corresponding author: wangxinpeng@qut.edu.cn

Keywords: Red mud, Encapsulation, UHPC, Selective chemisorption, Density functional theory (DFT) calculation

The use of RM in building materials is an effective way to efficiently utilize this resource. However, the current resource utilization of RM in construction materials faces challenges related to low cost-effectiveness, environmental safety, and high added value. RM exhibits low activity, poor stability, making it difficult for low-energy preparation and large-scale utilization. It also contains harmful impurities that pose environmental risks, making safe utilization challenging. Moreover, the existing disposal techniques for RM are inefficient and lack precise design, hindering high-value utilization. Therefore, the development of RM for its large-scale and safe use in building materials is urgently needed.

To alleviate the storage of red mud (RM) and the resulting pollution, this study presented an encapsulation-based strategy for the safe management of RM, and adopted ultra-high performance concrete (UHPC) as an encapsulating material due to its superior impermeability and chemisorption properties. It is noteworthy to find that encapsulated material suffered from a selective chemisorption according to the semi-quantitation calculation of chemical solidification and physical package. The density functional theory (DFT) calculations were innovatively employed to investigate the selective chemisorption mechanism. The simulation results suggested that distinct bonding forms lead to the selective chemisorption of heavy metals, with Pb being adsorbed by Si-O-Pb chemical bonds and a strong Si-O-Pb-O-Si long chain, while As and Cr only form relatively weak As-O and Cr-O bonds through their attraction to O atoms. With synergistic effect of chemical solidification and physical package, a stronger stabilization effect is achieved. The leaching results indicated that the encapsulated RM exhibited exceptionally low concentrations of hazardous components (i.e., Na at 1.580 mg/L, As at 0.003 mg/L, Cr at 0.027 mg/L, and undetected levels of Pb in encapsulated RM with a thickness of 0.5 mm), far below the limits set by the United States Environmental Protection Agency (EPA). This study opening a new window for the safe and effective utilization of hazardous solid waste.

Phosphorus removal improvement of porous concrete using highly adsorptive aggregates

Fan Wu^{1,2}, Qingliang Yu^{2,3,*}, H.J.H. Brouwers²

¹Key Laboratory of Mountain Hazards and Earth Surface Process, Institute of Mountain Hazards and Environment, Chinese Academy of Sciences, Chengdu 610299, P.R. China

²Department of the Built Environment, Eindhoven University of Technology, P.O. Box 513, 5600 MB Eindhoven, The Netherlands

³School of Civil Engineering, Wuhan University, Wuhan 430072, P.R. China.

Email of the corresponding author: q.yu@bwk.tue.nl

Keywords: Pervious concrete; Bio-based concrete; Adsorptive aggregate; Steel slag; Adsorption performance.

Stormwater runoff pollution has become one of the major contributors to water body pollution in urban building engineering with the development of urbanization, affecting the health of urban residents and the development of ecological cities. Permeable structures such as pavements, parking lots, and rain gardens have been widely used in recent years to achieve urban stormwater runoff management in countries, such as the United States, China, Europe, and others, based on the concept of low-impact development. Pervious concrete is critical in allowing stormwater runoff to penetrate through its porous structure and providing collected water to the underlying soil layer. However, very limited studies have been conducted to investigate the pollutants removal capacity of pervious concrete from stormwater runoff.

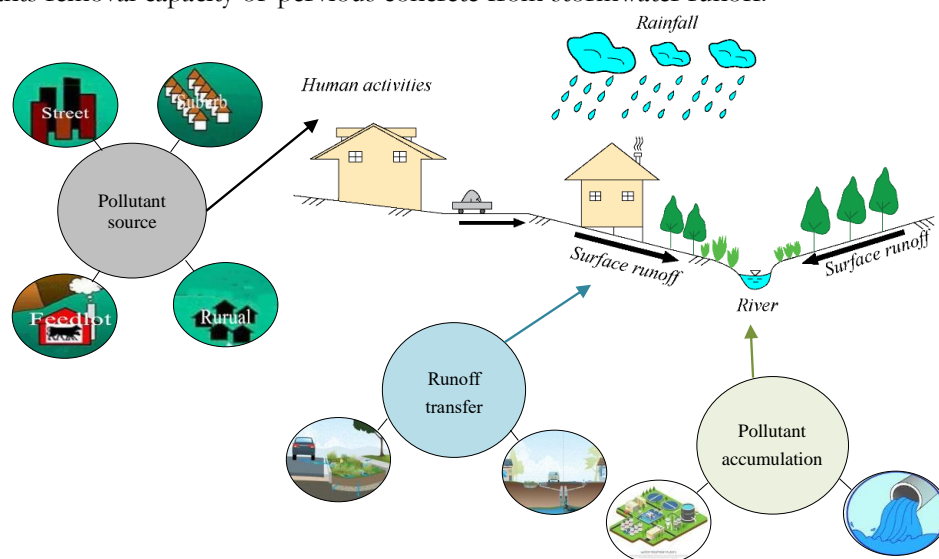


Fig. 1. Pollutant transfer process from the road surface to a nearby water body.

Some pollutants such as nitrogen, phosphorus (P), organic matter, and toxic pollution, can be carried into nearby water bodies during the rainy season, as shown in Fig. 1. The primary mode of transport for these pollutants is stormwater runoff. Among these pollutants, P has been identified as a major contributor to the poor water quality of the underlying soil layer, resulting in algae blooms and eutrophication. With the widespread use of pervious concrete, it is possible to remove some pollutants from stormwater runoff during the stormwater penetration process from the road surface to the underlying soil layer. Therefore, the adsorption capacity of pervious concrete should be significantly improved, particularly for P-removal, and its adsorption

mechanism and environmental impact should be evaluated.

Pervious concrete is typically made with no sand or very little sand to achieve a porous structure with high permeability for rapid water collection. The pollutant removal ability of pervious concrete has recently received widespread attention. Pervious concrete treated with TiO_2 , for example, is used to remove methylene blue, total P, and ammonia nitrogen with a removal rate of 60-90%. Calcium sulfoaluminate cement and coal bottom ash aggregates are used as pervious concrete components for nitrogen and P removal. Furthermore, various materials with high adsorption capacity are used as the components of highly adsorptive pervious concrete to improve pollutant removal, such as red mud, which is used to improve the removal rate of heavy metal ions from rainwater runoff, and alkali-activated slag, which is modified by chitosan and then used in pervious concrete to increase the adsorption capacity. Adsorption capacity of pervious concrete generally increases with increasing adsorbent dosage. However, despite the fact that conventional pervious concrete can be used to remove pollutants such as heavy metals (Mn, Co, Ni, Pb, As and Cs), fecal coliforms and P, etc., relatively poor adsorption performance and a long reaction time are observed during the adsorption process. To improve pollutant removal capacity, pervious concrete with high adsorption capacity should be developed.

This study aims to improve the adsorption performance of pervious concrete. Converter steel slag (SS) and manufactured adsorptive aggregate (AD) are applied as coarse aggregates for highly adsorptive pervious concrete, and conventional aggregate (basalt) is used as a comparison aggregate. The physical and mechanical properties, as well as the P-adsorption performance of pervious concrete are investigated. The cyclic adsorption characteristics, adsorption mechanism, and environmental impacts are studied. Adsorption isotherms and kinetics models are used to analyze the adsorption results.

The results show that the adsorptive aggregate type has a significant impact on the P-adsorption performance of pervious concrete. Concrete containing adsorptive aggregate and steel slag has a higher P-adsorption capacity than conventional aggregate concrete, increasing by 30.7% and 51.6%, respectively. The chemisorption of Ca-P precipitation is dominated by the concentration of Ca^{2+} released from concrete. P-adsorption capacity and removal rate of pervious concrete increase with P-concentration and reaction time. The Langmuir model and Elovich model fit the adsorption isotherm of pervious concrete well. Moreover, adsorptive aggregate concrete and steel slag aggregate concrete have low P-desorption, indicating that they can be used safely for P-removal from stormwater in sustainable permeable pavements with minimal environmental impact.

The positive effects of power ultrasound assisted mixing on Portland cement pastes: dispersion, hydration dynamics and products evolution

Guangqi Xiong^{1,2}

¹College of Materials Science and Engineering, Chongqing University, Chongqing, 400045, China

²Department of Civil and Environmental Engineering, The Hong Kong Polytechnic University, Hung Hom, Kowloon, Hong Kong, China

Yuanliang Ren¹

¹College of Materials Science and Engineering, Chongqing University, Chongqing, 400045, China

Zheng Fang¹

¹College of Materials Science and Engineering, Chongqing University, Chongqing, 400045, China

Xiaolong Jia¹

¹College of Materials Science and Engineering, Chongqing University, Chongqing, 400045, China

Chong Wang^{1*}

¹College of Materials Science and Engineering, Chongqing University, Chongqing, 400045, China

*Corresponding author

Shuai Zhou^{1*}

¹College of Materials Science and Engineering, Chongqing University, Chongqing, 400045, China

*Corresponding author

Email of the corresponding author: chongwang@cqu.edu.cn ; shuaizhou@cqu.edu.cn

Keywords: Power ultrasound assisted mixing; Dispersion; Hydration dynamics; Products evolution

This paper developed a novel power ultrasonic-assisted mixing technology to prepare cement paste at a water-to-cement ratio of 0.40. Three ultrasonic power levels (0 W, 480 W and 912 W) were adopted. Rheology, sedimentary stability experiments and compressive strength were tested. The hydration process was determined by means of inductively coupled plasma-optical emission spectrometry (ICP-OES), isothermal calorimetry, X-ray diffraction (XRD) with the Rietveld method, Fourier transform infrared spectroscopy (FTIR) and Thermogravimetric analysis (TGA). The results indicated that high-intensity power ultrasound (e.g., 912 W) decreased the apparent viscosity of fresh cement paste. The time required to reach 250 ml precipitation volume was increased by 76.4%, which indicated that the PUS acted on the particles in the form of vibration, combined with the mechanical shear energy generated by mechanical mixing, weakening the agglomeration energy and dispersing the particles. The rapid formation of calcium hydroxide (CH), ettringite and C-S-H gels was promoted by power ultrasound, which accelerated the crystallization nucleation process. The CH content of the 480 W and 912 W groups increased 5.27% and 3.79% at 1 day and 2.86% and 1.57% at 28 days, respectively. The hydration exothermic results showed that the hydration kinetic process of cement paste prepared by the PUS-assisted mixing process can be described by the nucleation and crystal growth (NG), phase boundary reaction (I) and diffusion (D) stages. The transition time from NG to D in the ultrasound group was faster than that in the reference group. Moreover, power ultrasound shortened the induction period and increased the accumulated heat release of cement paste at early hydration ages. The total heat release of the 480 W and 912 W groups increased by 7.83% and 11.89%, respectively, compared with that of 0 W when the cement paste was hydrated

ICSBM 2023

3rd International Conference of Sustainable Building Materials
25-27 September, Wuhan, China

for 36 h. The capillary pores and gel pores were both reduced at 28 days hydration ages by applying high intensity power ultrasound (e.g., 912 W) treatment. The porosity, including middle and large capillary pores, decreased with increasing ultrasonic power from 2.25% in the 0 W group to 0.62% in the 912 W group. The small capillary porosity increased from 8.20% to 8.79%. The changes in capillary pores that were closely related to the permeability indicated that high intensity power ultrasound may improve the resistance to ion attack or gas penetration in cement paste. Moreover, the gel porosity of the 912 W group decreased 35.17% and 31.87% compared with that of the 0 W and 480 W groups, respectively. The power ultrasound also enhanced the early age strength and ensured the strength increment rate at late hydration ages. The compressive strength of the 912 W group increased by 26.1% at 1 day and 18.3% at 28 days compared with that of the control group. This study also found that ultrasonic irradiation increased the gel-space ratio of the cement matrix, which had a linear correlation with the increase in the compressive strength of the matrix. The model performance was also the motivation to present predictions for the compressive strength of cement pastes under different power ultrasound irradiation. Furthermore, considering the pore refinement effect of power ultrasound, it is worth noting that power ultrasound may also have a positive impact on the durability of cement paste, which is worthy of further study.

Study on the Internal Generation Mechanism of Nano-SiO₂ for Modification of Cement-based Materials

Zhishan Xu¹, Yongsheng Ji^{1,*}

1 State Key Laboratory for Geomechanics & Deep Underground Engineering, School of Mechanics & Civil Engineering, China University of Mining & Technology, Xuzhou, Jiangsu 221116, China

Email of the corresponding author: jiyongsheng@cumt.edu.cn

Keywords: cement-based materials; nano-SiO₂ precursor solution; internal generation mechanism; microstructure; compressive strength

Modification of cement concrete using nano- SiO₂ is one of the main ways of concrete material evolution. However, nano-silica has high surface energy which is easy to appear agglomeration phenomenon. Not only can the nanomaterials not be fully utilized, but the agglomerated nanoparticles tend to form defects in the concrete. In turn, it reduces the strength and durability of concrete. Existing methods such as high-speed and prolonged stirring, ultrasonic dispersion, and surfactant dispersion have played a certain effect in reducing the degree of agglomeration of nanomaterials. However, all these methods consume large amounts of energy, greatly increase the production cost of cement concrete, and still do not allow the nanoparticles to be adequately dispersed uniformly. As a result, the effect of nanomaterials on the modification of cementitious materials and people's expectations of nanomaterials are far from each other.

The liquid phase method is a common method for synthesizing nano-SiO₂ mineral powder, which mainly includes steps of chemical synthesis, filtration and drying. In the chemical synthesis stage, nano-SiO₂ has been generated, and the subsequent steps are only to obtain pure nano-SiO₂ solid powder. And the nano-SiO₂ mineral powder is usually dispersed in water first and then mixed with cement. Therefore, it is advisable to directly use the nano-SiO₂ precursor solution (NP) in the chemical synthesis stage as an admixture instead of the nano-SiO₂ mineral powder to modify the cement-based material.

This paper uses nano-silica precursor solution (NP) instead of nano-SiO₂ mineral powder to modify cement-based materials. The NP is made of acetic acid and liquid sodium silicate as raw materials. Used to solve the problem that the nano-effect is difficult to be fully played. Firstly, highly stable NP is synthesized by using acetic acid and liquid sodium silicate as raw materials. And the existence state and precipitation evolution of SiO₂ in NP is studied based on the silicic acid polymerization theory and rheological reaction kinetic principle. Then the effects of NP on the compressive strength, microstructure and hydration process of cement-based materials are studied in combination with multi-scale tests. The internal generation mechanism of nano-SiO₂ in NP-modified cement paste is also analyzed.

The results show that SiO₂ in NP exists mainly in the form of silicate molecules, silicate oligomers and nanogel particles, and there is no agglomeration problem similar to that of solid nanoparticles. When NP is mixed with cement, the original NP dispersion system is destabilized and SiO₂ is precipitated in the form of nano-particles, and the nano-effect is given full play. To make the cement paste more denser in microstructure after hardening and significantly increase the compressive strength.

The Effect of CNTs on the diffusivity of Chloride Ions in C-A-S-H Gel

Yiting Zhang¹, Huali Hao¹

¹ School of Civil Engineering, Wuhan University, Wuhan, Hubei, 430072

Email of the corresponding author: haohuali@whu.edu.cn

Keywords: C-A-S-H gel, Carbon nanotubes, Diffusion of chloride ions, Molecular dynamics.

Geopolymers are new cementitious materials synthesized under alkaline or acidic conditions by natural minerals, industrial wastes and liquid excitants containing silica-aluminium components. They are environmentally friendly cementitious materials with low energy consumption and emission, which is now considered to be the most likely replacement for ordinary cement materials in concrete structures. Similar to cement-based materials, geopolymers typically have pores and cracks ranging from the nanoscale to the microscale, which leads to the disadvantages of brittle fracture and poor application reliability. Researchers have doped carbon nanotubes (CNTs) into geopolymers and have demonstrated that CNTs refine the pore structure of geopolymer and enhance its mechanical properties. However, the strong adsorption force exists among the tubes of CNTs, and it is easy to agglomerate into bundles and twist, which seriously limits its application. The modification by grafting functional groups on CNTs can effectively reduce the agglomeration of CNTs. For concrete structures, durability and mechanical properties are equally important. Studies on the durability of CNTs on geopolymers are less and need further attention. Premature failure of concrete structures due to chloride ion attack is a major factor in reducing the durability of concrete structures. The most critical effect of chloride attack on concrete is the corrosion of steel reinforcement, which reduces the load-bearing capacity of the concrete structures. Chloride ions from the environment enter the concrete by diffusion and accumulate to a certain extent on the surface of the steel reinforcement, which begins to rust. The free chloride ions from the concrete pore solution mainly attack the steel reinforcement. Previous studies have shown that cement hydration products can adsorb and solidify part of the chloride ions and reduce the diffusion rate of chloride ions in concrete. Moreover, the main hydration product of the alkali activated slag geopolymer is C-A-S-H gel. In view of this, the objective of this study is to investigate the effect mechanism of modified CNTs on the diffusion properties of chloride ions in C-A-S-H gel.

In this study, molecular dynamics simulations were used to model the diffusion behaviours and patterns of chloride ions in the C-A-S-H gel. CNTs surface was functionalized to understand the effect of the different functional groups on the diffusion properties of chloride ions in C-A-S-H gel. By comparing the interaction energy between components and the diffusion rate of chloride ions, the microscopic mechanism and dynamic behavior of chloride ion diffusion in C-A-S-H gel were revealed and the effect of modified CNTs on the diffusion of chloride ions in C-A-S-H gel was analysed. The results show that water molecules are more adsorbed around the functional groups on the surface of CNTs and the diffusion rate of water molecules decreased. The modified carbon nanotubes affected the diffusive motion of water molecules, while the diffusive motion of chloride ions was also changed. The modified CNTs can improve the ability of whole materials to cure chloride ions. The chloride ions are mainly solidified in the material by means of physical absorption and chemical bonding. These findings have important theoretical guidance for the practical application of CNTs modified with different functional groups in concrete cementitious materials and further promotes the development of related disciplines.

Electromagnetic absorption characteristics of alkali-activated slag-fly ash composite cementitious material

Peiqi Zheng¹, KaiXuan Zhang¹, Xiuzhi Zhang^{1,*}

¹ College of Materials Science and Engineering, University of Jinan, Jinan 250022, China

Email of the corresponding author: mse_zhangxz@ujn.edu.cn(X. Z.)

Keywords: Alkali-activated; Fly ash; Micron graphite; Electromagnetic absorption; Electromagnetic parameters.

In order to mitigate the adverse effects of electromagnetic pollution on military, medical, and human health, as well as reduce carbon emissions from building engineering materials, the development of green building materials with electromagnetic protection function is considered as one of an effective solution. Alkali-activated cementitious materials as green cementitious materials that have attracted much attention, which is becoming a common trend in electromagnetic protection research. In this experiment, a composite absorbing cementitious material was prepared by using slag and fly ash as precursors. The principal objective of this study was to investigate the effects of slag and fly ash ratio, micron graphite particle size (15 μm , 80 μm , and 150 μm), and content on the electromagnetic wave absorption capacity and mechanical properties of alkali slag-fly ash cementitious materials. The results indicated that when the slag and fly ash ratio was 7:3, the cementitious material exhibited the highest compressive strength performance at 95.87 MPa after curing 28 days. The observed increase in compressive strength of the composite material could be attributed to the increase in micron graphite content, but showed a downward trend when micron graphite content was over 4 wt.%. In addition, with the increase in micron graphite particle size, mechanical properties of composite material became worse substantially. SEM test was undertaken to explore the state of micro-graphite in high alkalinity environment, micron graphite did not participate in the hydration reaction, and a complete sheet structure of micron graphite can be clearly seen. Meanwhile, the conductivity test revealed that when the incorporation of micron graphite exceeded the seepage threshold of 4 wt.%, the conductivity of alkali slag-fly ash cementitious material became stable. This is because the deterioration of the dispersion of micron graphite and the composite materials had already established a conductive network, further increased the content of micron graphite did not result in a significant increase in conductivity. Additionally, the incorporation of 150 μm micron graphite was found to be more favourable for the formation of a conductive network inside the composite materials compared to 15 and 80 μm micron graphite. Alkali slag-fly ash cementitious material exhibited good performance of absorbing electromagnetic waves in the frequency range of 8.2~18GHz, which was characterized and calculated by using a vector network analyser. Especially, the addition of 4 wt.% 15 μm micron graphite to the alkali slag-fly ash cementitious material resulted in a minimum reflectivity of -30.63 dB at 14.19 GHz. The inclusion of micron graphite significantly improved the dielectric constant and loss coefficient of the composite, where the iron oxide contained in fly ash increased the magnetic permeability. The synergistic effect of fly ash and micron graphite was also discussed. The findings can contribute to a better understanding of green building materials with electromagnetic radiation protection capabilities.

Novel C-M/A/F-S-H seeds: Synthesis, characterization and the effect on cement hydration

Hongwei Zhu, Chuanlin Hu*, Fazhou Wang

State Key Laboratory of Silicate Materials for Architectures, Wuhan University of Technology, 430070 Wuhan, China

Email of the corresponding author: chuanlin@whut.edu.cn

Keywords: C-M-S-H seeds, C-A-S-H seeds, C-F-S-H seeds, Seeding effect, Hydration

Currently, blended cement where Portland cement/clinker is partially replaced by supplementary cementitious materials (SCMs) can reduce CO₂ emissions linked to the clinker production. However, with the increase of substitution level, the early performance of blended cement is limited because of the relatively low reactivity of SCMs. It is well-known that the calcium silicate hydrate (C-S-H) gel is the main hydration product of Portland cement, which accounts for 50-70 % by volume of the total hydration products. Recent researches proved that the synthetic C-S-H presented the similar composition and structure to C-S-H gel, thus the synthetic C-S-H could serve as the “seeds” in cement hydration, which substantially stimulated the growth of C-S-H gel. Meanwhile, the addition of the C-S-H seeds had no apparent negative effect on the later strength of concrete. Therefore, the C-S-H seeds were regarded as a novel and efficient early-strength agent. But they are still not widely used due to the high manufacture cost and lack of green production technology. Meanwhile, the SCMs contain abundant calcium and silicon elements necessary for the preparation of C-S-H seeds and thus it is feasible to prepare the C-S-H seeds from SCMs. Whilst the SCMs are diverse in composition and contain other metal elements such as Al, Mg and Fe. And it is widely reported that these metal elements can be incorporated into the poorly crystalline C-S-H. Therefore, the first and most important step is to investigate the effect of these metal elements on the structure and properties of C-S-H seeds.

In this study, the novel C-M-S-H seeds, C-A-S-H seeds and C-F-S-H seeds were prepared with PCE by the co-precipitation method successfully. Their seeding effect on cement hydration was measured by isothermal heat flow calorimetry. And the seeds were characterized by DLS (dynamic light scattering), TOC (total organic carbon) and ICP-OES (inductively coupled plasma-optical emission spectroscopy). The synthesis process of the C-S-H, C-M-S-H, C-A-S-H and C-F-S-H seeds was detailed as follows. The pH of the PCE solution was adjusted to 7.0 by NaOH first. Then the Ca(NO₃)₂ solution, Ca(NO₃)₂-Mg(NO₃)₂ mixture, Ca(NO₃)₂-Al(NO₃)₃ mixture and Ca(NO₃)₂-Fe(NO₃)₃ mixture were respectively dropped into each PCE solution with four Na₂SiO₃ solutions simultaneously in one hour. The pH was kept at 11.7 during the dripping. After that, the suspension was stirred for another 24 hours and the seeds were made finally. The designed molar Ca/Si of all seeds is 1.0. The respective designed molar Mg/Si, Al/Si and Fe/Si of C-M-S-H, C-A-S-H and C-F-S-H seeds are all 0.05.

The seeding effect of the C-M/A/F-S-H seeds on cement hydration were tested by isothermal heat flow calorimetry. The dosage of the seeds accounted for 1 wt.% of the cement, and water to cement ratio (w/c) was 0.35 of all samples including the water in seeds suspension. The testing temperature was set as 20 °C. The seeds suspension was diluted to 0.1 g/L by deionized water for DLS measurement. The seeds suspension was centrifuged to obtain the supernatant by the ultrafiltration tube. Then the supernatant was characterized by TOC and ICP-OES analysis.

It was found that the C-M/A/F-S-H seeds showed much better seeding effect on the cement hydration than the commonly used C-S-H seeds. The seeding effect of the seeds was related to the average size and absorbed PCE in the suspension. Smaller size and more absorbed PCE led to enhanced seeding effect of the seeds. Thus, this study proved the feasibility for the preparation of C-S-H seeds by incorporating extra Mg, Al and Fe. And it also provided a basis for the production of green and cheap seeds from SCMs.

ICSBM 2023

3rd International Conference of Sustainable Building Materials
25-27 September, Wuhan, China

Temperature-responsive clays containing heat-sensitive gelatin for 3D printing

Haidong Zhuang¹, Zhengyao Qu¹ *

¹State Key Laboratory of Silicate Materials for Architectures and Wuhan University of Technology

Email of the corresponding author: quzhengyao@whut.edu.cn

Keywords: 3D printing, clay, gelatin, temperature response

3D printing technology has broad application prospects in the traditional construction field, which can greatly shorten the construction period and improve the design of building structures, and it is also a construction technology with great potential in extreme environments. When clay is applied in the 3D printing process, the printed object is usually vulnerable to external damage or deformation, relatively low strength compared to other 3D printing materials, and does not have enough stability to maintain complex shapes. In this study, a temperature-stimulating responsive intelligent clay 3D printing formula was innovatively proposed by combining clay and gelatin. The combination of these two materials overcomes the limitations of traditional materials. Gelatin can enhance the bonding strength between layers of the clay system, improve the printable performance and mechanical strength of the clay, and increase its early bearing capacity. During the experiment, the gelatin is cross-linked first by adjusting the temperature, which achieves higher design flexibility and printing accuracy in the 3D printing process. Make the printing process more fine and stable. At the same time, the plastic properties of clay and the adjustable pore structure of gelatin combine to provide the necessary support and deformation ability for printing, ensuring the stability and structural integrity of the printed object, and making the printed structure more stable.

TOPIC E: Green products & Bio-based materials

Bio-concrete-organic-soil

The primary objective of this experimental protocol was to investigate the potential optimization of bio-concrete in underground environments by incorporating bacteria in the surrounding soil. The study focused on examining the incubation process of cracked mortar specimens in three distinct soil types: fully saturated organic soil, fully saturated natural soil, and fully saturated mixed soil containing both organic and natural constituents. Throughout the incubation period, the healing process of crack sealing in the specimens was evaluated and compared under the conditions of saturated soil. To analyse the cracks and their characteristics, an open-source software called ImageJ was utilized for image post-processing. This software demonstrated effectiveness in automatically identifying and locating the unique features of cracks, including their point of origin. The assessment of crack sealing was conducted through visual inspection, as well as by employing scanning electron microscopy (SEM) and Energy Dispersive X-ray (EDX) analysis.

ICSBM 2023

3rd International Conference of Sustainable Building Materials
25-27 September, Wuhan, China

The use of organic soil to create a bio-protection system for concrete for sustainable underground structures.

College of Engineering and Technology, University of Derby, Derby DE22 3AW, UK:

College of Natural and Life Science, University of Derby, Derby DE22 1GB, UK

First author, Abdurahim Abogdera¹

a.abogdera2@derby.ac.uk

Second author, Omar Hamza¹

o.hamza@derby.ac.uk

Third author, David Elliott²

d.r.elliott@derby.ac.uk

Email of the corresponding author: o.hamza@derby.ac.uk

Keywords: MICP, pH, Organic soil, Sterilized soil.

Abstract: The purpose of this study protocol is to evaluate the possibility of enhancing the performance of bio-concrete in underground environments by incorporating bacteria into the soil surrounding the concrete. The study focused on evaluating the incubation process of cracked mortar specimens in four distinct soil types: fully serialized saturated soil, fully saturated organic soil, fully saturated natural soil, as well as fully saturated mixed soil containing both organic and natural constituents. A study was conducted under saturated soil conditions to assess and compare the healing process of crack sealing in the specimens. To analyse the cracks and their characteristics, including their origin point, we used a Nikon microscope to perform image post-processing on the images after they had been captured. An inspection of crack sealing was conducted visually, using scanning electron microscopy (SEM), and using energy dispersive x-ray (EDX) analysis as methods of assessing crack sealing. Considering the fact that organic soil contains a wide variety of nutrients and organisms, we decided to incorporate organic soil into the process of manufacturing bio-concrete to increase its visibility.

Research on Mechanical-Electro-Magnetic Properties and Microstructure of Carbon Fiber-Graphite Modified Foam Concrete

Ying-hua Bai^{1,2}, Yuan-liang Xie¹, Kang Shen^{3*}, Yao Lu¹, De-yue Zhang¹

1. School of Civil Engineering, Architecture and Environment, Hubei University of Technology, Wuhan, 430068, China

2. Innovation Demonstration Base of Ecological Environment Geotechnical and Ecological Restoration of Rivers and Lakes, Hubei University of Technology, Wuhan, 430068, China

3. Department of Civil Engineering, Hubei University of Technology Engineering and Technology College, Wuhan, 430068, China

Email of the corresponding author: 837980624@qq.com

Keywords: carbon fiber(D); XCT(B); magnetic property(C)

Abstract: In this paper, foam concrete is modified using graphite and carbon fiber as absorbents. The mechanical properties of the foam concrete are then analysed in conjunction with hydration products, SEM test and XCT test. Further, the resistivity, complex permittivity and complex permeability are tested to study the influence of absorbents on the electromagnetic properties. The results demonstrate that carbon fiber can increase the proportion of the pore size range from 0 to 200 μm in foam concrete, and significantly improve its flexural strength. Besides, adding graphite compensates for the delaying effect of carbon fiber on the hydration of sulphoaluminate cement at early stages, increases the average pore size of carbon fiber foam concrete, and reduces the compressive strength. When carbon fiber is added alone with a content of 0.6wt.%, the percolation threshold is reached. When more than 2wt.% graphite is further mixed, little effect will be generated on the conductivity of carbon fiber foam concrete. Graphite and carbon fibre compounding brings excellent electromagnetic wave loss performance to the foam concrete, with an effective bandwidth of less than -10 dB of reflection loss reaching 2.5 GHz at a specimen thickness of 6 mm, accounting for 52.08% of the tested frequency band.

High performance bio-lightweight concrete using eco-aerogel coated miscanthus fibers

Yuxuan Chen, School of Civil Engineering, Wuhan University, Wuhan, 430072, PR China

Qingliang Yu, School of Civil Engineering, Wuhan University, Wuhan, 430072, PR China

Email of the corresponding author: q.yu@bwk.tue.nl (Q. Yu).

Keywords: Miscanthus fiber; silica aerogel; hydrophobicity; thermal conductivity, .Compressive strength

Recently the plant based cementitious material is becoming popular because the context on the energy conservation and emission reduction over the world. One example of this plants fibers used in cement and concrete is miscanthus fibers. The miscanthus fibers are widely grown in EU and harvested three times a year. The negative CO₂ footprint of miscanthus make it a suitable bio-materials to use in the high CO₂ emission materials like cement and concrete. However, the main concerns of using large volume of plant fibers in cement is the high water absorption and great amount of sugar leached from the plant, especially for coconut fibers or other fibers of high sugar content. Therefore, the smart utilization of bio-fibers applied in lightweight concrete is of growing interests. Silica aerogel is a super-insulating inorganic material [7], consisting of a 3D network of crosslinking silica nanoparticles and 95%–99% of air. Ambient drying process of aerogel includes a surface modification process in advance, where the surface -OH group on silica gel surface to -CH₃ group with silane and organic solvent as agents. The hydrophobicity of aerogel could be applied in miscanthus fibers to reduce the water absorption and sugar leaching significantly. Therefore, this study mainly investigates the application of hydrophobic silica aerogel in the miscanthus fibers to increase the compatibility between cement and miscanthus fibers.

Miscanthus is provided by NNRGY Company (the Netherlands). Silica aerogel is produced from olivine to increase the sustainability of the materials. The hydrophobic miscanthus is produced as follows: 1) Hydrophobic silica aerogel is firstly dissolved in ethanol to create a silica aerogel suspension solution. 2) proper amount of miscanthus fibers is placed in the silica aerogel suspension to absorb the solution into the porous structures of the biofibers. 3) After a certain amount of time, the miscanthus fibers in saturated condition is air dried for 24hours to remove the ethanol while the silica aerogel is dispersed in the fibers. The PREPARED hydrophobic miscanthus fibers is ready for use. In order to analyze the effect of hydrophobic miscanthus fibers on cement matrix, a series of experiments were conducted, including the XRD, TG, calorimeter and SEM. The macro-properties of miscanthus fiber reinforced concrete were examined, including mechanical performance, thermal conductivity and specific strength.

The results show that silica aerogel modified miscanthus fibers can be used as an excellent fiber in cement matrix. Compared with control group, silica aerogel modified miscanthus fibers can enhance the strength and thermal insulating performance of the produced bio-concrete. The enhanced performance is mainly due to the increased compatibility with cement matrix and the increased thermal barrier contributed by the silica aerogel. Microstructural analysis provide more evidence to explain this results.

In summary, this study investigates the application of aerogel modified miscanthus fibers in OPC concrete to increase the mechanical performance and thermal insulating properties. The use of superhydrophobic aerogel particles reduce the sugar leached from miscanthus and The hydration heat peak is only slightly delayed with the incorporation of aerogel coated fibers.. Silica aerogel can lower the density and increase the strength of MLC. The ratio of compressive strength vs density significantly increased. The thermal conductivity of aerogel coated miscanthus fibers decreased to 0.35 compared to the plain miscanthus fibers concrete of 0.40.

Effects of lime content on properties of autoclaved aerated concrete made of circulating fluidized bed ash

Du Xusheng ¹

¹ Design Department, Industrial Materials Engineering Design and Research Institute, Xi'an University of Architecture and Technology Design and Research Institute Co., Ltd., Xi'an, China

Xu Zhe ¹

¹ Design Department, Industrial Materials Engineering Design and Research Institute, Xi'an University of Architecture and Technology Design and Research Institute Co., Ltd., Xi'an, China

Wang Lei ^{2*}

² College of Materials Science and Engineering, Xi'an University of Architecture and Technology, Xi'an 710055, China

Li Junjiang ²

² College of Materials Science and Engineering, Xi'an University of Architecture and Technology, Xi'an 710055, China

Email of the corresponding author: 535250684@qq.com (Wang Lei)

Keywords: lime, circulating fluidized bed ash, autoclaved aerated concrete, compressive strength

About 120 million tons of circulating fluidized bed ash (CFBA) are discharged annually in China, and they are usually disposed of landfills. In order to make good use of CFBA to produce autoclaved aerated concrete (AAC) and reduce cement consumption during the AAC production, this paper utilized lime to partially replace cement, and investigated the effects of five different lime contents (namely 6 wt.%, 9 wt.%, 12 wt.%, 16 wt.% and 19 wt.%) on the appearance quality, dry density, water absorption, compressive strength of AAC proportioned with 75 wt.% CFBA, 3 wt.% gypsum, some cement and lime (22 wt.% in total). XRD and SEM were also adopted to study the hydration products and micro-morphology of AAC. The results show that, after cured in autoclave at temperature of 190 °C and vapor pressure 1.2 MPa for 7 hours, the dry density and compressive strength of AAC specimens gradually increased with the increase of lime content up to 16 wt.%, while the water absorption rate gradually decreased. Moreover, under the CaO content of 16 wt.%, no CaO diffraction peaks were exhibited while the density of tobermorite peaks increased gradually as the CaO content increased. Meanwhile the pore structure gradually became dense. When the lime content exceeded 16 wt.%, the compressive strength of AAC decreased while the water absorption and dry density increased. In addition, the CaO diffraction peaks were obviously presented and the tobermorite peaks didn't change compared with that added with 16 wt.% lime. Moreover, the pore structure of AAC became relatively loose. Under the current experimental conditions, 16 wt.% lime and 6 wt.% cement can work together to effectively stimulate the activity of CFBA to a maximum extent, thus the mechanical properties of AAC made of 75 wt.% CFBA can be improved, its water absorption can be reduced and the microstructure can be optimized.

Use of rice husk ash for mitigating the autogenous shrinkage of UHPC

Hao Huang¹, Guang Ye¹

¹Faculty of Civil Engineering and Geoscience, Delft University of Technology, Netherlands

Email of the corresponding author: h.huang.tud@gmail.com

Keywords: autogenous shrinkage, rice husk ash, internal RH, UHPC

It is recognized that the high risk of early-age micro-crack of HPC/UHPC is attributed to the large magnitude of early-age autogenous shrinkage caused by self-desiccation in binder hydration. Over the years, several methods have been proposed to mitigate autogenous shrinkage based on internal curing theory, and a better internal curing agent is always being sought.

Rice husk ash (RHA) was recognized as having the potential to be an internal curing agent. In this paper, the effect of RHA on mitigating autogenous shrinkage has been evaluated by different sizes and dosages of RHA, and the internal RH change is measured simultaneously. The results show a high efficiency of RHA for internal curing purposes, to drastically reduce the autogenous shrinkage of cement pastes. Compared to the cement paste without RHA, the internal RH results show that the internal RH in pastes with RHA is evidently higher at either early or later ages. These were addressed to explain the mechanism RHA mitigates the autogenous shrinkage of pastes.

With the optimized particle size and dosage, RHA is used for mitigating the autogenous shrinkage in UHPC. The result shows that the addition of RHA can reduce the autogenous shrinkage in UHPC at early ages as it did in cement pastes. The result of the restrained ring test also proves that the cracking potential of UHPC at early ages is decreased because of the incorporation of RHA.

Retarding the setting time of alkali-activated slag paste by processing the alkali activator into pills and capsules

Yanlin Huo¹, School of Civil Engineering, Harbin Institute of Technology,

Jinguang Huang², Technology and Quality Department, China MCC5 Group Corp. Ltd.

Dong Lu¹, School of Civil Engineering, Harbin Institute of Technology,

Yingzi Yang^{1,*}, School of Civil Engineering, Harbin Institute of Technology

Email of the corresponding author: yzyang@hit.edu.cn

Keywords: Alkali-activated slag concrete; Alkali activator; Setting time; Mechanical properties; Durability

Alkali activated slag concrete (AASC) is a new form of eco-friendly construction material using ground granulated blast furnace slag (GGBFS) as a raw material. Despite the environmental and performance advantages, the rapid setting properties are considered a significant limitation to the in-situ use of AASC. The most direct solution to this problem is the research and development of retarders. However, in recent years, as AASC's research on retarders has intensified, it has been found that some negative effects are observed for both organic and inorganic retarders. For example, it may highly reduce the strength development of concrete, increase the chemical shrinkage of AASC, and reduce the frost durability. Additionally, there is an issue that has to be considered that the cost of using high concentrations of retarders is quite expensive.

For these reasons, we attempted to reduce the contact surface between the binder and water in AASC by processing the solid alkali activator in a physical way, thus achieving a retarding effect. And another advantage of this method is that there is almost no variation in the ratio of the mixture. The negative impact on mechanical properties is expected to be limited. Other benefits of AASP, such as enhanced durability and crack repair, can also be promoted due to the sustained release effect of processed capsules and pills.

In this study, we explored a new method to retard the curing of AASP. Solid sodium silicate, a commonly used alkaline activator, was processed into pills and capsules. The properties of AASP, including strength, setting time, drying shrinkage, and resistance to carbonization, were tested to evaluate the effect of the processed activator. In addition, the pre-crack widths of AASP with and without processed pills were compared after re-curing to clarify the effect of pill-induced crack repair.

The initial and final setting times of the control mixture are 60 and 113 mins, respectively. With the utilization of the capsules and pills, the initial and final setting times are obviously prolonged. When the substantial ratio of the capsules is 20%, the initial and final setting times are increased by approximately 61.67% and 38.94%, respectively, compared with the control mixture. When the substantial ratio of the capsules increases to 40%, the initial and final setting times are 145 and 230 mins, respectively. The utilization of pills in AASP shows similar setting time results with the capsules when the substantial ratio is the same. The reason for the retarded setting time caused by the utilization of capsules and pills is generally attributed to the reduction of the contact surface between the alkali activator and GGBFS. In the early age of the hydration, only the surface part of the pills could contact with water and GGBFS, most volumes of the processed pills are stored up, and cannot directly contact with water and GGBFS. Similar to the utilization of pills, the reduction of the contact surface of the alkali activator and GGBFS is the main reason for the setting retardant of AASP by using capsules.

The main findings are as follows:

(1) The initial setting time of AASP can be highly extended from 60 to 145 min using processed pills and capsules. The final setting time of the AASP with pills and capsules are also in the

ICSBM 2023

3rd International Conference of Sustainable Building Materials

25-27 September, Wuhan, China

acceptable range. It is considered the utilization of the processed pills and capsules may provide a solution for the rapid setting of the AASC and help for the in-situ use.

(2) Utilizing processed pills and capsules may reduce the early age strength development of AASP. However, the negative influence caused by using pills and capsules changes smaller with age developing. Mixture with 20% processed pills show similar strength with the control mixture.

(3) Using processed pills and capsules can decline the drying shrinkage of the AASP, especially in the first 7 days. It is generally due to the lower hydration heat release caused by using pills and capsules.

(4) Carbonation resistances of the AASPs with pills and capsules are lower than the control mixture in the early age due to the lower hydration degree. However, for the long age of carbonation resistance, using pills and capsules may provide superior carbonation resistance owing to the sustained hydration effect and the healing of the cracks.

Calcined Clay Binders

Harald Justnes, SINTEF Community, Trondheim, Norway

Email of the corresponding author: harald.justnes@sintef.no

Keywords: Blended cement, calcined clay, durability, microstructure, performance, reactivity.

The fastest route to reduce the CO₂ emission from cement and concrete is either to replace the clinker in cement, or cement in concrete, with a supplementary cementitious material (SCM). The SCM which is sufficiently abundant to serve the industry world-wide is clay and limestone filler. This keynote goes through all aspects of calcined clay as SCM; what it is, how it is produced, how does it react with cement as well as what the benefits are when using it in concrete in terms of strength development and durability. The challenges and potential benefits of extremely high calcined clay loadings are also addressed.

Clay is just defined as an earth-like material with particle size < 2 µm originating from weathering or erosion of rocks. It may consist of several clay minerals (kaolinite, smectite, illite etc.) in the same clay together with mineral grains like quartz and feldspars being more or less inert at ordinary temperatures. Ordinary blue clays containing only 50% clay minerals and iron oxide making them unsuitable for high end products like porcelain can still be used beneficially as cement substitution in concrete after calcination at modest temperatures (800-850 °C) compared to cement clinker manufacturing at 1450 °C.

Calcined clay minerals are pozzolanic in nature consuming calcium hydroxide from cement hydration resulting in more amorphous C-S-H binder and crystalline calcium aluminate hydrates (CAHs) of various kinds. While CAHs may be beneficial in making denser microstructure due to increased water binding (crystal water) and reducing chloride ingress due to additional chloride binding as Friedel's salt, they are not resilient to carbonation and will actually lead to a more open pore structure than carbonated OPC due to release of the crystal water upon carbonation.

Replacing clinker in blended cement, or cement in concrete, with >35% calcined clay may consume all calcium hydroxide in the binder and lower the pH < 10 so the reinforcement steel is no longer in a passive state with respect to corrosion. Some argue that the less permeable microstructure and increased electrical resistance may prevent or slow down rebar corrosion, so the structure still performs within the intended service life. However, binders with pH < 10 may open up for other reinforcement materials that does not thrive in high pH environment like aluminium metal, ordinary glass fibres and natural organic fibres. Such reinforcing materials will allow the use of the best accelerator ever, calcium chloride, to counteract the inherent low early strength of binders with high cement replacements, and even allow the use of seawater as mixing water along with dredged sand from the sea. Examples are given for concrete with 55% replacement of cement by calcined clay and using 4% CaCl₂ as accelerator achieving 1-day compressive strength > 10 MPa and 3 days strength 35 MPa ending at 55 MPa at 28 days, even when entrained with 4.5 vol% air.

Concrete with a calcium hydroxide depleted binder and pH < 10 will also enable utilization of alkali-reactive aggregate for increased resource utilization and will have excellent sulphate resistance.

Oxygen diffusion into unsaturated concrete and affecting chloride-induced corrosion of steel bars

Li Shicai ^{a,b}, Jin Zuquan^{a,b,*}, Gao Yuan^b

a. School of Civil Engineering, Qingdao University of Technology, Qingdao 266520, PR China

b. Engineering Research Center of Concrete Technology under Marine Environment, Ministry of Education, Qingdao 266520, PR China

Email of the corresponding author: jinzuquan@126.com

Keywords: oxygen diffusion; chloride ions; wire beam electrode; non-uniform corrosion; unsaturated concrete

Oxygen diffusion in reinforced concrete (RC) is a crucial factor affecting the corrosion of steel bars under a high chloride environment, while it is controlled strongly by the relative humidity (RH) of the concrete. Therefore, the objective of this work is to elucidate the diffusion of oxygen in unsaturated concrete and its effect on the corrosion of steel bars. In this work, a self-made device is developed to study the oxygen diffusion in concrete and the wire beam electrode (WBE) technology is innovatively used to investigate the effect of oxygen on the non-uniform corrosion of steel bars. The oxygen diffusion coefficient of concrete is decreased maximum by 97.3% and 96.5% with the increased RH (12%–88%) of concrete and the decreased water-binder ratio (0.48–0.18), respectively. Meanwhile, a multi-factor coupling model is developed to estimate the oxygen diffusion coefficient of concrete and used for durability prediction. The corrosion process of steel bars was tracked by WBE technology and it presented as the formation and propagation of local anode zone. However, the electrodes remain passivated after 120 d of corrosion in low oxygen (5%) environment. Therefore, the pitting anode zone will be shrunk and the corroded steel bars were re-passivated with insufficient oxygen supply.

Solidification and stabilization of heavy metals in municipal solid waste incineration fly ash using nano-alumina by alkali-activated treatment

Tianru Li, School of Civil Engineering, Dalian University of Technology, Dalian city, Liaoning Province, 116024, China

Baomin Wang, School of Civil Engineering, Dalian University of Technology, Dalian city, Liaoning Province, 116024, China

Email of the corresponding author: wangbm@dlut.edu.cn

Keywords: Solidification and stabilization; Heavy metal; MSWI fly ash; Nano-alumina; Alkali-activated treatment.

With the increase in population and the improvement of people's living standards, a large amount of municipal solid waste incineration (MSWI) fly ash is subsequently generated. MSWI fly ash containing heavy metals is hazardous solid waste that requires safe disposal. Alkali-activated treatment can effectively improve the environmental safety of MSWI fly ash. Due to the low alumina content of MSWI fly ash, the addition of nano-alumina (NA) solves the defect to enhance the ability of solidification/stabilization (S/S) and maximize the utilization of MSWI fly ash. NA/MSWI fly ash solidified body was prepared and relative mechanisms of solidifying heavy metals were carried out in this study, and the details are as follows: (i) investigate the environment risk of MSWI fly ash and solidified bodies including leaching experiment and chemical speciation; (ii) elucidate the compressive strength of specimens under different dosages of NA at various curing time; and (iii) discuss the mechanism of S/S heavy metals based on the characteristics of X-ray diffraction (XRD), Fourier transform infrared (FTIR) spectrography, nuclear magnetic resonance (NMR), and scanning electron microscopy (SEM). In this study, NA was added (0-3 wt.%) to explore its effects on mechanical properties and heavy metal immobilization efficiency of NA/MSWI fly ash solidified body. Research results revealed that when the addition of NA was 2 wt.%, the compressive strength of solidified bodies can significantly increase by 38.0% and 42.8% at 7 days and 28 days, respectively. Meanwhile, the leaching concentration of heavy metals in NA/MSWI fly ash solidified body can noticeably reduce with the immobilization efficiency of above 99.5%. Adding NA promoted the ratio of stable state on Pb and Zn in solidified bodies. A series of microscopic characterization analyses indicated that NA stimulated gels and Friedel's salt formation, and there was also found N-A-S-H existed in NA/MSWI fly ash solidified body, which all enhance S/S heavy metals by physical adsorption, physical encapsulation, and chemical bonding. Therefore, this study paves a potential new way for the application of nanomaterials in S/S MSWI fly ash through alkali-activated technology, and nano-alumina is a more promising candidate.

New insights in the preparation of artificial aggregates: towards sustainable concrete

¹Yunpeng Liu, ¹State Key Laboratory of Silicate Materials for Architectures, Wuhan University of Technology; 122# Luoshi Road, Wuhan City, China

²Wei Zheng, ²Chongqing Fresi Energy Saving Technology Development Co., Ltd; No.57 Xishan Road, Chongqing, China

³Huanghuang Huang, ³School of Materials Science and Engineering, Wuhan University of Technology, 122# Luoshi Road, Wuhan City, China

Email of the corresponding author: liyunpeng@whut.edu.cn

Keywords: artificial aggregates; machine-made sand; lightweight aggregates; intelligent aggregates

Aggregates occupy 60 – 70 % volume of cement concrete, which significantly affects the performance of concrete. Due to the natural aggregate resource shortage, artificial aggregates have been widely used in concrete production. Artificial aggregates are obtained by mechanical processing according to specific standards. This abstract mainly introduces the team's work in some novel artificial aggregates, which includes three parts:

a. improving the quality of machine-made limestone sand by energy-matched equipment

Machine-made sand is the most widely used artificial aggregate. Limestone machine-made sand has found wide applications due to its wide distribution with a large reservation of limestone. Moreover, limestone machine-made sand could meet the requirements of C30-C40 concretes, which occupied most of the concrete industry. Compared to natural sand, machine-made usually has a high powder content and poor grading related to the production equipment. For example, a vertical shaft impact crusher is usually employed due to its high crushing and shaping ability by multiple high-power impacts. Therefore, the obtained machine-made sand usually has a good shape. However, much powder was also generated after multiple impact cycles. In other words, the curing energy provided by a vertical shaft impact crusher is much higher than limestone sand required, which may have over-grinding effects, resulting in high powder content. The high amount of powder requires high storage space while reusing stone powder is difficult. Based on the characteristics of limestone, the crushing equipment with matching impact crushing energy has been selected to complete the coarse aggregates crushing, which can initially adjust the sand grading. Then, the grading and shapes of the sands are adjusted through double-layer differential crushing. The powder amount produced by the two-step process will be significantly reduced without requiring separate storage. The obtained sands possess a well-controlled powder content and proper gradation, which could prepare high-performance concrete with low cement content.

b. improving the performance of lightweight aggregate through the design of matrix composition

Lightweight aggregate is an essential component of lightweight concrete with high strength. The primary raw materials of lightweight aggregate have been changed from natural shale and clay to industrial solid waste. Although the raw materials have changed, the design method of lightweight aggregate is still according to Riley's scheme. Therefore, the main compositions of the matrix are still quartz and mullite, which does not improve the aggregate strength significantly. Diopside-based aggregates have been manufactured from waste glass and muck. The obtained aggregates showed a high mechanical strength (20.81 MPa @ 1.461 g/cm³) and low water absorption rate due to the formation of glass-ceramic phase—diopside.

ICSBM 2023

3rd International Conference of Sustainable Building Materials
25-27 September, Wuhan, China

Considering that the cold-bonding artificial aggregate has the characteristics of low energy consumption and a simple preparation process, carbonated steel-slag aggregates have been prepared, which can absorb CO₂ and have good physical properties. In addition, lightweight aggregates' designability facilitates concrete's functionalization by introducing functional components in the aggregates.

c. to prepare intelligent aggregates to make concrete intelligent.

The intelligence of concrete products is a forward-looking development direction. Intelligent aggregates have been developed by using carbon-mineralized materials to encapsulate small chips. Intelligent aggregates can be written into concrete product information and embedded in concrete products, whose information could be read through a unique reading system. Unlike QR codes, intelligent aggregates have the advantages of long recognition distance, high durability, and reusability. Moreover, intelligent aggregates have a higher temperature resistance than QR codes and other technologies due to the protection of calcium carbonates.

These are several promising applications of intelligent aggregates. One is to incorporate the intelligent aggregate into the concrete product, which can record the product's relevant information. The tracking of the concrete product can then be realized by combining it with GPS technology. At the same time, intelligent aggregates could be used to monitor the healthy state of the product by using the MEMS sensor, which can monitor the product's stress, strain, temperature, and vibration.

In conclusion, designability is the most significant feature of artificial aggregates compared with natural aggregates. From the improvement of equipment, the design of composition and structure, artificial aggregates with excellent performance, multi-functions, and intelligence can be obtained, which could be used to prepare sustainable concrete.

Development of Low-carbon Supersulfated Cement for Solidification and Stabilization of Hazardous Waste

¹ Jian-Xin Lu, affiliation and addresses: Department of Civil and Environmental Engineering, The Hong Kong Polytechnic University, Hung Hom, Kowloon, Hong Kong 999077, China

² Jiaying Ban, affiliation and addresses: Department of Civil and Environmental Engineering, The Hong Kong Polytechnic University, Hung Hom, Kowloon, Hong Kong 999077, China

³ Chi Sun Poon, affiliation and addresses: Department of Civil and Environmental Engineering, The Hong Kong Polytechnic University, Hung Hom, Kowloon, Hong Kong 999077, China

Email of the corresponding author: jixnlu@polyu.edu.hk

Keywords: Supersulfated cement; Pozzolanic reaction; Hazardous waste; Solidification and stabilization; Heavy metals.

To combat carbon emissions, this study developed a novel low-carbon supersulfated cement (SSC) prepared with pozzolanic-hazardous waste and investigated the synergetic mechanism of its pozzolanic reaction and immobilization behaviour of hazardous waste. The hydration characteristics of the SSC were explored using IC, XRD, and hydration heat tests. To reveal the immobilization efficiency of SSC, OPC system was used for comparison. The immobilization efficiency of SSC was evaluated by toxicity characteristic leaching procedure and sequential extraction procedure tests, and the mechanisms were revealed by XRD, SEM, Zeta potential, NMR, and progressive leaching tests. The results indicated that the SSC system was more effective than OPC in immobilizing hazardous waste than OPC. The lower Ca/Si ratio and higher Al/Si ratio in SSC can formed hydration products with more negative charges, resulting in stronger physical adsorption to the heavy toxic metals than in OPC. Meanwhile, high content of ettringite crystals in SSC contributed to achieving chemical immobilization through the effect of Al ion exchange for heavy metals. The excess SO_4^{2-} ions in the pore solution of the SSC binder were able to immobilize the heavy metals by sulfate precipitation. Overall, this study provided new insights into the sustainable immobilization of hazardous waste by adopting SSC.

Preparation and Characterization of Portland Cement Clinker Made by Non-traditional Raw Material

Tao Lu, affiliation and addresses: College of Materials Science and Engineering, Nanjing Tech University, Nanjing, PR China

Chao Zhu, affiliation and addresses: College of Materials Science and Engineering, Nanjing Tech University, Nanjing, PR China

Zhuqing Yu^{1,2}, affiliation and addresses: ¹College of Materials Science and Engineering, Nanjing Tech University, Nanjing, PR China; ²State Key Laboratory of Materials-Oriented Chemical Engineering, Nanjing, P. R. China

Xiaodong Shen^{1,2}, affiliation and addresses: ¹College of Materials Science and Engineering, Nanjing Tech University, Nanjing, PR China; ²State Key Laboratory of Materials-Oriented Chemical Engineering, Nanjing, P. R. China

Email of the corresponding author: zyu@njtech.edu.cn

Keywords: High magnesium limestone, Iron tailings, Mineralizer, Portland cement clinker.

As the traditional raw material for Portland cement clinker production, such as high quality limestone, are gradually exhausted, the cement industry has for some time been seeking alternative raw material for clinker production. Recently, the studies on the utilization of low grade limestone in the cement industry are increasing. Also, some industrial solid wastes are used as an alternative raw material for clinker production, since they have a similar chemical composition with other raw materials used for cement clinker production. The use of low grade limestone and industrial solid wastes together by the cement industry can greatly reduce the amount of traditional raw material used for the production of cement clinker and reduce energy consumption and carbon dioxide emissions.

Iron tailings can be used in Portland cement clinker production to replace clay, as the chemical composition of iron tailings is similar to that of clay. Due to the existence of impure ions and particular mineral compositions, the use of tailings can effectively improve the burnability of raw meal, decline the sintering temperature and promote the formation of mineral phases, which can improve the mechanical properties of the cement clinker. But, the chemical composition of iron tailings is complex and varies with the region. It contain a variety of heavy metal elements. Some elements in iron tailings are not conducive to calcination. The usage dosages of tailings for cement clinker production are normally less than 5%.

High magnesium limestone is a kind of typical low grade limestone includes. Som MgO can promote the formation of mineral phases of clinker and contribute to the sintering of clinker during the process of Portland cement clinker calcination. More MgO will crystallize and form free periclase leading to the volume expansion of cement. The content of MgO in the production of cement clinker is required to be less than 3%. In order to satisfy this requirement, many high-magnesium limestone is stripped during the mining process of limestone resulting in a waste of resources. It is expected to improve the calcination process to increase the solid solution of MgO and the activity of periclase in order to use high magnesium limestone resources.

The aim of this work is to prepare a kind of Portland cement clinker made by non-traditional raw material, such as high magnesium limestone and iron tailing, and study the properties of this clinker. The effects of the substitution level of non-traditional raw material, calcination system, and fluorine doping on the sintering of cement clinker are investigated. Fluorine ion doping with different concentrations is used to improve the sinterzation and properties of clinker. The dosage of high magnesium limestone and iron tailing and four calcination temperatures (1300°C, 1350°C,

ICSBM 2023

3rd International Conference of Sustainable Building Materials
25-27 September, Wuhan, China

1400°C, and 1450°C) are considered.

In the experiment, all raw materials are prepared in the laboratory by the process of crushing, grinding and sifting (75 μm sieve) and dried at 105°C for 12 h in a air dry oven. The raw meal is prepared according to the planned ratio and then mixed evenly in a ball mill. 5% deionized water of the raw meal is added into the mixed raw material. The mixed raw meal is pressed to a sample with Ø 60 mm×10 mm and dried again in a air dry oven at 105°C for 10 h. The dried sample is calcined in a furnace at a set temperature for 60 min. The heating rate is 10°C/min, the cooling mode is rapid cooling. The cooled clinker is then ground and sieved. The mineral and chemical composition of the cement clinker is analyzed by X-ray diffraction (XRD) and X-ray fluorescence spectroscopy (XRF). The prepared cement clinker with gypsum dihydrate (5% of the cement clinker) is mixed together to prepare cement paste by using a mold with a size of 20 mm×20 mm×20 mm. The water to cement ratio (w/c) is 0.35. All sample is cured under water. The compressive strength is carried out after the curing age of 3 d, 7 d and 28 d. The mineral phases in the hydrated cement paste is determined by XRD. The stability of cement clinker is tested by autoclave experiment.

The current results show that the clinker phases are tricalcium silicate (C₃S), dicalcium silicate (C₂S), tricalcium aluminate (C₃A), iron phase (C₄AF) and periclase. The main cement hydration products are ettringite, C-S-H gels, and calcium hydroxide (Ca(OH)₂). These conclusions show that high-magnesium limestone and iron tailings can be used to produce Portland cement clinker, which is conducive to reducing the use of traditional cement production raw materials and the treatment and consumption of iron tailings.

Bio-inspired functionally layered prepacked aggregate fibrous concrete slab under low velocity drop weight impact test

Nandhu Prasad^{1,2*}, K. Saravana Raja Mohan¹, S. Sreenath¹

¹Research Scholar, ¹Professor & Dean, ¹Assistant Professor, School of Civil Engineering, SASTRA Deemed University, Thanjavur (613401), India.

²Assistant Professor, Department of Civil Engineering, Sree Chaitanya College of Engineering, Karimnagar (505527), India

Email of the corresponding author: nandhuprasad@yahoo.com, nandhuprasad@sastra.ac.in, nandhuprasad@scce.ac.in

The performance of Functionally Layered Prepacked Aggregate Fibrous Concrete (FLPAFC) slabs when subjected to repetitive falling mass impacts is experimentally investigated in this study. Tortoise shell's impact strength served as inspiration for the development of FLPAFC panels. In order to explore the possible usage of fibres in FLPAFC slabs for constructions requiring impact protection, twelve different concrete mixes were created with a 2.4% dose of single and hybridized combinations of steel and polypropylene fibres, resulting in the impact resistance has been greatly enhanced. To determine the effectiveness of three-layered FLPAFC slabs, an experiment was conducted concurrently to compare the efficacy of one-layered and two-layered concrete. The testing standards employed in the experiments were initial cracking and ultimate failure impact numbers, impact resistance ratio, service and ultimate crack resistance, ductility index, failure mode and force transfer mechanism. In addition, statistical analysis using two parametric Weibull distribution to analyse the best mix design fit for the real-world application and findings are presented in terms of reliability corresponding to impact strength. One-layered and two-layered concrete specimen might potentially be outperformed in terms of impact strength by three layered FLPAFC slabs by using the right dose of fibres and combinations of single and hybridized combination of fibres. The occurrence was a result of the fibre bridging mechanism, and the three layers led to a reduction in shear stress transfer in the Interfacial Transition Zone (ITZ). This study adds to the concept of creating stronger and more resilient fibre composites that could potentially be utilized in protective structures in the future.

Synthesis of aragonite whisker from recycled concrete waste by carbonation method

Peiliang Shen, Department of Civil and Environmental Engineering, The Hong Kong Polytechnic University, Hong Kong, China

Zhengjiang Gu, Department of Civil and Environmental Engineering, The Hong Kong Polytechnic University, Hong Kong, China

Yi Jiang, Department of Civil and Environmental Engineering, The Hong Kong Polytechnic University, Hong Kong, China

Chi Sun Poon, Department of Civil and Environmental Engineering, The Hong Kong Polytechnic University, Hong Kong, China

Email of the corresponding author: cecspon@polyu.edu.hk (C.S. Poon)

Keywords: Recycled concrete waste; carbonation; aragonite; magnesium; kinetics

The whole world is facing a critical environmental challenge due to the extensive release of greenhouse gas and CO₂ is the major contribution. The construction sector plays an important role. In order to achieve the “net” zero emission of CO₂ in the construction sector, effective waste CO₂ sequestration and utilization technologies in the cement industry are needed. However, few mineral carbonation technologies have been demonstrated at commercial scale. Therefore, further innovations in CO₂ capture and utilization based on carbonation of cement-based materials are urgently needed to make the CO₂ capture and storage technologies economically viable. As the same time, as a kind of cement-based material, concrete waste is one of the major municipal solid wastes, which is a suitable material that can be used for mineral carbonation because a huge amount of construction and demolition wastes (about 3 billion tonnes per year) is generated due to urban renewal, new infrastructure and housing developments. It mainly consists of old cement paste, which conveniently has a high carbonation reactivity due to the presence of cement hydrates including Ca(OH)₂, calcium silicate hydrate gel (C-S-H) and hydrated calcium sulpho-aluminate phases. Therefore, in this study, a wet carbonation method targeting high carbonation rate was developed to prepare aragonite whisker using fine recycled concrete waste (FRCW), aiming to effectively capture CO₂ and convert FRCW into high-value products. The effect of operational factors, including MgCl₂ concentration, temperature, CO₂ concentration and duration on the formation of aragonite was systemically investigated. The results indicated this carbonation process can not only produce needle-like aragonite whisker-rich materials but also capture a large amount of CO₂ (0.19 g CO₂ per g FRCW) within an hour. The MgCl₂ concentration and temperature were key parameters governing the nucleation of aragonite, while the formation of needle-like aragonite was favored in a MgCl₂-FRCW suspension with a minimum Mg²⁺/Ca²⁺ molar ratio > 0.16 at a temperature > 60 °C. A lower CO₂ concentration of < 50% only slightly decreased the carbonation rate without affecting the types of carbonation products formed, indicating the potential to sequester CO₂ from industrial flue gas directly. In addition, amorphous carbonation phases including silica gel, decalcified C-S-H and amorphous calcium carbonate were produced apart from the dominant reaction product-aragonite. Based on the results, the formation of aragonite could be divided into two steps: 1. the FRCW reacted with MgCl₂ to form a new FRCW-MgCl₂-Mg(OH)₂-CaCl₂ system. 2. the Ca²⁺ reacted with CO₃²⁻ to form aragonite and brucite was solubilized back to MgCl₂, resulting in possible recycling and reusing MgCl₂ for another carbonation cycle. The proposed approach exhibits a novel direction of sequestering CO₂.

Review of ultra-high performance concrete research

Tianwei Song, 1. Key Laboratory of Building Collapse Mechanism and Disaster Prevention, China Earthquake Administration, Langfang, 065201; 2. School of Civil Engineering, Institute of Disaster Prevention, Langfang, 065201

Yanfeng Zuo, 1. Key Laboratory of Building Collapse Mechanism and Disaster Prevention, China Earthquake Administration, Langfang, 065201; 2. School of Civil Engineering, Institute of Disaster Prevention, Langfang, 065201

Email of the corresponding author: 1159421999@qq.com

Keywords: ultra-high performance concrete; UHPC performance; raw materials; mix proportion

Ultra High Performance Concrete (UHPC) has received a lot of attention from scholars around the world because of its excellent performance in all aspects. However, the large amount of cementitious materials and the complicated preparation and maintenance process of UHPC have increased the cost and caused energy consumption and environmental pollution, which limit the application of UHPC in practical engineering. In order to improve these defects and make UHPC widely used, this paper reviews the effects of different cement dosages and changes in the proportion of major minerals in cement and mineral admixture types and dosages on the properties and microstructure of UHPC in the preparation of UHPC from the raw materials, mix ratios, mixing process and curing system of UHPC, and the effects of changes in the particle size and gradation of aggregates on the flowability of UHPC. The effect of the change of aggregate particle size and grading on the fluidity, mechanical properties, and dense stacking of UHPC; Among many kinds of fibers, steel fibers have the highest fit with UHPC, and the corresponding fiber-matrix interface bond strength and mechanical properties of UHPC are the most significant, but the cost of steel fibers is higher. Therefore, in order to further save costs, this paper reviews the effects of steel fibers on matrix properties when incorporated with different doping amounts, aspect ratios, and shapes, and the cost savings achieved by using hybrid fibers to replace some of the steel fibers, on the other hand, it summarizes and compares the effects of steel fibers on matrix properties under both directional and non-directional modes of incorporation, and the effect of fiber directional coefficient on matrix properties when buried with steel fibers. The effect of the change of fiber directional effect coefficient when the fiber is buried. The effect of the change in the type and amount of green materials used to meet the environmental requirements and cost savings on the properties of UHPC and the analysis of the mechanism provide a theoretical basis for the future direction of material selection in the preparation of UHPC. At the same time, this paper summarizes the design method of UHPC ratio: the improved formula based on the theory of close packing and the empirical formula based on a large amount of experimental data, and the UHPC prepared by the ratio designed with the two formulas has a small error with the actual. As well as the effects of different mixing processes on the flow and mechanical properties of UHPC and the effects of different maintenance systems on the properties of UHPC in order to further improve the properties of UHPC with the same materials and ratios, but the maintenance of UHPC is usually accompanied by high energy. However, the maintenance of UHPC is usually accompanied by high energy consumption, so in order to achieve the goal of energy saving and emission reduction, the preparation process of non-steam curing UHPC is also reviewed in this paper, and the existing problems and future development direction of UHPC are given at the end.

Thermal damage inhibitory effect of graphene oxide and silica fume synergy on the steam-cured manufactured sand concrete

Xin Su, Qi Li, Peipeng Li*, Zhigang Ren *

School of Civil Engineering and Architecture, Wuhan University of Technology, 430070 Wuhan, PR China

E-mail of the corresponding authors: lipp@whut.edu.cn (P. Li), renzg@whut.edu.cn (Z. Ren).

Keywords: manufactured sand concrete, graphene oxide, silica fume, steam curing, thermal damage inhibitory effect

With the rapid development of prefabricated buildings in China, the demand for precast concrete members has increased sharply. River sand is widely used as the fine aggregate in the traditional practice of preparing precast concrete. However, in recent years, the depletion of river resources, the rise of environmental awareness, and the shortage of natural river sand supply have led to the replacement of river sand with alternative materials such as manufactured sand, sea sand concrete, and desert sand. Among these alternatives, manufactured sand has become the most widely used option because it can be prepared by processing recycled waste, such as slag, stones, and construction waste, which not only helps reduce dependence on natural resources but also promotes sustainable development. The precast concrete members used in prefabricated buildings are factory-produced. To enhance the efficiency of turnover on-site and the demolding strength, lifting strength, and prestressing tension strength of precast concrete components, steam curing is employed to reduce the maintenance time required. However, it is important to note that while steam curing can improve curing efficiency, it may also have adverse effects on the microstructure, late strength, and durability of concrete due to the thermal damage caused by steam curing. Therefore, this paper investigated the thermal damage inhibitory effect of graphene oxide (GO) and silica fume (SF) synergy on the steam-cured manufactured sand concrete by the mechanical testing, XRD, SEM, and MIP. Therefore, this study investigates the inhibitory effect of a synergy between graphene oxide (GO) and silica fume (SF) on thermal damage in steam-cured manufactured sand concrete. The investigation includes mechanical testing, X-ray diffraction (XRD), scanning electron microscopy (SEM), and mercury intrusion porosimetry (MIP). The results demonstrated that the combination of GO and SF enhanced the mechanical properties of steam-cured manufactured sand concrete. The optimal dosage for the combination was determined as 0.03% GO and 7.5% SF, resulting in compressive strength, splitting tensile strength and flexural strength was increased by 17.66 %, 17.65 % and 21.57 % at 28 days compared with reference groups, respectively. This improvement can be attributed to the increased hydration and pozzolanic reaction degree, reduced content of calcium hydroxide (CH), and enhanced connection between concrete and aggregate facilitated by GO and SF. Furthermore, the combination of GO and SF leads to a strengthened interfacial transition zone (ITZ) and an increased proportion of harmless pores in concrete. Overall, the use of GO and SF in steam-cured manufactured sand concrete effectively addresses both the mechanical properties and durability concerns at a microscopic level, offering a novel manufacturing process for prefabricated concrete components. Additionally, the application of GO in steam-cured concrete promotes its utilization in building materials.

Control of peroxophosphate gypsum slag dry hard cement by adding aluminum phase

Jiaqi, Wen¹, affiliation and addresses (Department and Institution): State Key Laboratory of Silicate Materials for Architectures, Wuhan University of Technology, 430070 Wuhan, Hubei, PR China

Pei Tang², affiliation and addresses: State Key Laboratory of Silicate Materials for Architectures, Wuhan University of Technology, 430070 Wuhan, Hubei, PR China

Wei Chen³, affiliation and addresses: State Key Laboratory of Silicate Materials for Architectures, Wuhan University of Technology, 430070 Wuhan, Hubei, PR China

Email of the corresponding author: pei-tang@whut.edu.cn

Keywords: excess-sulfate phosphogypsum slag cement(PPSC); Sodium aluminate; Ettringite;

The persulfophosphogypsum slag cement was prepared by pressing, three kinds of sodium aluminate with different dosage were selected to prepare samples, which were mixed with powder after being prepared into solution. The effect of sodium aluminate dosage on the mechanical properties of the persulfophosphogypsum slag cement paste was investigated, and the mechanism of the effect of sodium aluminate addition on the hydration products and microstructure of the paste was explored through XRD, TG-DSC, SEM and MIP tests. The results show that adding sodium aluminate can improve the mechanical properties of the paste test block. When the content of sodium aluminate is 0.5 %, the strength of the test block in 3 days of hydration reaches 13.51 MPa, which is 129.4% higher than 5.89 MPa in the control group. When the hydration reaches 28 days, the strength of the test block added 0.5 % sodium aluminate reaches 41.34 MPa, which is 48 % higher than 27.85 MPa in the control group. After adding sodium aluminate, the characteristic peak of ettringite is enhanced, the diffraction peak of unhydrated gypsum is weakened and the decomposition endothermic peak of ettringite is also enhanced. After adding sodium aluminate, the amount and size of the hydrated ettringite increase, and the formation position of ettringite also changes. The porosity of the test block decreases at the early stage, and the structure becomes more compact.

Segregation Analysis of Hollow Microspheres as Lightweight Aggregate in Cementitious Composites

Jingwei Yang¹, ¹Department of Civil and Environmental Engineering, Seoul National University.

Juhyuk Moon¹, ¹Department of Civil and Environmental Engineering, Seoul National University.

Email of the corresponding author: snuyangjw@snu.ac.kr

Keywords: Hollow microsphere; lightweight concrete; Segregation; Microtomography images.

Due to the depletion of natural resources and rising temperatures, sustainable construction is becoming increasingly popular. Lightweight high-performance concrete, with its excellent thermal insulation and soundproofing properties, is a superior alternative to traditional concrete. Since the lower density of lightweight aggregates, they tend to float and cause segregation, which can significantly affect concrete performance. Hollow glass microspheres (HGMs) are lightweight aggregates with high strength and density commonly used in lightweight high-performance concrete. However, the segregation behavior of HGMs, which have sizes in the micro range, in cementitious materials is not yet well understood, and there is limited research on precise detection methods. Therefore, a comprehensive investigation of the segregation of lightweight HGMs in cementitious composites was conducted. In this study, lightweight high-performance cementitious composites were designed with ultra-high-performance concrete (UHPC) as a mix proportion. The raw materials included white Portland cement, silica fume, quartz powder, HGMs, water-reducing agent, and water. Segregation was induced by increasing the water-to-cement (w/c) ratio from 0.25 to 0.5. High-resolution micro-computed tomography (CT) is a powerful tool to analyze and visualize the internal architecture of cementitious materials. Therefore, the distribution of HGMs was quantitatively examined using Skyscan 1272 CT scanner (Bruker, Kontich, Belgium). Cylindrical samples with a diameter of 5 mm and a height of 20 mm were fabricated. The scanning resolution chosen was matched to the smallest particle size of the HGMs to accurately capture their distribution in cementitious composites. The sample was scanned in four passes from bottom to top. Each scanning session lasted for 4 hours. Furthermore, a rapid CT projection image combined with a grayscale analysis method was proposed, which assessed segregation by evaluating the X-ray absorption capacity of samples. The effects of segregation on the flowability, compressive strength, and density of the samples were compared. The CT quantitative results revealed that segregation of HGMs occurred only at higher w/c ratios (0.5), and the segregated samples exhibited agglomeration of HGMs. Rapid CT projections were used to determine segregation occurrence by comparing the X-ray absorption of the samples, and grayscale analysis of the projection images enabled quantitative comparisons and showed a strong linear relationship with sample density. The flowability increased with increasing water without any noticeable abrupt changes. The compressive strength of samples with higher w/c ratio experienced a sudden decrease, but the density still exhibited a linear relationship with the w/c ratio. In summary, HGMs performed well in lightweight high-performance cementitious composites designs with w/c ratios below 0.45. Higher w/c ratios resulted in the floating and agglomeration of HGMs. CT technology was the optimal quantitative measurement method for the segregation of lightweight aggregates like hollow microspheres. CT projection accelerated the analysis process and offered a fast, convenient, and accurate approach. The samples' compressive strength performance was extremely sensitive to segregation, while the sensitivity of flowability and density to segregation was relatively low. This study provided a new method for monitoring the segregation of lightweight concrete and investigated the conditions and performance of segregation in lightweight high-performance concrete. It contributed to a comprehensive understanding of lightweight high-performance sustainable building materials and promoted their real-world application.

Sustainable Ultra-High Performance Concrete Using Low-Grade Waste Glass

Xudong Zhao ^{a, b, c}, Jian-xin Lu ^c, Zhonghe Shui ^{a, b}

^a State Key Laboratory of Silicate Materials for Architectures, Wuhan University of Technology, Wuhan 430070, China

^b School of Materials Science and Engineering, Wuhan University of Technology, Wuhan 430070, China

^c Department of Civil and Environmental Engineering & Research Centre for Resources Engineering Towards Carbon Neutrality, The Hong Kong Polytechnic University, Hong Kong, China

Email of the corresponding author: zhshui@whut.edu.cn (Z. H. Shui)

Keywords: Ultra-high performance concrete, Waste glass, Volumetric stability, High temperature performance, Life-cycle assessment

The management of the waste glass has become an acute issue in Hong Kong. A huge amount of waste glass containers is generated (about 200 tonnes/daily in 2020) in the city. The high concentration of contaminants in waste glass can be harmful to concrete, and cleaning the glass is neither economical nor sustainable. Ultra-high performance concrete (UHPC) is a new high-value building material where large quantities of cement and quartz sand are used to obtain ultra-high performance, but this is not environmentally friendly. Limited research has investigated the use of low-grade waste glass in UHPC. Under this circumstance, a series of tests were carried out to determine the composition of low-grade waste glass, the properties of fresh concrete and hardened concrete. And, it investigated the suitability of unwashed glass powder and glass sand as a substitute for cement and fine aggregates in UHPC. The results showed that the addition of waste glass had a negative effect on the processability of UHPC samples due to the impurities in the waste glass. In addition, the compressive strength of UHPC made from waste glass could reach over 120 MPa, a reduction of less than 20% compared to conventional UHPC. Waste glass UHPC exhibited better volumetric stability and high temperature performance. Economic and environmental analysis indicated that using waste glass UHPC greatly reduced the unit cost and the impacts on the environment.

Mechanical and Microstructural Properties of Sustainable Ultra-High Performance Concrete Using Low-Grade Waste Glass

Xudong Zhao ^{a, b, c}, Jian-xin Lu ^c, Zhonghe Shui ^{a, b}

^a State Key Laboratory of Silicate Materials for Architectures, Wuhan University of Technology, Wuhan 430070, China

^b School of Materials Science and Engineering, Wuhan University of Technology, Wuhan 430070, China

^c Department of Civil and Environmental Engineering & Research Centre for Resources Engineering Towards Carbon Neutrality, The Hong Kong Polytechnic University, Hong Kong, China

Email of the corresponding author: zhshui@whut.edu.cn (Z. H. Shui)

Keywords: Ultra-high performance concrete, Waste glass, Volumetric stability, High temperature performance, Life-cycle assessment

The management of the waste glass has become an acute issue in Hong Kong. A huge amount of waste glass containers is generated (about 200 tonnes/daily in 2020) in the city. The high concentration of contaminants in waste glass can be harmful to concrete, and cleaning the glass is neither economical nor sustainable. Ultra-high performance concrete (UHPC) is a new high-value building material where large quantities of cement and quartz sand are used to obtain ultra-high performance, but this is not environmentally friendly. Limited research has investigated the use of low-grade waste glass in UHPC. Under this circumstance, a series of tests were carried out to determine the composition of low-grade waste glass, the properties of fresh concrete and hardened concrete. And, it investigated the suitability of unwashed glass powder and glass sand as a substitute for cement and fine aggregates in UHPC. The results showed that the addition of waste glass had a negative effect on the processability of UHPC samples due to the impurities in the waste glass. In addition, the compressive strength of UHPC made from waste glass could reach over 120 MPa, a reduction of less than 20% compared to conventional UHPC. Waste glass UHPC exhibited better volumetric stability and high temperature performance. Economic and environmental analysis indicated that using waste glass UHPC greatly reduced the unit cost and the impacts on the environment.

A comparative study of the composition and the corrosion products of concrete sewer pipes

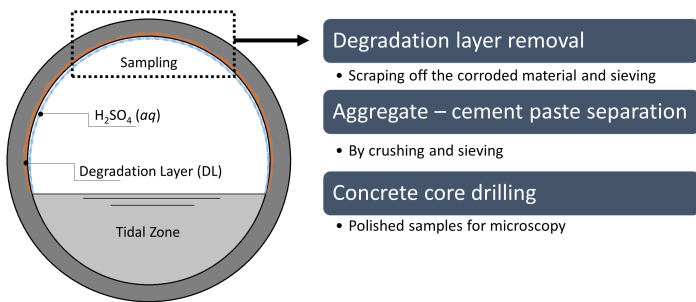
B. Cerrai*, K. Schollbach, H.J.H. Brouwers

Composition and corrosion of sewer pipes concrete

The investigation evaluates different concrete pipe samples from the Netherlands' sewer systems spanning from the 1920s to the late 1990s.

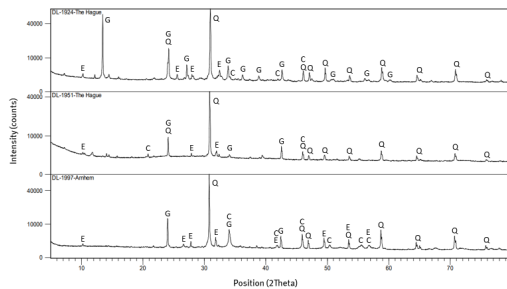
The purpose is to characterize the concrete composition and assess the degradation on a microscopic scale.

Microbiologically Induced Concrete Corrosion (MICC), is a deteriorating mechanism in concrete sewage systems caused by sulphate attack of the cement paste by sulfuric acid produced in the pipes' environment. The production of gypsum and ettringite affect concrete's structural support.



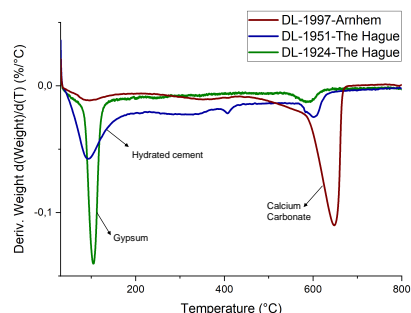
X-Ray Diffraction from Powders

Q: quartz (SiO_2); G: gypsum ($\text{CaSO}_4 \cdot 2\text{H}_2\text{O}$); C: calcite (CaCO_3); E: ettringite ($\text{Ca}_6\text{Al}_2(\text{SO}_4)_3(\text{OH})_{12} \cdot 25\text{H}_2\text{O}$)



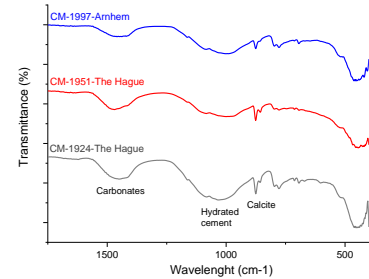
Diffractograms from XRD analysis of powdered corrosion material sampled from the pipes' degradation layers (DL)

Thermogravimetric Analysis

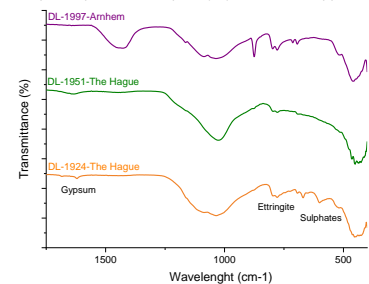


Graph of the derivative values of weight against temperature measured with TGA on powdered corrosion material sampled from the pipes' inner part (DL)

Fourier-Transform Infrared Spectroscopy

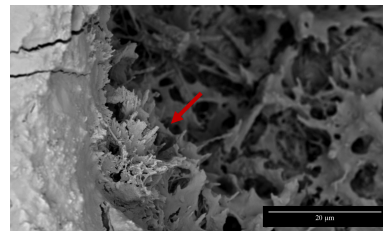


FR-IR spectra of powdered cement pastes (CM) extracted from the pipes' concrete

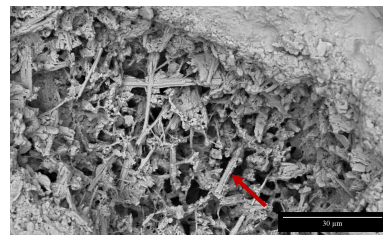


FR-IR spectra of powdered corrosion material sampled from the pipes' degradation layers (DL)

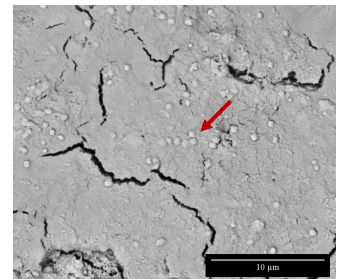
Scanning Electron Microscopy



SEM image displaying secondary ettringite formation (SEF) inside a pore



SEM image illustrating gypsum elongated crystals inside a pore



SEM image revealing calcite crystals (calcium carbonate)

Conclusions

- Optical microscopy, XRD, and FT-IR analyses revealed that the concrete mix was produced with OPC, natural gravel and sand as aggregates. The identified composition does not appear to have changed during the years of the pipes' construction.
- The MICC degradation products are ettringite and gypsum. The latter has been revealed in all the pipes' thicknesses, meaning that the sulphate attack may penetrate deep into the concrete structure over time. The quantity is proportionate to the date the pipe was installed.
- The presence of calcite is justified as a product of the carbonation process, which occurs after the diffusion of carbon dioxide in the hydrated cement paste and in the presence of moisture, a feasible circumstance in the sewage system.

Straw Wool Geopolymer Board

Straw-Geopolymer Compatibility and Its Insulation Performance

C.H. Koh*, F. Gauvin, K. Schollbach, J. Brouwers.

Department of the Built Environment, Building Physics and Services (BPS) unit, Eindhoven University of Technology (TU/e), Den Dolech 2, 5612 AZ Eindhoven, The Netherlands.

*k.c.h.koh.chuen.hon@tue.nl (presenting and corresponding author)

Introduction and Objectives

Wood wool cement board (WWCB) has gained widespread usage in the construction sector due to its numerous advantages, including resistance to decay and insects, lightweight nature, and favourable acoustic and thermal insulation properties.

This study aims to replace the high embodied energy raw material (OPC) with geopolymer, and wood wool with agriculture by-product straws (wheat and barley straws) in the production of straw geopolymer board (SGB), which are lightweight and have favourable thermal insulation properties

Results and Discussion

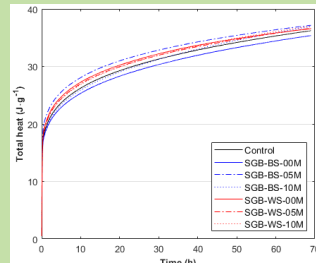


Figure 3 Compatibility when using different straws as fibers in SGB making

The replacement of fibres with straws do not impede the geopolymer forming process, showing compatibility of straw-geopolymer composite.

Material and Methodology

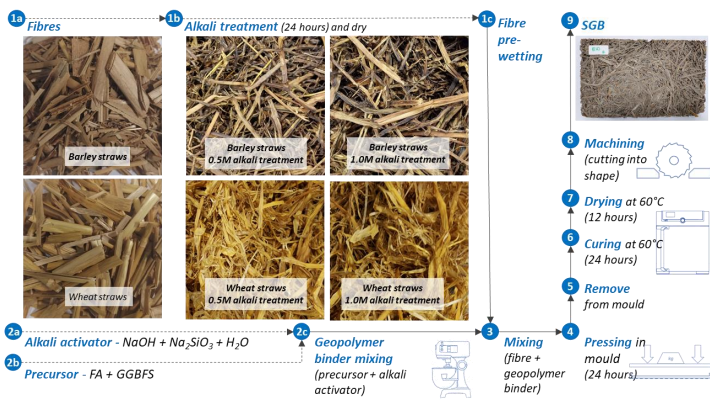


Figure 1 Production Method



Figure 2 Samples

Conclusions

This study highlights the potential of geopolymer as a sustainable alternative to OPC in the production of insulation boards, offering favourable thermal and mechanical properties and reduced environmental impact.

The replacement of fibres with straws also show compatibility of straw-geopolymer composite, however its mechanical strength is reduced.

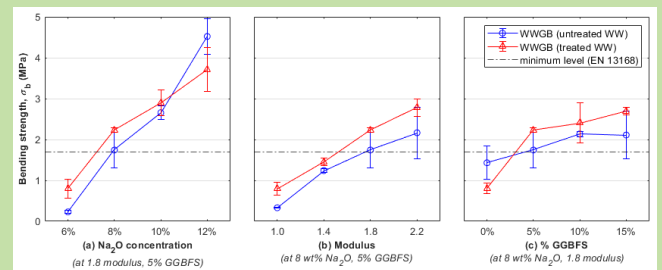


Figure 4a Bending Strength: Different geopolymer recipe using wood wool as fibers (reference)

The bending strength of the board is mainly determined by geopolymer recipe. When replacing fibres with straws, barley straw is more suitable in comparison to wheat straw; while alkali treatment improves the strength.

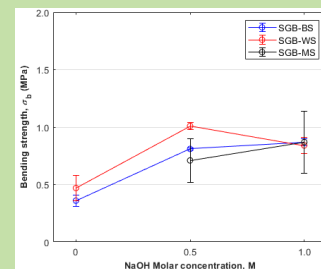


Figure 4b Bending Strength: Different straws as fibers

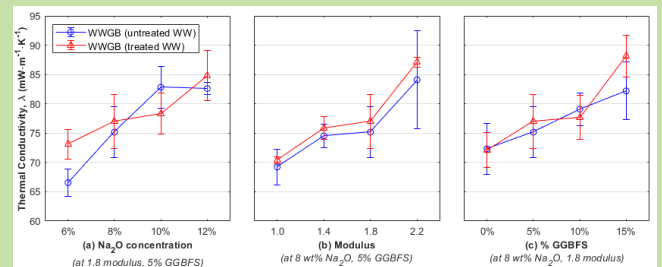


Figure 5a Thermal conductivities: Different geopolymer recipe using wood wool as fibers (reference)

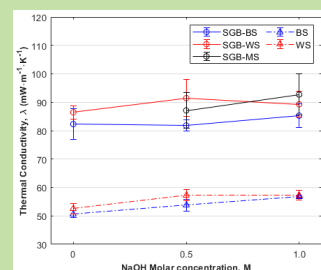


Figure 5b Thermal Conductivities: Different straws as fibers

The thermal conductivity of the board is correlated with the density and porosity of the boards. When replacing fibres with straws, boards made with wheat straws show lower thermal conductivities.

Hydroceramics for durable passive cooling of the built environment

Daoru Liu^{1,2}, Qingliang Yu^{1,2}, H.J.H Brouwers¹

¹Department of the Built Environment, Eindhoven University of Technology

²School of Civil Engineering, Wuhan University of Technology

Objectives

- Reduction of building energy for cooling
- Improvement in indoor thermal comfort
- Improvement in durability of radiative cooling materials

Research Significance

- Proposing a pathway to prepare efficient passive cooling materials for building application

Results and Discussion 1

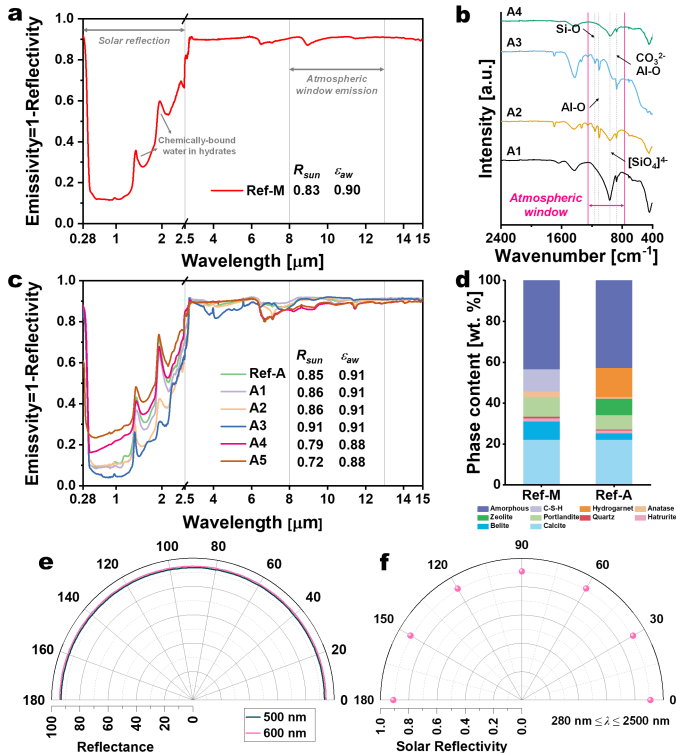


Fig. 1. (a) Emissivity spectrum of moisture-cured reference, (b) FTIR spectra of CHCs, (c) Emissivity spectra of CHCs, (d) Phase compositions (Q-XRD) of hydroceramics, (e) Polarization reflectance at $\lambda = 500$ nm and $\lambda = 600$ nm at different angles of A3, and (f) Solar reflectance at the polarization angle from 0 to 180° of A3.

Results and Discussion 2

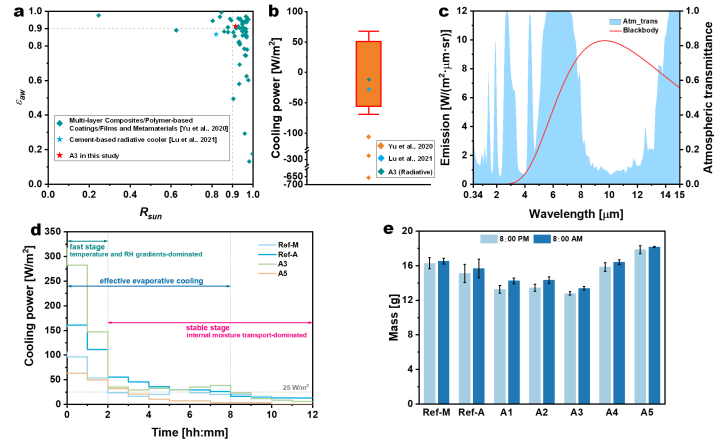


Fig. 2. (a, b) Basic optical properties and cooling power of A3 and other radiative coolers, (c) Spectra of blackbody emission and atmospheric window for cooling power calculation, and (d) Drying mass loss and evaporative cooling power.

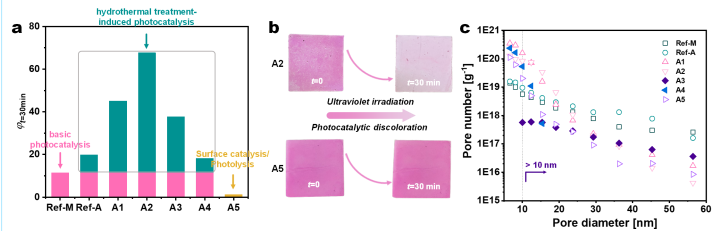


Fig. 3. (a) Self-cleaning performance at $t = 30$ min, (b) Discoloration of A2 and A5 at $t = 30$ min, and (c) Pore number distribution.

Conclusions

- The improvement in cooling optical properties is attributed to the increased whiteness and nano/micro particles and pores of the hydroceramics. The higher whiteness reduces chromatic solar absorption while the nano/micro particles and pores enhance Mie scattering in the solar range.
- The enhancement of self-cleaning performance is attributed to the microstructure change, especially the generation of nanosized C-(A)-C-H/(Al)-tobermorite "nanowires" with higher surface area, increased active sites, and stronger quantum effects.

A novel power ultrasound assisted mixing technology to prepare cement paste: Effect on hydration process and compressive strength

Guangqi Xiong¹, Chong Wang^{1*}

¹ College of Materials Science and Engineering, Chongqing University, Chongqing, China

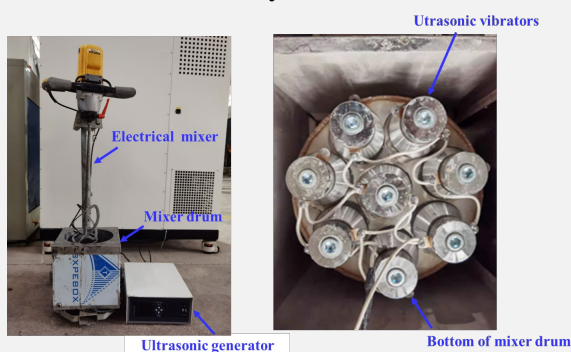
* Email: chongwang@cqu.edu.cn

Introduction

This paper developed a novel power ultrasound (PUS)-assisted mixing technology to prepare cement paste. The combination of PUS and mechanical mixing is expected to eliminate the mixing deficiency, poor dispersion and, more importantly, improve the hydration process and mechanical properties.

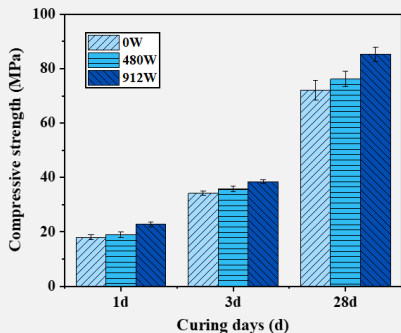
Experiment

The device is composed of an ultrasound generator, mixer drum with transducer array and high-speed electrical mixer. During the mixing process, clinker and gypsum were first added into the mixer. After mixing started, 25 °C water was poured into the mixing drum. The electrical mixer was turned on first and mixed for 20 s at 150 r/min. Then, the ultrasonic generator was turned on, and the specific power (e.g., 0 W, 480 W and 912 W) was chosen. After mixing for 3 minutes, the electrical mixer and ultrasonic generator were turned off simultaneously.



Results and discussion

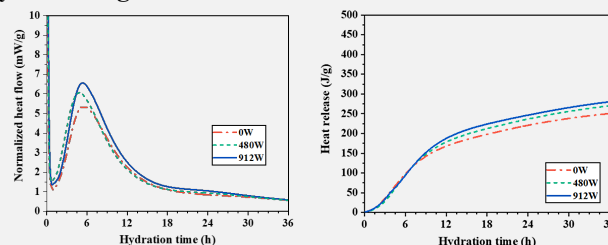
Compressive strength



➤ The PUS assisted mixing also enhanced the early age strength and maintained the strength increment rate at late hydration ages.

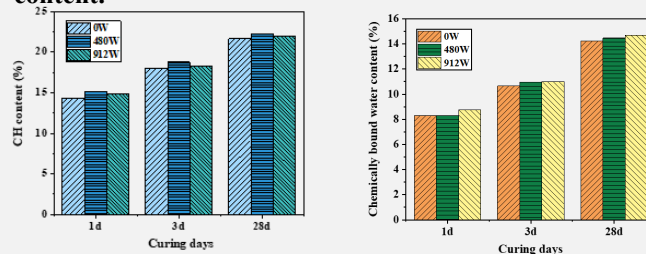
Isothermal calorimetry

➤ PUS assisted mixing shortened the induction period and increased the accumulated heat release of cement paste at early hydration ages.

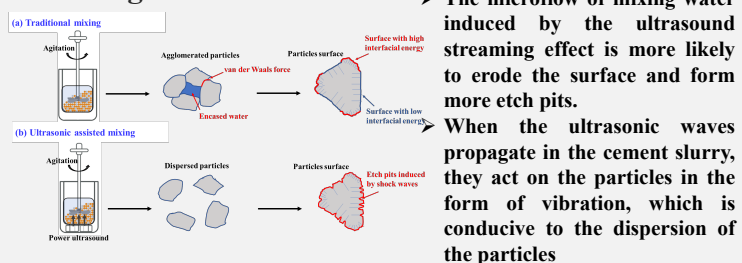


Thermal gravimetric analysis

➤ The technology significantly promoted the formation of calcium hydroxide (CH) and increased the chemically bound water content.



Dispersion mechanism of power ultrasonic assisted mixing



Conclusions

- During the initial hydration period, the induction period of cement paste is shortened slightly and the accumulated heat release is increased at early hydration ages. During the late hydration period, PUS is beneficial for the yield of hydration products, increasing the chemically bound water content of cement paste.
- PUS-assisted mixing can notably improve the compressive strength of cement paste. The compressive strength of the P912 group increased by 26.1% at 1 day and 18.3% at 28 days compared with that of the control group.

Publications

- [1] G. Xiong, C. Wang, et al, Effect of power ultrasound assisted mixing on the hydration and microstructural development of cement paste, J. Sustain. Cem-Based. (2022) 1-12.
- [2] G. Xiong, C. Wang, et al. Understanding the thermal effect of power ultrasound in cement paste, Appl. Therm. Eng. 232 (2023) 120946.

Combined effect of NaAlO_2 and NaOH on the early age hydration of Portland cement with a high concentration of borate solution

Ma Haosen, Li Qiu

State Key Laboratory of Silicate Materials for Architectures, Wuhan University of Technology

Objectives

- In this study, the effect of NaOH and NaAlO_2 on the early age hydration of Portland cement with a high concentration of borate solution (5M) was investigated.
- A range of analytical techniques was employed, aiming to reveal the hydration process, hydration products and mechanism of solidification of high concentrations of borate solution in Portland cement with the addition of NaOH and NaAlO_2 .
- The hydration kinetics, hydration products and transformation of boron and aluminum phases during early age hydration were characterized and are discussed.

Results and Discussion 1

- Samples were hydrated with $w/c=0.6$ for the value **solidification value $\geq 45\%$** , 25°C for periods ranging from 0 hours to 48 hours.
- Fig.1 shows that PC with borate solution and/or alkali activators had different hydration process. Addition of borate solution strongly retarded the hydration of PC which alkali activators break the retardation effect.
- Typical TEM image of S0A0 is shown in Fig.1, which shows the cement clinker core and ulexite coating layers.
- Typical TEM image of S5A5 is shown in Fig.2, which shows the dissolution of coating layers.

Results and Discussion 2

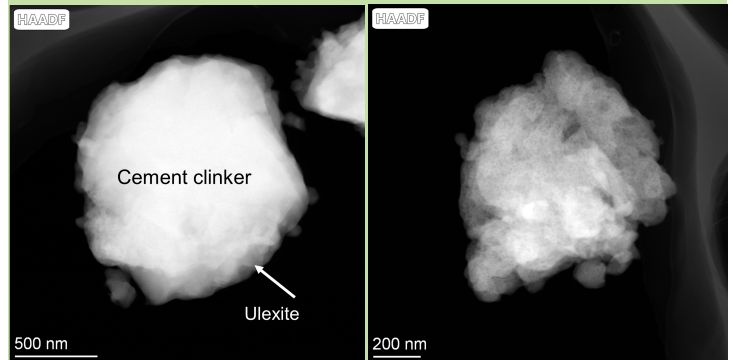


Fig. 1 STEM-HAADF image of S0A0 hydrated for 48 hours.

Fig. 2 STEM-HAADF image of S5A5 hydrated for 48 hours.

Conclusions

- In **5M borate solution**, the hydration of ordinary Portland cement was severely retarded by formation of **protective coating layer of amorphous ulexite** on the surface of cement particles, resulting in the prevention of further dissolution of anhydrous cement phases to postpone the hydration process.
- The addition of NaAlO_2 or NaOH cannot overcome the retardation effect caused by high concentration borate solution. The hydration products of OPC in high concentration borate solution with NaAlO_2 or NaOH addition were **amorphous ulexite or ulexite and B-Aft**, respectively.
- The mechanism of the combined addition of NaAlO_2 and NaOH to overcome the retardation effect is to **transform the amorphous ulexite into B-Aft and gowerite**. The disappearance of ulexite phase indicated the nonexistence of protective coating layer, resulting in the continuous hydration of cement particles. By increasing pH value by addition of NaOH and introducing aluminate by addition of NaAlO_2 , sufficient amount of B-Aft were favored to formation to incorporate boron in the structure of B-Aft, resulting in the decrease of concentration of borate solution, so as to alter the ion environment and thermodynamics of hydration process to form gowerite instead of ulexite.

Investigations on the effect of surface treatment of hemp fibers on the mechanical and micro-performance of fiber-cement composites

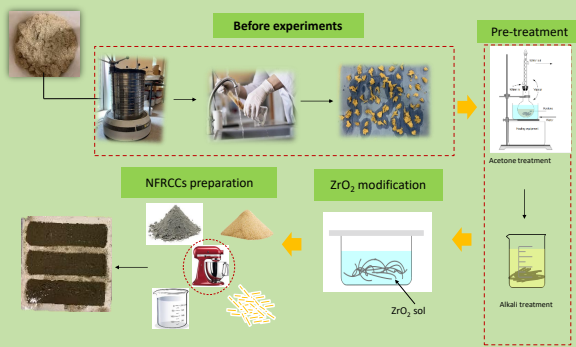
Helong Song¹, Tao Liu², Florent Gauvin^{1*}, H.J.H Brouwers¹

¹ Department of the Built Environment, Eindhoven University of Technology, The Netherlands
² Department of Environmental and Resource Engineering, Technical University of Denmark, Denmark

Abstract

The poor durability of natural fiber reinforced cement composites (NFRCCs) is mostly due to alkaline degradation of the embedded fibers in cement, which hinders the application of these materials in building and construction fields. Therefore, this work aims to improve the alkali resistance of fibers, using zirconia to coat hemp fiber through a sol-gel technique. 2 wt% of different fibers (i.e. untreated, pre-treated, and ZrO₂ modified) are added to a cement mortar mix. The difference in the mechanical strength, cross-section, and interface compatibility between fiber and cementitious matrix of 28 days hardened were investigated.

Methodology

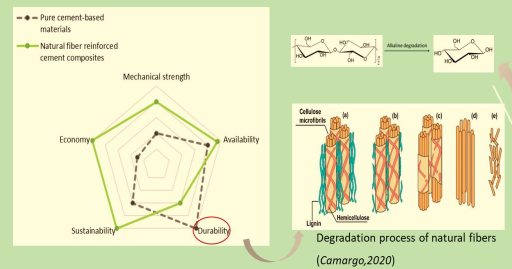


Backgrounds

- Tons of agricultural natural fibers are produced in the world. The Food and Agriculture Organization of the United Nations (FAO) reported that an average of 93,000 tons/annum was produced during 2000–2015.



- Natural fiber reinforced cement composites (NFRCCs) have a huge potential in the civil structure and building fields due to their high tensile strength and significantly enhanced ductility.
- However, NFRCC composites encounter the bottleneck that the durability in the alkaline environment of cement-based materials is particularly poor on account of the alkaline hydrolysis and the mineralization of natural fiber.



Results

The composites reinforced by ZrO₂ modified fibers present the highest flexural strength at 3, 7 and 28 days of curing (Fig. 1) due to the resistance of ZrO₂ to the degradation of alkaline cement hydration products on the fiber surface (Fig. 3), and even better interfacial bonding (Fig. 2).

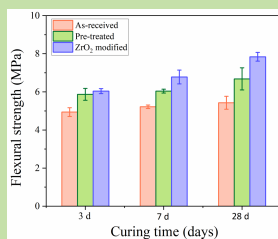


Fig. 1 Flexural strength of NFRCCs

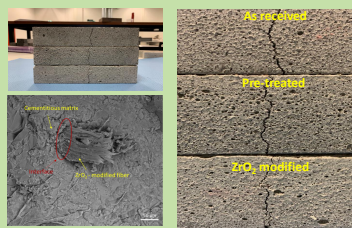


Fig. 2 The crack gap after testing

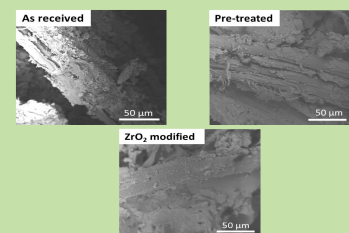


Fig. 3 The surface of embedded fibers

Conclusion

- Compared to the cementitious composites reinforced by two different fibers (as received and pre-treated), ZrO₂-modified fiber reinforced composites exhibit better flexural strength and interfacial compatibility.
- After the ZrO₂ modification of fibers, relatively fewer cement hydration products are deposited on the fiber surface.

References

- Camargo, Marfa Molano, et al. "A Review on Natural Fiber-Reinforced Geopolymer and Cement-Based Composites." *Materials* 13.20 (2020): 4603.

Micro-mechanism of SCMs on the chloride penetration of UHPFRC

Jia He, Qingliang Yu, H.J.H. Brouwers

Department of the Built Environment, Eindhoven University of Technology, the Netherlands

Background

- Due to the high CO₂ emission, large consumption and high cost of cement, the development of ultra-high performance concrete (UHPC) has been severely restricted.
- Replacing cement with supplementary cementitious materials (SCMs) with industrial waste is a feasible way to promote the development of the eco-friendly UHPFRC.
- In this study, ground granulated blast furnace slag (GGBS) and limestone powder (LP) are used in UHPFRC with three different replacement levels of cement. In this study, experimental evaluation of early hydration kinetics, mechanical properties and durability properties are determined for UHPFRC with different contents of GGBS or LS.

Materials & experiment methods

1) Materials

- The cement used in this study is Ordinary Portland Cement (OPC) CEM I 52.5 R, provided by ENCI (the Netherlands). A polycarboxylic ether based superplasticizer is used to adjust the workability of UHPC. The GGBS and LP are used to replace cement. Two types of sand are used, one is a normal sand with the fraction 0-2 mm and the other one is fine sand with the fraction 0-1 mm.

2) Mix proportion for UHPFRC

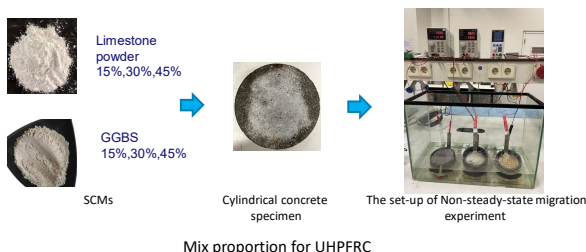
- In this study, the modified Andreasen and Andersen model is utilized to design all the concrete mixtures. The final mix proportions for UHPC incorporating high volume of GGBS or LS are given in Table 1.

Table 1. Mix proportion for UHPFRC

Samples	CEM I 52.5 (kg/m ³)	GGBS (kg/m ³)	LS (kg/m ³)	Fine sand (kg/m ³)	Sand 0-2 (kg/m ³)	Water (kg/m ³)	SP (kg/m ³)	Steel fiber (kg/m ³)
REF	949	0	0	275	1027	155	54	156
GGBS15	807	142	0	275	1027	155	54	156
GGBS30	664	285	0	275	1027	155	54	156
GGBS45	522	427	0	275	1027	155	54	156
LS15	807	0	142	275	1027	131	46	156
LS30	664	0	285	275	1027	108	38	156
LS45	522	0	427	275	1027	85	30	156

3) Specimen preparation and test methods

- 50 × 50 × 50mm cube moulds and 40 × 160 × 160mm prism moulds were filled to prepare specimens for compressive strength test and three-point bending test. In this study, experimental evaluation of mechanical properties like compressive strength and flexural strength, early hydration kinetics and durability are determined for UHPFRC with different volumes of GGBS and LS.

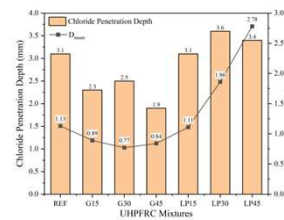


Results

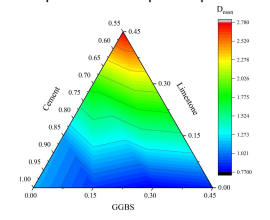
Rapid chloride ion migration (RCM) of UHPFRC



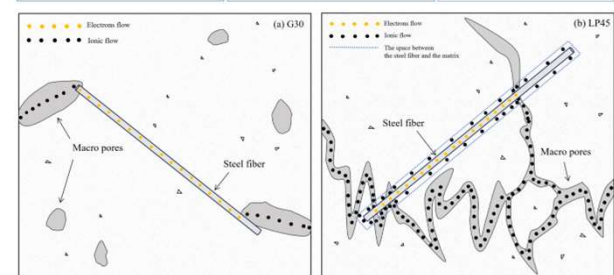
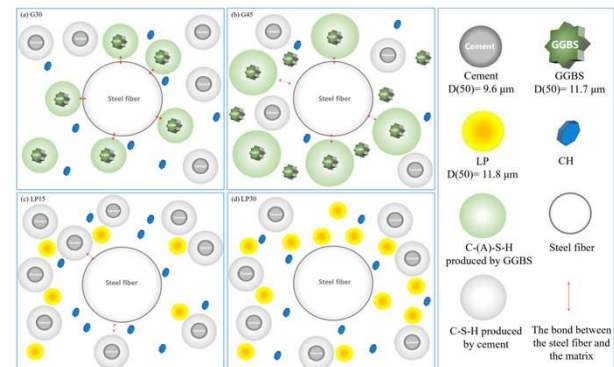
Cylindrical concrete specimens after test



The penetration depth of specimen



Synergistic interaction of steel fiber and SCMs



Conclusion

- The synergistic interaction analysis of steel fiber and SCMs during RCM test reveals distinct mechanisms of GGBS and LP in the ionic flow and electrons flow within UHPFRC specimens.
- In the GGBS-cement binder system, GGBS at a replacement rate of 30 wt% contributes to the formation of secondary C-(A)-S-H around the fibers which makes the steel fibers densely wrapped.
- As the incorporation of LP exceeds 15 wt%, it results in weak bonding between the steel fiber and the matrix, leading to the formation of the network channels for ion transport together with capillary pores and macro pores, which decreases the chloride penetration resistance of UHPFRC significantly.

Effects of calcined phosphogypsum replacement on hydration and properties of CSA cement at different curing temperatures

Jiawen Chen, Yishun Liao, Jinxin Yao, et al.

School of Urban Construction, Wuhan University of Science and Technology, Wuhan 430065, China

Objectives

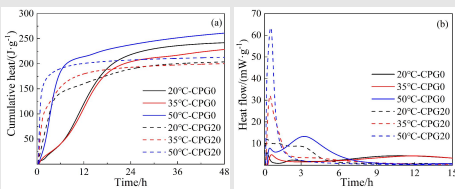
- To understand the cement hydration and microstructure formation mechanism of CPG-supplemented CSA pastes cured under hot-weather temperatures.
- To ensure the appropriate application and effective service of such CSA cement-based materials.

Research Significance

- Significantly improve the utilization rate of calcined phosphogypsum and contribute to the "double carbon".
- Preparation of high-performance CSA cements.

Results - experiments

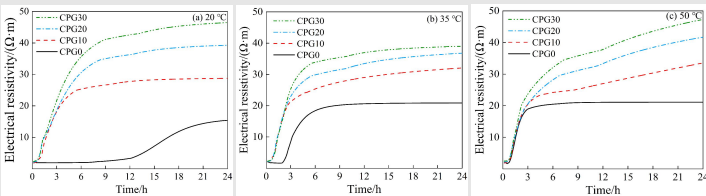
Isothermal calorimetry



- The accelerating effect of the increase of temperature on the hydration of CSA cement mixed with CPG was more obvious.

Heat release of CSA cements at different temperatures

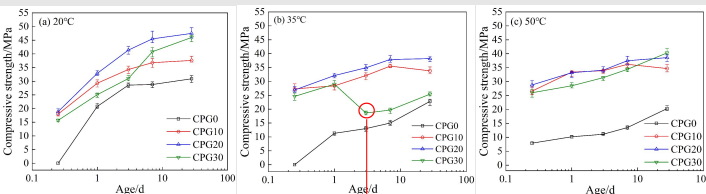
Electrical resistivity



Electrical resistivity of CSA cement pastes at different temperatures

- At elevated temperatures, the heterogeneous distribution of the hydration products resulted in the loose structure and the decrease of electrical resistivity.

Compressive strength



Compressive strength of CPG-CSA cement pastes cured at 20°C, 35°C, and 50°C

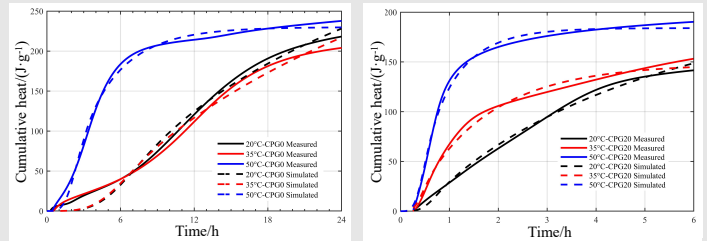
- The presence of excessive AFt formation in the CPG30 sample during curing at 35°C for three days resulted in the development of cracks caused by expansion.



- a transformation of a portion of AFt to AFm occurs at 50°C, resulting in the absence of cracks in the CPG30 sample.

Results - models

Hydration kinetics model

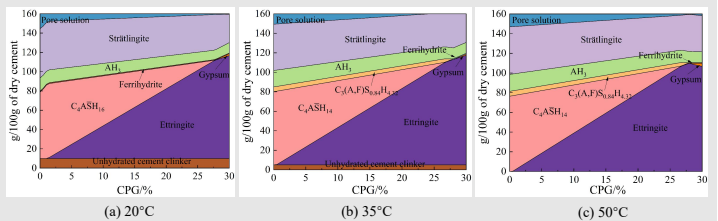


Hydration kinetics model of CSA cement pastes at different temperatures

CPG content	Parameters	20°C	35°C	50°C
0(Control)	$A/(J/g)$	371.874	399.925	229.964
	k_0/h^3	0.02118	0.01726	0.13867
	k_0/h^3	0.00475	0.00633	0.09304
20%	$A/(J/g)$	208.376	148.161	184.023
	k_0/h^3	0.10596	0.31896	0.66899
	k_0/h^3	4.51059	11.53772	17.04408

- The growth rate constant and nucleation rate constant of cement paste increased with the addition of CPG at different curing temperatures.

Thermodynamic model



Evolution of the hydration phases of 28-d CPG-CSA cement pastes cured at different temperatures

- The incorporation of CPG shifts the interconversion of AFt and AFm towards the reaction direction of producing AFt.

Conclusions

- CSA cement hydrated faster at elevated temperatures, and the amount of CPG played a major role in the acceleration of hydration.
- The electrical resistivity test results show that the early hydration of the cement pastes was accelerated, and the time interval between the induction period and the acceleration period was shortened at 50°C.
- The compressive strength of CSA cement pastes was influenced by curing temperature and CPG content. The transformation of a portion of AFt to AFm at high temperatures mitigated the risk of sample cracking caused by excessive AFt in CSA cement pastes with high CPG content.
- Elevated temperature and the presence of CPG modify the hydration kinetics of the cement paste.
- The ettringite content of CSA cement obtained by thermodynamic modelling is nearly close to the experimental results.

References

- Y. Tao, A. V. Rahul, M.K. Mohan, G. De Schutter, K. Van Tittelboom, Recent progress and technical challenges in using calcium sulfoaluminate (CSA) cement, *Cem Concr Compos.* 137 (2023) 104908.
- T. Hanein, J.L. Galvez-Martos, M.N. Bannerman, Carbon footprint of calcium sulfoaluminate clinker production, *J Clean Prod.* 172 (2018) 2278–2287.
- E. Gartner, Industrially interesting approaches to "low-CO₂" cements, *Cem Concr Res.* 34 (2004) 1489–1498.

Segregation Analysis of Hollow Microspheres as Lightweight Aggregate in Cementitious Composites



Jingwei Yang¹, Juhyuk Moon^{1*}

¹ Department of Civil and Environmental Engineering, Seoul National University, Seoul, Republic of Korea

1. Introduction

- Lightweight concrete is more susceptible to segregation than traditional concrete.
- Hollow glass microspheres (HGMs) have very low density, they tend to float upward in the cementitious mixtures.
- Suitable W/C for HGMs application in lightweight concrete? How to detect segregation?
- Purpose: To investigate the stability of lightweight HGMs in cementitious matrix with different w/c ratios and determined the potential w/c ratio at which segregation might occur.

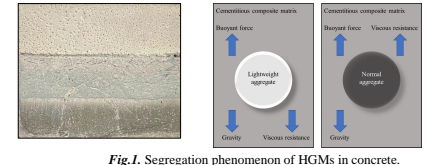


Fig. 1. Segregation phenomenon of HGMs in concrete.

2. Experimental design and detection technologies

❖ HGMs information

- HGMs density: 0.125-0.6 g/cc; crush strength: 250-27000 psi; Thermal conductivity: 0.05-0.2 W/mK.

❖ Concrete mix design

- Specimens were prepared according to Table 1 and Fig. 3.
- Specimens were cured at 20 °C and 60% relative humidity until the testing day.

Table 1. Mix proportions of L-HPC.

Mixture ID	W%	HGM %	C%	SF%	QP%	SP%
HS25	25	0				
LW25	25					
LW30	30					
LW35	35	30	100	25	35	6
LW40	40					
LW45	45					
LW50	50					

* HGM=hollow glass microspheres; W=water; C=cement; SF=silica fume; QP= quartz powder; SP=superplasticizer; %=weight percentage.

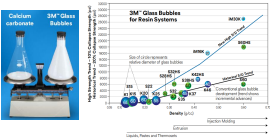


Fig. 2. HGMs information.

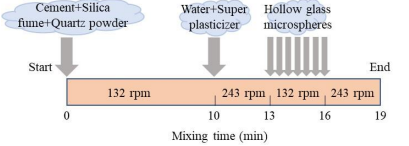


Fig. 3. Feeding sequence, mixing time and mixing rate of L-HPC.

❖ Detection technologies

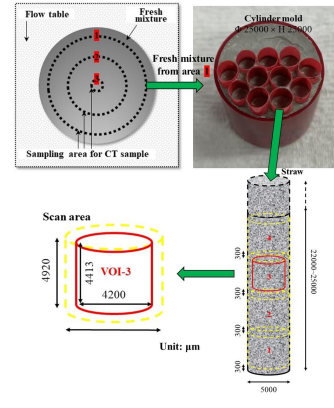


Fig. 4. Sampling of fresh mixtures after flowability test to prepare CT specimens.

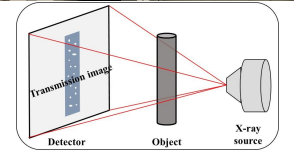
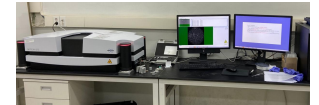


Fig. 5. X-ray computed tomography equipment and its working principle.

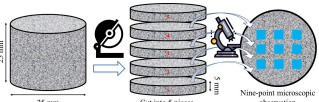


Fig. 6. Optical microscopy analysis method.

3. Segregation test results

❖ Flowability

- The fluidity of mixtures containing HGMs increased with increasing water content.

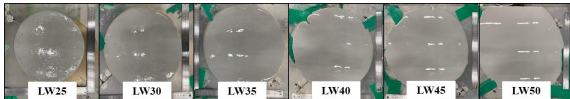


Fig. 7. Flow diameter of lightweight mixtures.

❖ Rapid assessment by CT projection

- HGMs float and agglomerate on the top of the sample, so X-ray transmission and grayscale value on top is high.

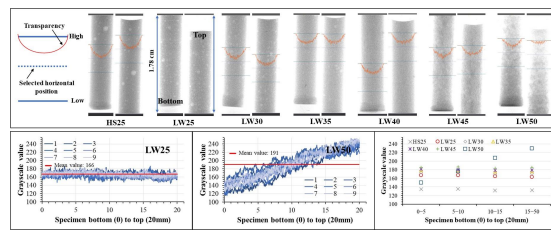


Fig. 8. Rapid assessment test and visual presentation of lightweight specimens; grayscale values of the projection images.

❖ Quantitative evaluation of segregation by CT images

- The porosity of the LW25 sample is evenly distributed from bottom to top, while the LW50 sample has higher porosity at the top due to segregation.

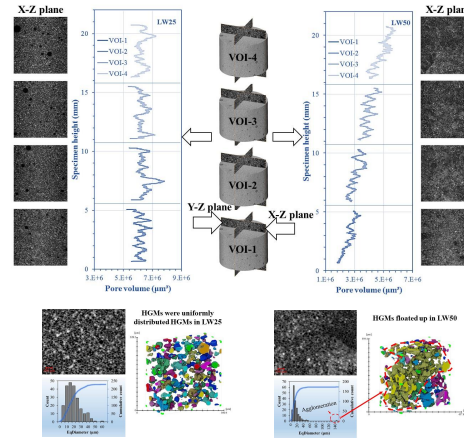


Fig. 9. Variation of pore volume with height in the X-Y cross section for LW25 and LW50 specimens; Typical distribution of HGMs in LW25 and LW50 specimens.

❖ Optical microscopy

- LW50 has fewer HGMs at the bottom than at the top.

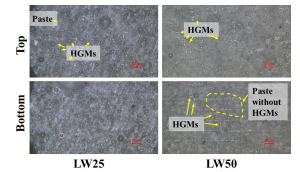


Fig. 10. Typical OM images of cutting surface of LW25 and LW50 specimens.

❖ Mechanical property

- LW50 has the lowest compressive strength growth rate.

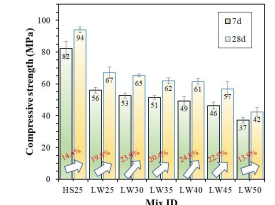


Fig. 11. Compressive strength and density of L-HPC.

4. Conclusion

- HGMs were evenly distributed at w/c values of 0.25 to 0.40, but slightly segregated at 0.45 and severely segregated at 0.5.
- CT projection can quantitatively evaluate the segregation behavior of aggregates and visualize the specimen in 2D. Projection analysis has the major advantage of allowing a test to be completed in just two minutes, saving time and money.
- The compressive strength growth rate of cementitious composites would be slowed down from 7 days to 28 days when segregation occurred.

5. Acknowledgements

- This work is supported by the Korea Agency for Infrastructure Technology Advancement (KAIA) grant funded by the Ministry of Land, Infrastructure and Transport (Grant RS-2020-KA156177). The Institute of Engineering Research at Seoul National University provided research facilities for this work.

6. Publication

- J. Yang, H. Kang, C. Shi, X. Hu, J. Moon, Tomographic analysis of segregation behavior of hollow glass microspheres in lightweight cementitious composites, Cement and Concrete Research, Under review (2023).

Two-dimensional concrete meso-aggregate modeling method based on Voronoi method

Jinyang Li
Eindhoven University of Technology

Objectives

- Effective simulation of the shape of crushed and pebble aggregates has always been the key to the study of concrete meso-mechanical models.
- The aggregate gradation theory should be considered

Research Significance

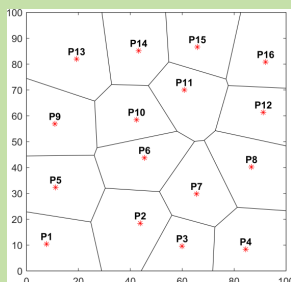
- The meso-mechanics of concrete aims to understand the mechanical behavior and properties of concrete by examining its constituent materials and their interactions at this level. However, achieving accurate replication of the natural characteristics of aggregates and fibers poses challenges in the meso-scale numerical simulation of concrete.

Methodology

- The modified Andreasen and Andersen equation

$$P(D) = \frac{D^q - D_{min}^q}{D_{max}^q - D_{min}^q}$$

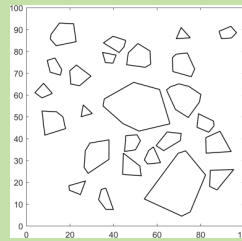
- Voronoi diagrams



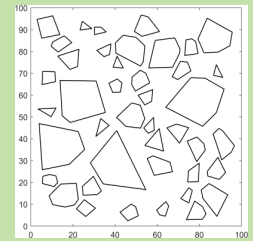
- B-spline curves

Results and Discussion

- Simulation of crushed aggregates

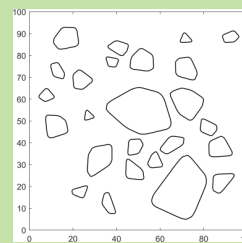


(a) 40% volume fraction

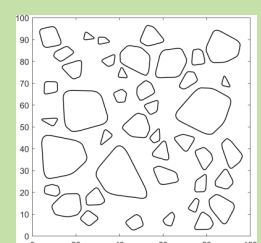


(b) 60% volume fraction

- Simulation of pebble aggregates

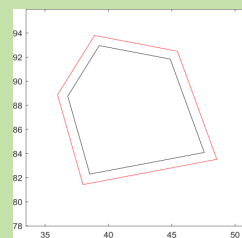


(a) 40% volume fraction

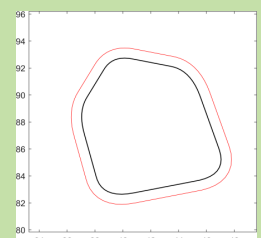


(b) 60% volume fraction

- Simulation of interface transition zone (ITZ)



(a) ITZ of crushed aggregates



(b) ITZ of pebble aggregates

Conclusions

- The results demonstrate that the proposed concrete meso-aggregate modeling method based on the Voronoi method not only effectively simulates the geometric shapes of crushed stone and pebble aggregates but also overcomes the aggregate grading problem. In particular, the generated elliptical aggregates closely resemble the shape of pebble aggregates while retaining the geometric features of convex polygonal aggregates.

Life Cycle Assessment of geopolymers for sustainable transition of cement industry

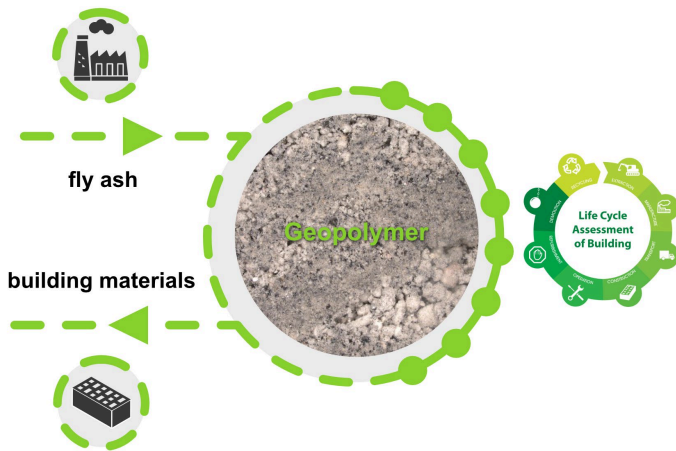
Jakub Szczurowski¹, Katarzyna Zarębska², Adrian Lubecki¹

¹Faculty of Energy and Fuels, AGH University of Krakow, Al. Mickiewicza 30, 30-059 Krakow, Poland;

²Faculty of Environmental Engineering, Geomatics and Renewable Energy, Kielce University of Technology, 25-314 Kielce, Poland corresponding author: kzarebska@tu.kielce.pl

Introduction

The construction industry has a significant impact on the environment, accounting for a substantial portion of resource consumption. Life Cycle Assessment (LCA) studies quantify impacts such as carbon emissions, energy consumption, water usage, air pollution, waste generation and ecosystem depletion.



Methods

The study presents a comparison of the carbon footprint generated by cement made from geopolymers and traditional Portland cement. The LCA study was conducted in line with international standards. Due to the fact that geopolymer cement production process was scaling up from lab scale, to ensure better comparability, uncertainty analysis using the Monte Carlo method was performed.

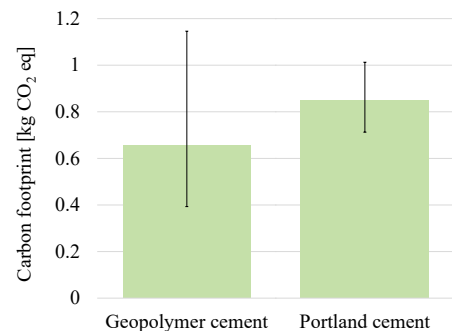
Research Significance

- Considering the life cycle impacts, LCA helps optimize the environmental performance of construction projects.
- It guides material selection, design modifications, energy efficiency improvements and waste reduction strategies, ultimately leading to more sustainable and eco-conscious designs.
- It promotes environmentally responsible decision-making and encourages the adoption of sustainable practices in the construction Industry.

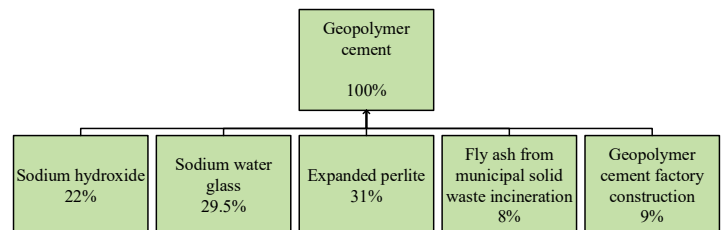
Results and Discussion

- The results demonstrate that geopolymer cement has the potential to revolutionize the cement industry's environmental sustainability.
- The geopolymer technology offers a promising avenue to decouple cement production from excessive carbon emissions, contributing to global efforts in combatting climate change.
- Areas where environmental improvements can be made during the geopolymer cement production process: optimizing raw material sourcing and reducing energy consumption during activation.

Carbon footprint comparison with uncertainties bars



Carbon footprint share in geopolymer production process



Conclusions

The environmental LCA of geopolymer cement has demonstrated its potential to reduce the carbon footprint of the cement industry. Geopolymer cement, with its potentially lower greenhouse gas emissions and environmental performance compared to Portland cement, offers a compelling solution for sustainable construction.

Funding: This research was funded by National Science Centre, Poland grant number OPUS-22 UMO-2021/43/B/ST8/1636.

Formation of a layered structure porous glass-ceramics for neutron shielding

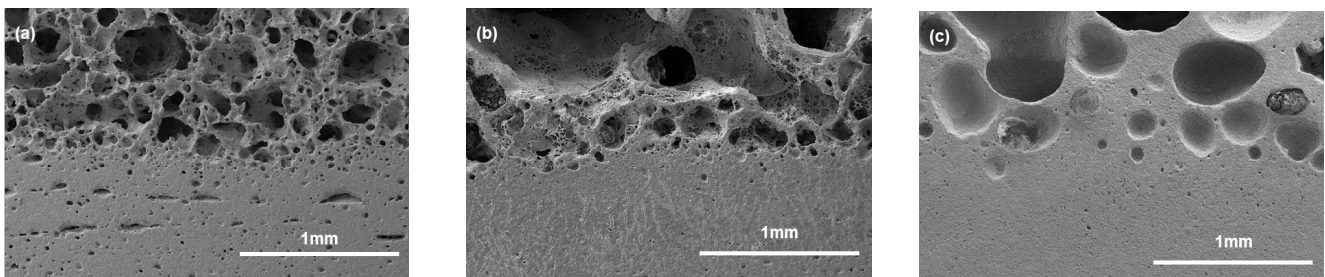
Kefeng. Jiang¹ and Wei. Chen^{2*}

¹ School of Materials Science and Engineering, Wuhan University of Technology, Wuhan, China
² State Key Laboratory of Silicate Materials for Architectures, Wuhan University of Technology, Wuhan, China

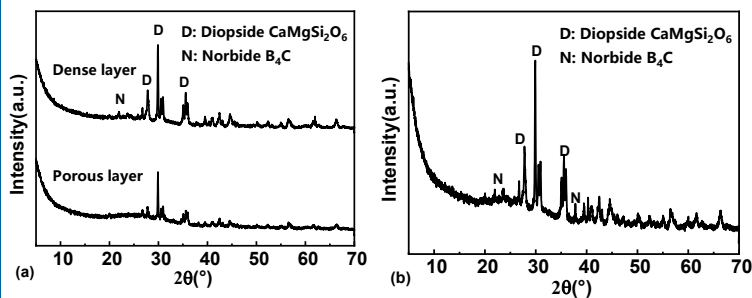
Introduction

In this work, in-situ foaming was used to prepare dense/porous bi-layered porous glass-ceramics. The influence of B_4C on the pore structure, properties, performances and neutron shielding rate of bi-layered porous glass-ceramics was investigated. The forming process of bi-layered structure was explained. The oxidation of B_4C and the in-situ B_2O_3 formation would reduce the viscosity of glassy phase and help the formation of bi-layered structure. The prepared bi-layered porous glass-ceramics possess advantages of lightweight, high flexural strength and excellent thermal insulation performance. In addition, the exist of boron gives the bi-layered porous glass-ceramics neutron shielding ability.

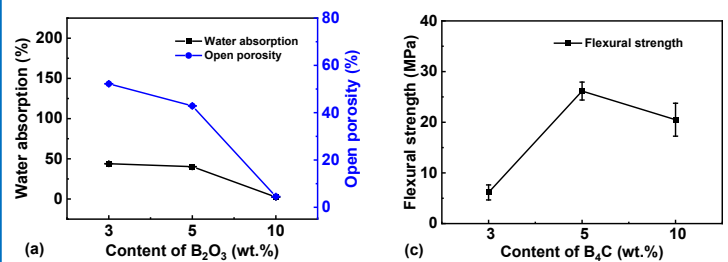
Results and discussion



SEM images of porous glass-ceramics with different amount of B_4C sintered at 950 °C for 60 min: (a) 3 wt.%, (b) 5 wt.%, (c) 10 wt.%



XRD patterns of porous glass-ceramics with different amount of B_4C sintered at 950 °C for 60 min: (a) 5 wt.%, (b) 10 wt.%



(a) Water absorption and open porosity, (c) flexural strength of porous glass-ceramics with different amount of B_4C sintered at 950 °C for 60 min

Conclusion

- The B_4C was oxidized to form boron oxide, the formation of boron carbide reduced the viscosity of glass phase and foaming temperature.
- Samples with 5 wt.% possess highest flexural strength of 26.15 MPa, lowest density of $1.06 \text{ g}\cdot\text{cm}^{-3}$ and thermal conductivity of $0.10 \text{ W}\cdot\text{m}^{-1}\cdot\text{K}^{-1}$. The performance is much better than normal porous glass-ceramics.

Effective iron removal from coal gangue applied in cement industry

Kenan Zhang, Xingjian Kang, Qinfu Liu
School of Geoscience and Survey Engineering, China University of Mining and Technology-Beijing

Background

- The main component of coal gangue (CG) is coal series kaolinite, which would be transformed into metakaolinite with high pozzolanic activity after activation process.
- The use of calcined CG (CCG) would reduce cement consumption, the relevant energy consumption, and environmental pollution.
- Iron in CG would affect the overall color of cement-based materials and limit the high-volume application of CCG in cement industry.
- The aim of this research is to support the high value utilization of coal gangue (CG) in the cement industry, through a practical and affordable method of pre-removing iron from CG

Methods and Materials

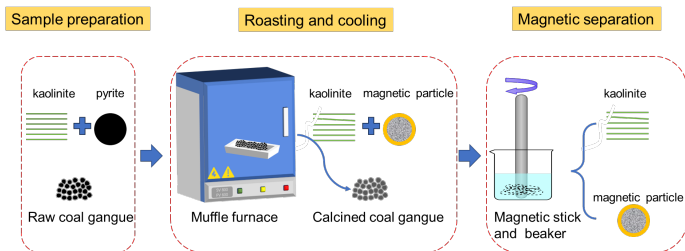


Fig. 1 Graphical abstract

The iron recovery rate of CCG was:

$$\varepsilon = \frac{(100\alpha - \gamma\beta)}{100\alpha} \times 100\%$$

ε : the recovery rate of iron, %

α : Fe_2O_3 content of CG, wt.% (loss on ignition deducted)

γ : yield of the nonmagnetic product, wt.%

β : Fe_2O_3 content of the nonmagnetic product, wt.%

Results and Discussion ①

Table 1. Iron phase analysis of CG

Iron phase	Fe in magnetite	Fe in sulfide	Fe in hematite, limonite	Fe in carbonate	Fe in silicate	Total
Content, wt. %	0.024	1.97	0.01	0.01	0.30	2.31
Percentage, %	1.04	85.13	0.43	0.43	12.96	100

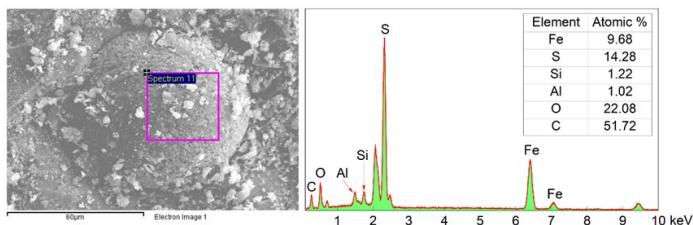


Fig. 2 Framboidal spherical pyrite in the CG

- Most of iron in the CG was present in the form of pyrite

Results and Discussion ②

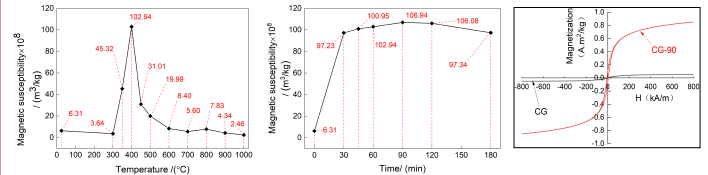


Fig. 3 Effect of calcination temperature and holding time on the saturation magnetic susceptibility of samples

- The CG held for 90 min at 400 ° C (CG-90) reached the highest magnetism

Table 2. magnetic separation results of CG and CCG

Samples	Fe_2O_3 content in the iron-removal products /wt. %	Fe_2O_3 content in the magnetic products /wt. %	Yield of magnetic product /wt. %	Recovery rate of iron /%
CG	-	-	0.09	-
CG-60	1.01	37.48	7.27	83.17
CG-90	1.02	37.04	8.95	83.37
CG-120	1.00	40.31	8.46	83.61
CG (HGMS)	3.28	6.33	25.60	56.28
CG-90 (HGMS)	1.05	9.90	31.53	87.12

HGMS: high gradient magnetic separation; The Fe_2O_3 content of CG is 5.58%

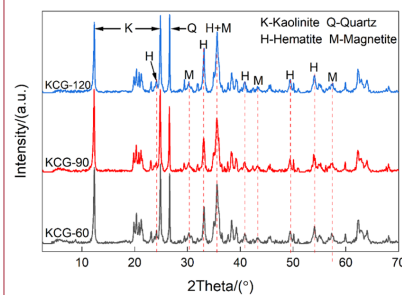


Fig. 4 XRD pattern for the magnetic products from CCG

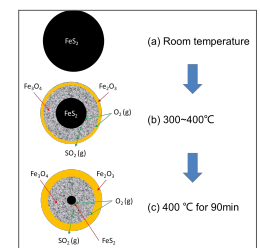


Fig. 5 Schematic diagram for calcination of the framboidal pyrite in CG-90

- Retention of the strongly magnetic magnetite enabled the effective removal of iron from CG.

Conclusions

- ✓ By calcining, the pyrite in CG was converted to hematite and strongly magnetic magnetite, which significantly enhanced the magnetism of CG, with the maximum magnetic susceptibility of CCG reaching roughly 17 times that of the CG.
- ✓ Magnetic separation including laboratory methods and HGMS effectively removed magnetic iron-containing particles.
- ✓ The iron recovery rates exceeded 83.17%, and the Fe_2O_3 contents of CCG's iron removal products were less than 1.02%, down from 5.58% for CG

Publications

- Publication 1, Dispersibility of kaolinite-rich coal gangue in rubber matrix and the mechanical properties and thermal stability of the composites
- Publication 2, Iron removal from kaolinitic coal gangue via magnetic separation after oxidizing calcination with the crystal structure of kaolinite protected (under review)

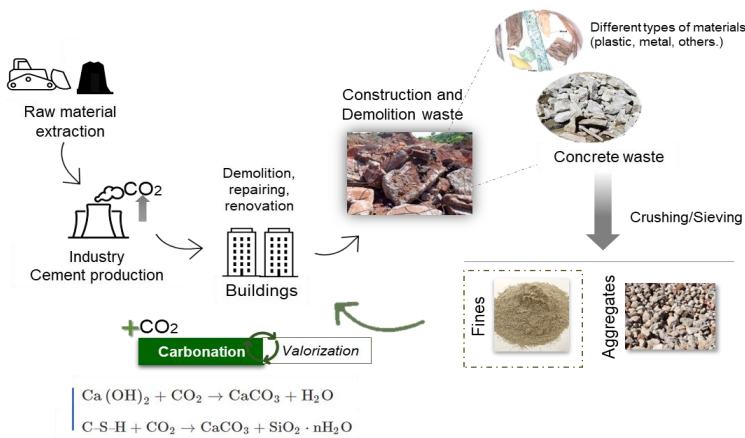
Influence of Temperature in Accelerated Dry Carbonation of Recycled Concrete Fines

L.N. Sousa¹, A.C.S. Bezerra², K. Schollbach¹, and H.J.H. Brouwers¹

¹ Department of the Built Environment, Eindhoven University of Technology, Eindhoven, the Netherlands
² Department of Civil Engineering, Federal Center for Technological Education of Minas Gerais, Belo Horizonte, Brazil

Introduction

- During the crushing process of concrete waste, a fine fraction of concrete is generated and has a high content of cement paste. The valorization of concrete waste fines/recycled concrete fines has been studied through semi-dry carbonation, aiming to improve the RCf properties to be further incorporated into new building materials.



Materials and Methods

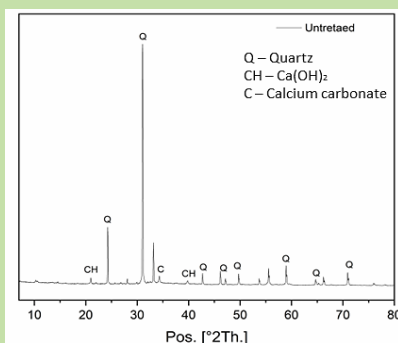
The RCf sample was provided and generated by industry partners. The fines were dried and sieved below 250µm to be further carbonated.

The semi-dry carbonation of RCf was conducted in a climate chamber under temperatures of 20, 35, and 50°C for 3 days. The relative humidity and CO₂ were fixed at 80% and 20%, respectively.

Chemical composition (XRF) and phase identification (XRD) of RCf before carbonation. The fines provided by industry were <250 µm, and the d_{50µm} is 148.98 µm.

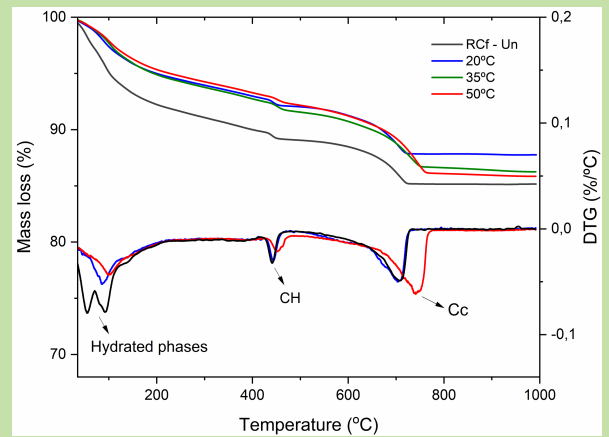
Oxides	%wt
SiO ₂	48.8
CaO	26.2
Al ₂ O ₃	3.9
Fe ₂ O ₃	3.0
MgO	0.8
K ₂ O	0.6
Others	2.1
LOI	14.6

RCf
D₍₅₀₎ = 148.98 µm



Results and Discussion

TGA and DTG profiles of samples before (RCf-Un) and after carbonation are presented below:



The %Cc content and the SSA (by BET method) are presented in Table 1.

Table 1 – SSA and Cc (% wt) of RCf and carbonated samples.

Temperature	SSA(m ² /g)	%Cc ¹
Rcf – Un	3.05	-
50°C	7.42	4.53%
35°C	8.53	5.10%
20°C	6.26	5.05%

¹ %Cc were calculated as: $\%CO_2Cc = \%Cc_{after} - \%Cc_{before}$.

where the is the Cc content before (RCf) and after the carbonation (carbonated samples).

All samples formed Cc product during the accelerated carbonation. However, there is a residual content of portlandite. That might be related to the formation of a Cc layer around the CH phase, which impairs the ion exchange. Then, after 3 days of carbonation, it seems that even at different temperatures, the carbonation presented a similar trend and a patamar of %Cc formed.

Outlook and Future Issues

- The RCf was generated during the crushing of concrete waste in industry. Then, the fines have already a content of Cc due to the long-term natural carbonation. Which could impair the complete reaction of CH.
- Further studies have been done to understand the kinetic of carbonation of concrete fines generated in industry.

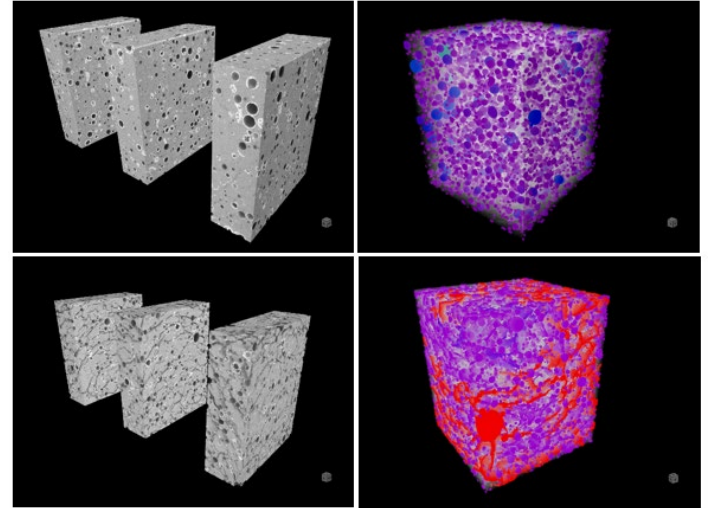
Ceramizable geopolymer-based fire-resistant coating

Li Zonggang Jiang Yuhang Li Qiu Chen Wei
State Key Laboratory of Silicate Materials for Architecture, Wuhan University of Technology

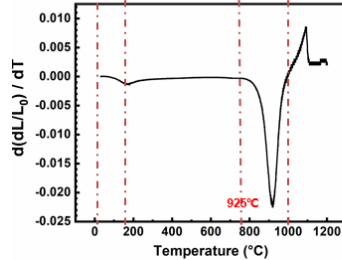
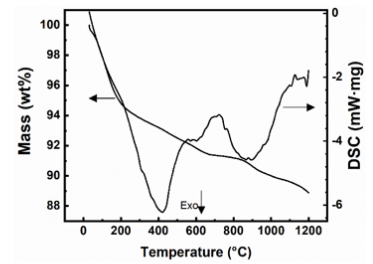
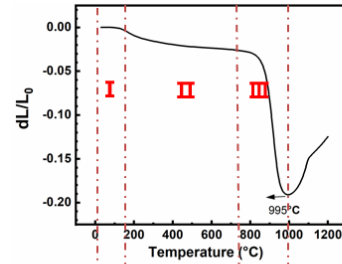
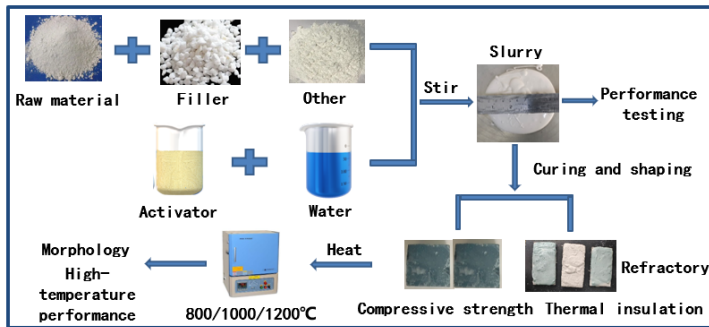
Introduction

This study utilizes aluminum silicate polymer and preferred thermal insulation fillers as the main raw materials to produce a geopolymer-based fire-resistant coating with fast curing, high refractoriness, and the ability to undergo ceramic transformation at high temperatures while improving mechanical properties. The working properties of the fire-resistant coating were controlled by designing the particle size distribution of thermal insulation fillers. The mechanism of geopolymer binder undergoing ceramic transformation in high-temperature environments was investigated through tests such as XRD and SEM.

Results and discussion

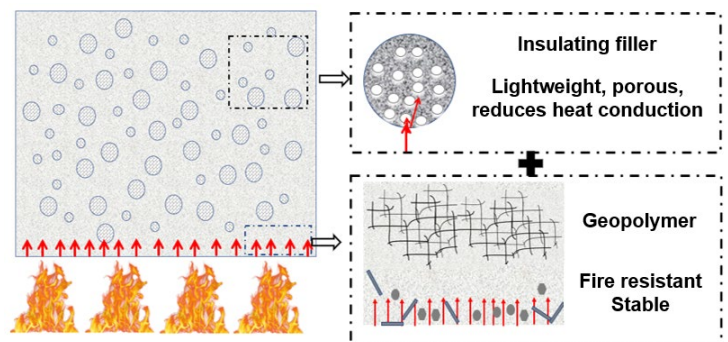
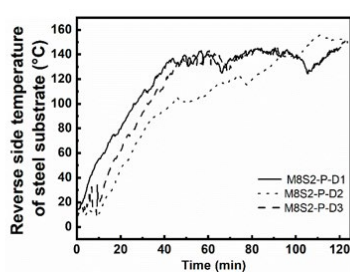
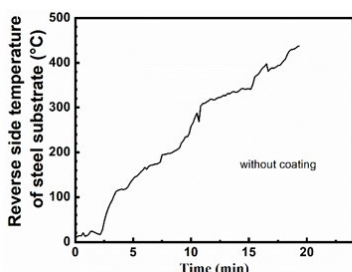
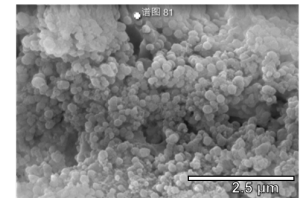
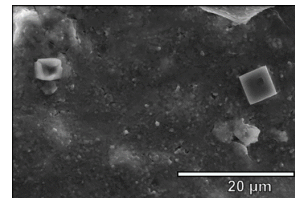
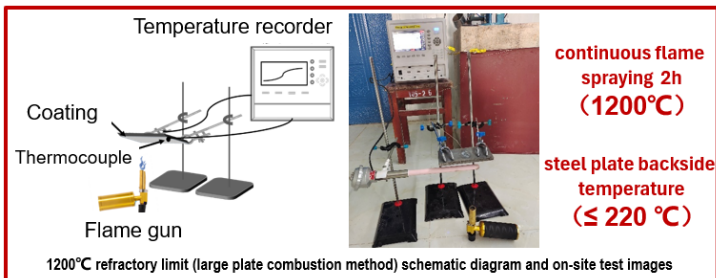


Experimental design



Stage	Heat shrink	Reason
I	RT—200°C	1.5% Adsorbed water volatilization
II	200°C—800°C	1.2% hydroxyl condensation
III	800°C—1000°C	16% melting and densification

1000°C—1200°C, Thermal expansion of the geopolymer.



Objectives

- Carbon capture, utilization and storage
- Carbonation curing
- Pre-curing
- Water-cement ratios
- Pore water saturation
- Cement-based materials

Research Significance

- Carbonation curing has attracted extensive attention as an effective method for carbon capture, utilization and storage (CCUS), as well as for improving the mechanical properties of cement-based materials. However, pore structure and pore water saturation which can control the diffusion of CO₂ and the leaching of Ca²⁺, are found to be the key factors restricting the carbonation reaction rate.

Results and Discussion 1

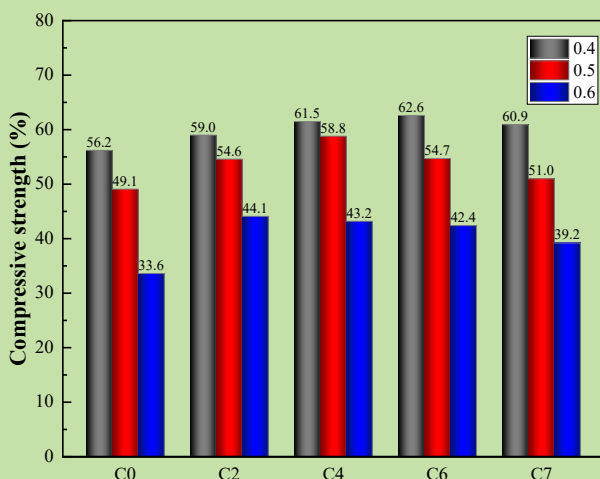


Fig. 1 Compressive strength of different w/b on different pre-curing

- The compressive strength decreased with the increase of w/c.
- There was a maximum compressive strength at different pre-curing ages for different w/c.
- When w/c was 0.4, 0.5 and 0.6 respectively, the highest compressive strength of cement mortars after pre-curing for 1 day, 3 days and 5 days, which were 62.6 MPa, 58.8 MPa and 44.1 MPa, respectively.

Results and Discussion 2

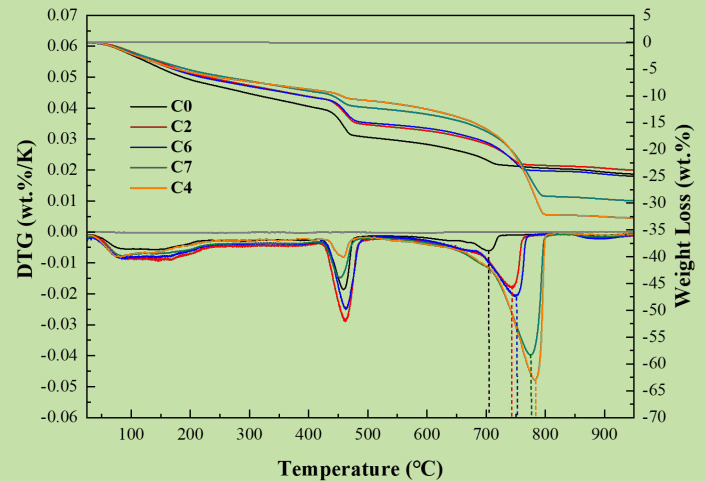


Fig. 2 TG-DTG results of 0.5 w/b on different pre-curing

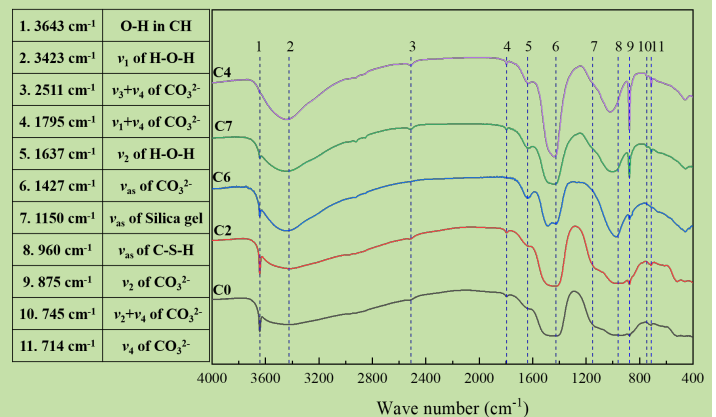


Fig. 3 FTIR results of 0.5 w/b on different pre-curing

- The peak value of TG-DTG curve was different from 500°C to 950°C for different pre-curing.
- The higher the temperature corresponding to the peak, the higher the crystallinity of CaCO₃.
- The FTIR showed that the increase of strength was related to the production of CaCO₃, and the different was relevant to the content of high-polymerization degree silica gel.

Conclusions

- Different w/c had different optimal pre-curing.
- An appropriate pre-curing age can significantly improve the mechanical properties of carbonated cement-based materials, while the refinement of pore structure due to carbonation also can decrease the negative impact of large pores formed in the cement-based materials prepared with high w/c.

Objectives

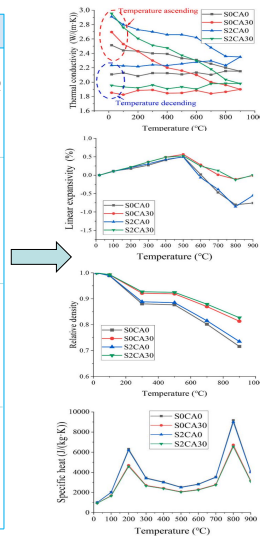
This paper presents the experimental and numerical investigation on the thermal properties of steel fibre-reinforced alkali-activated concrete (AAC) made by using multiple precursors at elevated temperatures. The temperature-dependent thermal properties such as mass change, thermal conductivity, density, specific heat, and thermal expansion are reported. The effects of temperature heating AAC, coarse aggregate, and steel fibre on the thermal performance of AAC are evaluated quantitatively. Based on the test results, a multi-phase mesoscale model is developed to predict the thermal properties considering volume fractions of steel fibre and coarse aggregate, which can be used in the fire safety design of AAC structures.

Research Significance

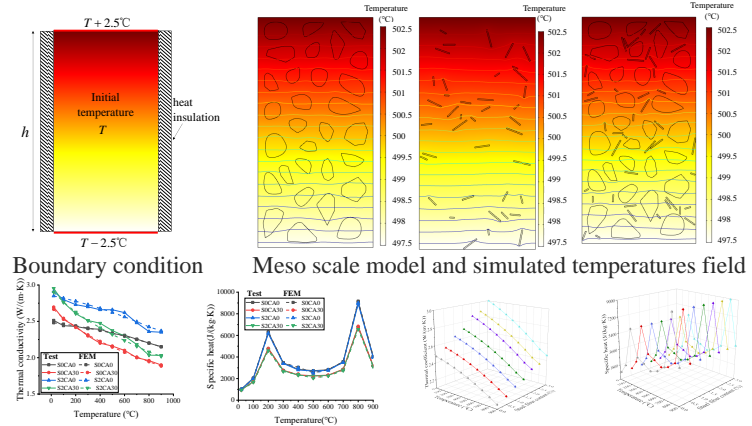
The experimental work involves the tests to determine the temperature-dependent thermal conductivity, density, specific heat, and thermal expansion. The numerical work involves the development of multi-phase model which can be used to evaluate the effect of individual components on the effective thermal properties of the steel fibre reinforced AAC.

Experimental works

Test type	Specimen size	Specimen number	Test set-up	Method
Thermal conductivity	Cuboid: L:230mm, W:114mm, H:64mm	X(Mix number) >2(one group) >3(repeated) =6X	Furnace, Heating curve	$\lambda = \frac{Q \cdot L}{A \cdot \Delta T \cdot t}$
Mass Loss	Cylinder: Φ 50mm, H:100mm	X(Mix number) >6(temperature) >3(repeated) =18X	Before heating, After heating, Furnace	$\frac{m_T}{m_0} = \frac{m_T}{m_0}$
Specific heat	Cube: L:100mm	X(Mix number) >3(repeated) =3X	Optimization, FEA	Optimization, FEA
Thermal expansion	Cylinder: Φ 50mm, H:100mm	X(Mix number) >3(repeated) =3X	Furnace, Heating curve	$\epsilon = \frac{\Delta L}{L}$



Numerical works



- The effective thermal properties of the steel fibre-reinforced AAC can be predicted by using the multi-phase model if the thermal properties of individual components are known.

Conclusions

- High temperature greatly affects the thermal properties of AAC.
- Coarse aggregate and steel fibre also have a considerable influence on the thermal properties.
- The effective thermal properties of the steel fibre-reinforced AAC can be predicted by using the multi-phase model.

Outlook and Future Issues

- In our mesoscale model, the matrix is considered as homogeneity material, we will consider the homogeneity of the matrix in the further works.
- The model considering the thermal and force coupling should be developed.

Publications

- Min Yu, Hanjie Lin, Tan Wang, Feiyu Shi, Dawang Li, Yin Chi, Long-yuan Li. Experimental and numerical investigation on thermal properties of alkali-activated concrete at elevated temperatures. Journal of Building Engineering, 2023, 74:106924.

Objectives

- Insight into the role of Temperature Rising Inhibitor (TRI) on the early hydration of Portland cement.
- The changes in the efficiency of TRI in the presence of supplementary cementitious materials (SCMs).
- The role of TRI on the filler effect of SCMs.

Materials and Methods

- Chemical compositions of cement and SCMs

Oxides	CaO	SiO ₂	Al ₂ O ₃	SO ₃	Fe ₂ O ₃	MgO	Na ₂ O	K ₂ O	Others
PC	63.35	23.02	4.14	2.18	3.64	1.25	0.21	0.53	-1.68
GBS	45.18	26.24	15.36	1.89	1.08	6.80	0.34	0.42	-2.69
FA	5.92	44.36	30.44	0.76	9.67	1.01	0.75	2.63	-4.46
QZ	0.09	98.30	0.72	0.00	0.07	0.06	0.05	0.54	-0.17

- Temperature rising inhibitor

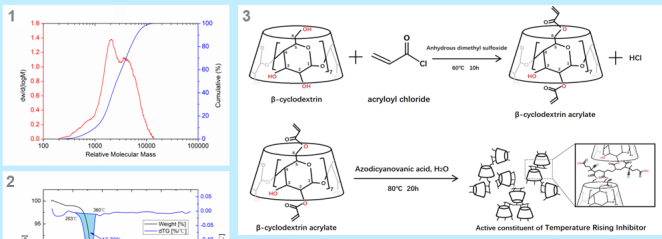


Fig.1 The relative molecular mass distribution of TRI measured by GPC

Fig.2 TG and DTG curves of TRI

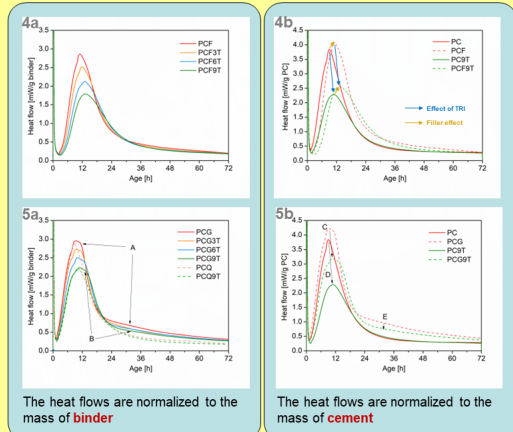
Fig.3 The synthetic process of the active constituent of TRI

- Mixing proportion of testing groups

	cement	fly ash	slag	quartz	TRI	TRI/cement	TRI/cement	water
PC	100							38
PC9T	100				0.9	0.9%		38
PCF	70	30						38
PCF3T	70	30			0.21	0.3%		38
PCF6T	70	30			0.42	0.6%		38
PCF9T	70	30			0.63	0.9%		38
PCG	70		30					38
PCG3T	70		30		0.21	0.3%		38
PCG6T	70		30		0.42	0.6%		38
PCG9T	70		30		0.63	0.9%		38
PCQ	70			30				38
PCQ9T	70			30	0.63	0.9%		38

Results and Discussion

- Isothermal calorimetry



Fly ash blended cement:

- The maximum heat flow decreases linearly with the increase of TRI.
- The inhibitory efficiency of TRI (on cement) is barely changed in the presence of fly ash.
- The filler effect is still visible when TRI is added.

GGBS blended cement:

- The individual reaction of GGBS can be detected (labelled A and B).
- The inhibitory efficiency of TRI (on cement) is evidently weakened by the GGBS (comparing C and D).

Fig.4 & 5 The calorimetry curves of fly ash blended cement (4) and GGBS blended cement (5)

Research Significance

- The mechanism of TRI was revealed by means of the synthesis experiment of C-S-H gel.
- The efficiency of TRI in blended cements was estimated and attributed to the adsorption capacity of SCMs.

- Adsorption capacity

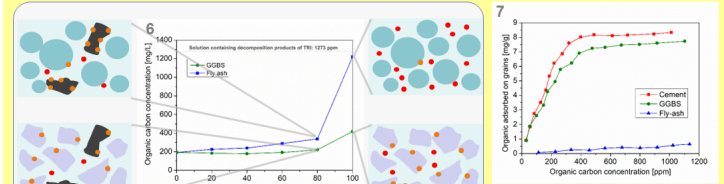


Fig.6 The relationship between the amount of organic adsorbed on grains and the organic concentrations in solutions.

Fig.7 The organic carbon concentrations of TRI solutions after being adsorbed by blended cement powders with various SCM content

In GGBS blended cement, a portion of TRI is adsorbed on GGBS grains, which leads to a weakened efficiency of TRI. While in fly ash blended cement, the negligible adsorption capacity of fly ash has no impact on the efficiency of TRI.

- Phase assembly

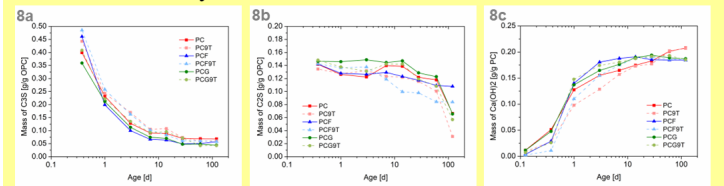


Fig.8 C₂S (8a), C-S (8b), and CH (8c) contents of hardened blended cement pastes based on Rietveld refinement. It is evident that the impact of TRI on the hydration degree of cement diminishes in long-term.

- Synthesis of C-S-H gel

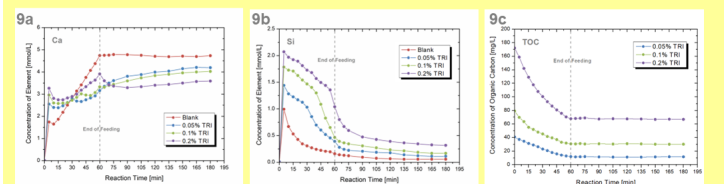


Fig.9 Evolution of Ca concentration (9a), Si concentration (9b), and total organic concentration (9c) during the continuous feeding of Ca(NO₃)₂ and Na₂SiO₃ solutions and precipitation of C-S-H. The Si concentration remains relatively high in the presence of TRI, and the Ca concentration becomes lower in consequence. The decrease of organic concentration of the solutions implies that TRI is adsorbed on the C-S-H.

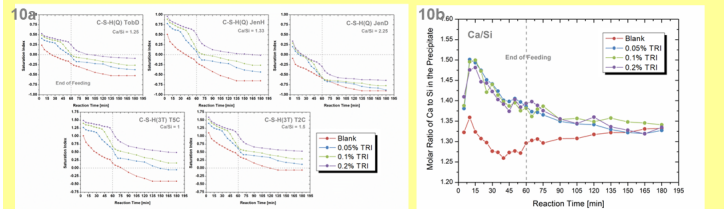


Fig.10 Evolution of saturation indices of several types of C-S-H (10a) and the molar ratio of Ca to Si in the precipitate (10b). The presence of TRI greatly increases the oversaturation degree required for precipitation of C-S-H with low Ca/Si. The Ca/Si of the precipitate becomes higher when TRI exists.

Conclusions

- The inhibitory effect of TRI on cement hydration in blended cement is barely changed by FA but evidently weakened by GGBS.
- GGBS grains have a strong adsorption capacity for TRI whereas fly ash grains barely adsorb TRI. This results in the different roles of SCMs in the inhibitory effect of TRI.
- The presence of TRI hinders the precipitation process of C-S-H, and increase the Ca/Si of the C-S-H.

Publications

- Weiyi Chen, Yuqi Zhou, Peiyu Yan, et al. Impact of Temperature Rising Inhibitor on Hydration of Cement-Fly Ash Cementitious Materials and Performance of Concrete [J]. Journal of the Chinese Ceramic Society. 2021, 49(8), 1609-1618. doi: 10.14067/j.issn.0454-5648.20200724

Alkalinity optimization and long-term life prediction for BFRP bars serving in marine concrete environment with different $\text{Ca}(\text{OH})_2$ content

Xiang Liu, Pei Tang*, Wei Chen*

State Key Laboratory of Silicate Materials for Architectures, Wuhan University of Technology

Research background

BFRP bars replace steel bars

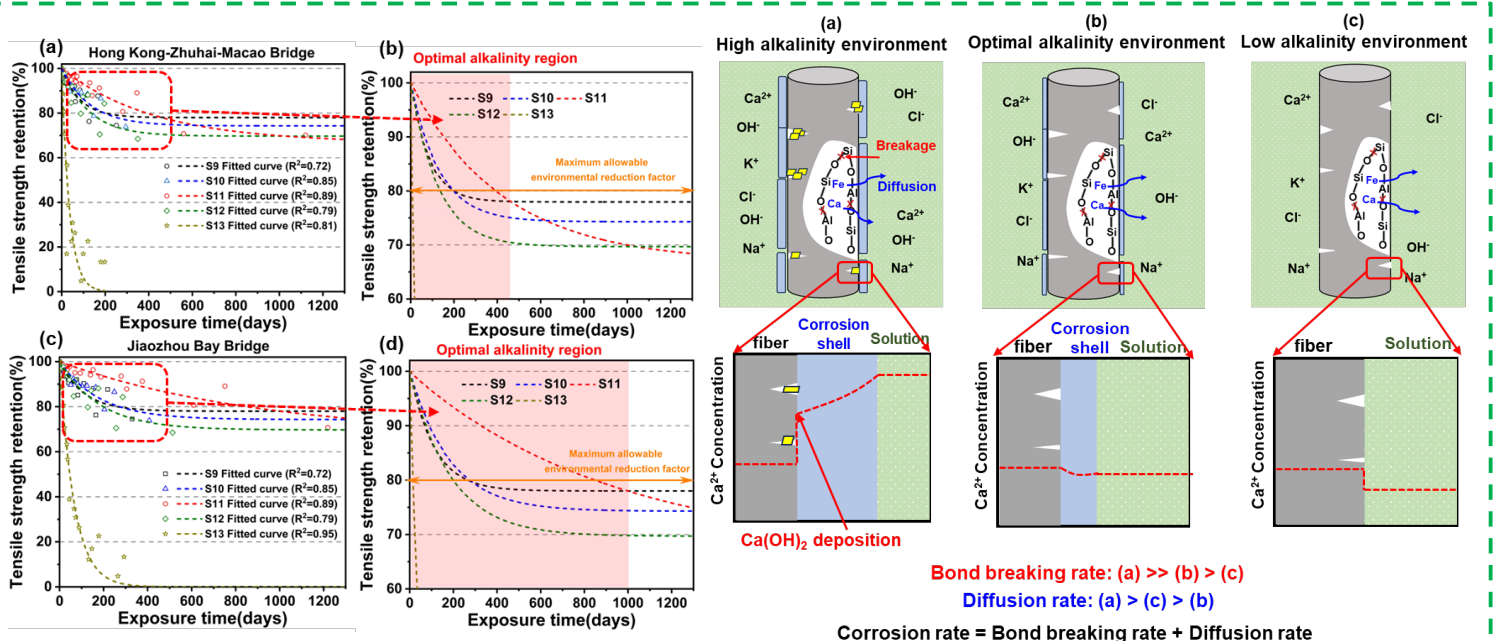
Basalt fiber + Epoxy resin → Pultrusion → BFRP bars

Degradation mechanism in seawater sea sand concrete

- Swelling of Interface
- Resin matrix
- Dissolution of resin into Interface
- Cracking of Fiber
- Cracking of Resin matrix
- Breaking of polymer chains
- In situ reaction
- Through solution reactions

BFRP bars can replace steel bars as the reinforcement skeleton of seawalls, which can avoid the structural damage caused by corrosion and expansion of steel bars, but the high alkalinity of concrete matrices also limits the applicability of BFRP bars

Result and discussion



Long-term service life prediction

Deterioration mechanism of BFRP bars under different alkalinities

The different contents of $\text{Ca}(\text{OH})_2$ in simulated marine concrete pore solution may lead to the existence of optimal alkalinity that minimizes the properties degradation rate of BFRP bars.

Influence of expansive agent on the mechanical properties of steel-tube-confined high-performance concrete (STCHPC)

Yangyueye Cao and Dianyi Song
National University of Defense Technology

Objectives



- Shrinkage of HPC is higher than that of normal concrete
- HPC tends to debond from the steel tube in STCHPC, making it difficult to realize their joint work
- Expansive agent (EA) is added to reduce the shrinkage and improve the co-working properties of HPC and steel tube

Experimental methods

- **Restrained shrinkages** of the HPC with **0%, 5%, 10% and 15%** of EA are measured
- Influences of EA dosage on the **compressive strengths** are studied
 - 100mm×100mm×100mm HPC cubes → effects on the **HPC material**
 - STCHPC specimens (cross-sectional side length of 70 and 116mm) → effects on **STCHPC structure**

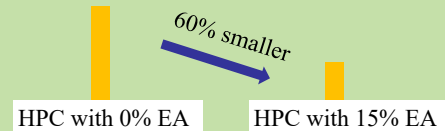


- **Pushout tests** are conducted to evaluate the **bond strength** between the steel tube and the HPC in the STCHPC

Results and Discussions

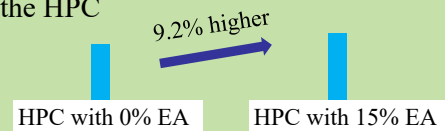
Effects on the **restrained shrinkage**

- The 28d shrinkage of the HPC is reduced



Effects on the **compressive strength**

- The **early strength** of HPC is slightly reduced
- EA improves the **28d compressive strength** of the HPC



- The 28d compressive strength of the **STCHPC** are improved with the use of EA

Effects on the **bond strength**

- The maximum pushout force is observed when 15% EA is used in the case of STCHPC specimen with a side length of **70mm**
- The maximum pushout force is achieved with 5% of EA when the side length of the STCHPC specimen is **116mm**

Conclusions

- On the **HPC material level**:
 - EA can reduce the restrained shrinkage of HPC, contributing to the joint work of the steel tube and the HPC in the STCHPC specimen
 - EA has a the positive effect on the 28d compressive strength of the HPC
- On the **STCHPC structural level**:
 - The higher EA dosage the higher compressive strength of the STCHPC specimen
 - In terms of the bond strength, the optimum dosage of the EA varies with different STCHPC specimen dimensions

Effects of calcined phosphogypsum replacement on hydration and properties of calcium sulfoaluminate cement at different curing temperatures

Yishun Liao, Jinxin Yao at al.
School of Urban Construction, Wuhan University of Science and Technology, Wuhan 430065, China

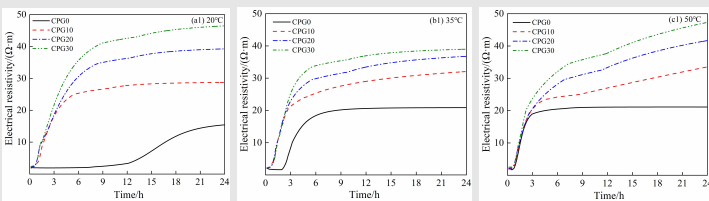
Objectives

- The present research aims to understand the cement hydration and microstructure formation mechanism of calcined phosphogypsum (CPG)-supplemented calcined phosphogypsum (CSA) pastes cured under hot-weather temperatures.
- It is analyzed mainly through experiments on heat of hydration, strength development, electrical resistivity, hydration kinetics, and thermodynamic modeling.

Research Significance

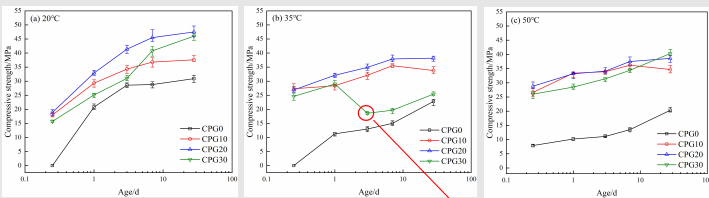
- Since CSA cement is insensitive to impurities, the application of phosphogypsum in clinker of sulphur-aluminate cement can not only significantly increase the utilization rate of calcined phosphogypsum, but also promote the goal of "double carbon".

Results-experiments



Electrical resistivity of CSA cement pastes at different temperatures

- At elevated temperatures, the heterogeneous distribution of the hydration products resulted in the loose structure and the decrease of electrical resistivity.



Compressive strength of CPG-CSA cement pastes cured at 20°C, 35°C, and 50°C

- The presence of excessive AFt formation in the CPG30 sample during curing at 35°C for three days resulted in the development of cracks caused by expansion.
- a transformation of a portion of AFt into AFm occurs at 50°C, resulting in the absence of cracks in the CPG30 sample.

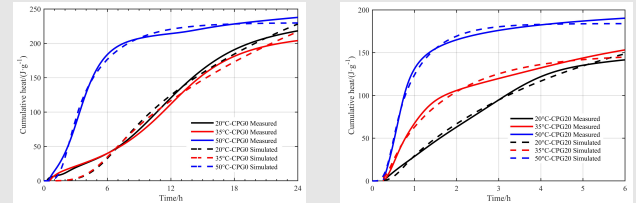


Results-models

Hydration kinetics model

$$V = 1 - \exp\left\{-2pSGt \int_0^1 \left[1 - \exp\left(-\frac{\pi N}{3} gG^2 t^3 (1-u)^2 (1+2u)\right)\right] du\right\}$$

$$V = 1 - \exp\left\{-2k_G t \int_0^1 \left[1 - \exp(-k_N t^3 (1-u)^2 (1+2u))\right] du\right\}$$

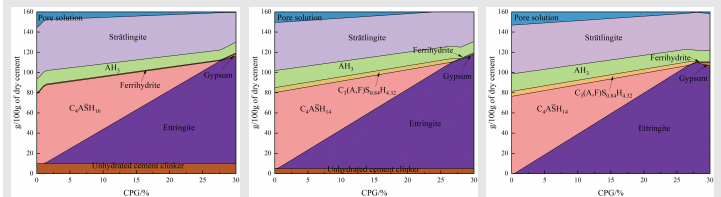


Hydration kinetics model of CSA cement pastes at different temperatures

CPG content	Parameters	20°C	35°C	50°C
0(Control)	$A(J/g)$	371.874	399.925	229.964
	k_h/h^*	0.02118	0.01726	0.13867
	k_n/h^*	0.00475	0.00633	0.09304
20%	$A(J/g)$	208.376	148.161	184.023
	k_h/h^*	0.10596	0.31896	0.66899
	k_n/h^*	4.51059	11.53772	17.04408

- The growth rate constant and nucleation rate constant of cement paste increased with the addition of CPG at different curing temperatures.

Thermodynamic model



- The incorporation of CPG shifts the interconversion of AFt and AFm towards the reaction direction of producing AFt.

Conclusions

- The electrical resistivity test results show that the early hydration of the cement pastes was accelerated, and the time interval between the induction period and the acceleration period was shortened at 50°C.
- The compressive strength of CSA cement pastes was influenced by curing temperature and CPG content.
- At 50°C, the growth rate and nucleation rate of CSA cement increased significantly compared with that at 20°C.
- The ettringite content of CSA cement obtained by thermodynamic modelling is nearly close to the experimental results.

References

- Y. Tao, A. V. Rahul, M.K. Mohan, G. De Schutter, K. Van Tittelboom, Recent progress and technical challenges in using calcium sulfoaluminate (CSA) cement, *Cem Concr Compos.* 137 (2023) 104908.
- T. Hanein, J.L. Galvez-Martos, M.N. Bannerman, Carbon footprint of calcium sulfoaluminate clinker production, *J Clean Prod.* 172 (2018) 2278–2287.
- F. Bertola, D. Gastaldi, S. Irico, G. Paul, F. Canonico, Influence of the amount of calcium sulfate on physical/mineralogical properties and carbonation resistance of CSA-based cements, *Cem Concr Res.* 151 (2022) 106634.
- E. Gartner, Industrially interesting approaches to "low-CO₂" cements, *Cem Concr Res.* 34 (2004) 1489–1498.

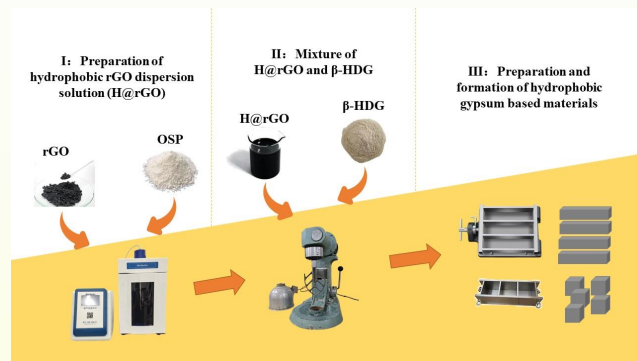
Characterization and Hydrophobic Surface Study of Gypsum based Composite by Modified Reduced Graphene Oxide

Zhi Zhenzhen, Guo Yanfei*, Wang Liting, Tan Hongbo, Liu Bo, Dong Binbin, Zhang Hua
Luoyang Institute of Science and Technology, Luoyang, China
Wuhan University of Technology, Wuhan, China

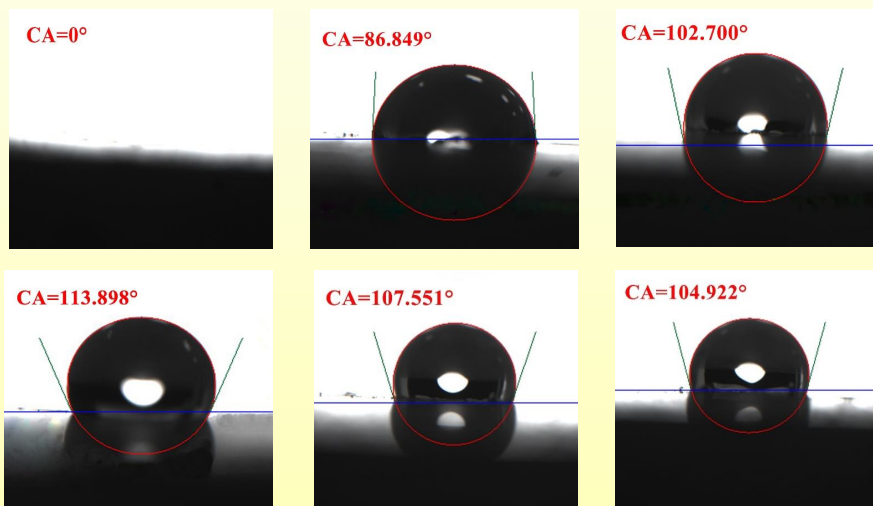
Introduction

- With the implementation of the strategy “peak carbon dioxide emissions and carbon neutrality”, the large-scale application of industrial by-product gypsum is continuously advancing.
- Functional gypsum based materials as one of the green, environmentally friendly, and low-carbon building material, are widely used in building decoration.
- However, its inherent poor water resistance and other defects seriously restrict its application scope.
- This paper aims to study the effect of modified hydrophobic graphene on the surface hydrophobicity, mechanical strength, and water resistance of gypsum based materials, and obtain hydrophobic gypsum based building materials.

Materials and methods



Results and Discussion

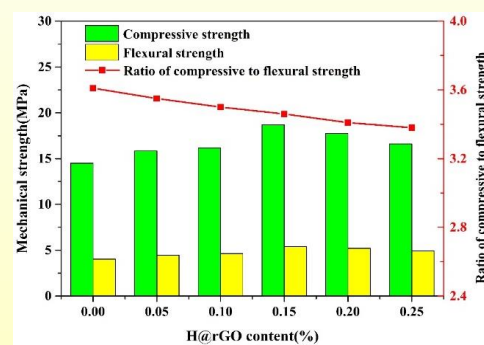


The surface contact angle of specimens with different contents of H@rGO: (a) control, (b) 0.05 wt%, (c) 0.1 wt%, (d) 0.15 wt%, (e) 0.2 wt% and (f) 0.25 wt%.

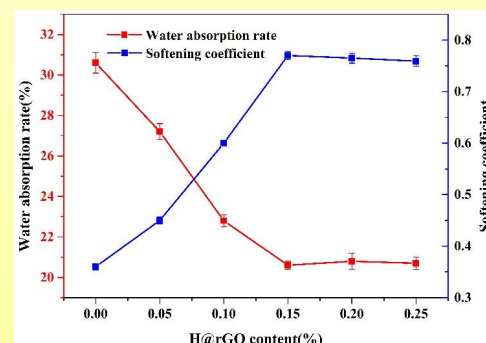
- The surface of control sample of gypsum hardened have strong hydrophilicity.
- The surface contact angle values increased significantly with the addition of H@rGO.
- The lower addition of H@rGO could improve the mechanical strength of hardened gypsum.
- The enhancement effect of H@rGO is declined when the addition of H@rGO more than a certain range
- The water absorption rates of gypsum specimens decreased significantly first and then slightly increased with the increasing content of H@rGO.

Conclusions

- With the content of 0.15wt% H@rGO, the surface contact angle was up to 113°, the compressive strength and softening coefficient were 18.7 MPa and 0.77, increasing by 35.33% and 113.89%.
- The pore size and total porosity of hardened samples decreased.
- The microstructure of hardened samples improved.



Mechanical strength of specimens with different contents of H@rGO



Water absorption rates and softening coefficients of specimens with different contents of H@rGO

Acknowledgement

Finance supported by the National Natural Science Foundation of China (No.52102024, No.52202064)

Contact

Email:
zhizhenzhen0607@163.com
guoyfvip@163.com



Sustainable BOF slag binder activated by EDTA-4Na

Building Materials Group, Department of Built Environment

Zhihan Jiang
z.jiang@tue.nl, pro_jzh@163.com

Supervisor:
Dr. Katrin, Schollbach
Prof. Dr. Jos, Brouwers

Introduction

Problems of BOF slag: **occupation of lands** and **potential pollutions**



- Application potential: as a **cementitious binder** due to abundant **belite** and **brownmillerite**
- Barrier: **low hydration reactivity** due to the dense structure and excessive iron-based phases
- Existing solutions: alkaline or salt activators with very **limited effects**
- Research contents: hydration activated by **EDTA-4Na**

Research program

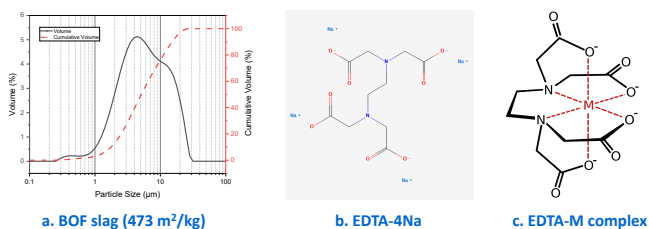


Fig. 1 Raw materials and activators

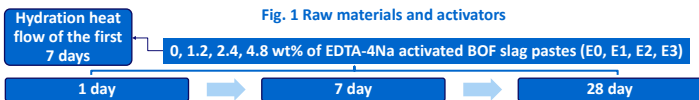


Fig. 2 Experiments design

Parts of Results and disussions

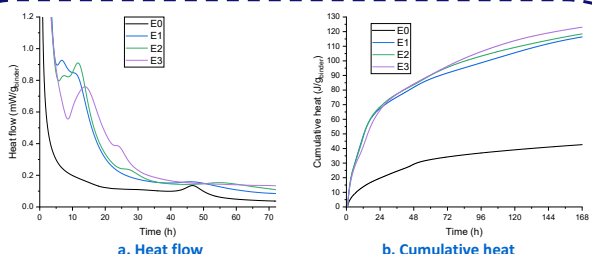


Fig. 3 Normalized hydration heat of pure and EDTA-4Na-activated BOF slag pastes

- Only **minor exothermic peak** for **pure BOF slag** paste after 2 days
- Short induction stage** and **distinct heat release peaks** for **EDTA-4Na-activated**; Peaks **retarded** at **increased dosages**
- Cumulative heat** of 7 d hydration **increased significantly** for **EDTA-4Na-activated pastes**

Main crystalline hydrates: **hydrogarnet** and **hydrocalcite**

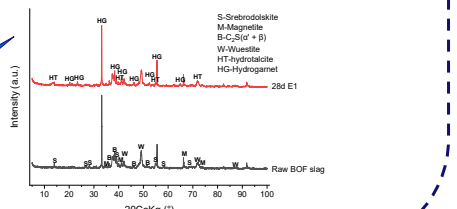


Fig. 4 XRD patterns (Internal standard silicon not labeled)

Parts of Results and disussions

Table 1 Quantitative phase compositions of BOF slag pastes

Phase	Raw BOF	1 day				7 day				28 day			
		E0	E1	E2	E3	E0	E1	E2	E3	E0	E1	E2	E3
Wuestite	21.9	21.4	19.2	16.4	15.3	14.9	15.0	14.8	14.2	14.4	16.7	14.9	15.7
Magnetite	4.5	6.0	4.3	4.6	3.9	4.7	4.3	3.8	4.0	5.0	4.2	3.8	3.7
Srebrodolskite	13.0	12.0	6.9	5.8	3.8	10.1	5.6	5.6	4.3	11.2	5.2	4.0	3.8
C ₂ S (α' + β)	35.4	34.9	31.8	34.8	26.3	28.1	28.9	26.5	26.4	28.7	26.4	25.4	22.9
Hydrogarnet	0.0	1.6	5.3	9.6	9.2	2.4	8.3	9.8	12.1	3.6	9.2	12.5	12.2
Hydrocalcite	0.0	2.1	2.9	4.4	3.8	3.3	3.1	2.2	2.9	3.9	2.7	3.2	3.6
Lime	0.7	0.1	0.3	0.2	0.4	0.1	0.1	0.6	0.3	0.2	0.3	0.3	0.1
Portlandite	0.6	0.3	0.1	0.2	0.4	0.5	0.1	0.3	0.7	1.0	0.4	0.8	1.4
Calcite	0.3	0.0	0.5	1.0	0.6	0.5	0.6	0.8	1.0	0.9	1.0	0.9	1.1
Amorphous	23.6	21.6	28.8	22.9	36.3	35.4	33.8	35.5	34.2	31.1	33.9	34.2	35.4
R _{wp} (%)	3.6	3.9	3.9	3.9	3.9	3.9	3.9	3.9	3.9	3.9	3.5	3.5	3.5

- Wuestite and belite (early) hydration accelerated with addition of (high) dosage of EDTA-4Na
- Most of srebrodolskite hydrated after only one day of hydration

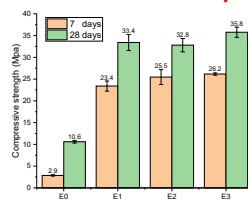


Fig. 5 Compressive strength of BOF slag pastes

- Pure BOF slag: **ignorable strength**
- EDTA-4Na-activated: **significantly improved strength**
- Dosage effects: **hard to distinguish**

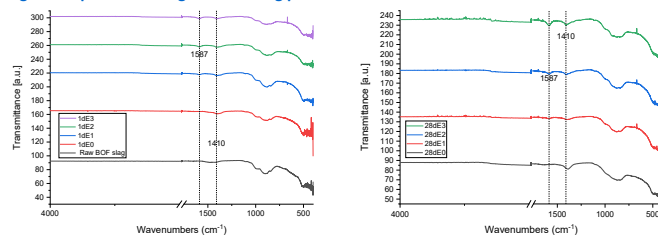


Fig. 6 FTIR spectra of raw BOF slag and hydrated pastes (by ATR)

- Infrared peaks at **1587 and 1410 cm⁻¹** are most likely due to the **asymmetric and symmetric u₃(COO⁻)**
- 1 day spectra: presence of EDTA-M complexes within hydration products, **hard to differentiate effects of dosages, bonding of EDTA-M complexes with hydrates not enough**
- 28 day spectra: **enhanced bonding of EDTA-M complexes** with hydration products after longer hydration time

Conclusions

- EDTA-4Na apparently **accelerated the early hydration** of **wuestite** and **belite**
- Srebrodolskite (low Al brownmillerite)** hydration significantly improved after only one day
- Main crystalline hydration products were **hydrogarnet** and **hydrocalcite**
- The **compressive strengths** were **enhanced dramatically**
- EDTA-M complexes were **bonded into hydrates** after longer hydration time

Outlook and Future Issues

- Outlook: significantly promote the **reuse of BOF slag** as a **sustainable binder**
- Future issues: **durabilities** of EDTA-4Na-activated BOF slag, such as **chloride resistance** and **anti-carbonation property**

Towards performance carbonation improvement of supersulfated cement by nano-silica

Zhongxu song, Heng chen*, Pengkun hou, Xin cheng
University of jinan

Introduction

- 1. Supersulfate cement (SSC) is a typical low-carbon cement with ettringite(Aft) and C-(A)-S-H gel as hydration products. Due to its low alkalinity and lack of calcium hydroxide in its hydration products, SSC demonstrates weak carbonation resistance, thereby limiting its practical applications.
- 2. The high pozzolanic and micro-filling effect of the nano-silica can significantly improve the compressive strength, and the performance following the process of carbonation, extending its service life.
- 3. Nano-silica facilitates the formation of C-(A)-S-H gel, and a large amount of C-(A)-S-H covers Aft, which slows the carbonation of Aft and improves the performance of carbonated supersulfate cement.
- 4. After carbonation, a significant amount of calcium carbonate is produced in SSC, and the addition of nano-silica reduces the formation of calcium carbonate. It is evident from quantitative analysis and morphological observations that the addition of nano-silica and silica fume increases the presence of various calcium carbonate crystalline forms (vaterite and aragonite).

Research Significance

Supersulfate cement is a typical low-carbon cement that has not been widely used due partially to its slow early age strength gain and poor resistance to carbonation. This study investigates whether the incorporation of nanosilica can improve the early strength along with its post-carbonation properties and increase the life cycle of supersulfate cement

Results and Discussion

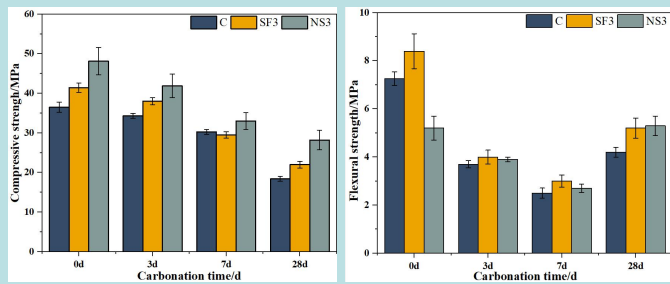
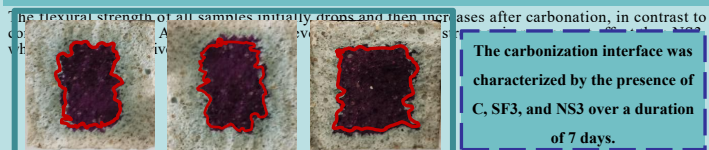


Figure 1. The flexural and compressive strength of supersulfated cement with 0%(C), 3% nano silica(NS3), 3% silica fume(SF3).

After carbonation, there is a decrease in compressive strength for all samples. NS3 and SF3 exhibit relatively better compressive strength, with NS3 still retaining a strength of 28 MPa after 7 days of carbonation.



The carbonization interface was characterized by the presence of C, SF3, and NS3 over a duration of 7 days.

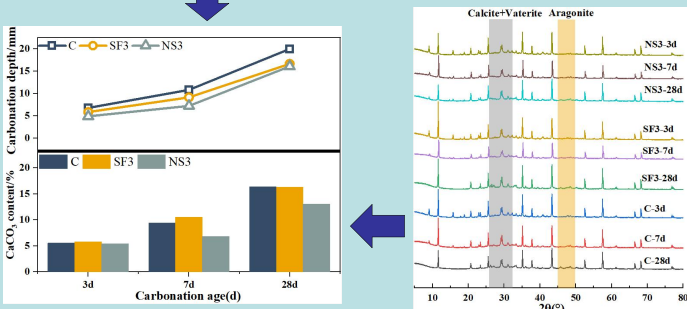


Figure 2. At 3, 7, and 28 days of carbonation, the carbonation depth and the total amount of calcium carbonate for C, SF3, and NS3 were determined.

The depth of carbonation and calcium carbonate content in the figure can reflect the progress of carbonation of C, SF3, and NS3, where the calcium carbonate produced by the carbonation of supersulfate cement includes three crystalline types (aragonite, spherulite, and calcite). The addition of SF and NS both reduces the amount of calcium carbonate generated, with NS maintaining better performance even after 28 days of carbonation.

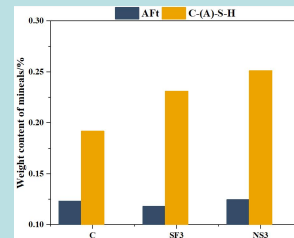


Figure 3. The influence of nano-silica on the proportion of hydration products in SSC before carbonation.

As shown in the figure, the proportion of C-(A)-S-H increases with the addition of silicon materials, and NS3 has the best improvement effect. The proportion of Aft did not change much.

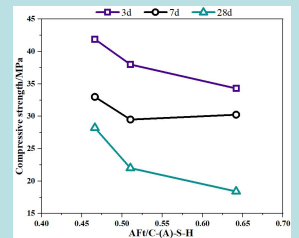
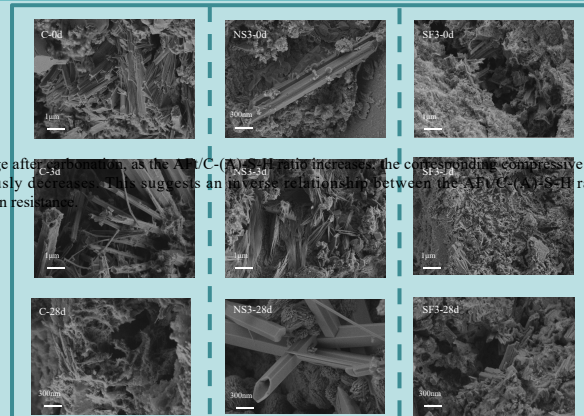


Figure 4. The influence of nano-silica on the proportion of hydration products in SSC before carbonation.



At each age after carbonation, as the AF/C-(A)-S-H ratio increases, the corresponding compressive strength continuously decreases. This suggests an inverse relationship between the AF/C-(A)-S-H ratio and carbonation resistance.

Figure 3. At 3, 7, and 28 days of carbonation, the carbonation depth and the total amount of calcium carbonate for C, SF3, and NS3 were determined.

As shown in SF3 and NS3, the addition of silica-based admixtures increases the amount of C-(A)-S-H gel enclosing Aft. Additionally, with the inclusion of NS, nanoparticles of silica are observed adhering to the surface of the hydration products.

After carbonation, in the control group, Aft is exposed on the surface and has undergone carbonation in the early stages. The addition of nano-silica causes the covering of Aft by C-(A)-S-H, and the carbonation of C-(A)-S-H results in the formation of calcite and amorphous silica gel on the surface.

Conclusions

- 1. The incorporation of nano-silica enhanced the compressive strength of the supersulfate cement and retarded the decrease in compressive and flexural strength after carbonation. The improvement effect of silica fume was weaker than that of nano-silica.
- 2. It was found that the degree of the carbonation depth of the comparison samples increased and the generation of calcium carbonate decreased compared to the control group. This indicates that the addition of silica-based admixtures has a positive effect on the carbonation resistance of supersulfate cement
- 3. The addition of nano-silica increased the amount of C-(A)-S-H gel formation, allowing Aft to be encapsulated in the dense C-(A)-S-H gel, thus reducing the amount of carbonation of Aft and enhancing the carbonation resistance of supersulfate cement.



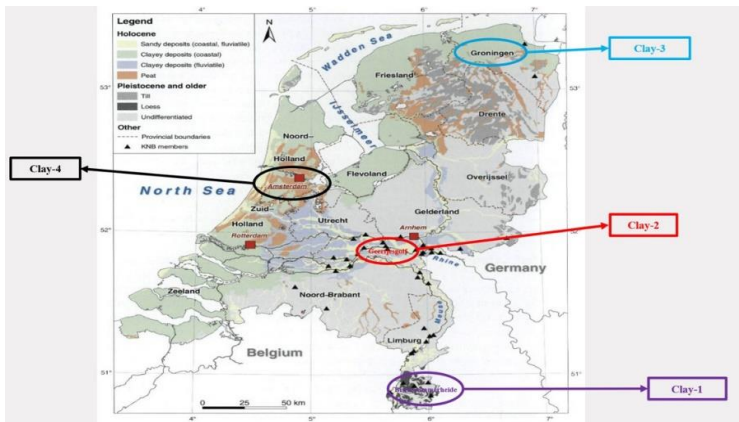
Assessing the feasibility of partially replacing Portland cement with calcined Dutch clay

Zixing Liu, K. Schollbach, H.J.H. Brouwers

Department of the Built Environment, Eindhoven University of Technology

Introduction

Portland cement is one of the most manufactured materials in the world. Global demand is expected to grow due to rapid infrastructure development in emerging economies, with cement production exceeding 3 billion tons in 2012. However, the calcination process of cement clinker is a significant source of greenhouse gas emissions (GHG), usually expressed as carbon dioxide equivalent (CO_{2eq}), sometimes referred to as embedded carbon. Therefore, effective remedies are necessary to control carbon emissions and mitigate climate change. In this regard, the use of supplementary cementitious materials (SCMs) has been extensively studied and implemented. Granulated blast furnace slag, silica fume, fly ash, etc. have been commonly used in the construction industry as cement substitutes. However, the quality and quantity of these materials is limited in the global cement substitution strategy, limiting the efficacy of these SCMs in reducing CO_2 . On the other hand, clay is abundant worldwide and has been studied and proven to be a viable cement substitute when it is calcined.



The distribution of low-grade clays in Netherlands

Objectives

In this paper, there are four low-grade Dutch clays with different kaolinite content (32.80%, 16.80%, 16.28%, and 14.80%) were incorporated into mortar and cement paste and the feasibility of partially replacing Portland cement with calcined Dutch clay was analyzed. In addition, significant advances in the characterization and utilization of these low-grade calcined Dutch clays will be possible through understanding of the mechanical properties, thereby helping to reduce production costs for large-scale construction project applications using low-grade Dutch clays.

Research Significance

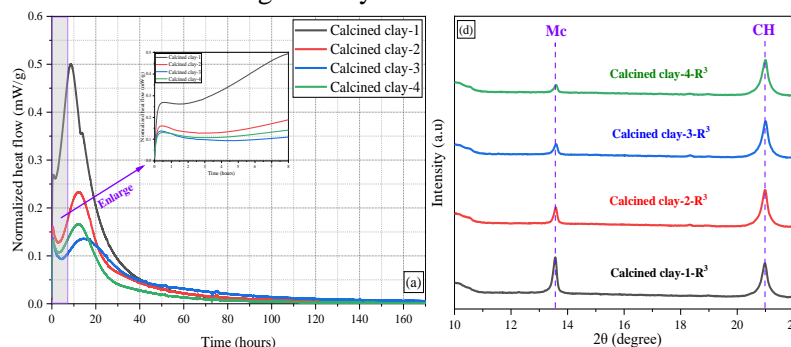
Clay is abundant in the Netherlands and is therefore very important as a building material. Despite the increasing use of concrete over the past few decades, clay bricks and roof tiles still define the look of Dutch towns and cities. About two-thirds of them are used in the structural ceramic industry and one-third in construction.

Results and Discussion

Iron (Fe) is the fourth most abundant element on Earth's crust. Clay usually contains iron (hydr)oxides as associated minerals. Hematite is formed in the presence of oxygen in the temperature range 300 °C–650 °C in clay materials heated in the temperature range 550 °C–850 °C. In a lower-oxygen environment, hematite is reduced to form magnetite, which remains stable even at temperatures close to 300 °C. At temperatures above 650 °C, regardless the presence of oxygen, the predominant iron phase formed is magnetite. During cooling, if oxygen is available, magnetite can convert back to hematite, and the calcined material will have a reddish color. In the absence of oxygen, magnetite will remain as the main stable phase. A higher percentage of bound water normally indicates higher pozzolanic reactivity and higher strength. The calcined clay-1 with a kaolinite content of 32.80% reacts the most, whereas the calcined clay-4 with a kaolinite content of 14.80% is the least reactive. In addition, carboaluminates form and remains in the systems. The height of the peaks of the carboaluminates increase with the calcined kaolinite content of calcined clays, which is also consisted with Avet et al. Although the relative compressive strengths of mortar with higher clay content (more than 10 wt.%) are still lower than the control groups, most of them are higher than 75% at 7 days and 28 days and meet the requirements of pozzolanic activity according to ASTM C618. But for the mortar with clay content of 40 wt.%, the relative compressive strengths are still the lowest, as compared to their counterpart and relative compressive strengths decrease as the clay content increase.



The color change of clays before and after calcination



Pozzolanic reactivity of calcined clays by using R3 test and XRD patterns (Mc = Monocarboaluminate, CH = Portlandite)

Thermal responsive clay-hydrogel composite for additive construction

Haidong Zhuang¹, Zhenbang Guo¹, Cristina Ruiz-Agudo², Fazhou Wang¹, Helmut Cölfen², Zhengyao Qu^{1,2*}
¹State Key Laboratory of Silicate Materials for Architectures, Wuhan University of Technology, Wuhan, China
²Physical Chemistry, University of Konstanz, Konstanz, Germany

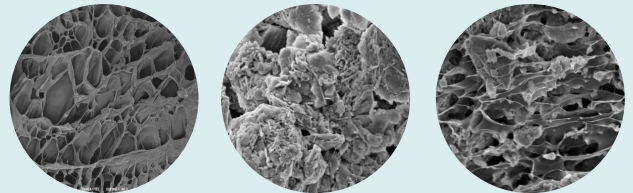
Research Significance

- ◆ The ability to control the fresh-state properties of concrete actively for 3D printing

Objectives

- ◆ To establish clay-gelatin thermal responsive 3D printing system
- ◆ To obtain the forming mechanism of **temperature stimulation response**
- ◆ To achieve the application in low temperature environment

Microstructure analysis



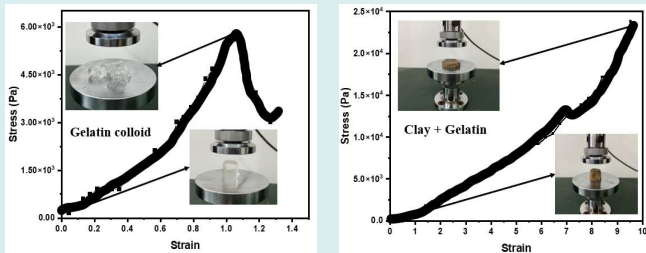
Gelatin

Clay+Water

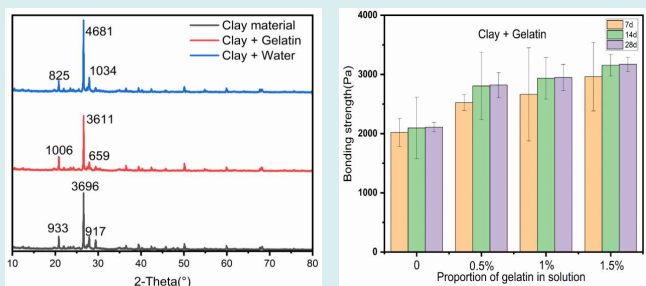
Clay+Gelatin

- ◆ Loose fiber network structure
- ◆ Layer stack structure and pin rod structure
- ◆ Composite cross-network structure

Rheology and mechanics



Comparison of loading capacity after storage at 5°C for 15min



XRD pattern of the sample

Interlayer bonding properties

Conclusions

- ◆ Temperature can be used as a trigger to control gelatin cross-links with clay particles, thereby improving the rheological properties of clay paste
- ◆ Interlayer bonding is enhanced while improving the printability and loading ability of the sample
- ◆ A clay-gelatin crosslinking structure is generated

Samples display



References

- Qu, Z., Yu, Q., Ong, G. P., Cardinaels, R., Ke, L., Long, Y., & Geng, G. (2023). 3D printing concrete containing thermal responsive gelatin: Towards cold environment applications. *Cement and Concrete Composites*, 140, 105029.
- Zhuang, H., Guo, Z., Ruiz Agudo, C., Wang, F., Cölfen, H., & Qu, Z. Temperature-responsive clays containing heat-sensitive gelatin for 3D printing. (In process)

Mechanism of Ba ion solution in LCCSB and its influence on carbonation reaction

Jianping Zhu*, Haole Wang, Xuemao Guan

Henan Polytechnic University, School of Materials Science and Engineering, Jiaozuo, China

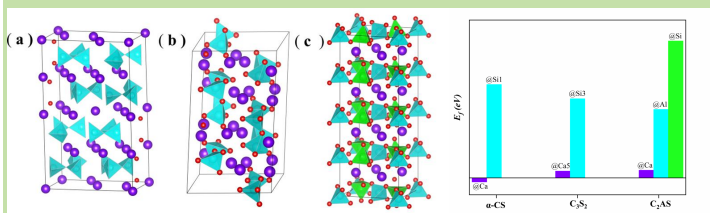
Objectives

- The solution tendency of Ba ion in LCCSB clinker was investigated in this study through experiments and DFT simulation, unveiling the influence mechanism of Ba ion solution on the carbonization reaction of LCCSB. Experimental tests were conducted to characterize the solid solubility of Ba in LCCSB and investigate the influence of doping conditions on the carbonation reactivity, carbonation hardening performance, carbonation products, and microstructure of LCCSB. The DFT simulation elucidated the impact of Ba substitution on cellular parameters and electronic properties in minerals, as evidenced by defect formation energy, BO-BL distribution, and EDD analysis. The bond strength and Ca^{2+} dissociation degree of the Ca-O bond were characterized using measures of bond strength and total bond order density (TBOD).

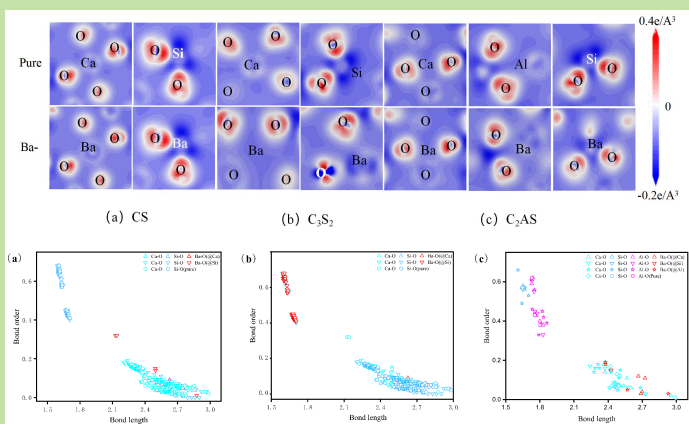
Research Significance

- It is imperative to further enhance the extensive application of barium slag BS in novel low-calcium cement, while concurrently optimizing the overall efficacy of CO_2 sequestration within the cement industry, thereby fostering synergistic development of solid waste utilization and energy conservation as well as emission reduction in this sector.

Tendency of Ba ions to solubilize in LCCSB clinker

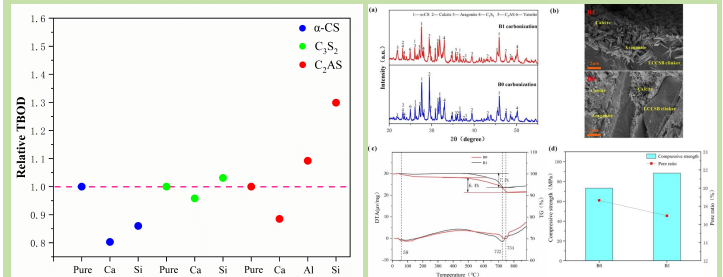


LCCSB : α -CS- C_3S_2 - C_2AS cell models



- The substitution order of Ba ions is : @Ca (α -CS > C_3S_2 > C_2AS)

Effect mechanism of Ba ion solution on carbonation reaction



- After the addition of Ba, it was observed that calcite aragonite growth was promoted and structural porosity was reduced. The incorporation of Ba ions in LCCSB resulted in a decrease in TBOD, as indicated by the TBOD analysis, facilitating the dissociation of Ca ions and further enhancing carbonation within the system.

Conclusions

- Ba exhibits a preference for doping into the Ca site in LCCSB. The solid solubility of Ba in LCCSB is approximately 1 mol%. Specifically, Ba ions preferentially occupy the Ca site of α -CS before entering the Ca site of C_3S_2 . However, the substitution mechanism of Ba ions at the Ca site of C_2AS remains unclear.
- After the dissolution of Ba ion solid into LCCSB, it facilitates the growth of calcium carbonate crystals, leading to an increase in calcite and aragonite content in carbonization products as well as enhanced compressive strength.
- It is evident from TBOD analysis that the presence of Ba ions significantly influences the dissociation rate of Ca ions in LCCSB, there is a decrease in the total bond sequence density (TBOD) of Ca-O bonds at the Ca site. A smaller TBOD value indicates reduced overall bond strength within the system and facilitates easier dissolution of Ca ions, thereby highlighting their potential for high carbonization reactivity.

Outlook and Future Issues

- The above results provide a potential application prospect for the preparation of highly carbonized LCCSB by sintering Barium-containing solid waste, and the research results are expected to further clarify the carbonization mechanism of LCCSB doped by solid waste ions, and bring better environmental benefits for CO_2 storage.

Understanding the microstructural evolution of 3D printing steel slag-cement with low-field NMR relaxation

Lingli Zhu^a, Wanting Zhao^a, Yu Zhao^b, Xuemao Guan^a

^aHenan Polytechnic University School of Materials Science and Engineering, Jiaozuo, 454000, China

^bHenan Polytechnic University School of Civil Engineering, Jiaozuo, 454000, China

Objectives

- The utilization of **steel slag** is enhanced and a sustainable, **eco-friendly solution** is provided through **3D printing technology**.
- The **low-field NMR** relaxation characteristics effectively characterize the early performance of 3D printing cementitious materials, **enabling non-destructive** and **rapid detection** at an early stage.

Research Significance

- Intelligent construction using 3D printing is the future trend. **Low-field NMR** can assist in conducting early nondestructive and rapid testing of 3D printing cementitious materials, **contributing to the development of intelligent construction**.

T2 relaxation distribution

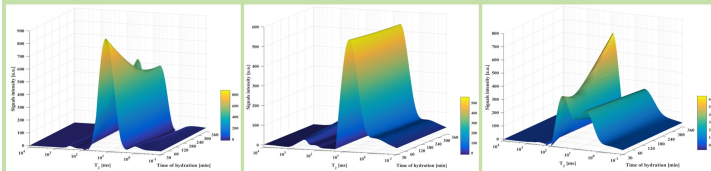


Fig.1 SS0

Fig.2 SS10

Fig.3 SS20

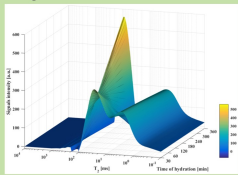


Fig.4 SS30

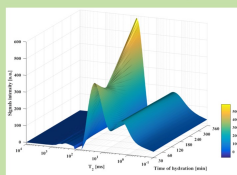


Fig.5 SS40

Low-field nuclear magnetic resonance (NMR) relaxation time measurements to characterize the microstructural evolution of 3D printed steel slag cementitious materials during the early 6h period, exploring the effect of steel slag properties on the early hydration microstructure. An appropriate amount of high alkalinity steel slag can effectively promote the formation of capillary pores and reduce porosity.

Rheological properties

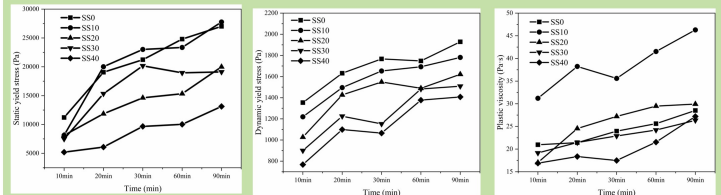


Fig.6

Fig.7

Fig.8

The impact of steel slag content on the rheological properties of 3D printed steel slag cement-based materials is illustrated in Fig. The yield stress and plastic viscosity of the slurry initially increased, followed by a subsequent decrease, as the steel slag content was increased from 0% to 40%. Time-dependent relaxation measurements effectively characterized the time-dependent rheological properties, where (0.1-10 μm) pore throat distribution was correlated with the static yield stress.

Conclusions

- The addition of 10% high-alkalinity steel slag instead of cement can enhance the compactness and reduce the porosity of the slurry.
- The composition of the slag significantly influences the rheology of the slurry. Optimal rheological properties of the slurry can be achieved when the steel slag content reaches 10%.
- The distribution of pore throat sizes (ranging from 0.1 to 10 μm) exhibited a positive correlation with the static yield stress.

Outlook and Future Issues

- At present, there is relatively little research on the early performance detection of 3D printed concrete based on solid waste preparation.
- How to conduct non-destructive and rapid testing of 3D printed concrete materials to improve the engineering application of 3D printed concrete

Publications

- Publication 1 Lingli Zhu, Jie Yao, Yu Zhao, et al. Effects of composite cementation system on rheological and working performances of fresh 3D-printable engineered cementitious composites [J]. Journal of Building Engineering, 2022, 12, 105801
- Publication 2 Lingli Zhu, Zhenghao Jin, Yu Zhao*, etc. Rheological Properties of Cemented Coal Gangue Backfill Based on Response Surface Methodology [J], Construction and Building Materials, 2021, 306, 124836

